Adsorptive Removal of Phosphorus from Aqueous Solution using Recycled Bricks and Modified Clay Pellets and the Potential for a Slow Release Fertilizer

Edet, Uduak

Award date:
2018

Awarding institution:
Coventry University

Adsorptive Removal of Phosphorus from Aqueous Solution using Recycled Bricks and Modified Clay Pellets and the Potential for Use as a Slow Release Fertilizer

By

Uduakobong Aniedi Edet

July 2018

Adsorptive Removal of Phosphorus from Aqueous Solution using Recycled Bricks and Modified Clay Pellets and the Potential for a Slow Release Fertilizer

By

Uduakobong Aniedi Edet

School of Energy, Construction and Environment
Faculty of Engineering, Environment and Computing
Coventry University

July 2018

A thesis submitted in partial fulfilment of the Coventry University requirements for the Degree of Doctor of Philosophy

DEDICATION

This project is dedicated to the Almighty God without his divine grace and favour, none of this would have been possible.

ACKNOWLEDGEMENT

My appreciation goes to the Niger Delta Development Commission (NDDC) of the Nigerian Government for funding this research.

My heartfelt appreciation goes to my husband and friend Colonel Aniedi Edet, who had to sacrifice so much to enable me attain this height. I could not do this without you. My children Edidiong, Semfon and Ekomobong I say thank you for coming with me on this journey and putting up with the disruptions in your lives. Your presence made the experience fun. Thank you for keeping me company in my office while I had to do my “work”. To my mom, Dinah U. Eshiet, thank you for coming to my rescue anytime I needed you. I also want to thank my brother and sisters: Akanimo Eshiet, Imaobong Maples and their families, especially my baby sister Ofonime Eshiet who has been a source of support, for showing I could always depend on them.

My gratitude goes to my director of studies Dr. Augustine Ifelebuegu, whose door was always open to attend to any problem I had. Your guidance and support got me through this, thank you for standing up for me. To my second supervisor, Dr Adrian Wood, thank you for your guidance and support. To Dr Mark Bateman, thank you for you guidance. To the members of staff of the Environmental Management laboratory, especially Dr Richard Collins and Anne Nuttal, who were never too busy to assist with any difficulties I encountered, I say thank you.

To my friends and colleagues too numerous to mention especially those I had to enlist for child minding duties, I appreciate every support I have received in the course of this pursuit, thank you all.

Abstract

The Urban Waste Water Treatment Directive increases government regulatory pressure required to ensure phosphate discharged by Waste Water Treatment Works (WWTWs) meet consent. Bricks from construction waste have been viewed as an alternative treatment medium for phosphate. This thesis examines the use of recycled bricks and novel brick-like materials to afford an opportunity for the provision of a green solution to issues associated with phosphate removal and recovery.

This thesis builds on existing studies on the use of recycled bricks, firstly eliminating the problem associated with use of powdered form of clay material by pelletising these materials. The pellets developed performed better than conventional brick dust. The composition of pelletised material was modified to ascertain the extent of phosphate adsorption. Optimization of pelletised material was carried out in batch studies, and phosphate removal was found to vary with elemental composition and increase with treatment time among other factors. The maximum adsorption capacity was 42.37 mg/g, 70.42 mg/g and 52.91 mg/g for AlMFCP, CaMFCP and FeMFCP respectively. The modified pellets show a faster kinetic that was up to five times faster than FCP signifying that the modified pellets will require a reactor that was five times smaller in size than FCP. Physisorption was the dominant adsorption mechanism supported by some pore diffusion for AlMFCP and FeMFCP but the dominant mechanism for adsorption using CaMFCP was chemisorption supported by some physical diffusion processes. Acidic pH favoured adsorption using FeMFCP, and slightly acidic pH for AlMFCP while adsorption using CaMFCP was favoured at acidic and neutral pH. Phosphate adsorption achieved using materials of this study was compared to materials of other studies through the comparison of adsorption isotherms. Pellets modified with calcium carbonate showed the best performance and was consequently used in further studies. Phosphate adsorption involved different mechanisms at different stages but tending to physisorption as the dominant mechanism.

Fixed bed column study performed on the pellets showed the practicability of a full-scale application in a wastewater treatment plant. Increase in bed height

and column diameter improved adsorption capacity due to longer empty bed contact time (EBCT) between the adsorbent and phosphate in solution. Higher flow rate hindered adsorption as a result of shorter contact between adsorbent and phosphate in solution. The column with column diameter of 2 cm, bed height of 10 cm and influent phosphate concentration of 20 mg/L showed the shortest retention time of 1.75 minutes, followed by the column with a bed height of 10 cm, column diameter of 5 cm and influent phosphate concentration of 20 mg/L.

Phosphate sorbed to materials in this study was recycled as a slow release fertilizer for agricultural production. The spent adsorbent compared favourably with yield obtained from KH_2PO_4 fertilizer. The yield increased with increase in application rate of phosphate with 382.17 kgP/ha producing the highest yield. The performance of pots with P added in the form of phosphate sorbed to CaMFCP was similar to pots with P added in the form of KH_2PO_4 when germination rate, plant height and WM yield were considered while pots with added KH_2PO_4 showed a better DM yield than pots with P added in the form of phosphate sorbed to CaMFCP. Relative effectiveness of fertilizer showed improvement as growth progressed. At the latter stages, yield using phosphate from spent filter materials surpassed KH_2PO_4 fertilizer. This demonstrated that spent fired clay pellets could be used as a slow release fertilizer for agricultural purpose thereby offering a green and cost effective option for phosphate removal in wastewater and the management of the resultant waste pellets.

Table of Contents

DEDICATION iii
ACKNOWLEDGEMENT iv
Abstract v
List of Tables v
List of Figures vi
Glossary of Terms i
1 Chapter One: Background of Study 1
1.1 Statement of the Problem 5
1.2 Research Aim and Objectives 6
1.3 Thesis Outline 6
2 Chapter Two Review of Related Literature 8
2.1 Phosphorus 8
2.2 Uses of phosphorus 9
2.2.1 Phosphorus and Eutrophication 9
2.2.1.1 Phosphorus and Wastewater 11
2.2.2 Processes and Operations of a Wastewater Treatment Plant 13
2.3 Phosphate Removal from Wastewater 16
2.3.1 Chemical Precipitation 17
2.3.2 Enhanced Biological Phosphorus Removal (EBPR) 21
2.4 Phosphate Removal through the Use of adsorbents 23
2.5 Adsorption of Phosphate from Wastewater Using Clay-Based Adsorbents 23
2.5.1 Properties of clay minerals 25
2.5.1.1 Charge 25
2.5.1.2 Swelling 27
2.5.2 Mechanism of phosphate adsorption by clay 27
2.5.3 Adsorption using Different Clay-based Adsorbent 28
2.5.3.1 Clay 28
2.5.4 Modification of clay 30
2.5.4.1 Modification using addition of polyvalent metals 31
2.5.4.2 Pillared Clays 31
2.5.4.3 Double layered hydroxides (LDH) 32
2.5.5 Man-made products 46
2.5.5.1 Light-Weight Aggregates (LWA) and Light Expanded Clay Aggregates (LECA) 46
2.5.5.2 Phoslock® 47
2.6 Adsorption Theory 48
1.1.2 Factors affecting Adsorption 49
2.6.1.1 Contact time 49
2.6.1.2 pH 49
2.6.1.3 Initial Concentration 50
2.6.1.4 Temperature 50
2.6.1.5 Surface area 50
2.6.1.6 Effect of Competing Anions 51
1.1.3 Kinetic Models 51
2.6.1.7 Pseudo First Order Kinetics 51
2.6.1.8 Pseudo Second Order Kinetics 52

2.6.1.9 Elovich Kinetic Model....52
2.6.1.10 The Bangham's Kinetic Model (Pore Diffusion Model)....53
2.6.1.11 Intraparticle Diffusion....54
2.6.2 Adsorption Isotherm....54
2.6.2.1 Langmuir Isotherm....54
2.6.2.2 Freundlich Isotherm....55
2.6.2.3 Tempkin Adsorption Isotherm....56
2.6.2.4 Dubinin-Radushkevich Adsorption Isotherm....57
2.7 Phosphorus retention in filter materials and suitability for plant production....58
2.7.1 Desorption of phosphates....58
2.7.2 Recovery and Plant Availability of Adsorbed Phosphate....59
2.8 Summary....60
3 Methodology....61
3.1 Materials....61
3.1.1 Analytical Reagents....61
3.1.2 Bricks and Clay:....61
3.1.3 Determination of Moisture Content of Clay....62
3.1.4 Preparation of Clay Pellets....62
3.1.5 Modification of Clay Pellets....64
3.1.6 Characterization of Clay Tiles....65
3.2 Equipments....66
3.2.1 Flow Injection Analyzer....66
3.2.2 Inductively Coupled Plasma Optical Emission Spectrometer (ICP-OES) 67
3.3 Preparation of Reagents:....68
3.3.1 Preparation of Ammonium Molybdate Reagent ●....68
3.3.2 Preparation of Stannous Chloride Reagent ●●....68
3.3.3 Preparation of Rinsing Solution....69
3.3.4 Preparation of Stock Standard Solution....69
3.3.5 Preparation of Calibrating Standard....69
3.3.6 Carrier Solution....69
3.3.7 Preparation of Hoagland's Solution....69
3.3.8 Preparation of Micronutrient Stock Solution....69
3.3.9 Preparation of Stock Iron Solution....69
3.4 Determination of Limit of Detection....70
3.5 Batch Experiment....70
3.5.1 Determination of the Effect of Phosphate Concentration....71
3.5.2 Determination of the Effect of Adsorbent Dosage....71
3.5.3 Determination of the Effect of pH....71
3.5.3.1 Determination of Point of Zero Charge (pH_{pzc})....72
3.5.3.2 Determination of the Effect of Temperature....72
3.5.3.3 Determination of the Effect of Contact Time....73
3.5.3.4 Determination of Effect of Firing Temperature....73
3.5.3.5 Determination of Effect of Clay Pellets Modification....73
3.6 Continuous Flow Experiment....74
3.6.1 Effect of bed height....76
3.6.2 Effect of initial phosphate concentration....76
3.6.3 Effect of column diameter....76
3.6.4 Effect of adsorbate flow rate....76

3.6.5 Determination of breakthrough point 77
3.7 Kinetic and Isotherm Experiment 79
3.7.1 Kinetic Experiment 79
3.7.2 Adsorption Isotherm 79
3.8 Thermodynamic Studies 80
3.9 Green House Experiment 80
3.9.1 Pot Experiment 81
3.9.2 Soil pH 83
3.9.3 Plant available Phosphorus 83
3.10 Data Analysis 83
3.10.1 Removal Efficiency 83
3.10.2 Adsorption Capacity 84
3.11 Health and Safety 84
4 A Mechanistic Evaluation of the Adsorption of Phosphate from Wastewater using Waste Bricks 85
4.1 Introduction 85
4.2 Effect of contact time 85
4.3 Effect of brick dosage 87
4.4 Effect of temperature 88
4.4.1 Adsorption kinetics modelling 89
4.4.2 Thermodynamic Study 93
4.5 Effect of initial concentration of phosphate 95
4.5.1 Adsorption Isotherm 97
4.6 Conclusions 100
4.7 Limitation of study 101
5 Adsorptive properties of Fired Clay Pellets (FCP) 102
5.1 Introduction 102
5.2 Characterization of Clay Tiles 103
5.3 Effect of Firing Temperature on the Adsorption of Phosphate by FCP 104
5.4 Effect of Adsorbent Dosage on the Removal of Phosphates 107
5.5 Effect of Contact Time on the Removal of Phosphate from Wastewater using FCP 108
5.5.1 Rate of Adsorption 108
5.6 Kinetic Models 110
5.6.1.1 Pseudo- First Order Kinetics 110
5.6.1.2 Pseudo Second Order Kinetics 110
5.6.1.3 Elovich Kinetic Model 111
5.6.1.4 The Bangham's Kinetic Model (Pore Diffusion Model) 112
5.6.1.5 Intra-particle Diffusion 115
5.7 Effect of pH on Phosphate Adsorption 117
5.8 Effect of Temperature on the adsorption of phosphate by FCP 122
5.8.1 Kinetic Model 125
5.8.2 Thermodynamic Parameters 126
5.9 Effect of initial concentration on the adsorption of phosphates by FCP 128
5.9.1 Effect of initial concentration on the adsorption of phosphate 128
5.9.2 Adsorption Isotherm 130
5.10 Effect of perforation 133
5.11 Summary and Conclusion 138

6 Evaluation of the impact of compositional modification on the adsorptive properties of clay pellets 140
6.1 Introduction 140
6.2 Effect of $Al_2(SO_4)_3$ modification on the performance of fired clay 143
6.3 Phosphate Adsorption using Fired Calcium Modified Clay Pellets (CaFMCP) 146
6.4 Phosphate Adsorption Using Fired Iron Modified Clay Pellets 149
6.4.1 $FeCl_3$ Modified Fired Clay Pellet 149
6.4.2 $FeSO_4$ modified fired clay pellets 151
6.5 Effect of combined compositional modification clay pellets 153
6.6 Adsorptive properties of modified fired clay pellets 157
6.6.1 Effect of contact time on the adsorption of phosphate using modified fired clay pellets 157
6.6.2 Effect of adsorbent dosage on the adsorption of phosphate using modified clay pellets 158
6.6.3 Effect of pH on the adsorption of phosphate using modified clay pellets 159
6.6.4 Effect of temperature 165
Adsorption Kinetic Model 166
6.6.4.1 Intra-particle Diffusion 173
6.6.4.2 Thermodynamic parameters 175
6.6.5 Effect of initial concentration 177
6.6.6 Adsorption Isotherms 179
6.7 Conclusion 188
7 Adsorption performance of a fixed bed column for the removal of phosphate using calcium carbonate modified clay pellets (CaMFCP) 189
7.1 Introduction 189
7.1.1 Effect of influent phosphate concentration 190
7.1.2 Effect of bed height 191
7.1.3 Effect of adsorbate flow rate 193
7.1.4 Effect of column diameter 195
7.2 Modelling of fixed bed adsorption data 196
7.2.1 Bed Depth Service Time (BSDT) 196
7.2.2 Thomas model 199
7.2.3 Yoon-Nelson Model 203
7.2.4 Adams-Bohart Model 207
7.3 Up scaling models 210
7.3.1 Up scaling using Empty Bed Contact Time (EBCT) 211
7.3.2 Up scaling using Bed Depth Service Time (BDST) 212
7.4 Summary and Conclusion 212
8 Calcium-modified fired clay pellet as an adsorbent for the removal of phosphate from waste water and its potential for a slow release fertilizer 214
8.1 Introduction 214
8.2 Soil analysis 214
8.2.1 Soil pH 214
8.2.2 Analysis of elemental content 215
8.3 Growth parameters 216
8.3.1 Germination rate 216
8.3.2 Plant height 218

8.3.3 Effect of phosphate application on the wet matter (WM) yield of ryegrass 221
8.3.4 Effect of phosphate application on the dry matter (DM) yield of ryegrass 223
8.3.5 Fertilizer Effectiveness of Applied Phosphate 225
8.3.6 Yield Response 226
8.4 Summary and conclusion 229
9 Summary, Conclusion and Recommendation for Further Research 231
9.1 Chapter 5 Summary 231
9.2 Chapter 6 Summary 232
9.3 Chapter 7 Summary 233
9.4 Chapter 8 Summary 234
9.5 Chapter 9 Summary 234
9.6 Conclusion 235
9.6.1 Contribution to Knowledge 235
9.7 Areas for Further Research 236

List of Tables

Table 2.1: Typical composition of untreated domestic wastewater 12
Table 2.2: The Grim's classification of clay minerals (Murray 2007) 25
Table 2.3: pHzpc of selected clay minerals 26
Table 3.1: Elements and Wavelengths for ICP-OES Analysis 68
Table 3.2: Application rate of phosphate (kgP/ha) 81
Table 4.1: Kinetic model adsorption parameters of adsorption of phosphate onto brick dust. Adsorption conditions: initial concentration 20mg/l, pH 6.7, adsorbent dose 33.33g/l, room temperature 92
Table 4.2: Gibbs free energy (ΔG) for the adsorption of phosphate by brick dust. ... 94
Table 4.3: Thermodynamic parameters for the adsorption of phosphate by brick dust 94
Table 4.4: Adsorption isotherm parameters for the adsorption of phosphate onto brick dust 99
Table 5.1: Kinetic model adsorption parameters of adsorption of phosphate onto FCP. Adsorption conditions: initial concentration 50mg/l, pH 6.7, adsorbent dose 20g/l, room temperature 114
Table 5.2: Kinetic model adsorption parameters of adsorption of phosphate onto clay pellets at different temperature. Adsorption conditions: initial concentration 50mg/l, pH 6.7, adsorbent dose 20g/l 125
Table 5.3: Thermodynamic parameters for the adsorption of phosphate by FCP. . 127
Table 5.4: Adsorption isotherm constants for the adsorption of phosphate onto FCP 133
Table 5.5: Kinetic model adsorption parameters of adsorption of phosphate onto perforated clay pellets at different temperature. Adsorption conditions: initial concentration 50mg/l, pH 6.7, adsorbent dose 20g/l 136

Table 6.1: Kinetic model adsorption parameters of adsorption of phosphate onto AlMFCP at different temperature. Adsorption conditions: initial concentration 50mg/l, pH 6.7, adsorbent dose 20g/l 170

Table 6.2: Kinetic model adsorption parameters of adsorption of phosphate onto CaMFCP at different temperature. Adsorption conditions: initial concentration 50mg/l, pH 6.7, adsorbent dose 20g/l 170

Table 6.3: Kinetic model adsorption parameters of adsorption of phosphate onto FeMFCP at different temperature. Adsorption conditions: initial concentration 50mg/l, pH 6.7, adsorbent dose 20g/l 171

Table 6.4: Gibbs free energy (∆Go) for the adsorption of phosphate using modified FCP..... 176

Table 6.5: Thermodynamic parameters for the adsorption of phosphate by modified FCP..... 176

Table 6.6: Adsorption isotherm parameters for the adsorption of phosphate onto modified FCP 182

Table 7.1: Fixed bed performance parameters of CaMFCP for the adsorption of phosphate 190

Table 7.2: BDST parameters for adsorption of phosphate onto CaMFCP..... 198

Table 7.3: Parameters of Adams-Bohart and Thomas models for the adsorption of phosphate by fired clay pellets under different experimental conditions..... 200

Table 7.4: Parameters of Yoon-Nelson model for the adsorption of phosphate by fired clay pellets under different experimental conditions..... 204

Table 7.5: Moreton WWTW Data (Littler 2011)..... 210

Table 7.6: Scaling up data..... 210

Table 8.1: Polynomial coefficient between yield response and fertilizer application rate of phosphate (kgP/ha)..... 228

List of Figures

Figure 2.1: Schematic of a typical wastewater treatment facility providing primary and secondary treatment..... 14

Figure 2.2: Cross-section of a trickling filter..... 16

Figure 2.3: A diagram showing the various points for addition of chemical precipitants 18

Figure 3.1: Firing temperature programme of furnace used in the production of the clay pellets 63

Figure 3.2: Clay Pellets a) during air drying; and b) after firing 64

Figure 3.3: Scanning Electron Microscope model JSM-6060LV 66

Figure 3.4: Schematic diagram of the fixed bed column experiment: (1) reservoir with phosphate solution; (2) peristaltic pump; (3) filter material; (4) glass wool; (5) effluent. 75

Figure 3.5: The set up for the fixed bed column experiment 75

Figure 3.6: Greenhouse experiment a) prior to harvest; b) post harvest. 82

Figure 4.1: Effect of contact time on the adsorption of phosphate using brick dust (n=3) standard error bars shown. Adsorption conditions: initial concentration 20mg/l, pH 6.7, adsorbent dose 5g, room temperature..... 86

Figure 4.2: Effect of adsorbent dosage on the adsorption of phosphate by brick dust using standard experimental conditions (n=3), standard error bars shown 87

Figure 4.3: Amount of phosphate adsorbed per unit mass of brick dust using standard experimental conditions (n=3), standard error bars shown 88

Figure 4.4: Effect of temperature on the adsorption of phosphate using brick dust. Adsorption conditions: initial concentration 20mg/l, pH 6.7, adsorbent dose 33.33g/l, room temperature..... 89

Figure 4.5: Kinetic model plot for the adsorption of phosphate using brick dust: a) Pseudo-first order kinetic model; b) Pseudo-second order kinetic model; c) Elovich kinetic model; and d) Bangham's kinetic model..... 90

Figure 4.6: Van't Hoff plot for the adsorption of phosphate using brick dust 94

Figure 4.7: Effect of initial concentration on removal efficiency of fired clay pellets using 5g FCP and 200ml phosphate solution (n=3), standard error bars shown 95

Figure 4.8: The effect of initial concentration on amount of phosphate adsorbed by FCP using 5g clay pellets and 200ml phosphate solution (n=3), standard error bars shown..... 96

Figure 4.9: The adsorption isotherm plots for the adsorption of phosphate using brick dust: a) Langmuir adsorption isotherm; b) Freundlich adsorption isotherm; c) Tempkin; and d) Dubinin-Radushkevich adsorption isotherm 98

Figure 5.1: (a) FCP before adsorption; (b) FCP after adsorption 104

Figure 5.2: Effect of firing temperature on the adsorption of phosphate using FCP using standard experimental conditions..... 104

Figure 5.3: The effect of firing temperature on the adsorption of phosphate FCP using standard experimental conditions..... 105

Figure 5.4: Effect of adsorbent dosage on the adsorption of phosphate by FCP using standard experimental conditions (n=3), standard error bars shown..... 107

Figure 5.5: Effect of contact time on the adsorption of phosphate by FCP. This experiment was carried out using 3g clay tiles, 150 ml of 50 mg/l phosphate solution. 109

Figure 5.6: Kinetic model plot for the adsorption of phosphate using FCP: a) Pseudo-first order kinetic model; b) Pseudo-second order kinetic model; c) Elovich kinetic model; and d) Gangham's kinetic model..... 113

Figure 5.7: Intraparticle diffusion model plot of qt (mg/g) against t1/2 (mins) for the adsorption of 50mg/l phosphate solution using 3g FCP..... 116

Figure 5.8: Effect of pH on the removal of phosphate by FCP using standard experimental conditions (n=3), standard error bars shown. 117

Figure 5.9: Final pH of phosphate solution at the end of contact using FCP..... 118

Figure 5.10: pH range for phosphate adsorption by different species Source: Petrik Laboratories Inc. In Taylor (2005)..... 120

Figure 5.11: The effect of temperature on the removal of phosphate by brown clay tiles using standard experimental conditions (n=3) standard error bars shown. 122

Figure 5.12: Kinetic model plot for the adsorption of phosphate using FCP: a) Pseudo-first order kinetic model; b) Pseudo-second order kinetic model; c) Elovich kinetic model; and d) Gangham's kinetic model..... 124

Figure 5.13: Van't Hoff plot for the adsorption of phosphate by FCP. 127

Figure 5.14: Effect of initial concentration on removal efficiency of clay pellets using 5g FCP and 200ml phosphate solution (n=3), standard error bars shown. 129

Figure 5.15: The effect of initial concentration on amount of phosphate adsorbed by FCP using 5g clay pellets and 200ml phosphate solution (n=3), standard error bars shown..... 130

Figure 5.16: The adsorption isotherm plots for the adsorption of phosphate using FCP: a) Langmuir adsorption isotherm; b) Freundlich adsorption isotherm; c) Tempkin; and d) Dubinin-Radushkevich adsorption Isotherm 131

Figure 5.17: The effect of perforation on the adsorption of clay pellets using standard experimental conditions..... 134

Figure 5.18: The effect of perforation on the performance of clay tiles within 30 minutes (n=3) standard error bars shown. 135

Figure 5.19: Kinetic model plot for the adsorption of phosphate using perforated FCP: a) Pseudo-first order kinetic model; b) Pseudo-second order kinetic model; c) Elovich kinetic model; and d) Bangham's kinetic model 137

Figure 6.1: SEM micrographs of the modified fires clay pellets (a) AlMFCP before adsorption; (b) AlMFCP after adsorption; (c) CaMFCP before adsorption; (d) CaMFCP after adsorption; (e) FeMFCP before adsorption; (f) FeMFCP after adsorption..... 142

Figure 6.2: Effect of $Al_2(SO_4)_3$ modification on the adsorption of phosphate by FCP using standard experimental conditions (n=3); standard error bars shown. 143

Figure 6.3: Effect of CaCO3 modification on the adsorption of phosphate by FCP using standard experimental conditions (n=3); standard error bars shown..... 147

Figure 6.4: Effect of FeCl3 addition on the adsorption of phosphate by FCP using standard experimental conditions (n=3); standard error bars shown..... 150

Figure 6.5: Effect of FeSO4 modification on the adsorption of phosphate by FCP using standard experimental conditions (n=3); standard error bars shown..... 151

Figure 6.6: Effect of composition modification on the adsorption of phosphate by FCP: a) addition of Al2(SO4)3 and other modifications; b) addition of CaCO3 and other modifications; and c) addition of FeSO4 and other modifications..... 154

Figure 6.7: Effect on contact time on the adsorption of phosphate by modified clay pellets using standard experimental conditions (n=3); standard error bars shown. 157

Figure 6.8: Effect of adsorbent dosage on the adsorption of phosphate by modified clay pellets using standard experimental conditions (n=3); standard error bars shown. 159

Figure 6.9: Effect of pH on the adsorption of phosphate by modified clay pellets using standard experimental conditions (n=3); standard error bars shown..... 160

Figure 6.10: Final pH of phosphate solution at the end of contact using modified FCP. 163

Figure 6.11: Distribution of phosphate species in solution as a function of pH (Kamiyango et al. 2009). 163

Figure 6.12: Effect of temperature on the adsorption of phosphate by modified clay pellets using standard experimental conditions (n=3); standard error bars shown. 165

Figure 6.13: Kinetic model plot for the adsorption of phosphate using AlMFCP: a) Pseudo-first order kinetic model; b) Pseudo-second order kinetic model; c) Bangham's kinetic model; and d) Elovich kinetic model 167

Figure 6.14: Kinetic model plot for the adsorption of phosphate using CaMFCP: a) Pseudo-first order kinetic model; b) Pseudo-second order kinetic model; c) Elovich kinetic model; and d) Bangham's kinetic model. 168

Figure 6.15: Kinetic model plot for the adsorption of phosphate using FeMFCP: a) Pseudo-first order kinetic model; b) Pseudo-second order kinetic model; c) Elovich kinetic model; and d) Bangham's kinetic model 169

Figure 6.16: Intraparticle diffusion model plot of qt (mg/g) against √t (mins) for the adsorption of 50mg/l phosphate solution using 3g FCP. 174

Figure 6.17: Van't Hoff plot for the adsorption of phosphate by modified FCP. 175

Figure 6.18: Effect of initial concentration on removal efficiency of clay pellets using 5g FCP and 200ml phosphate solution (n=3), standard error bars shown. 177

Figure 6.19: The effect of initial concentration on amount of phosphate adsorbed by FCP using 5g clay tiles and 200ml phosphate solution (n=3), standard error bars shown..... 178

Figure 6.20: The adsorption isotherm plots for the adsorption of phosphate using AlMFCP: a) Langmuir adsorption isotherm; b) Freundlich adsorption isotherm; c) Tempkin; and d) Dubinin-Radushkevich adsorption Isotherm. 180

Figure 6.21: The adsorption isotherm plots for the adsorption of phosphate using CaMFCP: a) Langmuir adsorption isotherm; b) Freundlich adsorption isotherm; c) Tempkin; and d) Dubinin-Radushkevich adsorption Isotherm 183

Figure 6.22: The adsorption isotherm plots for the adsorption of phosphate using FeMFCP: a) Langmuir adsorption isotherm; b) Freundlich adsorption isotherm; c) Tempkin; and d) Dubinin-Radushkevich adsorption Isotherm 186

Figure 7.1: Effect of influent phosphate concentration on the experimental breakthrough curves (bed height 10 cm; column diameter 6 cm; temperature 25oC ±2 oC; pH 6.5)..... 191

Figure 7.2: Effect of bed height on the experimental breakthrough curves (initial phosphate concentration 20 mg/l; column diameter 5 cm; temperature 25oC ±2 oC; pH 6.5)..... 193

Figure 7.3: Effect of adsorbate flow rate on the experimental breakthrough curves (initial phosphate concentration 20 mg/l; column diameter 4 cm; bed height 10 cm; temperature 25oC ±2 oC; pH 6.5) 194

Figure 7.4: Effect of column diameter on the experimental breakthrough curves (initial phosphate concentration 20 mg/l; flow rate 2.39 ml/min; bed height 10 cm; temperature 25oC ±2 oC; pH 6.5) 196

Figure 7.5: BDST plot for different bed height (flow rate 2.5 ml/min; influent phosphate concentration 20 mg/L)..... 198

Figure 7.6: Thomas plot for the adsorption of phosphate on CaMFCP: Effect of (a) bed height; (b) influent phosphate concentration; (c) flow rate; and (d) column diameter. 202

Figure 7.7: Yoon-Nelson plot for the adsorption of phosphate on CaMFCP: Effect of (a) bed height; (b) influent phosphate concentration; (c) flow rate; and (d) column diameter 205

Figure 7.8: Adams-Bohart plot for the adsorption of phosphate on CaMFCP: Effect of (a) bed height; (b) influent phosphate concentration; (c) flow rate; and (d) column diameter. 208

Figure 7.9: EBCT plot for columns of different bed heights (10, 20 and 30 cm; influent concentration 20 mg/L; column diameter 5 cm; flow rate 2.5 ml/min) 211

Figure 8.1: Concentration of elements in the soil pre-planting 215

Figure 8.2: Concentration of elements in the soil post-planting..... 215

Figure 8.3: Germination rate of ryegrass as a function of added phosphate sorbed to CaMFCP (n=3), standard error bars shown..... 217

Figure 8.4: Plant height of ryegrass: a) 1st growing cycle; b) 2nd growing cycle; c) 3rd growing cycle and d) 4th growing cycle; (n=3) standard error bars shown..... 219

Figure 8.5: Effect of phosphate application on the wet matter yield (WM) of ryegrass, (n=3) standard error bars shown 221

Figure 8.6: Effect of phosphate application on the dry matter yield (DM) of ryegrass, (n=3) standard error bars shown 223

Figure 8.7: Relative effectiveness of phosphate sorbed to CaMFCP; application rate: a) 127.39 kgP/ha; b) 382.17 kgP/ha..... 225

Figure 8.8: Quadratic yield response curve for phosphate application of ryegrass. 228

Glossary of Terms

2D	2-dimensional
A	Arrhenius constant (J/mol/k)
AlMFCP	$Al_2(SO_4)_3$ modified fired clay pelley
ANOVA	Analysis of variance
A_T	Tempkin isotherm equilibrium binding constant (L/g)
B	D-R isotherm constant (mol^2/KJ^2)
BDST	Bed depth service time
B_T	Tempkin isotherm constant
C_t	Adsorbed concentration at time t (mg/l)
Cad	Adsorbed phosphate concentration (mg/l)
C_b	Breakthrough concentration
C_o	Initial concentration
C_e	Exhaustion concentration
CW	Constructed wetland
ΔG^O	Gibb free energy (KJ/mol)
ΔS^O	Entropy (KJ/mol)
DM	Dry matter
DNA	Deoxyribonucleic acid
D-R	Dubinin-Radushkevich isotherm
DWF	Dry weather flow
ε	Polanyi potential
E	D-R free energy (KJ/mol)
EBCT	Empty Bed Contact Time
E^a	Activation energy (KJ/mol)
FST	Final Settling Tank
H	Bed height (cm)
H_o	Critical bed depth (cm)
k_1	Pseudo-first order kinetic constant
k_2	Pseudo-second order kinetic constant (g/mg/min)
K_{AB}	Adam-Bohart constant (mass transfer coefficient l/g/min)
kd	Rate constant
kdi	Intraparticle rate constant ($mg/g/mins^{-0.5}$)
K_f	Freundich isotherm constant
K_L	Langmuir isotherm constant (L/mg)
K_{BD}	BDST rate constant (l/mg/h)
K_{TH}	Thomas model rate constant (ml/h/mg)
K_{YN}	Yoon-Nelson constant (L/h)
LECA	Light weight expanded clay aggregates
M	Mass of adsorbent (g/L)

m	Mass of adsorbent (g)
Mc	Mass of adsorbent in column
Mtpa	Million tonnes per annum
MTZ	Mass transfer zone
n	Absorption intensity
N_o	Adsorption capacity of the bed
Na	Saturation concentration (mg/gl)
Vb	Bed volume to breakthrough
P_{total}	Amount of phosphate passing through the column
p.e.	Population equivalent
PET	Polyethylene terephthalate
PFC	Phosphate sorbed to CaMFCP
PILCs	Pillared clays
P_{MERP}	Most economical rate of phosphate application (kg P/ha)
	Adsorbed phosphate at time t (mg/g)
Q	Volumetric flow rate (l/hr)
q_e	Adsorbed phosphate at equilibrium (mg/g)
qt	Absorption capacity at time T (mg/g)
Qm	Maximum solid phase concentration (mg/g)
Q_{total}	Total phosphate adsorbed by the column
R	Universal gas constant (8.314 J/mol/k)
R^2	Coefficient of correlation
RNA	Ribonucleic acid
RO	Reverse osmosis
SEM	Scanning electron microscope
t	Time
T	Temperature (K)
T_{b50}	Time required for 50% breakthrough
tb	Breakthrough time
te	Exhaustion time
Uo	Superficial velocity (ml/min)
Ur	Absorbent usage rate (g/L)
V	Linear velocity (cm^3/hr)
Vc	Volume of adsorbent in bed
Vb	Breakthrough volume
Ve	Exhaustion volume
Veff	Effluent volume
WM	Wet matter
WWTWs	Waste Water Treatment Works
X_{max}	Fertilizer rate of maximum of yield response

1 Chapter One: Background of Study

The provision of access to clean water has always been a priority for many countries. With the global human population estimated at 7billion (UNFRA 2011 Estimate), there is a greater urgency for the provision of clean drinking water. There have been several arguments that a growth in population will presumably increase water scarcity (Postel 1998, Rijsberman 2006). Water scarcity can be categorised as physical scarcity with a physical absence or low presence of water and economic scarcity which could be attributed to insufficient investment or development of human capacity in the water sector (Kummu *et al* 2010, Rijsberman 2006). Physical water scarcity has been has been experienced in the arid and semi-arid regions of North Africa, Asia, and in parts of middle and southern Africa (Kummu *et al* 2010). The industrialised countries are currently not affected by water scarcity (Koehler 2008).

The availability of clean water can be affected by several factors and these include water pollution. Water pollution can be attributed to different sources, but anthropogenic sources such as industrial discharge, agricultural activity, and sewage discharge constitute a major cause of water pollution (Palma *et al* 2010, Donohue 2006). Pollutants from anthropogenic sources found in wastewater constitute a major channel for this pollution and the pollutants from these anthropogenic sources include BTEX (Nourmoradi 2013, Nourmoradi 2012, Aivalioti 2012), phenolic compounds (Tam *et al* 2009, Hameed 2008), Heavy metals (Feng 2012), PCBs (Prieto *et al* 2010), and nutrients such as nitrogen and phosphorus (Husband *et al* 2012, Kamiyango 2009 and Boujelben 2008). Excessive or elevated nutrients in the water system may enhance the increase in plant based organic matter hence causing eutrophication and algal blooms (Vohla *et al* 2011, Mateus and Pinho 2010, Smith and Schindler 2009, Tam *et al* 2009 and Wang *et al* 2005). Phosphate has been cited as a vital and limiting nutrient in freshwater system and has been suggested that a decrease in phosphate can effectively control eutrophication in coastal and fresh water systems (Mateus and Pinho 2009, Smith 2003 and Tyrrell 1999). Other researchers argue that nitrogen and phosphorus both play roles in the water systems and a reduction in both nutrients is essential in controlling eutrophication (Paerl 2009) and some others citing nitrogen as the limiting

nutrient in which a reduction will bring about a decrease in eutrophication (Lewis and Wurtzbaugh 2008).

Phosphates in wastewater may originate may originate from industrial use of phosphate as a raw material, domestic use of phosphate-containing detergents and runoff from application of phosphate fertilizers to agricultural lands (Kamiyango *et al* 2009). As eutrophication is a major issue, the effective and efficient removal of phosphate during wastewater treatment is crucial. The Urban Waste Water Treatment Directive (91/271/EEC) mandates an 80% reduction in phosphorus level or an effluent phosphorus concentration of 2mg/L P for 10,000- 100,000 p.e and 1mg/L for population estimate greater than 100,000. This directive has led to a decreasing low level of phosphorus in wastewater effluent during treatment through increased government regulatory pressure (Vohla *et al* 2011).

Several methods of phosphorus removal from wastewater have been employed in wastewater treatment. These include chemical precipitation involving the addition of calcium iron and aluminium salts, this is the commonly used and the most effective method of phosphorus removal in wastewater treatment plant (WWTP), and often resulting in high phosphorus removal levels (Clark *et al* 1997 Ebeling *et al* 2003). The major drawbacks of the method are the high volume of sludge produced (Hussain *et al* 2011) and the high cost of chemicals required for dosing (Kahraman *et al* 2012). Biological phosphorus removal has also been used in wastewater treatment (Hascoet and Florentz 1985, Hernandez *et al* 2006, Monclus *et al* 2010) and it depends on a combination of factors such as pH and temperature for effective performance (Jia *et al* 2013, Coma *et al* 2012). Consequently, it has a variable and inconsistent removal rate which may require a complimentary treatment to produce low effluent levels (Morse *et al* 1998, Brix and Arias 2005).

Adsorption of phosphate to suitable materials is becoming a frequently used method of removing phosphate in wastewater treatment. This could be attributed to its advantages over chemical precipitation and biological phosphorus removal. The advantages which include low cost, capacity to produce re-usable solids and simplicity makes this method a favourable option in wastewater treatment (Chen *et al* 2013, Jia *et al* 2013). Fe, Al and Ca are the

elements that are often credited with phosphate sorption and it is assumed that if these elements are present in any medium in a substantial amount, then that medium can be used for phosphate removal (Fondu *et al* 2010).

Several studies have been conducted using various low cost adsorbents such as: alunite (Ozacar 2006, Ozacar 2003), fly ash (Li *et al* 2006, Cheung *et al* 2000), opoka (Brogowski and Renman 2004, Hylander and Siman 2001 and Johansson and Gustafsson 2000), Polonite (Gustafsson *et al* 2008), sand (Vohla *et al* 2008, Farahbakhshazad and Morrison 2003), zeolite (Jiang *et* al 2013, Ning *et al* 2008), blast furnace slag (Johansson and Gustafsson 2000), LWA/LECA (Vohla *et al* 2005, Zhu *et al* 2003, Johansson 1997), ochre (Littler *et al* 2013), red mud (Huang *et al* 2008) and clay (Kaminyango *et al* 2009, Dable *et al* 2008) for the removal of phosphorus from wastewater. The studies have been carried out as a laboratory, small scale constructed wetland or a full scale constructed wetland with the adsorbents used as filter media (Vohla *et al* 2011).

Clay has been studied as a low cost adsorbent in the removal of phosphate from wastewater and different phosphate removal rates has been recorded. In a phosphate removal study done with raw and acid treated clay from Malawi, Kamiyango *et al* 2009 reported that a brick dosage of 60g/L was required for a removal rate of 80% using the acid treated clay while the raw clay only achieved a maximum removal rate of 60%. It was argued that different phosphate removal mechanisms were responsible for phosphate removal at different pH. At a low pH, removal is believed to occur through phosphate adsorption to iron oxide, while the phosphates were precipitated out by metal ions at a higher pH. A separate study conducted on two different clay types showed the uptake mechanism was adsorption to Aluminium oxides and 80% removal was achieved using 5g/L brick dosage (Dable *et al* 2008).

Bricks have been shown to be capable of removing wastewater pollutants. A study on the ability of bricks to adsorb ferrous ions showed that its ability increased after acid treatment (Dehou *et al* 2008). The adsorption characteristics of bricks has been shown to be higher that of sand beds (Selvaraju and Pushpavanam 2009), and this was attributed to the presence metal oxides and hydroxides particularly that of aluminium in the bricks. Another reason for the higher adsorptive property was the greater specific surface area

of the bricks as it leads to a larger reaction and binding sites for phosphates lending credence to the capability of bricks to remove pollutants from wastewater.

The use of bricks in the removal of phosphates from wastewater has been reported. Gurang 2005 reported a 75-98% removal using different bricks types. An analysis of the Fe:Al:Ca ratio showed that the removal best occurred when the ratio was between 1:4:4-1:4:6 with the optimum ratio at 1:4:5. Another study recorded average phosphate removal ratio 70% and it was observed that the phosphate removal decreased with increasing pH and the optimum pH range was between 3 and 4 (Taylor 2005).

Antwi (2009) studied the adsorption capacity of bricks from different geologic regions of the UK and found the bricks that had the best adsorption capacity were from the “Essex” region of the UK. The study showed that adsorption of the bricks occurred within two pH ranges, and was found to increase when pH decreased from 4 to 6 and increased when pH increased from neutral to 12. This finding is consistent with the assumption that different phosphate removal mechanism are responsible for phosphate uptake, at low pH, removal is by adsorption to Al or Fe ions while at high pH, removal is by precipitation by Ca ions (Dable *et al* 2008). The studies also showed that phosphate adsorption also increased with increasing brick dosage and a phosphate solution brick dosage ratio of 1:10 was optimum.

A study on the adsorptive characteristics of bricks showed an increased adsorption with increasing pH with the optimum pH range lies between 4 and 7. Phosphate adsorption was not found to be significantly affected by temperature, but the concentration of the phosphate solution affected the uptake of phosphate as it increased with an increase in phosphate solution (Jia *et al* 2013).

The potential of the bricks to be used as an adsorbent for an extended period was shown in the study by Antwi 2009, by saturating bricks with phosphate solution over a period of time and the bricks dust was found to reach saturation after 43 days.

The generation of huge amounts of bricks from the building and construction industry poses a huge environmental challenge with its disposal. A reuse or recycling of these bricks in wastewater treatment will provide an environment-friendly method of disposal, thus making a valuable resource out of waste. As little study has been conducted in determining the feasibility of the use of bricks in wastewater treatment, an extended study could be done to determine how long it will take to saturate a laboratory scale treatment plant to assess its suitability and feasibility for use as an adsorbent in wastewater.

Using bricks in a dust or powdered form increased the turbidity of the water thus contributing to increased cost of treatment as additional cost will be required to remove the suspended solids from the water. The production of clay pellets which would be suitable for wastewater treatment will address the problem.

The recycling of the phosphate adsorbed by the pellets could be valuable when the disposal cost of the bricks after use in wastewater treatment and the finite global phosphorus pool are considered. The ability of the spent bricks to re-release the adsorbed phosphate could be studied and the potential of using the saturated pellets as a source of slow release fertilizer for plant growth assessed. Studies done on different filter material to evaluate its potential and availability of the adsorbed phosphorus to be used for plant production showed that adsorbed phosphorus in filter materials could be released for use by plant (Hylander *et al* 2006, Hylander and Siman 2001).

1.1 Statement of the Problem

The preceding introduction highlights the potential of fired clay pellets for use as a filter material and adsorbent in wastewater treatment (Jia *et al* 2013, Antwi 2009, Gurang 2005). This study seeks to provide an insight into the effectiveness of the use of fired clay pellets in wastewater treatment by determining the adsorption characteristics and evaluating the potential for its use as a slow release fertilizer.

The study will seek to answer the following questions:

i. What factors will affect the adsorption of phosphate by clay pellets?
ii. How will the composition of the clay pellets affect the adsorption?

iii. What is the mechanism for the removal of phosphate during the treatment?
iv. Which element(s) is primarily responsible for the uptake of phosphate?
v. Can elemental composition be modified to improve removal efficiency?
vi. How will the performance of the clay pellets be affected when used in a fixed bed column study?
vii. Can the adsorbed phosphate be used as a slow release fertilizer?

1.2 Research Aim and Objectives

The aim of this research was to assess the removal of phosphates from wastewater using clay tiles, maximise the phosphate adsorption capacity of the clay tiles, determine the suitability of the use of the clay tiles in a fixed bed column study and evaluate the potential for the production of a slow release fertilizer.

The specific objectives of this research will be to:

i. Investigate the optimum firing temperature for the clay pellets.
ii. Identify the key elements within the parent clay responsible for phosphate adsorption.
iii. Explore ways to optimise the capacity of clay pellets.
iv. Investigate the predominant phosphate removal mechanism.
v. investigate the performance of the clay tiles in a continuous flow column and its applicability in wastewater treatment, and
vi. Investigate the potential for the production of a slow release fertilizer.

1.3 Thesis Outline

This research will start by reviewing existing literature on the different methods used in wastewater treatment for the removal of phosphates. Emphasis will be placed on the use of different clay-based adsorbents in the removal of phosphates from wastewater. The performances of laboratory-scale experimental studies used for phosphates removal from wastewater will also be reviewed.

a. Chapter One will expound the background, problem statement of the study, aim and objectives of the study.
b. Chapter Two will review relevant published literature on studies conducted to assess the treatment of wastewater with particular emphasis on the phosphate removal using different adsorbents. The performance of clay-based materials as adsorbent for phosphate removal form wastewater will also be reviewed in the chapter.
c. Chapter Three will describe the experimental procedure for the laboratory and greenhouse experiments including the experimental design and methodology.
d. Chapter Four will present the data from the laboratory experiments using brick dust as phosphate adsorbing material.
e. Chapter Five will discuss the data from studies utilizing clay pellets fired in the laboratory.
f. Chapter Six will discuss the modification of the pellets using salts of calcium, aluminium and iron.
g. Chapter Seven will discuss the fixed bed column study using the pellets that performed best in the previous chapter.
h. Chapter Eight will discuss the results from the greenhouse trial using spent pellets obtained from the study in from Chapter Eight as a phosphate source
i. The summary and conclusion of the research will be presented in Chapter Nine.

2 Chapter Two Review of Related Literature

2.1 Phosphorus

Phosphorus is a poly atomic multivalent non-metal element with atomic number 15 and atomic weight of 30.974. It belongs to Period 3 and is the second element in Group 15 of the periodic table. The name phosphorus is derived from the Greek word *phosphoros* meaning bringer of light. Phosphorus was discovered by the German Alchemist Hennig Brand through the distillation of urine. It is a very reactive element and it is never found in its pure state in nature.

It commonly exists as three allotropes: white phosphorus, red phosphorus and black phosphorus. White phosphorus is a waxy, transparent solid which sometimes appears slightly yellowish. It has a boiling point of 280^{o}C and a melting point of 44^{o}C. White phosphorus can sublime when stored in a vacuum, if exposed to light. It is phosphorescent, giving off a greenish-white glow. It is the least stable and most reactive of the three allotropes. It self-ignites at 30^{o}C and is insoluble in water, but is soluble in benzene, carbon disulphide and chloroform.

Red phosphorus is a red powder that is produced by heating white phosphorus in the presence of a catalyst to 240^{o}C. It is a non-toxic, odourless, and chemically active allotrope of phosphorus. It is not phosphorescent unlike white phosphorus. Freshly prepared red phosphorus is highly reactive and ignites at temperature around 300 ^{o}C. Prolonged storage or heating produces a more stable product that does not spontaneously ignite in air. Red phosphorus is insoluble in most liquids. It has several uses including the production of safety matches, pyrotechnics, fertilizers, incendiary shells in organic synthesis reactions and certain flame retardants.

Black phosphorus is the least reactive allotrope of phosphorus. It is the most thermodynamically stable allotrope of phosphorus. It exists in three known crystalline state (orthorhombic, rhombohedral, and as a simple cubic). It is insoluble in most solvents, non-flammable and chemically inert (Zhao *et al* 2017). Black phosphorus can be produced by applying extreme pressure to white phosphorus or by using metal salts as catalyst at ambient conditions. It can conduct electricity despite being a non-metal. Black phosphorus can be

exfoliated to produce phosphorene, a graphene-like 2D material with thermal transport and charge properties. Black phosphorus has several uses in optical application and is also used in semi-conductors.

2.2 Uses of phosphorus

One of the most important uses of phosphorus is for the manufacture of ammonium fertilizers. Phosphorus also plays a vital role during the production of steel, and is also used for the production of special glasses and fine chinaware. It is also used in the manufacture of detergents.

Biologically, phosphorus is essential to all living things. It forms the phosphate-sugar backbone of DNA and RNA. It is also used for energy transfer within the cells as part of ATP (adenosine triphosphate).It also forms a major components of bones and teeth in vertebrates and exoskeletons of invertebrates.

2.2.1 Phosphorus and Eutrophication

The presence of excessive or elevated levels of nutrients such as nitrogen and phosphorus in water systems can stimulate an increase in plant based organic matter (Vohla *et al.* 2011, Mateus & Pinho 2010, Smith & Schindler 2009, Tam *et al.* 2009, Wang *et al.* 2005), this increase is commonly referred to as eutrophication is a critical water quality issue for aquatic ecosystems (Mainstone & Parr 2002, Jarvie *et al*. 2006, Paerl *et al.* 2009, Smith & Schindler 2009). Eutrophication produces a brown or green coloration to the water thereby decreasing the 'perceived aesthetic value' of the water body.

Phosphorus (P) has been cited as a vital and limiting nutrient in freshwater system and has been suggested that a decrease in phosphorus can effectively control eutrophication in coastal and fresh water systems (Mateus and Pinho 2010, Smith 2003 and Tyrrell 1999). The limitation factor of a nutrient element is a combination of the biological requirements of the proliferating species and the availability of the nutrients (Elser 2012). Phosphorus has been known to be the primary nutrient responsible for eutrophication in upstream freshwater and this could be attributed to the large watershed areas which are responsible for the capture, accumulation and mobilization of relatively huge quantity of biologically available nitrogen when compared to phosphorus (Wetzel 2001, Paerl 2009) Phosphorus as a nutrient element is generally in short supply in

freshwater systems and river and hence has the highest potential to limit plant growth (Mainstone & Parr 2002).

The concept of “limiting nutrient” is based on the premise that growth in all organisms occur as a result of each cell splitting into two identical cells and all the nutrients must be available in sufficient quantities for this to occur (Hilton *et al.* 2006). The cell multiplication will continue until one of more nutrients fall below a concentration where further growth cannot occur and that nutrient is termed “limited” and subsequent growth is determined by availability of the “limiting nutrient” (Hilton *et al.* 2006).

A reduction in phosphorus has been suggested to control eutrophication in freshwater and marine ecosystems (Paerl *et al.* 2009). Other researchers argue that nitrogen and phosphorus both play roles in the water systems and a reduction in both nutrients is essential in controlling eutrophication (Paerl 2009) and some others cite nitrogen as the limiting nutrient in which a reduction will bring about a decrease in eutrophication (Lewis & Wurtzbaugh 2008).

One of the major effects of eutrophication on aquatic environment is a series of significant changes to an ecological system. An assessment of Lake Victoria in Sub-Saharan Africa indicated that there had been a replacement of diatoms as the prevalent algal plankton by cyanobacteria (Kling *et al.* 2001). Other changes to the ecology of the lake as described by Nyenje *et al.* (2010) include the boom in algal and water-hyacinth production, a collapse of the indigenous fish stock. The collapse in the fish stock was attributed to the loss of deep water oxygen linked to eutrophication. Increased incidence of fish kill and loss of coral reef communities has also been reported by several sources (Smith 2003, Smith & Schindler 2009).

A visible effect of eutrophication can be seen in the proliferation of phytoplankton and aquatic macrophytes (Hilton 2006), this proliferation could result in the development of bloom of harmful nitrogen-fixing cyanobacteria. Increased nutrient loading is often linked to these harmful algal blooms which alter the interactions that exist between organisms and their aquatic environment (Nyenje *et al*. 2010). Toxins which have severe neuro- and hepatotoxic effects in humans and other animals are produced when water

containing these cyanobacteria are consumed (Heisler *et al.* 2008, Conley *et al.* 2009, Smith & Schindler 2009, Arai & Sparks 2007).

Another effect of eutrophication is the depletion of oxygen in the aquatic environment. The accumulation and subsequent decomposition of organic matter leads to loss of oxygen and the generation of harmful gases such as hydrogen sulphide and methane. This anaerobic condition can cause the suffocation of fishes and other invertebrate species (Nyenje *et al.* 2010, Smith & Schindler 2009).

The modification of the ecological integrity of aquatic environment is another effect associated with eutrophication. This could cause significant alteration in the physiology of the phytoplankton communities and their reaction to nutrients variation, and a decline in the composition and diversity of fish and other macro invertebrate species (Nyenje *et al.* 2010).

Eutrophication has also been shown to affect the biogeochemical cycling of organic and inorganic contaminants and intensify the uptake of airborne toxic contaminants by lakes and other water bodies as reported in the study of the behaviour of polychlorinated biphenyls (PCBs) and mercury in lakes in Canada (Smith & Schindler 2009).

2.2.1.1 Phosphorus and Wastewater

Wastewater is the spent or used water from various sources including households, industrial and commercial waste stream, and storm water. Wastewater typically contains about 0.06% dissolved or suspended solids, which is carried in 99.94% water flow. This high water to solid ratio is crucial for the transportation of solid through the sewer system (Drinan and Spellman 2013). The specific constituents of wastewater usually vary in concentration and type dependent on the source of wastewater. The typical composition of an average domestic wastewater is shown in **Table 2.1**.

Table 2.1: Typical composition of untreated domestic wastewater

Some materials have been removed due to 3rd party copyright. The unabridged version can be viewed in Lancester Library - Coventry University.

Source: Drinan and Spellman (2013)

The physical characteristic (colour, odour, and temperature) of domestic wastewater varies, and wastewater volume is usually expressed in cubic metre per person per day. Wastewater volume is an important parameter in design of wastewater treatment plant. Typical volume of wastewater received by a treatment works fluctuates throughout the day, ranging between 50 and 200% of the average daily flow. This is referred to as diurnal flow variation.

Phosphorus in water exists in different forms. Phosphorus in wastewater exists in many different forms. The common forms are orthophosphate, polyphosphates and organically-bound phosphates. Organically-bound phosphates are phosphate compounds with –P-O-C bonds and they constitute about 4% of total phosphorus in wastewater. Organic phosphate in wastewater comes from various sources as the form part of cell walls (phospoholipids), or are constituents of phosphoramides, phosphate esters or phosphor-organic insecticides. Organic phosphate can be degraded biologically and/or chemically to orthophosphates in a water environment.

Polyphosphates are condensed orthophosphates compounds with –P-O-P bonds and are basic constituents of detergents and water softeners. These different forms tend to end up as orthophosphate. Polyphosphates hydrolyze in water to produce soluble orthophosphate while the bacterial decomposition of organically-bound phosphate also produces orthophosphate. Orthophosphate

is the predominant phosphorus species found in wastewater (Hammer and Hammer 2008; Masters and Ella 2008).

2.2.2 Processes and Operations of a Wastewater Treatment Plant

Wastewater treatment usually comprises of primary, secondary or tertiary (advanced) treatment processes depending on the level of purification required. Primary treatment often employs physical processes to remove pollutants that are floatable, settleable or simply too large to pass through simple screening devices. These processes include skimming, sedimentation, and screening. Typically, 35% of biological oxygen demand (BOD) and 60% of suspended solids (SS) is removed during primary treatment. In secondary treatment, the physical processes are enhanced with the employment of micro-organisms for the removal of waste. These microbial actions oxidize organics present in the wastewater and this process occurs under controlled conditions. Secondary treatment can remove up to 90% of BOD and SS. Although the removal of BOD is the primary aim of secondary treatment, about one half of nitrogen and one third of phosphorus are also removed during the process. To reduce phosphorus concentration to consent levels, advanced or tertiary treatment is usually required. A flow diagram of a treatment plant employing primary and secondary treatment is shown in **Figure 2.1**.

Figure 2.1: Schematic of a typical wastewater treatment facility providing primary and secondary treatment
Source: Masters and Ela (2014)

Primary treatment usually begins with screening to remove large floating objects that may clog small pipes or damage the pumps. Screens typically consist of parallel steel bars with gaps between 2 and 7 cm followed by a wire mesh screen with smaller openings. To avoid problems associated with disposal of materials collected on the screens, a comminuter is used to grind the coarse material to small pieces that can be left in the wastewater flow. The wastewater then flows into a grit chamber where heavy sand and grit settle out and onto a primary settling tank (primary clarifier or sedimentation basin) where water flow is reduced to allow SS settle out by gravity. Detention time lasts between 1.5 and 3 hours and allows the removal of up to 40% of BOD and 65% of SS. The solid that settle out is known as primary sludge is usually removed for further processing.

The aim of secondary treatment is to remove BOD and SS beyond what can be achieve by sedimentation. Micro-organisms are employed in either suspended growth or attached growth treatment. In suspended growth treatment, the microbes are suspended and allowed to move with the water; while the microbes in the attached growth treatment are fixed on a stationary surface and water flows past the microbes. Activated sludge, aerated lagoons and membrane bioreactors are the commonly used suspended growth processes.

In activated sludge system, extra oxygen is usually injected into the system and the microbial mass is often increased artificially by the separation and return of a large portion of microbes in the reactor effluent to the activated sludge tank. Oxygen is injected into the bioreactor using diffusers which maintains the aerobic conditions required to facilitate the microbial decomposition of organic matter and also agitates the microbial cells and wastewater. The wastewater-microbial cells mixture is often referred to as mixed liquor. The main advantage of an activated sludge system is the small land area required as there is greater contact between the microbes and wastewater with a given volume of space.

Membrane bioreactor (MBR) is used in suspended growth bioreactors to reduce the size of secondary treatment tanks and improve SS separation efficiency. The MBR draws water from mixed liquor into hollow fibre membranes submerged in activated sludge aeration tanks. MBRs exude nearly all the microbial cells from the secondary effluent; hence sludge mixed liquor must be continuously bled off the aeration tank by a waste activated sludge line to maintain the desired mixed liquor concentration. The efficient removal of bacteria is a major advantage of MBR. Fouling of membranes poses a huge challenge that contributes to the high cost of building and and operating an MBR when compared to other treatment options.

The trickling filter is a commonly used attached growth system in wastewater treatment. A trickling filter consists of a rotating distribution arm that sprays wastewater over a circular bed of plastic packing or other coarse materials (Masters and Ela 2014). Plastic media is preferred as it can be engineered to produce a higher surface area for microbial growth per volume of filter. The gaps between the packing allow the circulation of air required to maintain aerobic conditions. A layer of slime, consisting mainly of bacteria but also including algae, protozoa, fungi, insect larvae, worms and snails, that can absorb and consume waste as it trickles through the bed is used to cover the media. A cross-sectional diagram of a trickling filter is shown in **Figure 2.2**.

Figure 2.2: Cross-section of a trickling filter
Source: Hammer and Hammer 2008

The accumulating slime periodically drops off the packing material into the wastewater where it is removed in the secondary settling tank. Effluent from the filter can be recycled into the incoming flow allowing a more efficient organics removal and preventing the biological slimes from drying out or dying during low flow conditions (Masters and Ela 2014).

Rotating Biological Contactors (RBC) is a variation of the trickling filter. An RBC consists of closely spaced, circular, plastic discs with a diameter of 3.6m that are attached to a horizontal rotating shaft. A biomass film grows on the surface of the discs and comes in contact with wastewater as the RBC rotates and the bottom of each disc is submerged in the tank containing the wastewater to be treated. While rotated out of the wastewater, the microbes are supplied with oxygen and they absorb organics when submerged in wastewater. Higher efficiency treatment can be achieved when the modular RBC units are placed in series. RBCs have an advantage over trickling filters as the solid media can be kept wet at all times under varying load conditions.

2.3 Phosphate Removal from Wastewater

Different methods have been employed for the removal of phosphorus from wastewater in conventional wastewater treatment plant. The methods commonly used are chemical precipitation, advanced biological removal, physical method or the combination of two or more methods.

2.3.1 Chemical Precipitation

The most reliable and well established process for phosphate removal from wastewater is the use of chemical precipitation. It involves the addition of calcium, iron or aluminium salts, and it is the most commonly used and effective method of phosphorus removal in wastewater treatment plant (WWTP), often resulting in high phosphorus removal levels (Clark *et al.* 1997 Ebeling *et al.* 2003). Chemical precipitation as a method for removing phosphates from wastewater several advantages and these include the simplicity of its application (Wang *et al*. 2006). The major disadvantage of chemical precipitation is the production of chemical sludge with its attendant high cost of treatment and final disposal (Bertanza *et al.* 2013). Chemical precipitation of phosphorus can occur either as a pre-treatment, co-treatment or post-treatment.

a. Pre-Treatment:

In pre-treatment, the chemicals are usually added before the primary settling tank (PST). The addition of the salt is followed by rapid mixing, flocculation and primary sedimentation and has a removal efficiency of 90% with the final phosphorus concentration lower than 0.5mg/L. Solids separation is often enhanced by the addition of anionic polymers before flocculation. The advantage of pretreatment is that the same amount of chemical is required for the removal of Biological oxygen demand (BOD) and settled solids (SS). The disadvantages of pre-treatment include the production of more sludge and the use of more chemical than required for co-treatment or post-treatment.

b. Co-Treatment:

Co-treatment or precipitation is suitable for use in activated sludge plant and the chemicals are added directly to the aeration tanks or just before it. This is advantageous because there is a lower need for chemicals in co-treatment as a result of the coagulation-flocculation and adsorption processes occurring in the activated sludge alongside continuous sludge circulation. Co-treatment leads to the creation of best available conditions for coagulation and flocculation as it allows for the choice of

best dosage point. Rapid mixing and flocculation is usually not achieved as the velocity gradient and turbulence levels may not provide the ideal conditions required. This is one of the disadvantages of co-treatment. Another disadvantage is a lower phosphorus removal efficiency of about 85% is obtained and phosphorus concentration in the final effluent could also be higher at about 1mg/L.

c. Post-Treatment:

In post-treatment, chemicals are added after secondary clarification to the inflow of the final settling tank (FST). Post-treatment is usually done in the tertiary or final settling tank and it gives the highest phosphorus removal efficiency of about 95% removal with phosphorus concentration in the effluent lower than 0.5%. The chemical reaction is usually stronger due to the formation of orthophosphates by the microbial activity in previous treatments. The disadvantages of post-treatment include the high cost of treatment plant as big ponds are required, and the ratio of metal ion to phosphorus is usually higher than required for other dosing points.

The various points that could be used for the addition of chemical precipitate are shown in **Figure 2.3**.

Source: Morse *et al.* 1998

Figure 2.3: A diagram showing the various points for addition of chemical precipitants

Salts of multivalent ions of Al, Fe and Ca are most commonly used to precipitate phosphate from the wastewater and the general reaction involved in the precipitation of phosphate in wastewater is represented in **Equation 2.1**:

$$M^{3+} + PO_4^{3-} \rightarrow MPO_4\downarrow \qquad \textbf{Equation 2.1}$$

Where M is a multivalent metal.

The commonly used salts for chemical precipitation are:

i. Iron salts:

In the precipitation of phosphorus from wastewater various forms of iron salts are commonly used. Fe^{2+} and Fe^{3+} forms of iron can react with orthophosphates to form strengite ($FePO_4$) and vivianite $Fe_3(PO_4)_2.8H_2O$ respectively. Fe^{3+} is the principally responsible for the removal of phosphorus; Fe^{3+} forms strong complexes or precipitates with tripolyphosphates and pyrophosphates before adsorbing onto iron (III) hydroxo-phosphates surfaces (Yeoman *et al.* 1988). This precipitation is dependent on the phosphate concentration, Fe^{3+} dosage, pH and temperature.

When Fe^{2+} form is to be used it has to be first oxidized to Fe^{3+}. This oxidation is dependent on different operating conditions such as a high oxygen concentration of 0.15g O_2/ Fe^{2+}g, catalytic activity, pH and the presence of inhibitory material e.g. sulphur (Yeoman *et al.* 1988). The use of Fe^{2+} from the removal of wastewater has been the subject of several studies. Wang *et al.* (2006) achieved a 90.6% reduction in total phosphorus using ferrous sulphate at a Fe:P ratio of 1.3:1. An earlier study achieved an 85% total phosphorus removal using a Fe:P of 1.5:1 (Clark *et al.* 1997).

Stoichiometrically, 1 mol of Fe^{3+} is required to remove 1 mol of phosphorus. However, during the precipitating process, a competing reaction of Fe^{3+} with hydroxyl ions to form hydroxides also occurs. This competing reaction of hydroxyl ions phosphate ions for Fe^{3+} for along with the need to destabilize colloids such as influent organics and iron phosphates, and the reaction of bicarbonate ions to produce iron hydroxides indicates that a higher stoichiometric mass ratio of Fe:P is required (Yeoman *et al.*1988, de Haas *et al.* 2000).

Ferric chloride is most widely used iron salt for chemical precipitation (de Haas 2000), other iron salt such as ferric sulphate, ferrous sulphate and ferrous chloride are also used in precipitating phosphate in wastewater treatment. The Fe^{3+} combines with PO_4^{3-} to form ferric phosphate; the basic reaction is represented in **Equation 2.2**:

$Fe^{3+} + H_nPO_4^{3-n} \leftrightarrow FePO_4 + nH^+$ **Equation 2.2**

The reaction is slow under neutral pH and lime is often added as a pH corrector to enhance coagulation. Zhou *et al*. (2008) achieved over 95% phosphorus removal using ferric chloride as a precipitant.

ii. **Aluminium salts:**

Aluminium sulphate or alum ($Al_2(SO_4)_3.18H_2O$) and aluminium chloride ($AlCl_3$) are also commonly used in WWTP for precipitating phosphates. It requires three times the amount of ferric salts. The basic reaction is represented in **Equation 2.3**

$Al^{3+} + H_nPO_4^{3-n} \leftrightarrow AlPO_4\ nH^+$ **Equation 2.3**

The chemical reaction for the precipitation of phosphates from wastewater using aluminium sulphate is represented as shown in **Equation 2.4**:

$Al_2(SO4)_3.14H_2O + 2PO_4^{3-} \rightarrow 2AlPO_4\downarrow + 3SO_4^{2-} + 14H_2O$ **Equation 2.4**

The quantity of aluminium required for effective precipitation is dependent on the concentration of soluble phosphate and colloids in the wastewater (Yeoman *et al.* 1988). The pH also affects precipitation significantly, for effective removal to be achieved the pH must be high enough to buffer the aluminium sulphate (Yeoman *et al.* 1988). Other factors that influence the precipitation of aluminium phosphates are the metal to phosphate dosage level, calcium and bicarbonate activity of the water

When alum is added to water, it dissociates to produce trivalent Al^{3+} ions which further hydrates to form hexa aquo aluminium ion $(Al(H_2O_6)^{3+}$. These hexa aquo aluminium ions can undergo quick hydrolytic reactions to produce solid aluminum hydroxide $Al(OH)_3$, $[Al(H_2O)_5OH]^{2+}$ as well as other soluble polymeric and oligomeric compounds (Yang *et al.* 2006, Omoike and vanLoon 1999).

Aluminium hydroxide is a strong precipitant for orthophosphates with precipitation occurring almost immediately (de Bashan and Bashan 2004). Removal of phosphates by $Al(OH)_3$ can occur through adsorption on the surface or co precipitation by incorporating soluble phosphorus into its

structure, through the integration of Al-OH-Al and Al-PO_4-Al linkages into an aluminium hydroxypahosphate (Omoike and vanLoon 1999).

High adsorption capacity of phosphates by aluminum hydroxide can be sustained over long periods. Baker *et al (*1998) obtained over 99% phosphate removal after two years using a column packed with activated aluminum oxide, silica sand and limestone. A 55% phosphate adsorption within the first 20 minutes after application was obtained using air-dried alum sludge.

iii **Calcium salts:**

Calcium hydroxide or slaked lime is also used for the precipitation of phosphates. It is commonly used to raise the pH of wastewater primarily to enhance removal of suspended solids. When the pH value increases above 10, the excess Ca^{2+} will react with phosphate to produce hydroxylapatite. The reactions can be summarized as shown in **Equations 2.5 and 2.6**:

$$Ca(HCO_3)_2 + Ca(OH)_2 \rightarrow 2CaCO_3\downarrow + 2H_2O \qquad \textbf{Equation 2.5}$$

$$10Ca^{2+} + 6PO_4^{3-} + 2OH^- \leftrightarrow Ca_{10}(PO_4)*6(OH)\downarrow \qquad \textbf{Equation 2.6}$$

The quantity of lime required is dependent on the pH of the wastewater and pH correction to neutral is often required before subsequent treatment or disposal.

The major drawbacks of precipitation using lime is the high volume of sludge produced (Hussain *et al* 2011) and the cost of chemicals required for dosing (Kahraman *et al* 2012).

2.3.2 Enhanced Biological Phosphorus Removal (EBPR)

Biological phosphorus removal has also been used in wastewater treatment (Hascoet and Florentz 1985, Hernandez *et al* 2006, Monclus *et al* 2010). It involves the use of polyphosphate accumulating organisms (PAOs). Conventional biological nutrient removal (BNR) processes is inadequate for the maximization of nutrients and organics removal as all microbial population, phosphorus accumulating bacteria, autotrophic and heterotrophic bacteria, compete with each other for growth and maintenance under the same operating conditions (Peng *et al.* 2011). As a result, the need to optimize the BNR process to provide favourable growth conditions for the microbes is essential.

Enhanced biological phosphorus removal (EBPR) was developed as a wastewater treatment method based on the selective enrichment of bacteria accumulating inorganic polyphosphate as a building block for their cells (De-Bashan and Bashan 2004). It involves microbial metabolic cycling through several microbial-accumulated polymers such as polyphosphates, poly-β-hydroxyalkanoates (PHA), and glycogen which is induced by the alternation of the incubating conditions of wastewater between an initial carbon rich anaerobic incubation and a carbon deficient aerobic condition (De-Bashan and Bashan 2004). EBPR requires the presence of anaerobic and/or anoxic zone with a high readily degradable chemical oxygen demand before the aerobic zone in an activated sludge system making the anaerobic-aerobic cycle an integral requirement for EBPR (Morse *et al* 1998, de Bashan and Bashan 2004).

PAOs have the ability to take up phosphate in excess over their basic metabolic requirements and store them as intracellular polyphosphate; hence net phosphorus removal is obtained when PAOs are removed in waste activated sludge (Bertanza *et* al 2013, Oehmen 2007). PAOs are micro-organisms that can take up carbon sources such as volatile fatty acids (VFAs) under anaerobic conditions and store them as carbon polymers such as poly-β-hydroxyalkanoates (PHAs) intracellularly (Zhang *et al* 2011). The energy required for the transformation of VFAs to carbon polymer is generated primarily through the splitting of polyphosphates and the release of phosphates from the cells (Oehmen *et al.* 2007).

Under aerobic conditions, PAOs are capable of using the stored PHA as energy source for biomass growth, phosphorus uptake, glycogen replenishment and storage of polyphosphate (Oehmen *et al.* 2007). The uptake of orthophosphates in the aerobic zone is greater than that taken up in the anaerobic zone and the orthophosphates are incorporated into new intracellular microbial polyphosphates. Some PAOs known as denitrifying PAOs (DPAOs) are able to use nitrate or nitrite as electron acceptors in place of oxygen under anoxic conditions as such performing simultaneous phosphorus uptake and denitrification.

Total phosphorus removal have been reported in long term operation of a typical anaerobic-anoxic-aerobic EBPR (Chaung and Ouyang 2000; Merzouki *et al.* 1999) EBPR often produces an inconsistent phosphorus removal rate which may require complimentary treatment to produce low effluent levels (Morse *et al* 1998, Brix and Arias 2005).

2.4 Phosphate Removal through the Use of adsorbents

Adsorption of phosphorus to suitable materials is becoming a frequently used method of removing phosphorus in wastewater treatment. This could be attributed to its advantages over chemical precipitation and biological phosphorus removal. These advantages include low cost, capacity to produce re-usable solid, simplicity make this method a favourable option in wastewater treatment (Chen *et al.* 2013, Jia *et al.* 2013). Fe, Al and Ca are the elements that are often credited with phosphate sorption and it is assumed that if these elements are present in any medium in a substantial amount, then that medium can be used as a substrate for phosphate removal (Fondu *et al.* 2010). Removal of phosphates by adsorption occurs when phosphates in the wastewater is bound to the oxyhydroxides of Al or Fe (Pratt *et al.* 2012, Pratt *et al.* 2007 Arias *et al.* 2001).

Several studies have been conducted using various low cost adsorbents such as: alunite (Ozacar 2006, Ozacar 2003), fly ash (Li *et al* 2006, Cheung *et al* 2000), opoka (Brogowski and Renman 2004, Hylander and Siman 2001 and Johansson and Gustafsson 2000), Polonite (Gustafsson *et al* 2008), sand (Vohla *et al* 2007, Farahbakhshazad and Morrison 2003), zeolite (Jiang *et* al 2013, Ning *et al* 2008), blast furnace slag (Johansson and Gustafsson 2000), LWA/LECA (Vohla *et al* 2005, Zhu *et al* 2003, Johansson 1997), ochre (Littler *et al* 2013), red mud (Huang *et al* 2008) and clay (Kaminyango *et al* 2009, Dable *et al* 2008) for the removal of phosphorus from wastewater. The studies have been carried out as a laboratory, small scale constructed wetland or a full scale constructed wetland with the adsorbents used as filter media (Vohla *et al* 2009).

2.5 Adsorption of Phosphate from Wastewater Using Clay-Based Adsorbents

Clay refers to naturally occurring material composed of fine-grained minerals with a maximum particle dimension of 5 µm that become plastic when wet and hard when dried or fired (Aksu *et al.* 2015; Guggenheim and Martin 1995). Clay

minerals refer to the phyllosilicate minerals or other minerals that impart plasticity to clay (Guggenheim and Martin 1995). They belong to the family of phyllosilicates minerals and are characterised by platy morphology due to the arrangement of atoms in their structure. Clay minerals are differentiated by the presence of layered polymeric silicate tetrahedral sheets linked to Al, Fe, or Mg oxide octahedral sheets (Ismadji *et al* 2015). They are formed by chemical weathering actions involving other silicate containing mineral found on the earth surface.

Clay minerals were initially classified by Grim (1962) based on the differences between the clay minerals into two broad categories as either amorphous or crystalline. The details of the classification are shown in **Table 2.2**.

Table 2.2: The Grim's classification of clay minerals (Murray 2007)

Some materials have been removed due to 3rd party copyright. The unabridged version can be viewed in Lancester Library - Coventry University.

Source: Ismadji *et al* (2015)

2.5.1 Properties of clay minerals

The presence of charges within the clay mineral is responsible for the properties exhibited by the clay minerals (Gupta *et al*. 2009). Swelling and cation exchange capacity are some of the important properties of clay mineral that is attributed to the presence of these charges (Ismadji *et al*. 2015).

2.5.1.1 Charge

Clay minerals commonly carry charges which are the basis for their exchange capacity and swelling properties. These charges are either structural or surface. The structural charges are permanent charges which can occur as a result of

the ion substitution or in some instances due to structural defect (Eslinger and Pevear 1988). These charges charges originate from the interior of the layers in the clay minerals (Ismadji *et al.* 2015). The surface charge on the other hand, occurs as a result of chemical reactions on the surface of the clay minerals or by adsorption of surfactant ions (Eslinger and Pevear 1988). Surface charges originate from the basal surface of tetrahedral sheets for clay minerals with 2:1 layer type, basal surface of the octahedral and tetrahedral sheets for clay minerals with 1:1 layer type clay minerals and the edges of the layers of 1:1 and 2:1 clay minerals (Eslinger and Pevear 1988).

Surface charge is produced as a result of the hydrolysis of Al-OH or Si-OH bonds along the clay lattices and depending on the pH of the solution and silica structure, the net surface charge can either be positive or negative as shown in **Equations 2.6 and 2.7**.

$$SiOH + OH^- \rightarrow SiO^- + H_2O \ (pH > pH_{zpc}) \qquad \textbf{Equation 2.6}$$

$$SiOH + H^+ \rightarrow SiOH^+ \ (pH < pH_{zpc}) \qquad \textbf{Equation 2.7}$$

The pH at which the net surface charge is zero is referred to as zero point of charge (pH_{zpc}). Clay has a higher affinity for cations when the pH is higher than pH_{zpc} as the clay net surface charge is negative, while at pH lower than pH_{zpc} the net surface charge is positive and the attraction for anions is higher. The pH_{zpc} of selected clay minerals is shown in **Table 2.3**

Table 2.3: pHzpc of selected clay minerals

Some materials have been removed due to 3rd party copyright. The unabridged version can be viewed in Lancester Library - Coventry University.

Source: Ismadji *et al.* (2015)

2.5.1.2 *Swelling*

Swelling refers to hydration of clay leading to increase in volume. The swelling capacity of the clay is dependent on the clay mineral present. A 1:1 clay mineral such as Kaolinite has a low cation exchange capacity about 3.3 meq/100g, and is a non-swelling clay that is migratory and easily dispersible. A 2:1 layer clay such montmorillonite, on the other hand, possess a high cation exchange capacity between 90 and 150 meq/100g and will easily adsorb cations which would increase dispersion and degree of swelling (Aksu *et al.* 2015).

2.5.2 Mechanism of phosphate adsorption by clay

Phosphate adsorption on Fe and Al oxides involves ligand exchange mechanism and is believed to be improved by increasing ionic strength (Cornell and Schwertmann 2003). Ligand exchange occurs when anions with specific affinity for metal ions in hydroxylated minerals are absorbed out of proportion to their concentration or behaviour in aqueous solutions. (Goldberg and Sposito 1985). These anions, such as phosphate ions are adsorbed beyond the neutralisation limit of positive surface sites and adsorption on negatively charged surfaces have been known to occur. The mechanism for this as proposed by Rajan *et al.* (1974) suggested the reaction of protons dissociated from anions with surface hydroxyls to form water could lead to the displacement of the formed water by the anions on negatively charged surface.

In ligand exchange, hydroxyl groups present on metal ions of the clay are replaced with phosphate ions in aqueous solution hence capturing the phosphate ions by forming inner-sphere complex on the clay surface and releasing the hydroxyl ions into the solution (Zhu and Zhu 2007). The release of hydroxyl ions leads to an increase in the pH of the solution and this is a crucial indication of the presence of ligand exchange mechanism.

The generalised ligand exchange reaction for phosphate adsorption is expressed in **Equation 2.8**:

$$_{a}SOH_{(s)} + H_nPO^{n-3}_{(aq)} + {}_{n}H^{+}_{(aq)} \leftrightarrow S_aH_nPO_{4(s)} + {}_{n}H_2O + {}_{a-n}OH_{(aq)} \quad \textbf{Equation 2.8}$$

where S is the metal ion in the clay, n ≤ 3 is the degree of protonation of the phosphate ion.

The surface complexes formed by ligand exchange are referred to as inner-sphere complexes as they do not contain water between the surface Lewis acid sites. The phosphate ions and are held together by covalent or ionic bonds (Goldberg and Sposito 1985), and is represented as **Equations 2.9 and 2.10**:

$$\equiv M\text{-}OH + H_2PO_4^- \leftrightarrow \equiv M - (H_2PO_4) + OH^- \qquad \textbf{Equation 2.9}$$

$$2 \equiv M\text{-}OH + HPO_4^{2-} \leftrightarrow M_2 - (HPO_4) + 2OH^- \qquad \textbf{Equation 2.10}$$

Outersphere complexes can also be formed by electrostatic attraction with water retained between the ligand and the exchange sites; the reaction is represented as **Equations 2.11 and 2.12**:

$$\equiv M\text{-}OH_2^+ + H_{2+}PO_4^- \leftrightarrow \equiv M - (OH_2^+)\,(H_2PO_4^-) \qquad \textbf{Equation 2.11}$$

$$\equiv M - OH_2^+ + HPO_4^{2-} \leftrightarrow \equiv M - (OH_2^+)\,(HPO_4^{2-} \qquad \textbf{Equation 2.12}$$

Precipitation is another mechanism which phosphate is removed from wastewater by clay. Precipitation of phosphate occurs when the solubility of the product of the precipitate is exceeded by the product of the solution concentrations of the components of the precipitate (Loganathan *et al*. 2014). The precipitation reaction for Al, Fe and Ca is expressed as **Equations 2.13-2.15**:

$$Al^{3+} + PO_4^{3-} \rightarrow AlPO_4\downarrow \qquad \textbf{Equation 2.13}$$

$$Fe^{3+} + PO_4^{3-} \rightarrow FePO_4\downarrow \qquad \textbf{Equation 2.14}$$

$$5Ca^{2-} + 4OH^- + 3HPO_4^- \rightarrow Ca_2OH(PO_4)_3 + 3H_2O \qquad \textbf{Equation 2.15}$$

2.5.3 Adsorption using Different Clay-based Adsorbent

The efficiencies of removing phosphates by various clay-based adsorbents, the methods used and kinetic and equilibrium models explaining the sorption data are presented in **Table 2.4**.

2.5.3.1 Clay

The use of clay as an adsorbent for water pollutant has been widely reported. Weng *et al.* (2007) investigated the adsorption of Cu (II) using spent activated clay derived from the refining edible oil. Adsorption of Cu (II) ions was reported to occur within 5 min following pseudo-second order kinetics and obeying

Langmuir isotherm with ΔG^o values between -5.73 and -7.26 kcal/mol suggesting a spontaneous process and an adsorption mechanism that was predominantly controlled by specific surface interaction. The high surface area and net negative charges on clay surfaces have been suggested to be responsible for the adsorption capacity for cations exhibited by clay (Gupta *et al*. 2009). It has been suggested that the predominantly negatively charged surface of clays does not allow for substantial anions adsorption (Loganathan *et al.* 2014). This contradicts the result reported by Dable *et al*. (2008), in that study, about 80% phosphate adsorption was achieved using Neiki-Agneby clay and adsorption increased with increasing pH and optimum adsorption was found to occur between pH 3 and 6. However, the presence of alkali and metallic trivalent oxides and hydroxides within the clay was suggested to be responsible for the adsorption.

A lower phosphate adsorption rate was reported using using Kaolinite and bentonite from Iran (Moharami and Jalali 2013). In that study, adsorption capacity was 0.32 and 0.28 mg/g respectively. Bentonite was unaffected by pH while Kaolinite achieved optimum adsorption at pH 2. Adsorption could be described by Langmuir and Freundlich isotherms. Adsorption was suggested to occur through precipitation by Ca^{2+} as shown by the speciation of phosphates.

Precipitation by Ca^{2+} was also suggested as the mechanism of adsorption of phosphate using Kaolinite from Malawi (Kamiyango *et al*. 2009). Adsorption using raw clay was favoured at acidic pH 3, while clay treatment with acid increased the pH range to slightly acidic pH of 5. Acid treatment also improved phosphate adsorption by increasing removal efficiency to 98.5% from 69.7%, adsorption using raw clay was reported to follow pseudo-second order kinetics. Similar rate order was also reported for adsorption using smectite and kaolin from Tunisia with optimum pH for adsorption at pH 5 described by Freundlich isotherm (Hamdi and Srasra 2012). Adsorption capacity (26.38 and 28.01 mg/g) was better when derived from the pseudo-second order kinetic model compared to 0.23 and 0.24 mg/g when derived from pseudo-first order kinetics for kaolinite and smectite respectively. Vyshak and Jayalekshmi (2014) investigating phosphate removal using Kattand clay reported a decrease in

phosphate with increase in pH with optimum adsorption at acidic pH while Mallikarjun and Mise (2013) achieved optimum adsorption at pH 9.

pH is an important factor affecting adsorption of anions in solid-liquid interface. The surface charge on the surface of clay is known to change with pH hence affecting adsorption of phosphate at different pH. (Hamdi and Srasra 2012). Adsorption is believed to be greater at pH lower than pH_{zpc} which is the pH at which the net surface charge is zero.

2.5.4 Modification of clay

Modification is suggested to affect improve adsorption capacity by improving the surface area through its effect on the surface and micropore structure of the clay (Kim *et al.* 1997, Wu *et al.* 2001). Modification of clay could occur through the addition of a metallic ion or through heat and acid treatment among others. Calcination is one of the methods of heat treatment for clay. Calcined Kanuma clay achieved an adsorption capacity of 2.24 mg/g with adsorption decreasing with increase in pH and temperature. Adsorption followed pseudo-second order kinetic and was described by Freundlich isotherm. The inner-sphere ion exchange was suggested as the removal mechanism and adsorbed phosphate could be desorbed using NaoH indicating a possible use of the adsorbed phosphate as fertilizer. Gu *et al* (2013) and Jia *et al.* (2013) reported the potential of brick for use as adsorbent for phosphate removal. Adsorption capacity using novel porous bricks was 3.6 mg/g and adsorption was controlled by the pseudo-first order kinetics and Langmuir isotherm could be used to describe the adsorption (Gu *et al.* 2013). Jia *et al.* (2013) suggested the protonation of Al^{3+} and Fe^{3+} on the surface of the brick as affected by pH was responsible for the variation in adsorption. Coating of bricks with manganese and iron oxide was reported to affect adsorption as a function of pH. Optimum pH was between 4 and 5 using manganese coated bricks and pH 5 using iron coated bricks (Boujelben *et al.* 2008, Boujelben *et al.* 2014). Coating Light Expanded Clay Aggregates (LECA) improved the adsorption of phosphate. Adsorption was found to be higher using Al-coated LECA than Fe-coated LECA at pH higher than 6 (Yaghi and Hartikainen 2013) due to the fact that at higher pH, Al maintains more aqua groups in its coordinated sphere than Fe. Phosphate adsorption was higher at pH 4 using Fe-LECA, this contradicts

results by Boujelben *et al.* (2008) where optimum pH was achieved at pH 5. Phosphate adsorption using Fe is believed to be optimum at pH between 3 and 4.

2.5.4.1 Modification using addition of polyvalent metals

The addition of polyvalent metal to clay improves the adsorption capacity as a result of increase in the cation content. Increased cation would result in the uptake of negatively charged ions. The addition of 10% Al_2O_3 to bentonite improved the adsorption of phosphate from 14 to 18 mg/g (Osalo *et al*. 2013). It was suggested the addition of Al_2O_3 to bentonite increased the increased the surface area and polarity of the bentonite hence increasing adsorption. Langmuir isotherm could be used to describe adsorption. Sips isotherm was used to describe the adsorption of phosphate on Al/Mg-montmorillonite rich bentonite (Chmielewska *et al*. 2013) with maximum adsorption capacity derived from the Sips isotherm as 58.9 mg/g while the adsorption followed pseudo-first order rate order.

2.5.4.2 Pillared Clays

The modification of the adsorbent can be done by interchanging a layer in the structure of the absorbent as is known in pillaring. The polycations of multivalent metals act as “pillars” between the clay layer give rise to modified clay known as pillared clays (PILCs) with specific surface area and permanent porosity, and on calcination the resulting material have metal oxide pillars which prop open the clay sheets, as such exposing the internal surfaces of the clay layers (Shanableh and Elsergany 2013, Baksh 1992). In principle, any metal oxide or salt that can form polynuclear species on hydrolysis can be inserted as pillars (Tian *et al*. 2009) and all layered clay of the phyllosilicate family and other layered clay can be used as host (Baksh *et al* 1992).

Pillared clay has been reported to improve phosphate adsorption (Tian *et al*. 2009, Yan *et al.* 2010, El-Sergany and Shanableh 2012, Shanableh and El-Sergany 2013, Shanableh *et al* 2016). Two-metal pillaring was reported to improve adsorption better than pillaring with a single metal. Tian *et al*. (2009) reported an increase in adsorption from 6.67 to 8.9 mg/g when lanthanum was added with aluminium during pillaring. Adsorption decreased with increase in temperature and followed pseudo-first order kinetic and was described by

Freundlich isotherm. Fe/Al pillared clay (PILC) was reported to perform better than Fe or Al PILC (Shanableh and El-Sergany 2013, Shanableh *et al* 2016). Faster adsorption was achieved using Al-PILC but Al/Fe-PILC recorded higher adsorption (Shanableh and El-Sergany 2013). Optimum adsorption was achieved when equal proportion of Al and Fe was used to prepare Al/Fe-PILC (Shanableh *et al* 2016). However, Yan *et al*. (2010) reported a decrease in the performance of Fe and Al-PILC when combined. The removal efficiency decreased from 99% using Fe-PILC to 97% when Fe-Al-PILC was used.

Different adsorption mechanisms have been suggested for PILCs. Yan *et al*. (2010) suggested adsorption of Fe-Al-PILC occurred through ligand exchange where the surface functional groups of Al-OH and Fe-OH contributed to adsorption through protonation. It was suggested adsorption was chemisorption following pseudo-second order kinetics. Ion exchange was suggested as the mechanism for the adsorption of Fe-PILC, Al-PILC and Fe-Al-PILC where OH^- was exchanged with phosphate. The adsorption of phosphate using Al-PILC and LaAl-PILC was described using the Langmuir isotherm and followed pseudo-first second kinetics (Tian *et al.* 2009). The adsorption was spontaneous and exothermic as confirmed by the relative values of ΔG^o (-18.14 – 16.48 kJ/mol and -19.24 – 18.67 kJ/mol) and ΔH^o (-61.33 and -36.73 kJ/mol) for LaAl-PILC and Al-PILC respectively.

pH is one of the factors affecting adsorption of phosphate using PILCs, adsorption was favoured at acidic pH with optimum adsorption between pH 3 and 4 (Tian *et al*. 2009, Yan *et al.* 2010, El-Sergany and Shanableh 2012, Shanableh and El-Sergany 2013, Shanableh *et al* 2016).

2.5.4.3 Double layered hydroxides (LDH)

Double layered hydroxides (LDHs) also known as hydrotalcite-like-compounds (HTIcs) or anionic clays are clay minerals with hydroxide sheets that has a net positive charge on the layer as result of the partial substituition of trivalent for divalent cations (Das *et. al.* 2006, Zhou *et. al*. 2011). The net positive charge is balanced by intercalated anions and water molecules present within the interlayer space (Das *et. al.* 2006). Positive charges are produced through isomorphous substitution of Mg^{2+} in the brucite-like sheet with multivalent

cations and ionization of surface hydroxyl groups (Loganathan *et al*. 2014). The calcination of LDHs causes the formation of active composite metal oxides through the loss of the layer structure. Subsequent rehydration leads to the reconstruction of the original structure and adsorption of anions occurs via anion intercalation, this process is known as memory effect (Loganathan *et al.* 2014). Reconstruction of calcined LDH precursors using the memory effect is one of the mechanisms for removal of anions by LDH. The other mechanisms are surface precipitation, surface sorption and interlayer anion exchange (Loganathan *et al*. 2014). The presence of a high charge density sheet and an exchangeable anion interlayer makes LDHs excellent adsorbents (Cheng *et al*. 2010).

Mg/Fe LDH was used to investigate the adsorption of phosphate in batch and column studies using artificial wastewater and wastewater effluent (Seida and Nakano 2002). Adsortion was reported to increase with a decrease in pH, this was due to an increase in Mg^{2+} released from LDH into the solution at lower pH leading to higher phosphate removal.

Calcination is reported to improve the sorption of anions using LDHs. An increase in the surface area of Zn-Al LDH from 51.87 to 81.2 m^2/g as calcination temperature increased from 0 to 300^oC before decreasing to 29.28 m^2/g when the calcination temperature increased to 600^oC was reported by Cheng *et al*. (2010). This increase in surface area corresponded with an increase in phosphate adsorption achieving a maximum adsorption of 41.26 mg/g when LDH was calcined at 300^oC. Calcination at 600^oC caused the formation of $ZnAl_2O_3$ which do not partake in the reconstruction of the layered structure, from the mineral phase. Adsorption followed pseudo-second order kinetic and was better described using Langmuir isotherm.

The adsorption of phosphate by LDH can be improved by the release of polyvalent cations. The release of Ca^{2+} from CaFe-LDH was shown to promote the adsorption of phosphate which followed a pseudo-second order kinetics and Freundlich isotherm could also be used describe the process while adsorption using MgAl-NO_3 LDH could be described using Langmuir isotherm but also followed pseudo-second order kinetics (Khitous *et. al.* 2016). Adsorption using Mg/Al-NO_3 LDH was unaffected by pH between pH 3 and 7, this however,

indicated different mechanisms were responsible for adsorption at different pH. Adsorption at lower pH was dominated by electrostatic attraction which occurred between positively charged surface of the LDH and negatively charged phosphate ions. While anion exchange of $H_2PO_4^-$ with NO_3^- present within the interlayer was the major adsorption mechanism at higher pH (Khitous *et. al*. 2016).

Higher valency cations within the interlayer of LDH can increase phosphate sorption due to the production of more positive charges and the ratio of divalent to trivalent cation can have a significant effect on phosphate sorption. Das *et al.* (2006) compared the ability of LDH with Mg-Al molar ratio of 2:1, 3:1 and 4:1 to remove phosphate from artificial wastewater. A decrease in phosphate adsorption with increasing Mg-Al ration was reported. This decrease was attributed to a higher Al^{3+} concentration at lower Mg-Al molar ratio leading to a higher net positive charge on the LDH interlayer compared to samples with lower Al^{3+} concentration at higher Mg-Al molar ratio.

Table 2.4: Characteristics of sorptive removal of phosphate from water by clay-based adsorbents

Adsorbent	Adsorption method Column (C), Batch (B), Field (F), Constructed wetland (CW); Water type wastewater (W), artificial(A), fresh river (R), brackish (Br)	Concentration (mg/L) Initial (I) Equilibrium (E)	Volume of solution-ml (vol), Adsorbent dosage (S) Column diameter (D), bed height (H), Flow rate (Q)	pH/Temp	Adsorption capacity and major findings	Isotherm models used. *Best to fit data	Kinetic models used. *Best to fit data	Adsorption Efficiency (%)	References
Kaolinite (raw)	B; A	I 10	Vol 10 S 40 g/L	2-12/; 20 and 40^{o}C	0.15 mg/g Optimum pH 3	-	Pseudo-first order, pseudo-second order*	69.7	Kamiyango et al. 2009
Kaolinite (acid treated)					Optimum pH 5			98.5	
Neiki-Agneby clay	B; A	I 100	Vol 25 S 200 g/L	3-6				80	Dable et al. 2008
Green Anyama Clay									
Beige Anyama Clay									
Bentonite	B; A	5-250 mg/L	Vol 20 S 25-250 g/L	2-10; 25-45 ^{o}C	0.28 mg/g Sorption was unaffected by pH	Freundlich, Langmuir* isotherm		38	Moharami and Jalali 2013
Kaolinite					0.32 mg/g Optimum sorption pH 2	Freundlich*, Langmuir isotherms		75	
Zeolite					0.37 mg/g			34	

					Optimum sorption pH 6				
Clay	B; A	5 mg/L	Vol 100 S 0.05 g/L	4-10	Sorption increased with pH to pH 9	Freundlich, Langmuir* isotherms	-	-	Mallikarjun and Mise 2013
Kuttanad clay	B; A	2-20 mg/L	Vol 100 S 2.5-25 g/L	2-12 Room temp.	0.61 mg/g Optimum pH 3. Sorption declined as pH increased to 9 before increasing.	Freundlich*, Langmuir isotherms	Pseudo-first order*, pseudo second order models	61-84	Vyshak and Jayalekshmi 2014
Tarbarka clay (Clay T)	B; A	50-1000 mg/L	Vol 30 S 6.67 g/L	3-9	Sorption increased slightly with increase in pH to pH 5 before reducing	Freundlich*, Langmuir isotherms	Pseudo-first order, pseudo second order*	-	Hamdi and Srasra 2011
Gabes clay (Clay G)									
Zeolite					Optimum pH 4-5. Sorption increases steeply as pH increased from 3 to 4 before reducing sharply as pH increased to 7.				
Bentonite	B; A	0.5-5 mg/L	Vol 100 S 10 g/L	Room temp.	14 mg/g	Freundlich, Langmuir* isotherms	-	90	Osalo *et al*. 2013
Bentonite-Alumina					18 mg/g Addition of Al_2O_3 improved sorption			97	
Al/Mg-montmorillonite rich bentonite	B; A	300 mg/L	Vol 30 S 10 g/L	8-8.9 25-60 ^oC	58.9 mg/g	Freundlich, Langmuir, Redlich-Peterson, Sips* isotherms	Lagergren-first order, pseudo-second order*, intra-particle diffusion, film and	-	Chmielewska *et al*. 2013

							pore diffusion models		
Calcined Kanuma clay	B; A	0.5-50 mg/L	Vol 20 S 50 g/L	2-12; 5-35 ^{o}C	2.24 mg/g Sorption decreased with increase in temp. Optimum pH 6. Sorption declined sharply as pH increased to 12.	Freundlich*, Langmuir isotherms	Pseudo-first order, pseudo-second order* models	-	Yang *et al*. 2015
Iron oxide-coated crushed bricks	B; A	5-30 mg/L	Vol 25/250 S 20/40 g/L	2.3-10.8 10-40 ^{o}C	Langmuir Q_m 1.75 mg/g Optimum pH 5 Decrease in sorption beyond pH 5	Langmuir*, Freundlich, isotherms	-	=	Boujelben *et. al.* 2008
Manganese oxide-coated crushed bricks	B; A	5-30 mg/L	Vol 25 and 250 S 20 and 40 g/L	2.3-10.8 10-40 ^{o}C	Optimum pH 4-5. Sorption decreased as pH increased from 5 to 10	Freundlich, Langmuir* isotherms	Pseudo-first order, pseudo second order* models	-	Boujelben *et. al*. 2014
Novel porous bricks	B; A	50-2000 mg/L	Vol 1.2 L	7 25 ^{o}C	3.6 mg/g	Freundlich, Langmuir* isotherm	Pseudo-first order*, pseudo second order, Elovich models	-	Gu *et. al*. 2013
Used bricks	B; A	5-50 mg/L	S 1-60 g/L	2-12 15-35 ^{o}C	Optimum adsorbent dosage 20 g/L. Optimum pH 5. Sorption increased when pH increased from 2 to 5 before declining	-	-	85.3	Jia *et. al*.2013

					sharply as pH increased to 12				
Light Expanded Clay Aggregates (Leca®)	C; A	200 mgP/L	D 30cm H 50 cm Q 0.6L/2hr	-	0.5 kgP/m^3	-	-	15	Johansson 1997
Leca-Opoka mixtire		160 mgP/L			1-1.37 kgP/m^3			52-71	
Lightweight aggregates (LWA)	B; A	0-320 mg/L	Vol 200 S 40	22 °C					Zhu *et. al.* 1997
LECA	B; A	10-200 µgP/L	Vol 50/100 S ½ g/L	3-8; room temp	Sorption was higher when coated with Al or Fe, decreasing with increase in pH. Fe-LECA had better sorption than Al-LECA at pH below 6.	Langmuir	Pseudo-first order* and pseudo-second order	-	Yaghi and Hartikainen 2013
Al-LECA									
Fe-LECA									
Leca Filtralite NR (LWA NR)	B, CW; A	7.7 mg/L	C: vol 500 S: NR 72g/L, MR 146.2 g/L CW: Liquid depth 0.4m H 0.47m	B: 7.5 22 °C	B: LWA MR shown to be better adsorbent CW: 1.1 gP/kg – LWA MR, 0.3 gP/kg LWA NR Life expectancy: Without plants- LWA NR 1 yr, LWA MR 2 yrs. Saturation not reached after six years	Langmuir* and Freundlich isotherms	-	-	Mateus and Pinho 2010
Leca Filtralite MR (LWA MR)									
Fe-pillared bentonite	B; A, W	A 0-50 mg/L W 7.8 mg/L	Vol 50 S: A 2 g/L, W 1-2 g/L	A 5-8 W 7.3;		Freundlich*, Langmuir*,	Pseudo-first order, pseudo	A 92 W 79.5-94	Shanableh and Elsergany 2013

Al-pillared bentonite 2.4				25 °C	Sorption declined with pH. Al bentonite exhibited faster initial adsorption rates, while Fe/Al-Fe bentonites achieved higher adsorption capacity	Temkin isotherms	second order* models	A 88 W 75.6-93.6	
Al-Fe-pillared bentonite A								A 94.4 W 72.4-92.6	
Al-Pillared montmorillonite	B; A	5 and 10 mgP/L	Vol 40 S 2.5 g/L	3-8; 25-35 °C	6.67 mg/g Sorption decreased with increase temp, optimum pH 3-4	Freundlich*, Langmuir and Tempkin isotherms	Pseudo-first order*, pseudo-second order, pseudo-third order models		Tian *et. al*. 2009
La-Al Pillared montmorillonite					8.90 mg/g Sorption decreased with increase temp optimum pH 3				
Al-pillared bentonite	B; A	50 mgP/L	Vol 50 S 2 g/L	5; 25 °C	Sorption increased with decrease in particle size	Freundlich, Langmuir isotherms	Pseudo-first order, pseudo second order*	-	El-Sergany and Shanableh 2012
Al-pillared bentonite	B; A	25-60 mg/L	Vol 25 S 4 g/L	1-10	Optimum sorption pH 3, declined sharply as pH increased	Freundlich, Langmuir isotherm	Pseudo-first order, pseudo second order*models	97	Yan *et al*. 2010
Fe-pillared bentonite					Sorption > 90% at all pH, optimum pH 3.			99	
Fe-Al-pillared bentonite					Optimum sorption pH 3,			97	

					declined sharply as pH increased				
Al-intercalated acid activated bentonite beads: Al-ABn, Al-ABn-AB	B, C; A, W	B: A: 2-60 mg/L W: 4.5 mg/L C: 2.3/4.54 mg/L	B: Vol 50 S 1-5 g/L C: D 1cm Q 0.75/0.2 ml/min	B: A: 3-10 25-65 °C W: 3/7.8 C: 3/5	Optimum pH 3. Sorption declined with increase in pH	Freundlich*, Langmuir isotherms	Pseudo-first order, pseudo second order*models	Al-ABn 98 Al-ABn-AB 95	Pawar *et al*. 2016
Ferric modified Laterite	B; A	5-50 mg/L	Vol 50 S 5 g/L	3-9; 25-45 °C	9-31.36 mg/g Sorption decreased with increase pH	Freundlich*, Langmuir isotherms	Pseudo-first order, pseudo-second order*models	50-90	Huang *et al*. 2013
Electrochemically modified clay	B; A	5-50 mg/L	Vol 50 S 4-20 g/L	2-12; 25-35 °C	Optimum pH 6	Freundlich*, Langmuir isotherms	Pseudo-first order, pseudo-second order* models	-	Yang *et al*. 2013
Chemically modified clay	B; A	5-50 mg/L	Vol 50 S 4-20 g/L	2-12; 15-35 °C	4.01 mg/g Optimum pH 6	Freundlich*, Langmuir isotherms	Pseudo-first order, pseudo-second order* models		Yang *et al.* 2013
Facile prepared magnetic diatomite clay (MDC)	B; A	0-500 mg/L	Vol 20 S 1-25 g/L	2-10; 25°C	MDC 11.8 mg/g, MIC 5.48 mg/g Sorption decreased with increase in pH.	Langmuir*, Freundlich, Dubinin-Radushkevich isotherms	Pseudo-first order, pseudo-second order* models	>90	Cheng *et al.* 2016
Facile prepared magnetic illite clay (MIC)									
Fe-modified Bentonite	B; A	5-250 mg/L	Vol 20 S 25-250 g/L	2-10; 25-45 °C	30.51 mg/Kg Sorption less dependent on pH, increased slightly when pH increased from 8 to 10	Freundlich*, Langmuir isotherms	-	91.04	Moharami and Jalali 2015
Fe-modified Kaolinite					30.90 mg/Kg Sorption dependent on			92.6	

					pH. Higher sorption at acidic pH				
Fe-modified Zeolite					32.70 mg/Kg Sorption increased with increase in pH.			98	
Modified clay mineral	B; A	10-200	Vol 50 S 2 g/L	3-9; 25 °C	4.88-75.98 mg/g Sorption generally increased with increase in pH	-	-	78.1-98.6	Jiang *et al*. 2014
Zenith bentonite	B; A	0.05-5 mg/L	Vol 50 S 0.4 g/L	5-9; 5-35 °C	4.12 mg/g Optimum pH 7, sorption declined as pH became alkaline.	Freundlich, Langmuir isotherm	Pseudo-first order, pseudo-second order*	49	Zamparas *et al*. 2012
Zenith/Fe bentonite					11.15 mg/g Optimum pH 6 and slight decline as pH increased			84	
Phoslock®					11.59 mg/g Optimum pH 6 and slight decline as pH increased			87	
Al_{10} SBA-15 (Al modified mesoporous silicate)	B; A	10 mg/L	Vol 100 S 0.1-0.4 g/L	6.7-7.2; Room temp	710 µmol/g	Langmuir isotherm	Pseudo-second order		Jang *et al*. 2004
Al_{30} SBA-15					315 µmol/g Sorption decreased with increase in added Al				

Mg/Al-hydrotalcite kaolin clay	B; A	50 mg/L	Vol 50 S 8 g/L	2.5-11.5 25-45 ^{o}C	2.49-10.95 mg/g Sorption >90 for pH 3-10	Langmuir*, Freundlich, Dubinin-Radushkevich isotherms	Pseudo-first order, pseudo-second order*	62.62-95	Deng and Shi 2015
La_5 exfoliated vermiculite	B; A	1-100 mg/L	Vol 50 and 200 S 0.1 and 1 g/L	3-11	20.8-71.7 mg/g High sorption recorded between pH 3 and 7 before declining sharply as pH increased to 8. Coexisting anions had no effect.	Freundlich, Langmuir* and Dubinin-Radushkevich isotherm	Pseudo-first order, pseudo-second order*		Huang *et al*. 2014
Mg/Fe layered double hydroxides	B, C; A, W	B 1-1500 mgP/L, C 0.2 mgP/L	B: Vol 10, S 5 g/L; C: H 1mm, Q 20 ml/h	B: pH 2-8 C: pH 7.4	Sorption increased with decrease in pH. Mg was released from LDH, increasing with decrease in pH	Langmuir		C >80	Seida and Nakano 2002
Calcined Mg/Al layered double hydroxides	B; A	30-70 mg/L	Vol 50 S 0.4-5 g/L	2-11	28.32-53.66 mg/g Optimum pH 5, sorption declined steeply as pH increased from 6 to 8. Sorption decreased as temp increased	Freundlich, Langmuir isotherms	First order	>90	Das *et. al*. 2006
MgAl-NO_3 layered double hydroxide	B; W	30-200 mg/L	Vol 50 S 0.5-5 g/L	2-8	Optimum sorbent dosage was 2 g/L.	Freundlich, Langmuir* and Dubinin-	Pseudo-second order	pH 2 90 pH 2-7 >98	Khitous *et. al.* 2016

					Sorption was constant bewtween pH 3 and 8.	Radushkevich isotherms			
Zn-Al layered double hydroxide	B; W	20 mg/L	Vol 50/250 S 0.4 g/L	6.8	49.98 mg/g Sorption increased with increase in calcination temperature to 300 ^{o}C the decreased.	Freundlich, Langmuir* isotherms	Pseudo-first order, pseudo-second order* and Elovich		Cheng *et al.* 2010
Kaolinite Geothite-kaolinite mixture (GKM) Geothite-kaolinite association (GKA)	B; A	0.05-10 mmol/L	Vol 50 S 1 g/L	5; 25 ^{o}C	Sorption GKA >GKM > kaolinite. One-site Langmuir described sorption on kaolinite better while two-site Langmuir described sorption on GKA and GKM better.	Freundlich, Langmuir* isotherms	-	-	Wei *et. a*l. 2013
Red soil/ground burnt patties	C	5 and 15 mg/L	D 4.5 cm; H 10-20 cm Q 2.5-7.5 ml/min		50 % breakthrough time declined with decrease in bed height, increased with increased flow rate and influent conc	-	-	-	Rout *et al*. 2014
Palygorskite Acid treated palygorskite	B; A	5-150 mgP/L	Vol 100, 500; S 1 g/L	4-9	2.5-6.1 mg/g Sorption declined with	Freundlich*, Langmuir isotherms	Pseudo-first order, pseudo-second order,	-	Ye *et al*. 2006

Acid/thermal treated palygoskite					increase in pH. Sorption acid/thermal treated > acid treated > unmodified		Elovich*, power function		
Palygorskite	B; A	5-1000 mg/L	Vol 25 S 20 g/L	3-9; 25°C	Sorption declined with increase in pH. Maximum sorption occurred when palygorskite was heated to 700 °C before reducing	Freundlich isotherm	Pseudo-first* order, pseudo-second order*, Elovich, intra-particle diffusion*		Gan *et al*. 2009
Thermal treated palygoskite							Pseudo-first order, pseudo-second order*, Elovich, intra-particle diffusion		
Phoslock®	B; R, Br	620 µg/L	Vol 40 S 0.6 g/L	7.5-8.9	Sorption declined as pH increased	-	-	-	Reitzel *et al*. 2013
Phoslock®	B; W, Diary W	Diary W: 8.33 mg/L W: 13.02 mg/L	Vol 100 S: Dairy W 0-10 g/L, W 0-8.28 g/L	Diary W 7.67, W 7.38; 25 °C	1:100 phosphate to adsorbent ratio optimum for total phosphate removal from diary effluent, higher ratio required for W.	Langmuir	-	50-100	Kurzbaum and Shalom 2016
Phoslock®	B, F; A, W	B 1 mg/L, F 0.98mg/L	Vol 4L S 0.23 g/L	B 5-9 10-40 °C; F 9	Maximum adsorption capacity increased with increase in initial concentration and pH. Sorption	Langmuir	Pseudo-second order	F 85	Haghseresht *et al*. 2009

					declined with increase in pH from 5 to 9 F: Total phosphorus conc declined sharply during the first three days.				
Bephos™	B; A	0.05-20 mg/L	Vol 50 S 0.4 g/L	5-9; 5-35 ^{o}C	Sorption > 80% reported at all pH studied optimum pH 7. Sorption declined as salinity increased	Freundlich*, Langmuir*, Redlich-Peterson, Temkin isotherms	Pseudo-first order, pseudo-second order*	87-94	Zamparas *et al*. 2013

2.5.5 Man-made products

2.5.5.1 Light-Weight Aggregates (LWA) and Light Expanded Clay Aggregates (LECA)

Light-weight aggregate (LWA) and Light Expanded Clay Aggregates (LECA) are commercially produced clay aggregates primarily used in the construction industry but have found application in wastewater treatment. LECA is an aggregate of burnt clay produced at high temperature around 1200^{o}C in a rotary kiln. During firing, organic compounds present in the clay are burnt off causing the clay to expand creating honeycombed bubble spaces inside the clay while the outside surface melts and is sintered. The resulting pellet is porous, lightweight, and chemically inert with a neutral pH and non-biodegradable (Malakootian *et al.* 2009; Nkansah *et al.* 2012).

Several studies have been conducted to show the effectiveness of LWA/LECA to remove pollutants from wastewater. Johansson (1997) reported a low phosphate removal (14-15%) averaging 0.5 kgP/m^3 when Swedish LECA was used in a column study. However, phosphate sorption increased 1.26 kg P/m^3 when LECA was mixed with Opoka and was suggested the $CaCO_3$ present in Opoka increased the reactivity and phosphate sorption capacity of the LECA. Drizo *et al.* (1999) also reported low phosphate removal when LECA was used in a batch study with a phosphate adsorption maximum of 0.42 g/Kg derived from the Langmuir equation. Similar results were obtained by Vohla *et al*. (2005) for the removal of phosphate using Estonian LWA in a batch study. They reported a phosphate retention capacity between 0.1 and 0.2 g P/mg.

Zhu *et al*. (1997) on the other hand, reported phosphate sorption capacity of 3465 mg P/kg using a US manufactured LWA. Phosphate sorption was shown to be dependent on the chemical properties of the LWA. The metal content of the LWA had a relationship with phosphate sorption with Ca having the strongest correlation. Precipitation of phosphate by Ca was suggested as the predominant removal mechanism when LWA was used.

Mateus and Pinho (2010) studied the performance of two types of LWA in a batch and constructed wetland (CW) system. The estimated design capacity of the CW was 1.1 g p/kg and 0.3 g P/kg and life expectancy of the bed without plants was 2 and 1 years for LWA MR and LWA NR respectively. The pilot scale CW study achieved a maximum

phosphate removal of 93% with the plants contributing only 7% of phosphate removal and bed saturation not achieved after six years.

2.5.5.2 Phoslock®

Phosphate precipitation by lanthanum was reported in the 1970s to be more effective than either aluminium or iron (III) salts over a wide pH range between 4.5 and 8.5 (Melnyk *et al*. 1974; Recht *et al*. 1970 in Haghseresht *et al*. 2009). Lanthanum precipitates phosphate in the reaction expressed in **Equation 2.16**:

$$La^{3+} + PO_4^{3-} \rightarrow LaPO_4 \qquad \textbf{Equation 2.16}$$

The La-PO_4 complex can form at low pH levels and is highly insoluble. The solubility of La-PO_4 complex is reported to reduce with an increase in temperature with a solubility product of up to K_{sp} = -26.40 at 70 ^oC, where K_{sp} is the solubility product (Firsching and Brune 1991).

The use of lanthanum in phosphate removal can be toxic to aquatic life depending on the concentration and application rates (Douglas *et al*. 2004). The incorporation of lanthanum into clay mineral, to overcome the toxic effect to aquatic life, produced a lanthanum-modified bentonite called Phoslock®. Phoslock® was developed in the late 1990s by the Commonwealth Scientific and Industrial Research Organisation (CSIRO) Australia.

Studies have shown a decrease in phosphate adsorption with increase in pH using Phoslock®. Haghseresht *et al.* (2009), reported a decline in phosphate adsorption as the pH increased from 5 to 9. Reitzel *et al.* (2013) also reported a decrease in phosphate adsorption as the pH increased from 7.5 to 8.9. The reduced adsorption at higher pH was attributed to the presence of insoluble $La(OH)_3$ formed at higher pH against $La(OH)^+$ being the most likely species formed between pH 5 and 7.

The theoretical adsorption capacity of Phoslock® is about 10.6 mgP/g, although an adsorption capacity of 14.4 mgP/g (Kurzbaum and Shalom 2016) and 11.06 mgP/g using Phoslock® modified bentonite (Zamparas *et al*. 2012) have ben reported. Haghseresht *et al.* (2009) obtained a maximum adsorption capacity that increased from 9.54 to 10.54 mg/g as the temperature increased from 10 to 30 ^oC. Adsorption of phosphate using Phoslock® followed the pseudo-second order kinetic.

2.6 Adsorption Theory

Adsorption is a process where a liquid or gas accumulates on the surface of a liquid or solid (also known as adsorbent), forming a film or adsorbate (Zamparas 2015). It can be defined as the enrichment of chemical species from a fluid phase on the surface of a liquid or a solid (Worch 2012). Adsorption usually occurs between two phases, specifically liquid-liquid, gas-liquid, gas-solid or liquid-solid interphases. Adsorption occurs in most natural systems and has wide industrial applications. Solid surfaces are usually characterized by active energy-rich sites that can interact with solutes in the adjacent fluid phase due to their specific spatial or electronic properties (Worch 2012). Interactions on the surface of the adsorbent occur due the active forces within the phase of surface boundaries resulting in characteristic boundary energies. Typically, active sites are energetically heterogeneous. The basic terms of adsorption is illustrated in **Figure 2.4**.

Figure 2.4: Basic terms of adsorption
Source: Worch 2012

One of the driving forces for adsorption is the affinity of the solute for the solid as a result of electrical attraction between the solute and the solid; hence adsorption occurs via van der Waals attraction (Cecen and Aktas 2012). This type of adsorption is termed physical adsorption or physisorption where intermolecular attraction occurs between favourable energy sites and no exchange of electrons is involved.

Chemical adsorption or chemisorption occurs where there is an exchange of electrons between specific surface sites and the solute molecules, forming a chemical bond. Chemically bonded adsorbed molecules cannot move freely on the surface or within the interphase.

1.1.2 Factors affecting Adsorption

2.6.1.1 Contact time

Contact time is one of the factors affecting adsorption of phosphate. Adsorption typically increases with increasing time. Uptake is usually rapid at the initial stages of adsorption as a result of a large concentration gradient between the fluid and available adsorption sites. As the adsorbate is taken out of solution, the rate of adsorption decreases until equilibrium is achieved. Contact time required to attain equilibrium varies between adsorbents and pollutants. Adsorption of phosphate by most adsorbents typically achieves equilibrium within 60 minutes. Adsorption of phosphate by calcite attained equilibrium after 15 minutes of contact (Karageorgious *et al.* 2007); while equilibrium was achieved after 30 minutes using iron hydroxide-eggshell waste (Mezenner and Bensmaili 2009). Slower phosphate uptake by adsorbents have also reported. Dable *et al.* (2008) reported the adsorption of phosphate using crude clays achieved equilibrium after 4 hours. Equilibrium was also achieved after 4 hours using layered double hydroxides (Das *et al*. 2006). Adsorption processes that occur in less than one hour are generally considered to be more favourable than those requiring longer contact times.

2.6.1.2 pH

pH of the solution is one of the factors that affect the adsorption of anions. The surface charges of clay adsorbents are dependent on the pH of the solution. At lower pH, the clay surface would have a net positive charge and its attraction to anions will increase leading to higher adsorption of anions. The net negative charge at higher pH results in a reduction in the adsorption of anions. The adsorption of phosphate has been studied at different pH. Kamiyango *et al.* (2009) obtained maximum adsorption of phosphate using raw kaolinite at pH 3. Similar results were also obtained by Huang *et al.* (2015) using Zr/Al pillared montmorillonite and Vyshak and Jayalekshmi (2014) using Kuttanad clay. High phosphate adsorption was obtained at pH between 5 and 5 using calcined Kanuma clay (Yang *et al.* 2015), used brick (Jia *et al.* 2013), acid treated kaolinite (Kamiyango *et al.* 2009), and iron oxide coated crushed bricks (Boujelben *et al.* 2008). Other studies have shown the adsorption of phosphate was unaffected by the pH of the solution. Deng and Shi (2015) reported high phosphate

sorption (over 90%) for pH 3 to 10 using Mg/Al hydrotalcite kaolin clay, while Moharami and Jalali (2013) reported phosphate adsorption using bentonite was unaffected by pH when studied at a pH range between 2-10.

The various results on the effect of pH on the adsorption of phosphates indicate its complicated nature. Most studies suggest the optimum pH for the adsorption of phosphate is between 4 and 7 (slightly acidic to near neutral).

2.6.1.3 Initial Concentration

Adsorption efficiency typically decreases with increase in the concentration of the adsorbate while the amount adsorbed increase with initial concentration. The removal efficiency of Kuttanad clay decreased as the concentration of phosphate in the solution increased from 2 to 20 mg/L (Vyshak and Jayalekshmi 2014). The amount of phosphate adsorbed using $ZnCl_2$ activated coir pith carbon increased from 1.45 to 4.15 mg/g as the concentration of phosphate increased from 10 to 40 mg/L (Namasivayam and Sangeetha 2004).

2.6.1.4 Temperature

Adsorption usually involves specific reactions between the adsorbent and adsorbate, therefore the effect of temperature is not the same for all adsorption processes (Cecen and Aktas 2012). Most adsorption reactions are endothermic with adsorption increasing with increasing temperature. Increase in temperature is suggested to increase the rate of diffusion of the adsorbate to the active sites of the adsorbent leading to increased adsorption (Cecen and Aktas 2012). Namasivayam and Sangeetha (2004) using $ZnCl_2$ activated coir pith carbon reported an increase in the adsorption of phosphate as the temperature increased for 35 to 60 ^{o}C. The study conducted by Das *et al.* (2006) contradicted that study. In the study, adsorption of phosphate decreased as the temperature increased from 30 to 70^{o}C when layered double hydroxide was used.

2.6.1.5 Surface area

The extent of adsorption is usually considered as a function of total available active sites on the adsorbent. This means that a larger surface area would enhance adsorption. Specific surface area refers to the proportion of the total surface area that

is available for adsorption. Particle size and porosity are two properties that influence the total surface area of an adsorbent. The more porous or finely divided an adsorbent is, the higher the adsorption per unit mass of the adsorbent (Cecen and Aktas 2012). The presence of bulges or cavities on or within the increase the porosity, and consequently, the surface area of the adsorbent.

2.6.1.6 Effect of Competing Anions

Wastewater contains different ions which could impacts its treatment, as there might be competitive adsorption between phosphates and other anions that co-exists in wastewater. These anions include, NO_3^-, CO_3^-, Cl^-, F^-, SO_4^{2-} and SeO_3^{2-}. It is suggested that divalent anions have a more disruptive effect on phosphate adsorption than monovalent anions Das *et al* (2006) studying the effect of two monovalent anions (NO_3^- and Cl^-) and two divalent anions (SO_4^{2-} and SeO_3^{2-}) on the adsorption of phosphate by LDH reported about 40 and 25% decline in phosphate adsorption when SeO_3^{2-} and SO_4^{2-} were introduced to the system. A 10 and 15% reduction in phosphate adsorption was reported in the same study when NO_3^- and Cl^- was added.

The presence of SO_4^{2-} was also reported to reduce the adsorption of phosphate by Al pillared clay from 92.2 to 78% (Tian *et al.* 2009). The presence of Cl^- has also been shown to compete with phosphate ions for adsorption sites thereby reducing adsorption of phosphate (Chen *et al.* 2002).

1.1.3 Kinetic Models

2.6.1.7 Pseudo First Order Kinetics

The pseudo-first order kinetic model explains the relationship between the rate the sorption sites of the adsorbents are occupied and the number of unoccupied sites. Pseudo-first order kinetic model is based on the assumption that the rate of occupation of the adsorption sites is proportional to the number of unoccupied sites (Ghasemi *et al.* 2012). It is defined using the Lagergreen equation as shown in **Equation 2.16**:

$$\ln (q_e - q_t) = \ln q_e - (k_1 t) \qquad \textbf{Equation 2.16 (Zhou } \textbf{\textit{et al.}} \textbf{ 2013)}$$

Where

q_e and q_t is the amount of phosphate adsorbed at equilibrium and time t (mins)
k_1 is the rate constant of adsorption (min^{-1}).

The linear plot of ln (qe-qt) against time was used to determine the rate constant k_1,

2.6.1.8 *Pseudo Second Order Kinetics*

The pseudo-second order kinetic is used to describe the dependency of the adsorption capacity of the adsorbent on time and can be determined from the equilibrium adsorption capacity and rate constant. The model is based on the assumption that chemical sorption involving valence forces through sharing or exchange of electrons between phosphate ions and the adsorbent may be a rate limiting step. Pseudo-second order model is used to determine initial rate of adsorption and half time adsorption. The pseudo-second order kinetic can be expressed as shown in **Equation 2.17**

$$t/qt = 1/k_2q_e^2 + t/q_e$$ **Equation 2.17 (Zhou *et al.* 2011)**

Where
q_t and q_e is the amount of phosphate adsorbed at equilibrium and time t (mins)
And k_2 is the pseudo-second order rate constant (g/mg/min)

The linear plot of t/qt against time is used to determine q_e and k_2 from the slope and intercept respectively.

2.6.1.9 *Elovich Kinetic Model*

Elovich kinetic model has been used to chemisorption of gases onto heterogeneous surfaces and solid systems and it is now used to study the removal of pollutants from aqueous solutions (Yuan 2015). It is used to describe second order kinetic with the assumption that the solid surface has heterogeneous energy but do not propose any mechanism for adsorption (Mezenner and Bensmaili 2009). The model assumes that adsorption sites increase exponentially with adsorption implying a multilayer adsorption. Elovich kinetic model is used to determine adsorption rate and desorption rate. The Elovich kinetic model is represented as shown in **Equation 2.18**:

$$\frac{dq}{dt} = a_e^{-\alpha q}$$ **Equation 2.18** (Qiu *et al.* 2009)

Where q is the amount of amount of phosphate adsorbed at time t

a is the adsorption constant

α is the initial rate of adsorption (mg/g/min)

Integration of **Equation 2.19** assuming the boundary conditions of q= 0 at t= 0 and q= q at t= t yields

$$q = \alpha \ln(a\alpha) + \alpha \ln t \qquad \textbf{Equation 2.19}$$

The linear form of **Equation 2.19** is **Equation 2.20**:

$$qt = \frac{ln\alpha b}{b} + \frac{1}{b} \ln t \qquad \textbf{Equation 2.20 (Yakout and Elsherif 2010)}$$

Where α is the initial rate of adsorption (mg/g/min), and

b is related to the extent of surface coverage and activation energy for chemisorption (g/mg)

A plot of qt against ln t yields a straight line with α and b determined using the slope and intercept respectively.

2.6.1.10 The Bangham's Kinetic Model (Pore Diffusion Model)

The Bangham's kinetic model is used to evaluate the dominance of pore diffusion in the adsorption process (Subha and Namasivayam 2008). The Bangham's kinetic model assumes that pore diffusion is the only rate controlling step during adsorption (Yaneva *et al.* 2012). It is expressed as **Equation 2.21**:

$$\textbf{Log Log} \left[\frac{Co}{Co - qtM}\right] = \textbf{Log} \left[\frac{ko}{2.3.3V}\right] + \alpha \textbf{Log t} \qquad \textbf{Equation 2.21}$$

Where C_o is the initial concentration (mg/L)

V is the volume of the solution (ml)

M is the mass of the adsorbent (g/L)

qt is the amount of phosphate adsorbed at time t, and

k_o and α are constants

The plot of Log Log [C_o/ (C_o- Mqt)] against Log yields a straight line and k_o and α were determined from the slope and intercept

2.6.1.11 *Intraparticle Diffusion*

The diffusion mechanism can be explained using the intra particle diffusion theory proposed by Weber and Morris (1963), the model in **Equation 2.22**:

$$q_t = K_{di}\sqrt{t} + C_i \qquad \textbf{Equation 2.22 (Acelas } \textbf{\textit{et al.}} \textbf{ 2015)}$$

Where K_{di} is the intra particle rate constant (mg g^{-1} $mins^{-0.5}$), C_i is the intercept, nd *t* is time (mins)

The model is based on a multi-step uptake process. The first step involves the mass transfer of phosphate molecules from the bulk phosphate solution to the clay surface, while the second step is the intra particle diffusion of phosphate molecules on the tiles (Zhou, Jiang and Wei 2013).

The plot of the adsorbate uptake qt (mg/g) against the square root of time (minutes) $t^{1/2}$ resulted in a linear relationship and K_{di} and C values were obtained from this plot.

2.6.2 Adsorption Isotherm

2.6.2.1 *Langmuir Isotherm*

The Langmuir model is used to describe a monolayer sorption on sets of distinct localized sorption sites. It was initially used to describe the adsorption of gases onto activated carbon but has also been used to generally describe the adsorption of adsorbates onto adsorbents. It is based on the following assumptions:

i) There is a fixed number of available adsorption sites on the surface of the adsorbent;
ii) No transmigration of the adsorbate occurs in the plane of the surfaces;
iii) There is uniform energy of monolayer sorption onto the adsorbent surface and each site can hold a maximum of one molecule;
iv) There is no interaction between the sorbed molecules;
v) All sorption sites are alike on a microscopic scale (Balouch *et al.* 2013).

The linear for of the Langmuir isotherm is represented as follows in **Equation 2.23**:

$$\frac{Ce}{Cads} = \frac{1}{Qb} + \frac{Ce}{Q}$$ **Equation 2.23** **(Balouch *et al.* 2013)**

Where C_e is the equilibrium concentration of phosphate (mg/L)

C_{ads} is the amount of phosphate sorbed at equilibrium

b is the sorption constant (L/mg) at a given temperature, related to the energy of sorption

And Q is the maximum sorption capacity (mg/g)

The Langmuir isotherm model is represented by **Equation 2.24**:

$$qe = \frac{QmKLCe}{1+KLCe}$$ **Equation 2.24** **(Dada *et al.* 2012)**

Where C_e is the equilibrium constant (mg/L)

q_e is the amount of phosphate adsorbed equilibrium (mg/g)

Q_m is the maximum monolayer coverage capacity (mg/g)

K_L is the Langmuir isotherm constant (L/mg)

A dimensionless constant or separation factor (R_L) is represented by **Equation 2.25**:

$$R_L = \frac{1}{1+KLCo}$$ **Equation 2.25** **(Foo and Hameed 2010)**

R_L is used to describe the favourable nature of the adsorption process where $R_L>1$ is unfavourable, $R_L= 0$ is linear, $0<R_L<1$ is favourable and $R_L=0$ is irreversible (Foo and Hameed 2010; Yuan *et al.* 2015). A plot of 1/qe against $1/C_e$ yielded a straight line graph with the values of Q_m and K_L calculated from the slope and intercept respectively.

2.6.2.2 Freundlich Isotherm

The Freundlich isotherm is used to describe the relationship solid phase capacity based on multilayer adsorption and equilibrium liquid (Balouch *et al.* 2013). This isotherm is based on the assumption that adsorption occurs on heterogeneous surfaces and active sites with different energy (Boujelben 2013). The linear form of the Freundlich isotherm model is represented as follows in **Equations 2.26 – 2.27**:

$$\ln Q = \ln K_f + \frac{1}{n}\ln C_e$$ **Equation 2.26 (Boujelben 2013)**

The isotherm is expressed as:

$$Q_e = K_f C_e^{1/n} \quad n > 1$$ **Equation 2.27 (Hutson and Yang 1997; Dada *et al.* 2012)**

Where K_f is the Freundlich isotherm constant

n is adsorption intensity

C_e is the equilibrium concentration of adsorbate (mg/L)

Q_e is the amount of phosphate adsorbed at equilibrium (mg/g)

The linear form of **Equation 2.28** is expressed as

$$\text{Log } Q_e = \text{Log } K_f + \frac{1}{n} \text{Log } C_e$$ **Equation 2.28 (Dada *et al.* 2012)**

The plot of Log qe against Log Ce yielded a straight line and n and K_f was calculated from the slope and intercept.

Where K_f and *n* are Freundlich constant and represent the adsorption capacity and adsorption intensity respectively. K_f and *n* are derived from the intercept and slope of a graph of ln Q against $\ln C_e$

Where Q is the sorbed phosphate and
C_e is the equilibrium concentration of phosphate in the solution

2.6.2.3 Tempkin Adsorption Isotherm

The Tempkin adsorption isotherm model was initially used to describe the adsorption of hydrogen onto platinum electrodes in an acidic solution (Foo and Hameed 2010). The isotherm contains a factor that considers interaction between adsorbate (Dada *et al.* 2012). The model is based on the assumption that heat of adsorption of all molecules in the layer will decrease linearly rather than logarithmic with coverage, when extremely low and high concentration are not considered (Tempkin and Pyzhev 1940; Foo and Hameed 2010, Dada *et al.* 2012). It also assumes that there is a uniform distribution of bounding energy up to some maximum bonding energy (Inyinbor *et al.*

2016). The heat of adsorption is characterized by uniform distribution of binding energies up to some maximum binding energy Foo and Hameed 2010). The model is represented as shown in **Equations 2.29 – 2.32**:

$$q_e = \frac{RT}{b} \ln (A_T C_e) \qquad \textbf{Equation 2.29 (Tempkin and Pyzhev 1940; Dada 2012)}$$

$$qe = \frac{RT}{bT} \ln A_T + \left[\frac{RT}{b}\right] \ln C_e \qquad \textbf{Equation 2.30}$$

$$B = \frac{RT}{bT} \qquad \textbf{Equation 2.31}$$

$$qe = B \ln A_T + B \ln C_e \qquad \textbf{Equation 2.32}$$

Where A_T is Tempkin isotherm equilibrium binding constant (L/g)

B_T is the Tempkin isotherm constant

R is universal gas constant (8.314 J/mol/K)

T is temperature at 298K

And B is constant related to heat of sorption (J/mol)

A_T and b_T was determined from the intercept and slope of the plot of qt against ln t.

2.6.2.4 Dubinin-Radushkevich Adsorption Isotherm

Dubinin-Radushkevich adsorption isotherm is used to describe the adsorption mechanism with a Gaussian energy distribution on to a heterogeneous surface (Dabrowski 2001; Dada 2012). Dubinin-Radushkevich adsorption isotherm does not assume homogeneous surface or constant sorption potential and but helps to determine the apparent energy of adsorption (Al-Anber 2011). The model is expressed as shown in **Equation 2.33**:

$$\ln qe = \ln q_s - \beta\varepsilon^2 \qquad \textbf{Equation 2.33}$$

Where qe is the amount of phosphate adsorbed at equilibrium (mg/g)

q_m is the theorethical isotherm saturation capacity (mg/g)

β is the Dubinin-Radushkevich isotherm constant (mol^2/kJ^2)

ε is the Polanyi potential, which is equal to

$$\varepsilon = RT \ln\left(1+\frac{1}{Ce}\right)$$ **Equation 2.34**

Where is the universal gas constant (8.314 J/mol/K)

The model is usually applied to distinguish the physical and chemical adsorption with its mean free energy, E (kJ/mol) which is the energy required to remove a molecule of adsorbate from its location in the sorption site to infinity (Foo and Hameed 2010). E is computed from **Equation 2.35**:

$$E = \left[\frac{1}{\sqrt{2\beta}}\right]$$ **Equation 2.35**

2.7 Phosphorus retention in filter materials and suitability for plant production

2.7.1 Desorption of phosphates

Desorption studies have been carried out to assess the re-usability of adsorbents and recovery of adsorbed phosphates. Desorption involves the immersion of spent adsorbents in acidic or alkaline solution, usually HCl or NaOH solution, or distilled water with different pH. Das *et al.* (2006) obtained a maximum desorption of 63% of adsorbed phosphate by spent LDH when 0.1M NaOH solution was used. Namasivayam and Sangeetha (2004) reported a desorption rate of around 30% for pH2 and 50% for pH 11 of adsorbed phosphate using spent $ZnCl_2$ activated coir pith carbon. Xia *et al.* (2016) obtained a desorption rate of 92.46, 93.04 and 98.84% in 5, 10, and 15% w/v NaOH solution using spent $MnFe_2O_4$ nanoparticles.

Competition between phosphate ions and OH^- for the adsorption sites is suggested to be one of the mechanisms for the release of adsorbed phosphate. Competition between phosphate ions and OH^- for the adsorption sites would lead to the release of phosphate ions from the surface of the adsorbents (Xia *et al*. 2016). An increase in the pH of the desorption solution indicates the adsorption of OH^- from the solution.

The ability of spent adsorbent to desorb adsorbed phosphates indicates the potential for the recovery of the phosphates or regeneration of adsorbed phosphates. The assessment of the plant availability of adsorbed phosphate is an important criterion on the feasibility of the use of the phosphate as plant fertilizer.

2.7.2 Recovery and Plant Availability of Adsorbed Phosphate

The regeneration of the phosphate adsorbed by the bricks could valuable when considering the disposal cost of the bricks after use in wastewater treatment and the finite global phosphorus pool. The potential of the bricks to re-release the adsorbed phosphate could be studied and the feasibility of using the spent bricks as a medium for plant growth assessed. Studies done on different filter materials to evaluate the potential and availability of the sorbed phosphorus to be used for plant production showed that adsorbed phosphorus in filter materials could be released for use by plant (Hylander *et al* 2006, Hylander and Siman 2001). Kvarnstrom *et al.* (2004) showed that substrates from two infiltration basins used in phosphorus adsorption studies could be used as nutrient source in agriculture even though the phosphorus accumulation in the materials were low and supplementary fertilization will be required.

Another study by Cucarella *et al.* 2008 carried out to investigate the plant availability of adsorbed phosphate on 3 different substrate showed that the substrates could be used as source of plant nutrition as yield was increased and soil fertility improved through increasing pH, cation exchange capacity and availability of nutrients.

The fertilizer effectiveness of recovered phosphate in terms of uptake could be similar to commercial fertilizer even though the recovered phosphates have lower solubility in water (Karunanithi *et al*. 2015). The biomass of total phosphate uptake can be used to compare the performance of adsorbed phosphates to commercial fertilizers.

Hylander *et al.* (2006) obtained a relative fertilizer effectiveness of 76% using phosphate adsorbed to crystalline steel-works furnace slag as a fertilizer source for the production of barley. Bauer *et al.* (2007) compared the effectiveness of calcium phosphate recovered from swine wastewater with triple super phosphate for the production of ryegrass and obtained similar results of 4.8 g/pot for both sources with the control producing 4.2 g/pot. Yao *et al.* (2013) obtained an 85% germination rate compared to 53% for control when phosphate adsorbed to engineered biochar was used as a source of fertilizer.

2.8 Summary

This chapter identified the problem associated with excess phosphorus in the environment which provides the basis of this research. The current methods of treating phosphorus in wastewater and their limitations were discussed.

The theories supporting the concepts investigated in this study was also described. These include the theories relating to adsorption, isotherms, kinetic modelling and fixed bed column study.

Previous studies on adsorption as a method for the removal of phosphate in wastewater was also discussed. There was an emphasis on the use of clay and clay-based adsorbents for phosphate removal. The factors that could influence the adsorption of phosphate were highlighted.

The use of fired clay pellets for the removal of phosphates has not been fully explored and will provide an aspect of this research. Ways of developing a method of pelletization that will be suitable for use in wastewater treatment will also be explored. This thesis will also explore ways of developing a “green” approach to the re-use of the pellets used in this study for a greenhouse experiment.

3 Methodology

This chapter presents details of the materials and experimental procedures utilized during the process of this research.

3.1 Materials

3.1.1 Analytical Reagents

Potassium dihydrogen phosphate (KH_2PO_4), was used as the source of orthophosphate throughout this study. Other reagents used include concentrated sulphuric acid (H_2SO_4 ρ=1.84g/ml), concentrated nitric acid (HNO_3 ρ=1.51 g/ml) Ammonium molybdate $(NH_4)_6Mo_7O_{24}.4H_2O$, Hydrazinium sulphate ($N_2H_6SO_4$), Tin (II) chloride $SnCl_2.H_2O$, Sodium Hydroxide (NaOH), Disodium ethylene diamine tetra-acetic acid (Na_2-EDTA $C_{10}H_{12}O_8N_2Na_2$), Iron (II) sulphate heptahydrate ($FeSO_4.7H_20$), Alumimium sulphate hexadecahydrate ($Al_2(SO_4)_3.16H_2O$), Calcium carbonate ($CaCO_3$), Potassium nitrate (KNO_3), Calcium nitrate $Ca(NO_3)_2.4H_2O$, Magnesium sulphate ($MgSO_4$), Manganese chloride $MnCl_2.4H_2O$), Zinc sulphate heptahydrate $(ZnSO_4.7H_2O)$, Copper (II) sulphate pentahydrate $(CuSO_4.5H_2O)$, Boric acid (H_3BO_3), Molybdic acid $(H_2MoO_4.H_2O)$, Ethylene diamine tetraacetic acid (EDTA), Potassium hydroxide (KOH) The reagents used in this study were of analytical grade and obtained from Fisher Scientific or Sigma Aldrich UK.

The reverse osmosis (RO) water used in the preparation of stock solution and standards was purified by reverse osmosis in Coventry University.

3.1.2 Bricks and Clay:

The materials used in this study are clay and bricks from the WH Collier Brickworks in Marks Tey, Colchester. The parent clay used by this brickwork was boulder clay formed from the middle Pleistocene Lacustrine sediments during the Hoxnian Interglacial period that occurred about 400,000 years ago. These sediments have several stratified layers from which an estimation of the duration of the Hoxnian Interglacial period can be made. An ancient manuscript described the boulder clay as sediments deposited in a north westerly direction, indicating that the ice flow was probably from the North Sea towards the Atlantic (Peach and Horne 1881).

The clay when dug from the ground was a bluish-grey material that slowly changed colour to brown on exposure to air caused by the oxidation of iron compounds found within the clay. The brick work was visited and samples of the freshly dug clay were collected in polyethene bags, the bags were sealed to prevent the clay from drying out due to moisture loss and stored at room temperature in the laboratory. Fired bricks were also collected from the brick work.

3.1.3 Determination of Moisture Content of Clay

An empty weighing tub was weighed using an analytical balance and the mass written down. Clay was added to the weighing tub and weighed; the mass of the added clay was determined by subtracting the mass of the empty clay from the mass of the weighing tub + clay. The clay + weighing tub was put in an oven at 105^{o}C for 24 hours or until a constant mass was attained. The clay and weighing boat was measured again and the moisture content determined using **Equation 3.1-3.4**:

Initial mass of clay = (Mass of clay + tub) – Mass of tub **Equation 3.1**

Final Mass of clay = (Mass of clay and tub after drying) – Mass of Tub **Equation 3.2**

Δ in mass of clay = Initial mass of clay – Final mass of clay **Equation 3.3**

$$\% \text{ Moisture content} = \frac{\Delta \text{ in mass of clay}}{\text{initial mass of clay}} \text{X} 100 \qquad \textbf{Equation 3.4}$$

3.1.4 Preparation of Clay Pellets

250g of clay was weighed out and reverse osmosis (RO) water added and worked into the clay to improve plasticity. The clay was then spread using a squeegee unto a stainless steel grid measuring 1cm x 1cm x 1.5mm which served as a mould for the pellets. It was left to air dry for 2 days before before firing in a Lenton Thermal Design General Purpose Chamber furnace ECF/12/22 using the following temperature programme shown in **(Figure 3.1)**:

i. The temperature of the furnace was raised to 120^{o}C by ramping the temperature by 8^{o}C every minute and allowed to remain at 120^{o}C for 15 minutes.

ii. The temperature was then increased by 12^{o}C every minute to 540^{o}C over a 30 minute period and allowed to remain at 540^{o}C for another 15 minutes.

iii. The temperature was further increased to 740^{o}C over a 30 minute period at an increase rate of 24^{o}C every minute and allowed to remain at 740^{o}C for another 15 minutes.

iv. The temperature was finally increased to 960^{o}C at an increase rate of 21^{o}C every minute for 45 minutes and allowed to remain at that temperature for 15 minutes the furnace switched off and allowed to cool overnight.

At the end of the firing regime, the clay pellets had a terracotta colour. The firing temperature was varied with the final firing temperature at 540^{o}C, 740^{o}C, 800^{o}C, 850 ^{o}C, 900 ^{o}C, 960^{o}C, 1000 ^{o}C, 1050^{o}C and 1200^{o}C.

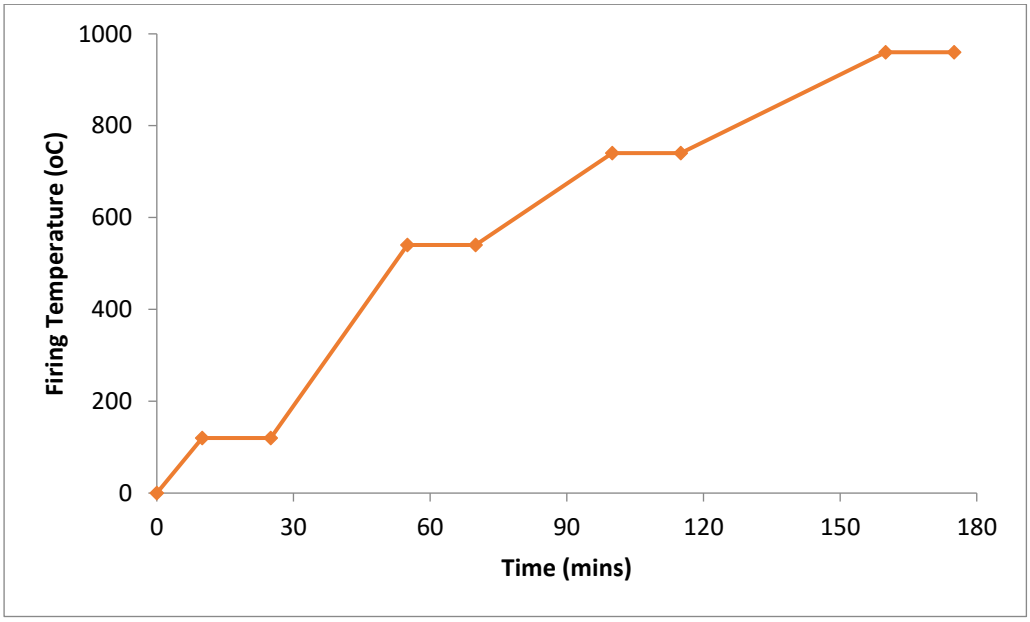

Figure 3.1: Firing temperature programme of furnace used in the production of the clay pellets

The firing regime was chosen based on the duration of the total firing time, and the final firing temperature programme was used for the optimization of firing temperature. The initial experiments were done at the final temperature of 960^{o}C, at this temperature there complete adsorption and there was the need to assess adsorption within this temperature range ±100^{o}C. The pellets during air drying and after firing are shown in **Figure 3.2.**

Figure 3.2: Clay Pellets a) during air drying; and b) after firing

3.1.5 Modification of Clay Pellets

Salts of iron (Fe), calcium (Ca) and aluminium (Al) commonly used as coagulants in wastewater treatment works were used to chemically modify the clay to optimize phosphorus absorption before use in the preparation of clay tiles. The salts used were Calcium carbonate ($CaCO_3$), Iron (II) sulphate heptahydrate ($FeSO_4.7H_20$), Alumimium sulphate hexadecahydrate ($Al_2(SO_4)_3.16H_2O$). Modification to the clay was done after water has been added before the drying stage and amendments were done by adding the appropriate quantity of aluminium, calcium or iron salt using the following ratio:

All modifications to the clay were done before the drying stage.

i. Ca modified fired clay pellets (CaFMCP) was prepared using the following ratio:

a. 0.2 g Ca — 0.5g of $CaCO_3$: 50g clay
b. 0.4 g Ca — 1g of $CaCO_3$: 50g clay
c. 1 g Ca — 2.5g of $CaCO_3$: 50g clay
d. 2 g Ca — 5g of $CaCO_3$: 50g clay
e. 4 g Ca — 10g of $CaCO_3$: 50g clay

ii. Al modified fired clay pellets (AlFMCP) was prepared using the following ratio:

a. 0.04 g Al 0.5g of $Al_2(SO_4)_3.16H_2O$: 50g clay
b. 0.08 g Al 1g of $Al_2(SO_4)_3.16H_2O$: 50g clay
c. 0.2 g Al 2.5g of $Al_2(SO_4)_3.16H_2O$: 50g clay
d. 0.4 g Al 5g of $Al_2(SO_4)_3.16H_2O$: 50g clay
e. 0.8 g Al 10g of $Al_2(SO_4)_3.16H_2O$: 50g clay

iii. Fe modified fired clay pellets (FeFMCP)

a. 0.2g Fe 1g $FeSO_47H_20$: 50 g clay
b. 0.4g Fe 2g $FeSO_47H_20$: 50 g clay
c. 1g Fe 5g $FeSO_47H_20$: 50 g clay
d. 2g Fe 10g $FeSO_47H_20$: 50 g clay
e. 4g Fe 20g $FeSO_47H_20$: 50 g clay

The clay tiles were then fired using the programme outlined previously.

The experimental levels for the preparation of modified clay pellets were determined by adding an increasing amount of the salts to the clay. The amount of metal added was determined from the mass of the salt. An attempt was made to maintain a constant amount of metal added for each sample. However, AlFMCP showed an negative effect on adsorption when the same amount of Ca was added, so the method was altered to add same mass of $CaCO_3$ and determine the concentrataion of Al added from the mass of $Al_2(SO_4)_3.16H_2O$. Hence, AlMFCP and CaMFCP have the same mass of added salt but FeMFCP and CaMFCP have the same amount of added metal.

3.1.6 Characterization of Clay Tiles

A microphotograph image of the clay tiles was obtained by using the Scanning Electron Microscope model JSM-6060LV JEOL Ltd, in the Advance Joining Research Centre, Faculty of Engineering Coventry University.

Some materials have been removed due to 3rd party copyright. The unabridged version can be viewed in Lancester Library - Coventry University.

Figure 3.3: Scanning Electron Microscope model JSM-6060LV

3.2 Equipments

3.2.1 Flow Injection Analyzer

The flow injection analyzer system is manufactured by FOSS and comprises of the FIAstar 5000 analyzer unit with a 120 vial 5057 sampler, and a method cassette P with 720nm and 1000nm interference filters. The parameter settings for detection are:

Wavelength (λ)	Measuring = 720nm, Reference = 1000nm
Signal filtration	1second sliding mean
Injection volume	40µl
Injection time	15 seconds
Fill time	30 seconds
Measuring Time	45 seconds
Sampler cup duration time	30 seconds
Sampler wash duration time	15 seconds
Pump speed	40 rpm
Evaluation	Absorbance peak height

The spectrophotometric method for the determination of dissolved phosphorus in water is based on the chemical reaction between orthophosphates and molybdate ions under acidic conditions to form 12-molybdophosphoric heteropolyacid. Detection

occurs either on a resultant molybdophosphate product when using molybdenum blue method or on the yellow molybdovanadophosphate complex, when using continuous flow methods like the flow injection method. The acceptance of the molybdenum blue method as a routine method for the determination of phosphorus can be attributed to its high sensitivity (Miro *et al.* 2003).

The use of hydrazine and Tin (II) chloride as reducing agents have proven to give the best overall results in terms of quicker reactions, wider dynamic ranges and lower detection limits, despite the relatively unstable nature of Tin (II) chloride (van Staden and van der Merwe 1997).

3.2.2 Inductively Coupled Plasma Optical Emission Spectrometer (ICP-OES)

A Perkin Elmer Optima 5300 inductively coupled plasma optical emission spectrometer (ICP-OES) was used for the multi element analysis. ICP-OES presents an efficient and effective method for the quick multi-element analysis of a wide range and scale of samples (Krejčová *et al.* 2007). Quantitative and qualitative information can be obtained from the ICP-OES about a sample. The qualitative information is derived from the wavelength at which electromagnetic radiation emission or radiation by the atom occurs and this indicates the element present in the sample, while the quantity of the emitted or absorbed radiation indicates the quantitative measurement of the level of the elements present (Cazes 2005).

During the analysis the samples were subjected to high temperatures which caused them to dissociate into atoms resulting in a significant amount of excitation and collision, which in turn caused the atoms to emit their characteristic radiation. The intensity of the light emitted at specific wavelength was measured and used to determine the concentration of the elements present (Cazes 2005).

The optimal operating conditions for the ICP-OES was as follows:

Plasma Viewing Height	5 mm
Peak Search Window	0.03 nm
Plasma Power	1.4 kW
Plasma Gas Flow Rate	15ml/min
Auxiliary Gas Flow Rate	1.5ml/min

Nebuliser Pressure 150 KPa

The viewing configuration of the atmospheric pressure argon plasma was axial. The emission wavelength (λ) used in this study is shown in **Table 3.1**

Table 3.1: Elements and Wavelengths for ICP-OES Analysis

Element	Emission Wavelength λ (nm)
Ca	317.933
Fe	238.204
Al	396.153
Mg	285.213
P	213.617

3.3 Preparation of Reagents:

3.3.1 Preparation of Ammonium Molybdate Reagent ●

In a 500ml volumetric flask, about 250ml of RO water was added, 5g of Ammonium molybdate ($(NH_4)_6Mo_7O_{24}•4H_2O$) was thed added to the flask and mixed. 17.5ml of concentrated sulfuric acid (H_2SO_4) was added, mixed carefully and made up to mark with RO water. The content was transferred to reagent bottle labeled ● to correspond to the mark on the designated tubing on the FIAstar 5000. The reagent was stable for several months.

3.3.2 Preparation of Stannous Chloride Reagent ●●

1g of Hydrazinium sulphate ($N_2H_6SO_4$) and 0.1g of stannous chloride ($SnCl_2$) was weighed into a 500ml volumetric flask and about 250ml of RO water was added and the flask was shaken vigorously to dissolve the salt. 14ml of concentrated sulphuric acid (H_2SO_4) was then added and carefully mixed and the reagent made up to mark with RO water and mixed again. The content was transferred into a reagent bottle labeled ●● corresponding to the tubing on the FIAstar 5000. The reagent was stable for one week when stored in a refrigerator and allowed to resume room temperature before use. A fresh reagent was prepared each week.

3.3.3 Preparation of Rinsing Solution

65g of sodium hydroxide (NaOH) and 6g of Disodium EDTA ($C_{10}H_{12}O_8N_2Na_2$) was dissolved in 1000ml volumetric flask and made up to mark with RO water. The solution was stable for one (1) month.

3.3.4 Preparation of Stock Standard Solution

0.4393g of Potassium dihydrogen phosphate was dissolved in RO water in a 1000ml volumetric flask and made up to mark. The solution was stored in an amber borosilicate glass bottle in a refrigerator. This solution was stable for at least three (3) months.

3.3.5 Preparation of Calibrating Standard

0.5ml, 1ml, 2mls, 3mls and 5mls of the stock standard solution were pipette into 100ml volumetric flask labeled 0.5mg/L PO_4, 1mg/L PO_4, 2mg/L PO_4, 3mg/L PO_4, and 5mg/L PO_4 respectively and made up to mark with RO water. The resulting solution a concentration of 0.5mg/L PO_4, 1mg/L PO_4, 2mg/L PO_4, 3mg/L PO_4 and 5mg/L PO_4. The calibrating standard was prepared daily and the Flow Injection Analyzer was calibrated daily.

3.3.6 Carrier Solution

The carrier solution used in the analysis was RO water.

3.3.7 Preparation of Hoagland's Solution

0.51g of KNO_3, 1.18g of $Ca(NO_3)_2.4H_2O$ and 0.49g of $MgSO_4.7H_2O$ were dissolved in a 1000ml volumetric flask.1 ml of micronutrient stock and 1ml of iron stock solution was added and made up to mark with RO water.

3.3.8 Preparation of Micronutrient Stock Solution

2.8mg of H_3BO_3, 1.81g $MnCl_2.4H_2O$, 0.22g $ZnSO_4.7H_2O$, 0.08g $CuSO_4.5H_2O$, and 0.02g $H_2MoO_4.H_2O$ was dissolved in a 1000ml volumetric flask containing RO water, 0.25 ml of the iron stock solution was added and made up to mark with RO water.

3.3.9 Preparation of Stock Iron Solution

26.1g of EDTA was dissolved in 286ml of RO water containing approximately 19g of KOH. In a 500ml volumetric flask, 24.9g $FeSO_4.7H_2O$ was dissolved and made up to

mark with RO water. The iron sulphate solution was added slowly to the potassium EDTA solution and aerated overnight while stirring. The solution was made up to 1000ml and stored in an amber borosilicate bottle.

3.4 Determination of Limit of Detection

The limit of detection and instrument Quantization Limit (IQL) was calculated using the slope of the calibration graph and the standard deviation of the response, as a daily calibration was carried out; these calculations were done using the graph that has the best R^2 value. This was to ensure accuracy and to minimize any error that may occur from a poor calibration. The mean and standard deviation (σ) was determined from 10 replicates of 1ppm calibration standard. Walfish (2006) expressed the equations used in calculating the Limit of Detection (LOD), Instrument Quantization Limit (IQL) and the relative standard deviation as shown in **Equations 3.5-3.7**:

$$LOD = 3.3\sigma/S \qquad \textbf{Equation 3.5}$$

$$IQL = 10\sigma/S \qquad \textbf{Equation 3.6}$$

$$RDS = \sigma n\text{-}1/mean*100 \qquad \textbf{Equation 3.7}$$

`Where: σ = standard deviation of the responses

S = slope of the calibration graph

3.5 Batch Experiment

Orthophosphate was the form of phosphate used in this study. Phosphorus in wastewater exists in many different forms. The common forms are orthophosphate, polyphosphates and organically-bound phosphates. These different forms tend to end up as orthophosphate. Polyphosphates which are condensed orthophosphates hydrolyze in water to produce soluble orthophosphate while the bacterial decomposition of organically-bound phosphate also produces orthophosphate. Orthophosphate is the predominant phosphorus species found in wastewater (Hammer and Hammer 2008; Masters and Ella 2008), hence orthophosphate was chosen as the phosphate species and an aqueous solution of KH_2PO_4 was used as

the artificial wastewater for this study. Typical phosphorus concentration in municipal wastewater averages 8-10 mg/L.

3.5.1 Determination of the Effect of Phosphate Concentration

5g clay tiles was measured into correctly labeled 250ml Erlenmeyer flasks containing 200 ml of 100mg/l, 250mg/l, 500mg/|l, 750mg/l and 1000mg/l phosphate solution. The Erlenmeyer flasks were then be placed in a rotary shaker for continuous shaking for 72 hours in an orbital motion at 170rpm. Aliquots were drawn into centrifuge tubes at regular interval; these were centrifuged at 5300 rpm for 45 minutes and filtered using a 125mm Whatman filter paper before analysis using the FIAstar 5000 analyzer. The experiment will be done in triplicates.

Adsorbed phosphate was calculated as the difference in the concentration of phosphate added and the phosphate concentration in the equilibrating solution.

3.5.2 Determination of the Effect of Adsorbent Dosage

150 ml of 50mg/l phosphate solution was measured into correctly labeled 250ml Erlenmeyer flasks containing 0.5g, 1g, 1.5g, 2g, 2.5g and 3g of FCP yielding a dosage concentration of 3.33 g/L, 6.67 g/L, 10 g/L, 13.33 g/L, 16.67 g/l, 20 g/L, and 33.33 g/L respectively. The Erlenmeyer flasks were then be placed in an orbital shaker for continuous shaking for 120 minutes in an orbital motion at 170rpm at room temperature. Aliquots were drawn into centrifuge tubes after 30, 60, 90, and 120 minutes, these were centrifuged at 5300 rpm for 45 minutes and filtered using a 125mm Whatman filter paper before analysis using the FIAstar 5000 analyzer. The experiments were done in triplicates.

Adsorbed phosphate was calculated as the difference in the concentration of phosphate added and the phosphate concentration in the equilibrating solution.

3.5.3 Determination of the Effect of pH

3g of FCP was measured into correctly labeled 250ml Erlenmeyer flask containing 150 ml of 50mg/L phosphate solution, the pH of the phosphate solution was adjusted to 2 by adding an adequate volume of dilute hydrochloric acid. The Erlenmeyer flasks were

placed in an orbital shaker for continuous shaking for 120 minutes in an orbital motion at 170rpm at room temperature. Aliquots were drawn into centrifuge tubes after 30, 60, 90, and 120 minutes, these were centrifuged at 5300 rpm for 45 minutes and filtered using a 125mm Whatman filter paper before analysis using the FIAstar 5000 analyzer. The experiments were done in triplicates. The steps were repeated for treatments at pH 3, 4, 5, 6, 7, 8, 10 and 12. For pH 7 – 11 the pH was adjusted by adding adequate volumes of NaOH solution.

Adsorbed phosphate was calculated as the difference in the concentration of phosphate added and the phosphate concentration in the equilibrating solution.

3.5.3.1 Determination of Point of Zero Charge (pH_{pzc})

The point of zero charge (pH_{pzc}) was determined using the pH drift method following the procedure described by Rivera-Utrilla *et al*. (2001). The pH drift method which provide a fast but reliable method for the determination of pH_{pzc} was originally developed for activated carbon has been used in the for the determination of pH_{pzc} in clay (Moharami and Jalali 2013). The method has been compared to the standard method of zeta potentiometric titration and mass titration with similar results.

20 ml of 0.01M NaCl into correctly labelled 50 ml Erlenmeyer flask. The pH of each flask adjusted to 2, 3, 4, 5, 6, 7, 8, 10, and 12 by adding the appropriate amount of 0.1M HCl or 0.1M NaOH solution. 0.06g of the adsorbents was added to each flask and left undisturbed for 48 hours. The final pH was measured after 48 hours. A graph of final pH was plotted against the initial pH and the pH_{pzc} was the point where the line of the final pH versus initial pH crossed the line equal to final pH.

3.5.3.2 Determination of the Effect of Temperature

3g of FCP was measured into correctly labeled 250ml Erlenmeyer flasks containing 150 ml of 50mg/L phosphate solution. The Erlenmeyer flasks will then be placed in a water bath shaker for continuous shaking for 120 minutes in an orbital motion at 170rpm, at a set temperature of 20^{o}C. Aliquots were drawn into centrifuge tubes every five minutes, these were centrifuged at 5300 rpm for 45 minutes and filtered using a 125mm Whatman filter paper before analysis using the FIAstar 5000 analyzer. The

experiment was done in triplicates. These steps were repeated for treatments at 25^{o}C, 30^{o}C and 35^{o}C.

Adsorbed phosphate was calculated as the difference in the concentration of phosphate added and the phosphate concentration in the equilibrating solution.

3.5.3.3 Determination of the Effect of Contact Time

3g of FCP was measured into correctly labeled 250ml Erlenmeyer flask containing 150ml of 50mg/l phosphate solution. The Erlenmeyer flask was then placed in an orbital shaker for continuous shaking for 120 minutes at 170rpm. Aliquots were drawn into centrifuge tubes every ten minutes for 30 minutes and every 30 minutes thereafter. These were centrifuged at 5300 rpm for 45 minutes and filtered using a 125mm Whatman filter paper before analysis using the FIAstar 5000 analyzer. This experiment was done in triplicates.

Adsorbed phosphate was calculated as the difference in the phosphate concentration added and the phosphate concentration in the equilibrating solution.

3.5.3.4 Determination of Effect of Firing Temperature

3g of FCP fired at a final temperature of 540^{o}C was measured into a 250ml Erlenmeyer flask containing 150ml of 50mg/l phosphate solution. The Erlenmeyer flask was then placed in an orbital shaker for continuous shaking for 120 minutes at 170rpm. Aliquots were drawn into centrifuge tubes after 30, 60, 90, and 120 minutes. These were centrifuged at 5300 rpm for 45 minutes and filtered using a 125mm Whatman filter paper before analysis using the FIAstar 5000 analyzer. This experiment was done in triplicates. The experiment was repeated for clay tiles that had final temperature of 740^{o}C, 800^{o}C, 850 ^{o}C, 900 ^{o}C, 960^{o}C, 1000 ^{o}C, 1050^{o}C and 1200^{o}C.

Adsorbed phosphate was calculated as the difference in the phosphate concentration added and the phosphate concentration in the equilibrating solution.

3.5.3.5 Determination of Effect of Clay Pellets Modification

3g of clay pellets modified by the addition of different aluminium, calcium and iron salt was measured into correctly labeled 250ml Erlenmeyer flask containing 150ml of

50mg/l phosphate solution. The Erlenmeyer flask was then placed in an orbital shaker for continuous shaking for 120 minutes at 170rpm. Aliquots were drawn into centrifuge tubes every five minutes for 30 minutes. These were centrifuged at 5300 rpm for 45 minutes and filtered using a 125mm Whatman filter paper before analysis using the FIAstar 5000 analyzer. This experiment was done in triplicates.

Adsorbed phosphate was calculated as the difference in the phosphate concentration added and the phosphate concentration in the equilibrating solution.

3.6 Continuous Flow Experiment

A fixed bed column experiment was performed in the laboratory to investigate the adsorption of phosphate using the Calcium modified fired clay pellets (CaMFCP) in a continuous flow mode. A fixed film reactor for phosphorus removal was not used in this study, the use of a biofilm allows for the biological removal of phosphorus by alternating between aerobic and anaerobic conditions. This study used a fixed bed column to assess the performance of the clay pellets for the removal of phosphate in a continuous flow mode.

Glass columns with internal diameter of 4cm and length of 100cm and PET (polyethylene terephthalate) plastic bottles with internal diameter 6cm and height 21cm was used in the column test. Glass wool was placed in the bottom of the column to prevent any loss of CaMFCP. The column was operated in a down flow mode and phosphate solution was pumped through the column using Gilson MINIPULS 3 peristaltic pump. The parameters investigated in the column experiment were bed height, initial phosphate concentration, flow rate and column diameter. Effluents were collected three times a week for analysis using FIAstar 5000 analyser. Adsorbed phosphate was calculated as the difference between influent phosphate concentration and the concentration of phosphate in the effluent. The schematic diagram and set up for the fixed bed column experiment is shown in **Figures 3.4** and **3.5** respectively.

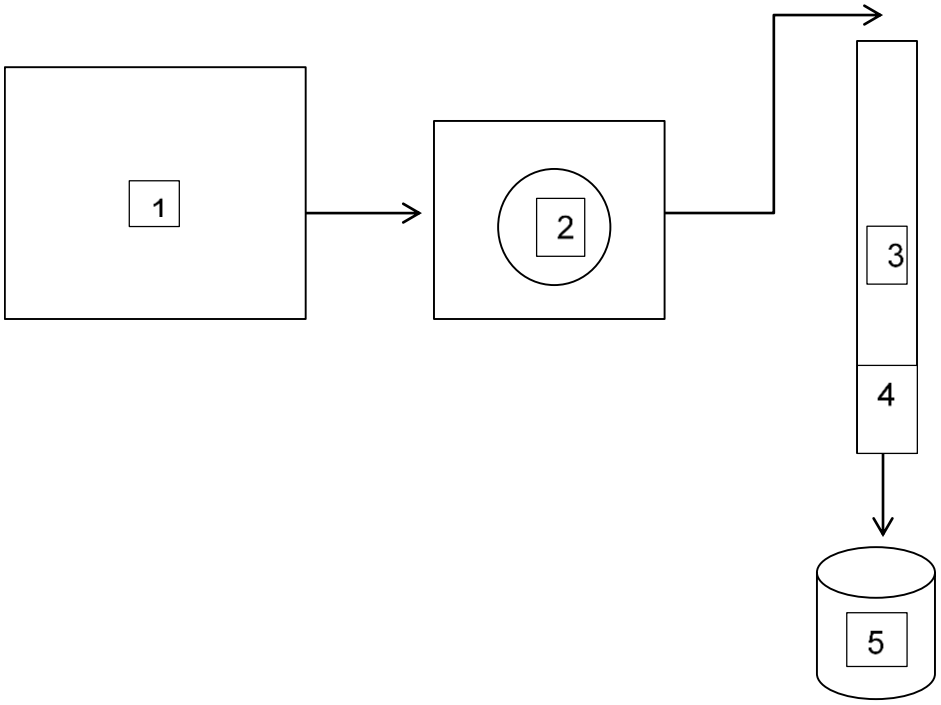

Figure 3.4: Schematic diagram of the fixed bed column experiment: (1) reservoir with phosphate solution; (2) peristaltic pump; (3) filter material; (4) glass wool; (5) effluent.

Figure 3.5: The set up for the fixed bed column experiment

3.6.1 Effect of bed height

The effect of bed height on the fixed bed adsorption of phosphate using CaMFCP was investigated at a constant initial phosphate concentration of 20mg/l. The glass columns with an internal diameter of 4 cm and length of 100 cm were filled to a height of 10 cm, 20cm and 30cm using 101.11g, 220.67g and 278.87 g of CaMFCP respectively. The flow rate was 2.25 ml/min.

3.6.2 Effect of initial phosphate concentration

The effect of initial phosphate concentration on the fixed bed adsorption of phosphate using CaMFCP was investigated using PET columns with internal diameter of 6 cm and length of 21 cm filled to a height of 10 cm with 208.66 g of CaMFCP. 10 mg/l, 20 mg/l and 50 mg/l phosphate solution was passed through Column 1, Column 2 and Column 3 respectively.

3.6.3 Effect of column diameter

In the laboratory the diameter of columns in continuous flow experiment can be scaled down on the condition that the H/d_{bed} ratio is greater than 1 as small H/d_{bed} ratio leads to low pressure drop.

The effect of column internal diameter on the fixed bed adsorption of phosphate using CaMFCP was investigated at a constant initial phosphate concentration of 20 mg/L. The columns with internal diameter of 2.5 cm, 5 cm and 6 cm were filled to a height of 10 cm using 32.57 g, 130.77g and 208.66 g of CaMFCP respectively. The flow rate was 2.4 ml/min.

3.6.4 Effect of adsorbate flow rate

The effect of adsorbate flow rate on the fixed bed adsorption of phosphate using CaMFCP was investigated using glass columns with an internal diameter of 4 cm filled to a height of 10 cm. Phosphate solution had a constant initial phosphate concentration of 20 mg/L and the flow rate was 1.7 ml/min, 2 ml/min and 2.6 ml/min for Column 1, Column 2, and Column 3 respectively.

The breakthrough concentration (C_b) was fixed at 10% of initial concentration (C_o) and the exhaustion concentration (C_e) was fixed at 50% of initial concentration. The time required to the breakthrough concentration and exhaustion concentration was

designated as t_b and t_e respectively, while the volume to breakthrough concentration and exhaustion concentration was V_b and V_e respectively. The column was allowed to run till total exhaustion.

3.6.5 Determination of breakthrough point

In a continuous flow column, the concentration profile of the adsorbate and adsorbent vary in time and space and could be described by the aid of a breakthrough curve (Chu 2004; Malkoc and Nuhoglu 2006). The breakthrough curve typically chows the progression of the area of mass transfer as the fluid moves through the column.

The mass transfer zone (MTZ) typically moves from the inlet point to the outlet point with the saturated zone behind the MTZ. As the MTZ progresses towards the outlet, the effluent concentration rises until a maximum is reached and this maximum concentration is referred to as breakthrough concentration. And beyond this point, the effluent concentration rises quickly up to the influent concentration at this point no more adsorption can be achieved. The breakthrough concentration could be described as the minimum detectable or maximum allowable concentration in the effluent.

The throughput effluent volume was calculated **Equation 3.8**

$$V_{eff} = Qt \qquad \textbf{Equation 3.8} \qquad \textbf{(Malkoc and Nuhoglu 2006)}$$

Where *Q* is the volumetric flow rate in l/hr

t is the total flow time (days)

The breakthrough curve also showed the loading behaviour of phosphate as it was removed in a fixed bed column and was expressed in terms of adsorbed phosphate concentration (C_{ad}), influent phosphate concentration (C_o), effluent phosphate concentration (C_t), or the ratio of the effluent phosphate concentration to the influent phosphate concentration (C_t/C_o) as a function of time or volume of effluent for a given bed height (Aksu and Gonen 2004; Malkoc and Nuhoglu 2006). The breakthrough curve could be derived from the plot of effluent concentration against the volume of phosphate solution treated (Littler 2011).

The area under the breakthrough curve *A* was obtained by plotting the adsorbed concentration (C_{ad}; mg/l) against time (*t*, hr). The total quantity of adsorbed phosphate (q_t) by the column for a given influent concentration and flow rate was calculated as:

$$qt = \frac{QA}{1000} = \frac{Q}{1000} \int_{t=0}^{t=t_{total}} C_{ad}\,dt$$ **Equation 3.9 (Gupta and Babu 2010)**

Where Q is the volumetric flow rate and $C_{ad} = C_o - C_t$.

The total amount of phosphate (P_t) passed through the column was calculated as

$$P_t = \frac{C_0 Q t_{total}}{1000}$$ **Equation 3.10 (Gupta and Babu 2010)**

The total percentage of phosphate (*S*) removed was calculated as

$$s = \frac{q_t}{P_t}\, x\, 100$$ **Equation 3.11 (Gupta and Babu 2010)**

The empty bed contact time (EBCT) can be described as the time required for the phosphate solution to fill the empty column. The EBCT was calculated from the following equation:

$$EBCT = Bed\,\frac{Volume}{flow\ rate}$$ **Equation 3.12 (Gupta and Babu 2010)**

The rate of saturation of adsorbent can also used to describe the performance of a fixed bed. The adsorbent usage rate U_r is defined as the rate of saturation of adsorbent per litre of solution passed through the column. U_r can be calculated from the equation:

$$U_r = \frac{mc}{Vb}\,\frac{Vc\rho}{VcNb} = \frac{\rho}{Nb}$$ **Equation 3.13 (Singh, Srivastava and Mall 2009)**

Where m_c is the mass of adsorbent in the column (g), V_b is the volume of solution treated at 50% breakthrough, V_c is the volume of adsorbent in the bed (l), N_b is bed

volumes to breakthrough, and ρ is the apparent density of adsorbent in the column (g/cm^3).

3.7 Kinetic and Isotherm Experiment

3.7.1 Kinetic Experiment

3g of clay tiles was weighed into correctly labeled 250ml Erlenmeyer flasks containing 150ml of 50mg/l phosphate solution. Two drops of chloroform will be added to inhibit microbial activity. The Erlenmeyer flasks will then be placed in a water bath shaker for continuous shaking for 120 minutes in an orbital motion at 170rpm, at a set temperature of 25^oC. Aliquots will be drawn into correctly labeled centrifuge tubes at 10, 20, 30, 40, 60, 90 and 120 minutes, these were centrifuged at 5300rpm for 45 minutes and filtered using a 125mm Whatman filter paper before analysis using the FIAstar 5000 analyzer. The absorbed PO_4 was calculated as the difference in PO_4 added and the phosphate in the equilibrating solution. An aliquot at time 0min was drawn immediately on the addition of the phosphate solution before shaking commences. The experiment was repeated for 20, 30 and 35^oC. The experiments were done in triplicates.

The rate of adsorption was determined from the amount of phosphate adsorbed at different times and the adsorption data from Section **3.8.1** used to evaluate for the pseudo-first order, pseudo-second order, Elovich kinetic and Bangham's pore diffusion models to determine which model best suits the adsorption.

3.7.2 Adsorption Isotherm

The result of the experiment described in **Section 3.6.1** was used in the study of the adsorption isotherm. The equilibrium adsorption capacity was derived from the isotherm data and Langmuir, Freundlich, Tempkin and Dubinin-Radushkeivich (D-R) isotherm models were used to analyze the relationship between the quantities of phosphate adsorbed onto the clay.

3.8 Thermodynamic Studies

A thermodynamic study was carried out to describe the relationship between temperature and the adsorption of phosphates using the data from experiments described in **Section 3.6.4**. The concept of thermodynamics assumes entropy is the driving force in an isolated system where energy cannot be gained or lost. Thermodynamics describes the energy changes between the molecules during collision. Gibbs free energy (ΔG), entropy (ΔS) and enthalpy (ΔH) and activation energy (E_a) was used to describe the energy changes during the adsorption of phosphates.

Gibbs free energy (ΔG), entropy (ΔS) and enthalpy (ΔH) was calculated using the following **Equations 3.14 and 3.15**:

$$\Delta G = -RT \ln(kd) \qquad \textbf{Equation 3.14}$$

$$\Delta G = \Delta H^o - \Delta S^o \qquad \textbf{Equation 3.15}$$

Where T is temperature in Kelvin and ΔH and ΔS corresponds to the slope and intercept respectively of a graph of ln K_d against 1/K.

While the activation energy E_a was derived from the Arrhenius equation as shown in **Equation 3.16**:

$$\ln K_d = \ln A - \frac{Ea}{RT} \qquad \textbf{Equation 3.16} \qquad \textbf{(Agarry } \textit{et al.} \textbf{ 2013)}$$

Where K_d is the rate constant

A is the Arrhenius constant J/mol/K)

E_a is the activation energy (KJ/mol)

R is the universal constant (J/molK)

T is temperature in K

E_a obtained from the slope of plotting ln K_d against 1/T

3.9 Green House Experiment

A greenhouse experiment was conduct to assess the availability of the adsorbed phosphate and evaluate its potential for use a slow release fertilizer. Ryegrass was

grown using the P-enriched filter materials as fertilizer. The experiment was conducted in the greenhouse in Coventry University, temperature within the greenhouse was between 19 and 22^{o}C with a minimum of a 16 hour photoperiod supplied by daylight and 400W high pressure sodium son/T lamps.

The experiment was carried out following the procedure by Hylander *et al.* (2006) and Hylander and Siman (2000) described as follows.

3.9.1 Pot Experiment

750ml pots was filled to about three quarters full with 400g artificial soil prepared using the OECD (1984) guideline for testing chemicals and consisted of 10% sphagnum peat, 20% kaolin clay and 70% industrial sand, the pH of which was adjusted to 6.0 ±0.5 using calcium carbonate. The soil was mixed with four different concentrations of phosphate (0.03g P, 0.1g P, 0.2g P and 0.3g P) in the form phosphate sorbed to CaMFCP (PSC) obtained from the fixed bed column experiment and allowed to equilibrate. Three control experiments were set up, the first two controls had 0.1g P and 0.3g P added in the form of KH_2PO_4 and the third control had no phosphorus loading. Each pot received as basic fertilizer 50 mL of a quarter strength Hoagland's solution during each cropping cycle. The experiment was done in triplicates. The phosphate application rate is presented in **Table 3.2**.

Table 3.2: Application rate of phosphate (kgP/ha)

Concentration of phosphate (mgP)	Application rate (kgP/ha)
0	0
0.03	38.22
0.1	127.39
0.2	254.78
0.3	382.17

Perennial ryegrass *Lolium perenne* L was used in this study. Ryegrass is a member of the grass family Poaceae, it is a widely cultivated and is often used for landscaping purposes. It is a quick growing grass with germination occurring within four days under favourable conditions. It is a low growing bunch-type grass that is considered as a high quality forage but could also be cultivated as a hay crop. Best yield is obtained in fertile, well-drained soils but could adapt to different soil type and climatic conditions.

It also has to ability to regenerate quickly. The perennial ryegrass seeds used in this study was obtained from Rolawan Ltd, UK.

0.1g (approximately 40 seeds) of ryegrass *Lolium perenne* was sown per pot and germination occurred from four days after planting. 3 pots were allocated to each treatment. The germination rate was determined from the emergence of the plant up to 15 days after planting. The moisture content of the soil was maintained at between 60% of the maximum water holding capacity by watering three times a week.

The plant height was measured at 3 and 7 days after germination, and on a weekly basis till harvest. The ryegrass was grown for a 30-day period after which the blades were cut 1cm above the soil surface, and weighed. The growth cycle was repeated four times. The harvested grass was dried at 55^{o}C in an oven for 3 days, fresh and dry weight was measured before and after drying. The data collect was subjected to ANOVA and linear regression using Excel.

The set up for the greenhouse experiment is presented in **Figure 3.6.**

Figure 3.6: Greenhouse experiment a) prior to harvest; b) post harvest.

The plant height was measured at 3 and 7 days after germination, and on a weekly basis till harvest. The ryegrass was grown for a 30-day period after which the blades will be cut 1cm above the soil surface, and weighed. The growth cycle was repeated four times. The harvested grass was dried at 55^{o}C in an oven for 3 days, fresh and dry weight was measured before and after drying and the dried grass was milled. The milled ryegrass was analysis for Al, B, Ca, Cu, Fe, K, Mg, Mn, Mo, P, S and Zn using ICP-OES after microwave assisted digestion.

The data collect was subjected to ANOVA and linear regression using Excel.

3.9.2 Soil pH

5g of air-dried soil was weighed into an Erlenmeyer flask and 12.5ml of RO water added to give a soil:water ratio of 1:2.5. The pH was measured using a JENWAY automated pH meter after calibration with pH buffer of 4 and 7 (Boen *et al.* 2013).

3.9.3 Plant available Phosphorus

Plant available phosphorus was extracted using Egner *et al.* (1960) as described by Hylander and Siman (2001). 5g of air-dried soil was weighed into an Erlenmeyer flask and 200ml of 0.4M acetic acid and 0.1M ammonium lactate solution with the pH adjusted to 3.75 by adding the appropriate volume of dilute HCL. This gave a soil weight:solution ratio of 1:20 (Hylander and Siman 2001, Cucarella 2008). The flask was then placed in a shaker for continuous orbital shaking for 90 minutes. The suspension was filtered using a 125mm Whatman filter paper before analysis using the FIAstar 5000 analyzer.

3.10 Data Analysis

The results obtained from the experiments carried out in this study was analyzed using the one way Analysis of Variance (ANOVA**)** and regression analysis using the Excel to analyze the effect of the operating conditions on the removal of phosphate. Correlation coefficient values was used to determine the confidence level of data from kinetic and isotherm experiments.

3.10.1 Removal Efficiency

Removal efficiency was calculated as

$$\textbf{\% Removal} = \frac{(Co - Ct)}{Co}100 \qquad \textbf{Equation 3.38}$$

Where C_o is the initial concentration of phosphates and

C_t is the concentration at time t

3.10.2 Adsorption Capacity

Adsorption capacity describes the amount of an adsorbate that can be held onto the surface of an adsorbent, it was determined from the following equation

$$Q_t = \frac{(Co - Ct)V}{m} \qquad \textbf{Equation 3.39}$$

Where q_t is the adsorption capacity at time t (mgP/g pellet)

C_o is the initial phosphate concentration

C_t is phosphate concentration at time t

V is the volume of the aliquot in (L), and

M is the mass of bricks (g)

3.11 Health and Safety

The ethical approval given to this project indicated that it was a low risk project. The COSHH requirements for this project were met. However, the following essential health and safety measures were taken into consideration during the period of laboratory analysis.

i. The general laboratory safety rules were strictly followed.
ii. The material Safety Data Sheet (MSDS) of all the reagents used in this study was consulted.
iii. The conditions for the handling and storage of all reagents requiring special conditions were followed as stipulated in those conditions.
iv. Appropriate personal protective equipments (PPE) were used throughout the analysis.
v. Waste disposal and handling was done in line with existing regulations.

4 A Mechanistic Evaluation of the Adsorption of Phosphate from Wastewater using Waste Bricks

4.1 Introduction

An estimated 30 – 40% of lakes and reservoirs all over the world have been affected by euthrophication, according to the United Nation Environment Programme (UNEP) (Zamparas *at al*. 2012; Pawar *et al*. 2016). Phosphate is an essential macronutrient, and excessive levels could trigger eutrophication through the proliferation of algae and aquatic plants (Yoon *et al.* 2014). It is therefore essential reduce phosphates to acceptable levels before discharge to receiving water bodies.

Chemical precipitation involving salts of aluminium, calcium and iron is a well-established and reliable method for the treatment of phosphate in wastewater to acceptable limit of 1-2 mg/L (Xie *et al*. 2015; Pawar *et al*. 2016). Adsorption is viewed as a low cost alternative to the commonly used chemical precipitation (Yan *et al*. 2014) and has been widely investigated using various materials such as: oyster shells (Chen *et al*. 2012), waste alum sludge (Babatunde and Zhao 2010), dolomite (Karaca *et al*. 2004), and oxide tailings (Zeng *et al*. 2004).

Clay minerals and clay adsorbents has also been used for the removal of phosphate Tunisian clay minerals (Hamdi and Srasra 2011), kaolinite (Kamiyango *et al*. 2009), used bricks (Jia *et al*. 2013), and Al^{3+}/Fe^{3+}-modified bentonite (Shanableh *et al*. 2016). Used bricks from construction waste could pose an environmental challenge in disposal. An estimated 31.8 million tonnes per annum of demolition waste is generated in England and Scotland annually (CRWP 2009). These demolition wastes have high content of aluminium, calcium and iron and could be applied for phosphate removal in wastewater. The aim of this study was to investigate the potential of used bricks to adsorb phosphate from wastewater.

4.2 Effect of contact time

An experiment was carried out to investigate the effect of contact time on the adsorption of phosphate using brick dust. The result is presented in **Figure 4.1**.

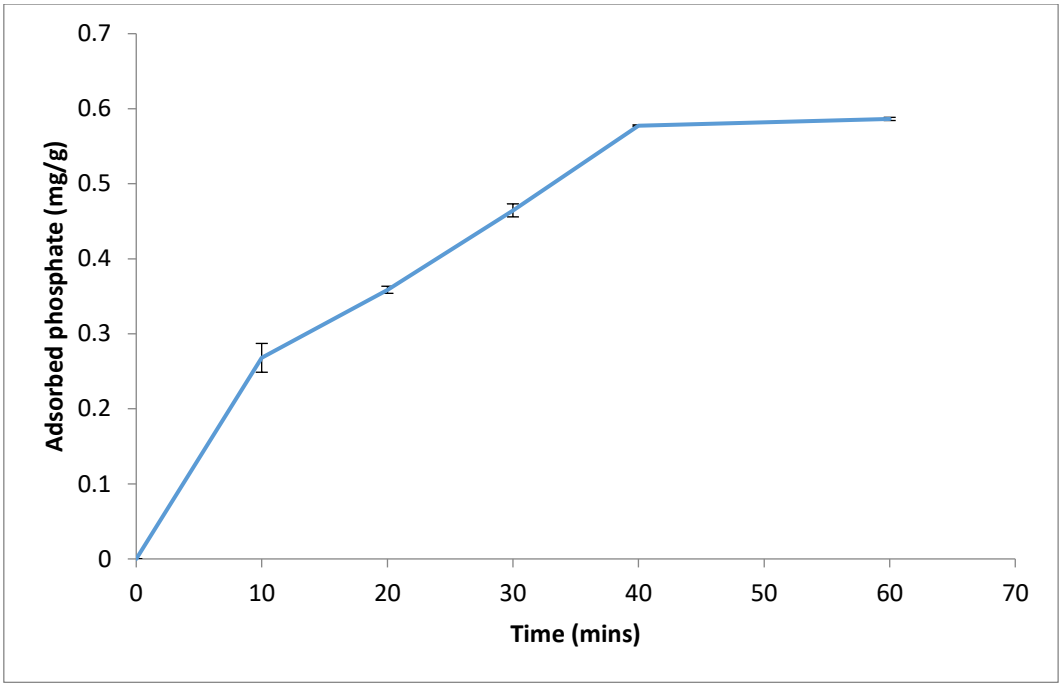

Figure 4.1: Effect of contact time on the adsorption of phosphate using brick dust (n=3) standard error bars shown. Adsorption conditions: initial concentration 20mg/l, pH 6.7, adsorbent dose 5g, room temperature.

Phosphate adsorption increased with increase in contact time from 0.27 to 0.59 mg/g as the contact time increased from 10 to 60 minutes. After the first 10 minutes, 45% of the phosphate was adsorbed, increasing to 60% during the next 10 minutes. Phosphate removal followed a typical adsorption pattern, where there was an initial fast removal of phosphate which slowed as the concentration declined until all the phosphate was taken out of the solution. The kinetic profile showed an initial fast uptake of phosphate during the first ten minutes of contact indicated by a steeper gradient before showing a more gradual uptake before plateauing after 40 minutes as the phosphate was taken out of solution. The initial fast uptake is due to the presence of a large number of empty adsorption sites available, as phosphate are taken out of solution, the number of these sites decreases and the slope becomes more gradual as the rate of adsorption reduces. The rate of reaction plateaus when it reaches equilibrium or all the phosphate has been taken out of solution.

The standard deviation for the curve was between 0 and ± 0.03, when compared with the value of the Y-axis, the error bars appeared larger.

4.3 Effect of brick dosage

The effect of the mass of brick dust on the adsorption of phosphate form wastewater was investigated using various dosage of brick dust from 6.67 to 33.33 g/L. Phosphate adsorption increased with increasing dosage of brick dust as shown in **Figure 4.2**.

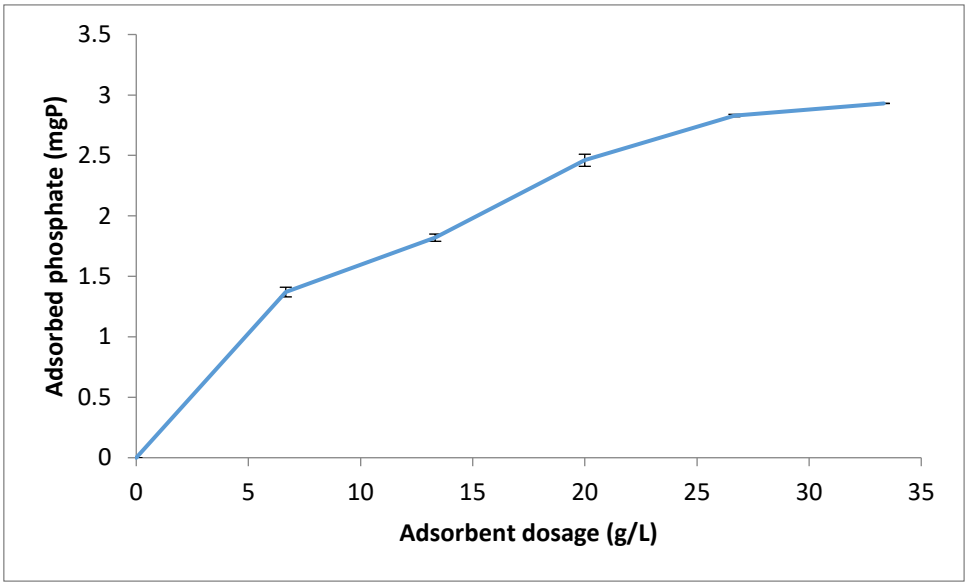

Figure 4.2: Effect of adsorbent dosage on the adsorption of phosphate by brick dust using standard experimental conditions (n=3), standard error bars shown

The increase in the amount of brick dust used led to an increase in the number of active sorption sites available for the adsorption of phosphate (Yaneva *et al*. 2013). Increase in the dosage of the adsorbent resulted in an increase in the surface area hence, provided more vacant available sites for adsorption (Mor *et al*. 2016). This result is consistent with results reported in various studies. Jia *et al*. (2013) reported an increase in the removal of phosphate as the dosage of used bricks increased from 5 to 30 g/L. Rahni *et al*. (2014) also reported an increase in phosphate adsorption with an increase in the dosage of modified bentonite-derived hydrogel from 10 to 40 g/L. Pawar *et al*. (2016) reported an increase in the removal of phosphate as the dosage of aluminium-pillared acid activated bentonite beads and alginate aluminium-pillared acid activated bentonite beads increased from 1 to 5 g/L.

The amount of phosphate adsorbed per unit mass of brick dust decreased as dosage increased as shown in **Figure 4.3**

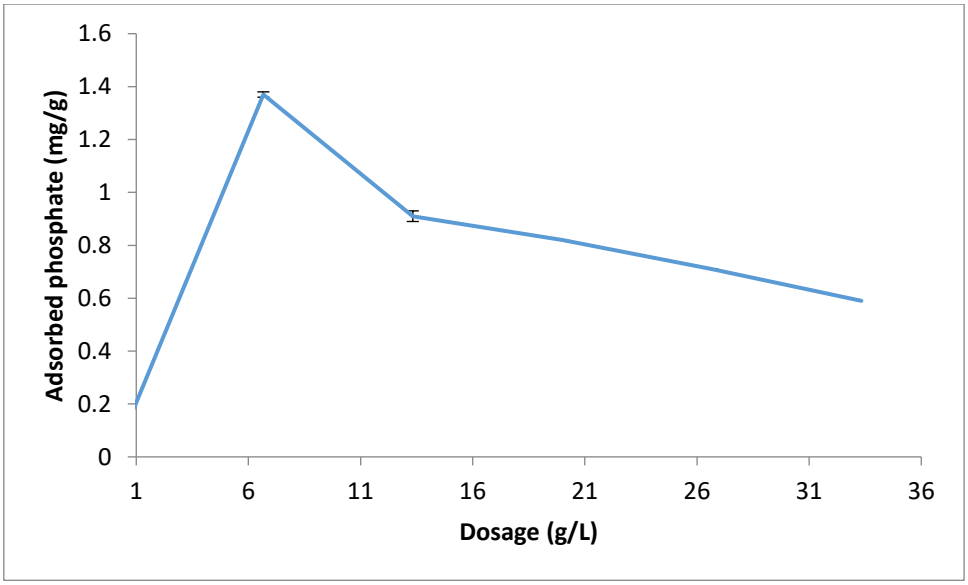

Figure 4.3: Amount of phosphate adsorbed per unit mass of brick dust using standard experimental conditions (n=3), standard error bars shown

The decrease in the amount of phosphate adsorbed per unit mass as the dosage increased could be attributed to surplus available sorption sites as a result of increased surface area (Albadarin *et al*. 2012). The decrease could also be as a result of the splitting effect of the concentration gradient (Albadarin *et al*. 2012). This is due to the fixed initial concentration of phosphate in the system and phosphate ions can only occupy a certain number of available active sites. When the mass of adsorbent increases the total number of phosphate ions in the system remains the same hence, the total amount of phosphate ions adsorbed is unaffected.

4.4 Effect of temperature

The effect of temperature on the adsorption of phosphate using brick dust was studied at different temperatures for 20 to 35^{o}C. The result is presented in **Figure 4.4.**

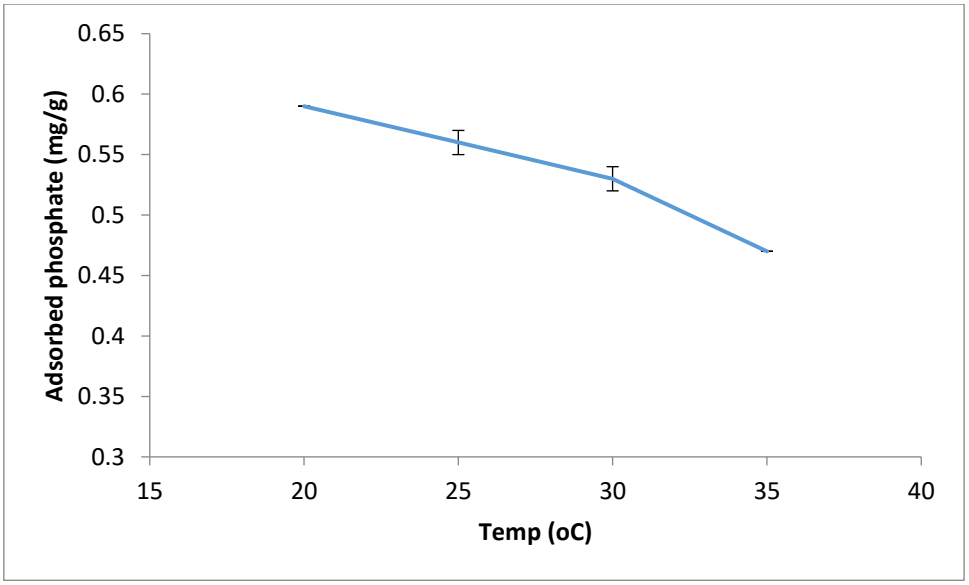

Figure 4.4: Effect of temperature on the adsorption of phosphate using brick dust. Adsorption conditions: initial concentration 20mg/l, pH 6.7, adsorbent dose 33.33g/l, room temperature.

Phosphate adsorption was shown to decrease with increase in temperature **(Figure 4.4)**. Decrease in the adsorption of phosphate from 0.59 mg/g at 20^{o}C to 0.47 mg/g at 35^{o}C suggests an exothermic reaction between the brick dust and phosphate molecules (Tian *et al.* 2009). Phosphate ions can exhibit the inclination to migrate to the bulk solution from the solid phase as the temperature of the solution increases (Karaca *et al.* 2004). This along with the increase in the rate of desorption of adsorbed phosphate from the surface of the brick dust could result in the decrease in the adsorption reported in this study (Mall *et al.* 1996). Decrease in the adsorption of phosphate with increase in temperature usually indicates low energy requirement for the adsorption. Phosphate adsorption like most adsorption process is usually endothermic, but Kose and Kivanc (2011) reported a decrease in phosphate adsorption with an increase in temperature using calcined waste eggshell, this result is similar to those reported in this study.

4.4.1 Adsorption kinetics modelling

The kinetics of adsorption of phosphate from wastewater was investigated using the pseudo-first order, pseudo-second order, Elovich, Bangham's and intraparticle diffusion kinetic models **(Section 2.7.1)** to determine the rate order and adsorption mechanism for brick dust.

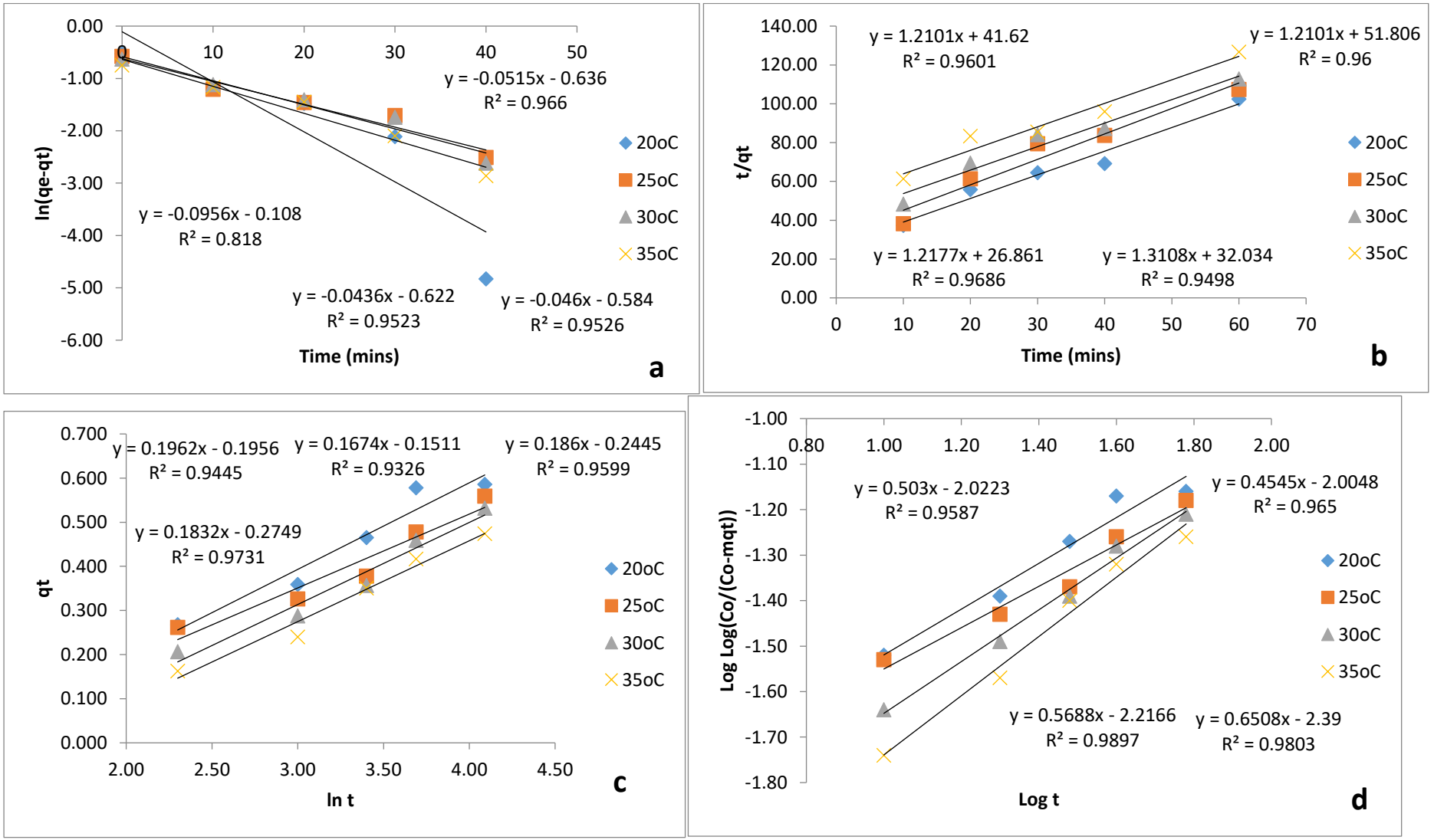

Figure 4.5: Kinetic model plot for the adsorption of phosphate using brick dust: a) Pseudo-first order kinetic model; b) Pseudo-second order kinetic model; c) Elovich kinetic model; and d) Bangham's kinetic model

The pseudo-first order plot of ln (qe-qt) showed a linear relationship that fits the experimental data **(Figure 4.5a)**. The first rate constant (k_1) decreased from -0.05 to -0.03/min as the temperature increased from 20 to 25^{o}C but was no change in the rate constant beyond 25^{o}C **(Table 4.1)**. The equilibrium adsorption capacity (qe) calculated from the slope increased from 10.46 to 22.94 mg/g when the temperature increased from 20 to 25^{o}C before reducing to 19.42 mg/g when the temperature increased to 35^{o}C. This inconsistency in the parameters of the pseudo-first order kinetic model indicates the model does not describe properly the adsorption of phosphate using brick dust.

The pseudo-second order showed a good linear relationship with the experimental data and also had a better fit than the pseudo-first order model with $R^2 > 0.94$ at all temperatures studied **(Figure 4.5b).** The pseudo-second order model is based on the assumption that each phosphate ion is adsorbed onto two adsorption sites which allows a stable binuclear bond to form. The rate constant (k_2) and initial rate of reaction (h) decreased with increase in temperature. The rate constant decreased from 0.06 to 0.03 g/mg/min while the initial rate of reaction decreased from 0.04 to 0.02 mg/g/min as temperature increased from 20 to 35^{o}C **(Table 4.1)**, this corresponds with the decrease in the rate of adsorption with increase in temperature reported in **Section 4.4.** The decrease in the value of k_2 as temperature increased could be attributed to the propensity of phosphate ions to migrate from the solid phase to the bulk phase as the temperature of the solution increases (Ho and McKay 1998; Karaca *et al*. 2004). Decrease in the rate constant with increase in temperature has been reported in literature. Karaca *et al.* (2004) reported a decrease in k_2 as the temperature increased when dolomite was used as an adsorbent for the removal of phosphate.

The applicability of Elovich equation showed the model could be used to describe the adsorption of phosphate using brick dust. The plot of qt against lnt showed a good fit to the experimental data **(Figure 4.5c)**. The values of the initial adsorption rate (α) and desorption constant (*b*) varied as a function of temperature. Initial adsorption rate increased from 0.82 to 0.86 mg/g/min as the temperature increased from 20 to 25 ^{o}C before declining to 0.76 mg/g/min as the temperature increased to 35^{o}C **(Table 4.1)**. The desorption constant fluctuated with temperature with *b* increasing from 5.1 to 5.9 g/mg when the temperature increased from 20 to 25^{o}C before reducing to 5.38 g/mg

at 30°C and increasing slightly to 5.46 g/mg at 35°C. Overall the desorption rate was lowest at 20°C, and could explain the higher adsorption at 20°C reported in **Section 4.4**.

Table 4.1: Kinetic model adsorption parameters of adsorption of phosphate onto brick dust. Adsorption conditions: initial concentration 20mg/l, pH 6.7, adsorbent dose 33.33g/l, room temperature

Kinetic model	Parameter	20°C	25°C	30°C	35°C
	Q_e exp (mg/g)	5.35			
Pseudo-first order	**k_1 (/min)**	-0.05	-0.03	-0.03	-0.03
	q_e (mg/g)	10.46	22.94	21.74	19.42
	R_2	0.818	0.9523	0.9526	0.966
Pseudo-second order	**k_2 (g/mg/min)**	0.06	0.05	0.04	0.03
	h (mg/g/min)	0.04	0.04	0.02	0.02
	R^2	0.9686	0.9498	0.9601	0.96
Elovich	**α (mg/g/min)**	0.82	0.86	0.78	0.76
	***b* (g/mg)**	5.1	5.97	5.38	5.46
	R^2	0.9445	0.9326	0.9599	0.9731
Bangham's	**k_o (mL/g/L**	44	39.35	51.20	61.84
	α	9.50×10^{-3}	9.90×10^{-3}	6.07×10^{-3}	4.07×10^{-3}
	R^2	0.9587	0.965	0.9897	0.9803

Bangham's kinetic model showed a good linear relationship with the R^2 values greater than 0.95 for all temperatures studied **(Figure 4.5d)**. Linearity of the kinetic plot was better than all the other models studied indicating the Bangham's equation can be used to describe the kinetic of adsorption of phosphate using brick dust. Bangham's constants k_o and α fluctuated with variation in temperature. The value of k_o decreased from 44 to 39.35 mL/g/L when the temperature increased from 20°C to 25°C before increasing to 51.2 mL/g/L and 61.84 mL/g/L as the temperature increased to 30 and 35°C respectively. α increased from 9.5 $\times 10^{-3}$ to 9.9 $\times 10^{-3}$ when the temperature increased from 20°C to 25°C before reducing to 6.07 $\times 10^{-3}$ and 4.07 $\times 10^{-3}$ as the

temperature increased to 30 and 35^{o}C respectively. The fluctuation in the parameters does not show a trend that could be derived as the function of temperature. The high R^2 shows indicated the involvement of pore diffusion but it was not a rate limiting step in the adsorption of phosphate using brick dust.

Adsorption is a complex multistep process with the adsorption mechanism involving mass transfer, surface reaction mechanisms and diffusion. The pseudo-second order model showed the best fit which indicates the adsorption of phosphate was primarily chemisorption and this suggests that each phosphate molecule was attached to two active sites on the adsorbent and the process was irreversible. The Bangham's diffusion model showed multi stage adsorption and the correlation coefficient (R^2) obtained from the Bangham's model ranged between 0.9587 – 0.9897 indicated that pore diffusion was involved in the uptake of phosphate onto brick dust, however it was not the only rate controlling step. It could be concluded that the adsorption of phosphate onto brick dust was a chemical reaction with physical diffusion process.

4.4.2 Thermodynamic Study

The temperature dependence of the adsorption process is often associated with changes in the thermodynamic parameters of Gibbs free energy (ΔG^o), enthalpy (ΔH^o) and entropy (ΔS^o) and are used to determine the spontaneous nature of the adsorption process and evaluate the applicability of the adsorbent (Huang *et al.* 2015). The parameters were determined using the following equations described in **Section 2.7.1**.

A plot of ln Kd against 1/T **(Figure 4.6)** using data obtained in **Figure 4.5a**, yielded a straight line graph showing a linear relationship between the logarithm of the rate constant and the inverse of temperature with ΔH^o and ΔS^o values calculated from the slope and intercept of the Van't Hoff plot and ΔG was calculated using **Equation 3.14** (Ifelebuegu 2012, Mezenner and Bensmaili 2009). The thermodynamic parameters for the adsorption of phosphate by brick dust are shown in **Table 4.2**.

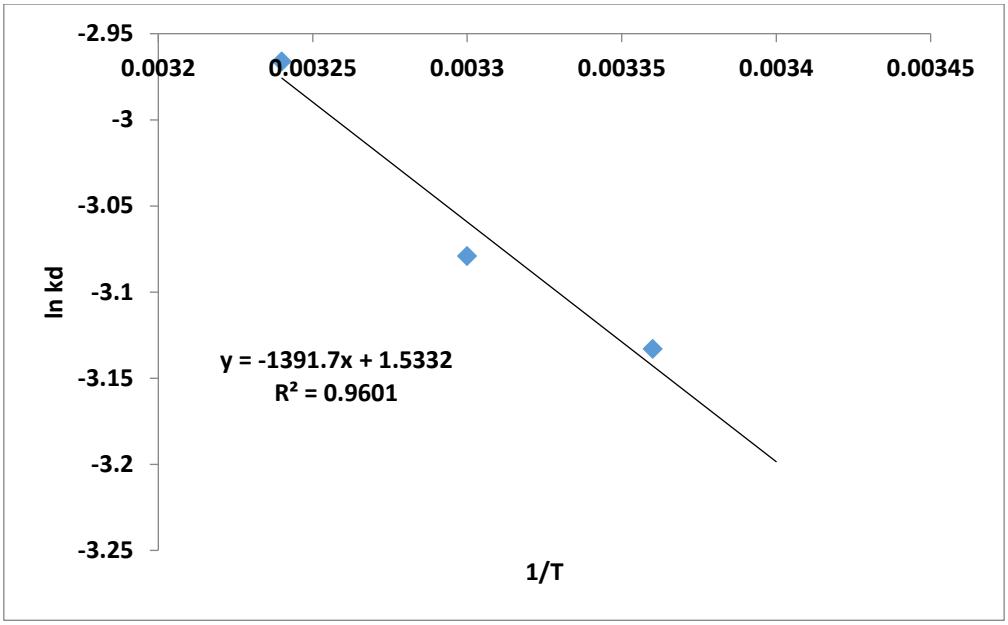

Figure 4.6: Van't Hoff plot for the adsorption of phosphate using brick dust

Table 4.2: Gibbs free energy (ΔG) for the adsorption of phosphate by brick dust.

Temp (°C)	ΔG°
20	-0.588
25	-0.595
30	-0.603
35	-0.61

Table 4.3: Thermodynamic parameters for the adsorption of phosphate by brick dust

Parameter	Brick dust
ΔH° (KJ/mol)	-0.139
ΔS° (KJ/mol/K)	1.53×10^{-3}
E_a (J/mol)	0.012
A	0.572

The values of Gibbs free energy (ΔG^o) obtained at all temperatures studied were negative, this indicates the spontaneous nature of the adsorption of phosphate onto brick dust and was a thermodynamically favourable process **(Table 4.2)**. The decrease in the ΔG^o from -0.588 KJ/mol to -0.61/mol implies an increase in the spontaneity of the adsorption process at higher temperature and is similar to those obtained by the

use of mixed lanthanum/aluminum pillared montmorillonite for the adsorption of phosphate (Tian *et al* 2009). This trend however, contradicts the results reported in **Section 4.4**, where adsorption decreased with increase in temperature. The values of ΔG^o suggests a physisorption process as values of ΔG^o for physisorption process are generally between -20 KJ/mol and 0 KJ/mol. The negative value of ΔH^o (-0.139KJ) confirmed the exothermic nature of the process **(Table 4.3)**. The positive value of ΔS^o (1.53 $x10^{-3}$ KJ/mol/K) indicated the increased randomness at the solid-solution interface during the adsorption of phosphate onto brick dust and a good affinity of phosphate ions towards brick dust (Huang 2015). The value of the activation energy E_a (0.012J/mol) indicated a relatively low energy barrier and confirmed the exothermic nature of the adsorption process.

4.5 Effect of initial concentration of phosphate

The effect of the initial concentration on the adsorption of phosphate was studied on various concentrations of phosphate ranging from 10 to 50 mg/L and the result is presented in **Figure 4.7**.

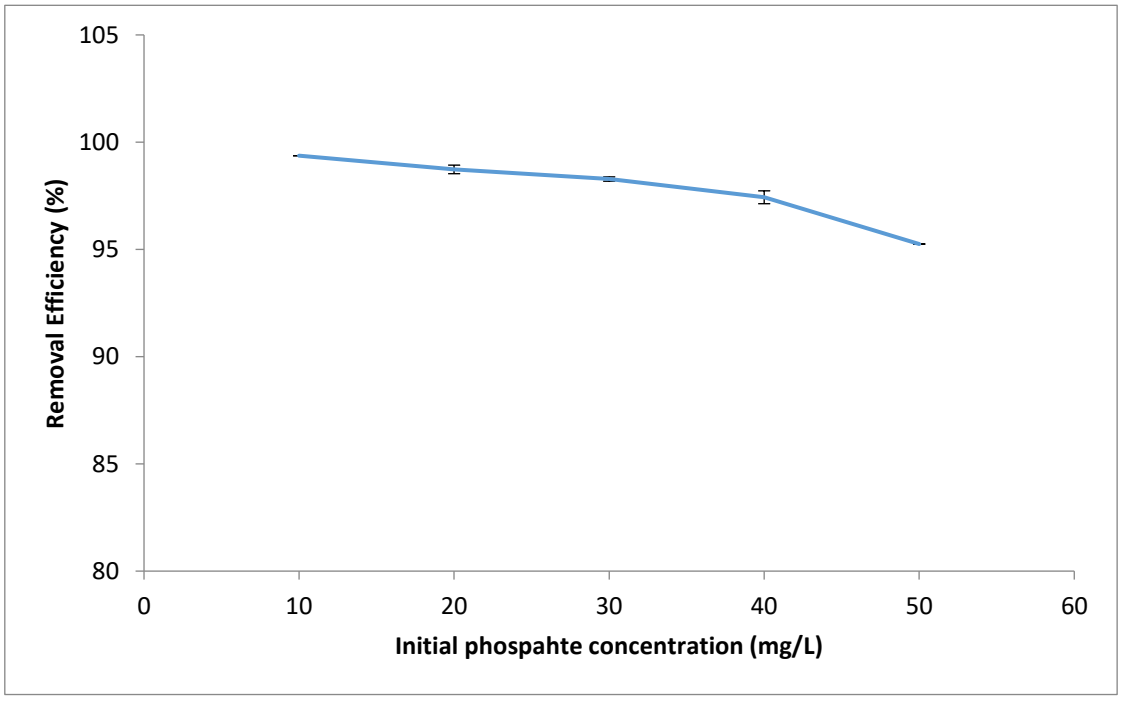

Figure 4.7: Effect of initial concentration on removal efficiency of fired clay pellets using 5g FCP and 200ml phosphate solution (n=3), standard error bars shown

Removal efficiency decreased as the initial concentration of phosphate increased. Higher removal efficiency at lower concentration could be attributed to the increase in the ratio of available active sites to the amount of phosphate ions present in the solution. At lower concentration, there is an excess of adsorption sites and as a result adsorption saturation could not be reached (Rout *et al*. 2014). As concentration increased, the ratio of adsorbent to phosphate ions present in solution decreased and active sites were more difficult to find due to the fixed number of available sites for any given mass of absorbent (Das *et al*. 2006). This result in greater competition between phosphate ions present in solution for the available active sites resulting in decreased removal efficiency as the concentration increased. These results are similar to the results obtained by Rout *et al.* (2014). In that study, the removal efficiency reduced from 99.97 to 94% when the initial concentration increased from 1 to 20 mg/L.

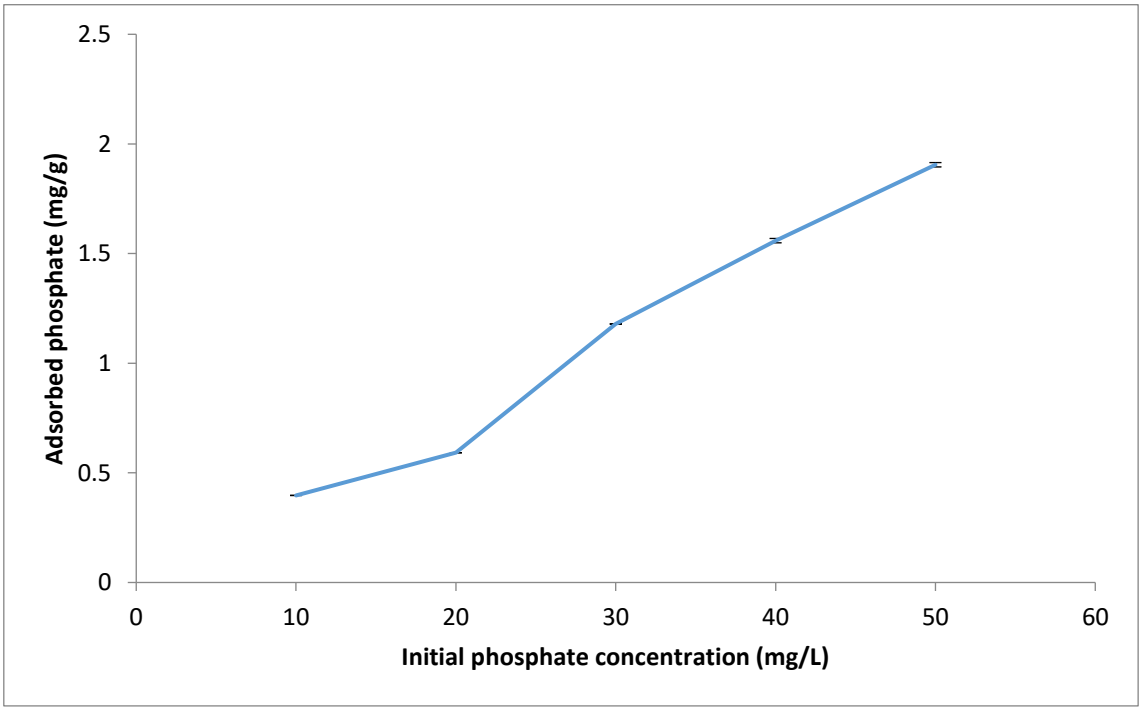

Figure 4.8: The effect of initial concentration on amount of phosphate adsorbed by FCP using 5g clay pellets and 200ml phosphate solution (n=3), standard error bars shown.

The amount of phosphate adsorbed increased with an increase in phosphate concentration **(Figure 4.8)** as a result of an increase in the number of phosphate ions available for binding unto the active sorption sites of the brick dust surface. This increase in the amount of phosphate ions led to a higher rate of collision between the phosphate ions and the surface of the brick dust (Dawodu and Akpomie (2014). The

increase in the phosphate ion concentration led to a corresponding increase in the generation of driving force required to lower the mass transfer resistance between the brick dust and the phosphate solution thus leading to an increase in the amount of phosphate ions adsorbed (Albadarin *et al.* 2012, Hameed and El-Khaiary 2008). These results are similar those reported by Karaca *et al*. (2004). The amount of phosphate adsorbed increased 9.74 to 52.91 mg/g as the concentration of phosphate increased from 10 to 60 mg/L when dolomite for the adsorption of phosphate.

4.5.1 Adsorption Isotherm

The adsorption isotherm of the adsorption of phosphate using brick dust was investigated using the Langmuir, Freundlich, Tempkin and Dubinin-Radushkeivich isotherm models to determine the model that describes the adsorption. The data from **Section 4.5** was used for the analysis of the adsorption isotherm. The isotherms were analysed using theories discussed in **Section 2.7.2**.

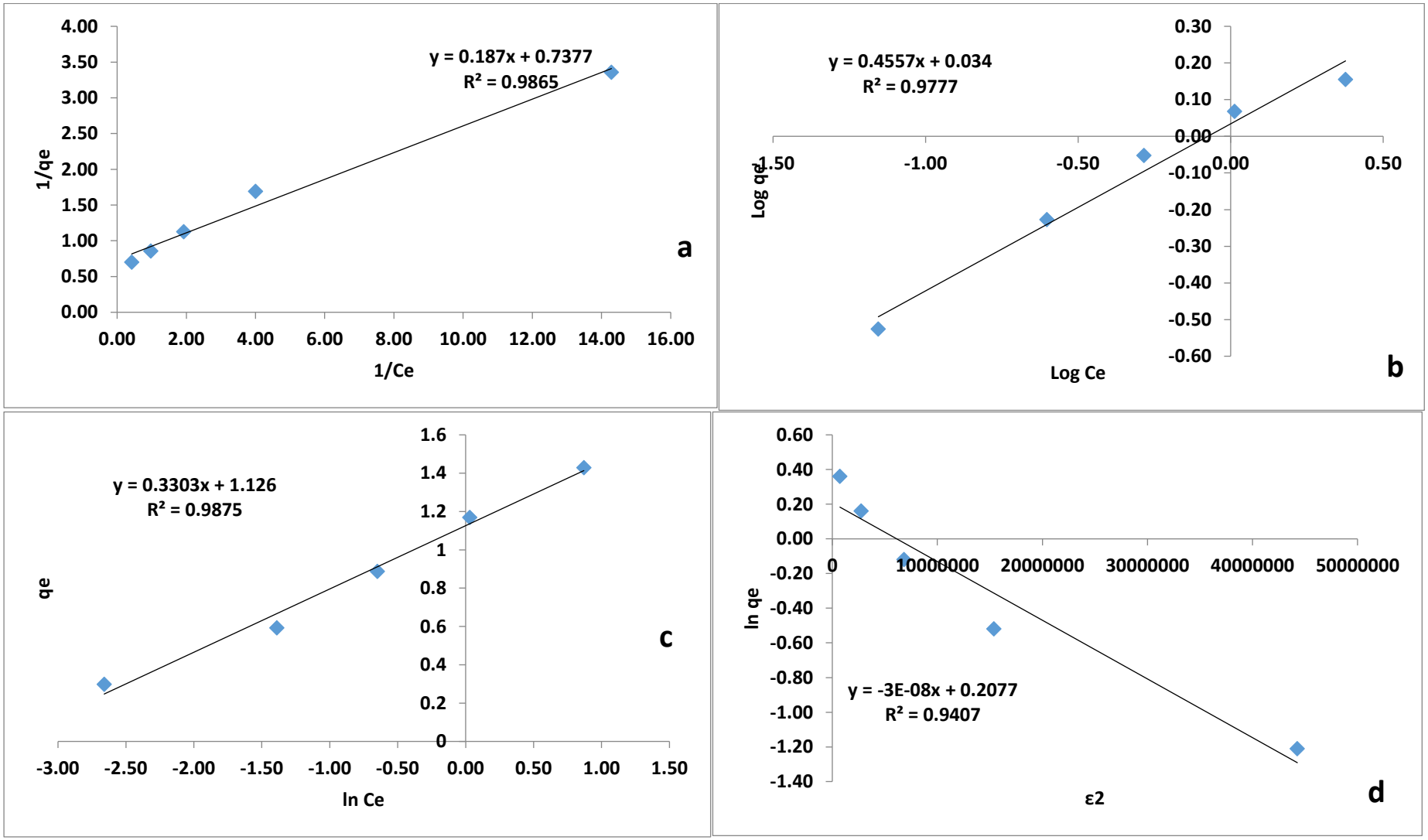

Figure 4.9: The adsorption isotherm plots for the adsorption of phosphate using brick dust: a) Langmuir adsorption isotherm; b) Freundlich adsorption isotherm; c) Tempkin; and d) Dubinin-Radushkevich adsorption isotherm

The maximum adsorption capacity, Q_m (5.35 mg/g) was determined from the slope of Langmuir isotherm **(Figure 4.9a)**. Langmuir isotherm constant (K_L) and R_L was determined as 0.25 L/mg and 0.04 respectively **(Table 4.4)**. Langmuir isotherm had the best fit out of all isotherm models studied except Tempkin isotherm. The R_L value was less than 1 indicating phosphate adsorption using brick dust was a favourable process. A good fit to Langmuir isotherm describes a monolayer sorption where each phosphate molecule is adsorbed on distinct localized sorption sites with no transmigration of the adsorbate in the plane of the surfaces giving uniform energies of monolayer sorption onto the adsorbent surface (Balouch *et al.* 2013). Adsorption that follows Langmuir isotherm model could indicate physiosorption as a mechanism of adsorption. The Q_m was similar to results obtained by Shanableh *et al*. (2016) using Al^{3+}-modified bentonite adsorbent for the adsorption of phosphate.

Table 4.4: Adsorption isotherm parameters for the adsorption of phosphate onto brick dust

Adsorption Isotherm Model	Parameter	Brick dust
Langmuir Isotherm	Q_m (mg/g)	5.35
	K_L (L/mg)	0.25
	R_L	0.04
	R^2	0.9865
Freundlich Isotherm	k_f (mg/g)	1.08
	$\frac{1}{n}$	0.4557
	n	2.19
	R^2	0.9777
Temkin Isotherm	A_T (L/mg)	1.19
	b	1287.51
	B (J/mol)	1.89
	R^2	0.9897
Dubinin-Radushkeivich Isotherm	B (mol^2/kJ^2)	2.84×10^{-7}
	E (kJ/mol)	1.35
	R^2	0.9351

Dubinin-Radushkevich (D-R) isotherm model was employed to determine the nature of the adsorption of phosphate on brick dust. The R^2 value of D-R isotherm (0.9351) was lower than Langmuir and Tempkin isotherms **(Figure 4.9d)**. The value of E is used to predict the type of adsorption, E value < 8 kJ/mol is classified as physical

adsorption. The value of E in this study was 1.35kJ/mol indicating the adsorption was a physical process **(Table 4.4)**. The E value obtained in this study was similar to result obtained by Kose and Kivanc (2011).

Freundlich isotherm model is used to determine the heterogeneity of the adsorption surface. The adsorption data showed a good fit with the isotherm as the R^2 (0.9777) **(Figure 4.9b)**. Adsorption intensity n is used to describe the heterogeneity of the adsorption surface, a smaller 1/n value indicates a more heterogeneous surface and an n value between one and ten indicates a favourable process. The value of 1/n and n study of 0.46 and 2.19 respectively obtained from this study showed the surface was heterogeneous and adsorption was favourable **(Table 4.4)**.

Tempkin adsorption can be used to determine heat of sorption which could be used to describe the adsorption process. Tempkin isotherm showed the good fit with the experimental data for all isotherms studied **(Figure 4.9c).** A_T and *B* value were 1.19 L/mg and 1.89 J/mol respectively **(Table 4.4).** The positive value of *B* means the adsorption was exothermic confirming the result of the kinetic study.

4.6 Conclusions

This study showed the potential for recycled house bricks for use as an adsorbent for phosphate removal from wastewater. Batch experiments indicated adsorption was affected by dosage of adsorbent, contact time, initial concentration of phosphate and temperature. Adsorption was shown to decrease with increase in temperature. This is advantageous as application in wastewater treatment would not require additional input of heat and could be carried out at prevailing temperature thereby saving operational cost.

The kinetic study indicated adsorption was governed by several mechanisms with various processes dominating different stages of adsorption.

Isotherm studies showed the adsorption could be described by Langmuir, Freundlich, Tempkin and Dubinin-Radushkeivich isotherms with maximum adsorption capacity of 5.35 mg/g.

Thermodynamic investigation showed removal of phosphate by brick dust was feasible, exothermic and spontaneous in nature.

4.7 Limitation of study

The application of ground brick as used in this study is shown to be low cost and highly efficient adsorbent for the removal of phosphate in wastewater treatment. However, there remain the problem of dispersed brick powder in solution increasing turbidity and attendant issues associated with the removal of suspended solids would pose technical challenges for its application.

Therefore there is a need to develop a material that can overcome this challenge. The next chapter will assess the development of clay pellets that could address the problem while maintaining its applicability.

5 Adsorptive properties of Fired Clay Pellets (FCP)

5.1 Introduction

Excessive or elevated nutrients in the water system may enhance the increase in plant-based organic matter hence causing eutrophication and algal blooms Vohla *et al.* (2011). Eutrophication is a major issue hence, the effective and efficient removal of phosphate during wastewater treatment is crucial. The Urban Waste Water Treatment Directive mandates an 80% reduction in phosphorus level or an effluent phosphate concentration of 2mg/L P for 10,000- 100,000 p.e and 1mg/L for population estimate greater than 100,000. This directive has led to a decreasing low level of phosphate in wastewater effluent during treatment through increased government regulatory pressure Vohla *et al.* (2011).

Several methods of phosphate removal have been employed in wastewater treatment. These include chemical precipitation involving the addition of calcium, iron and aluminium salts. It is the most commonly used and the most effective method of phosphate removal in wastewater treatment plant (WWTP), and often results in high phosphate removal levels Clark *et al.* (1997). The major drawbacks of the method are the high volume of sludge produced and the cost of chemicals required for dosing.

Adsorption of phosphate to suitable materials is becoming a frequently used method of removing phosphate in wastewater treatment. This could be attributed to its advantages over chemical precipitation and biological phosphorus removal. These advantages include low cost, capacity to produce re-usable solid, the simplicity make this method a favourable option in wastewater treatment (Jia *et al.* 2013). Fe, Al and Ca are the elements that are often credited with phosphate sorption, and it is assumed that if these elements are present in any medium in a substantial amount, then that medium can be used for phosphate removal (Fondu *et al.* 2010)

Several studies have been conducted using various low-cost adsorbents such as: alunite ((Ozacar 2003), fly ash (Cheung and Venkitachalam 2000), opoka (Brogowski and Renman 2004), Polonite (Gustafsson *et al*. 2008), Lightweight aggregate (LWA)/Light Expanded Clay Aggregate (LECA) (Johansson 1997, Zhu *et al.* 1997), ochre (Littler *et al.* 2013), red mud (Huang *et al*. 2008) and clay (Dable

et al. 2008, Kamiyango *et al* 2009) for the removal of phosphate from wastewater. The studies have been carried out in a laboratory, small-scale constructed wetland or a full-scale constructed wetland with the adsorbents used as filter media (Vohla *et al.* 2007).

The use of fired clay for removal of pollutants in wastewater treatment has been reported (Hauge *et al* 1994, Mohapatra *et al*. 2009, Tikariha *et al* 2013). The results from **Chapter 4** show the potential for bricks to be used as a suitable adsorbent for the treatment of phosphate pollution. However, there were problems associated with the use of brick dust as an adsorbent in wastewater treatment. Dust particles remained suspended in water hence increasing turbidity. This could lead to further technical problems to the operations and increased production cost. The development of a material that could address this problem could be seen viable solution.

The aim of this chapter was to develop a method of pelletization that was suitable for use in wastewater treatment. This chapter investigated the feasibility of employing fired clay pellets for the removal of phosphate from wastewater. The phosphate adsorptive properties such firing temperature of the pellets, pH, sorption kinetics, isotherm and thermodynamics) were investigated in batch experiments.

5.2 Characterization of Clay Tiles

SEM micrograph images of the clay tiles before adsorption showed a surface morphology with a rough and irregular surface with visible pores measuring between 2 and 10µm in diameter. The irregular surface and presence of pores could be assumed to contribute to the total surface area hence, acting as active sites for the uptake of phosphates **(Figure 5.1a)**. The surface of the tiles used in phosphate adsorption show the presence of prism-like crystals that are assumed to be phosphate crystallized out from the solution **(Figure 5.1b)**.

Figure 5.1: (a) FCP before adsorption; (b) FCP after adsorption

5.3 Effect of Firing Temperature on the Adsorption of Phosphate by FCP

The effect of final firing temperature on clay tiles on the removal of phosphate was studied at three temperatures: 540°C, 740°C and 960°C, to determine the optimum firing temperature for the tile. The experiment was conducted using 150 ml of 50mg/l orthophosphate solution, 3g clay tiles and samples were taken at 30, 60 and 120 minutes for analysis. An attempt was made to fire the tiles at 1200°C but this was not successful as it led to the vitrification of the clay which could be attributed to its high iron content (Big Ceramic Store n.d.).

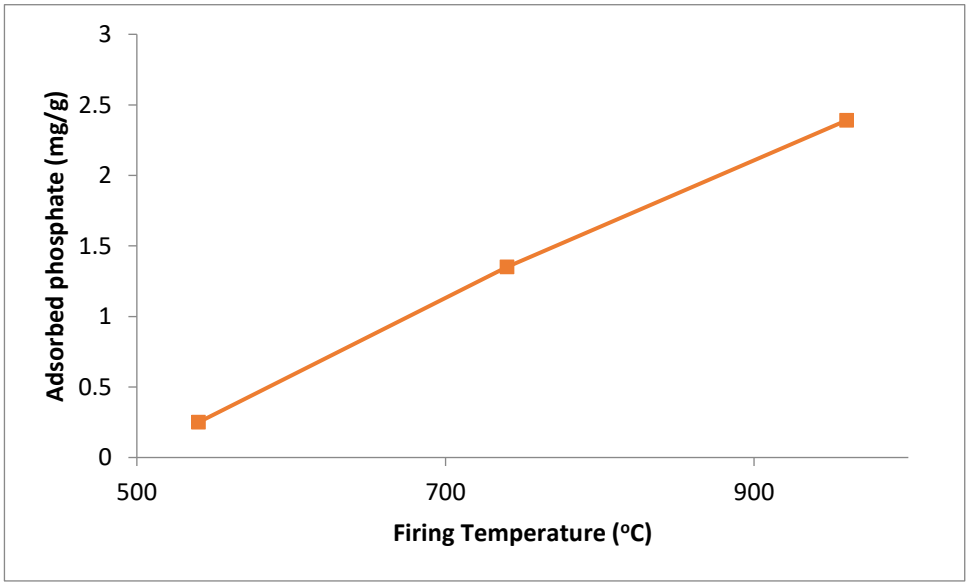

Figure 5.2: Effect of firing temperature on the adsorption of phosphate using FCP using standard experimental conditions

The adsorption of phosphate using the clay tiles was found to increase with increase in temperature (**Figure 5.2**) with complete adsorption occurring when the firing

temperature was increased to 960^{o}C consequently, the optimization of firing temperature was conducted **(Figure 5.3)**.

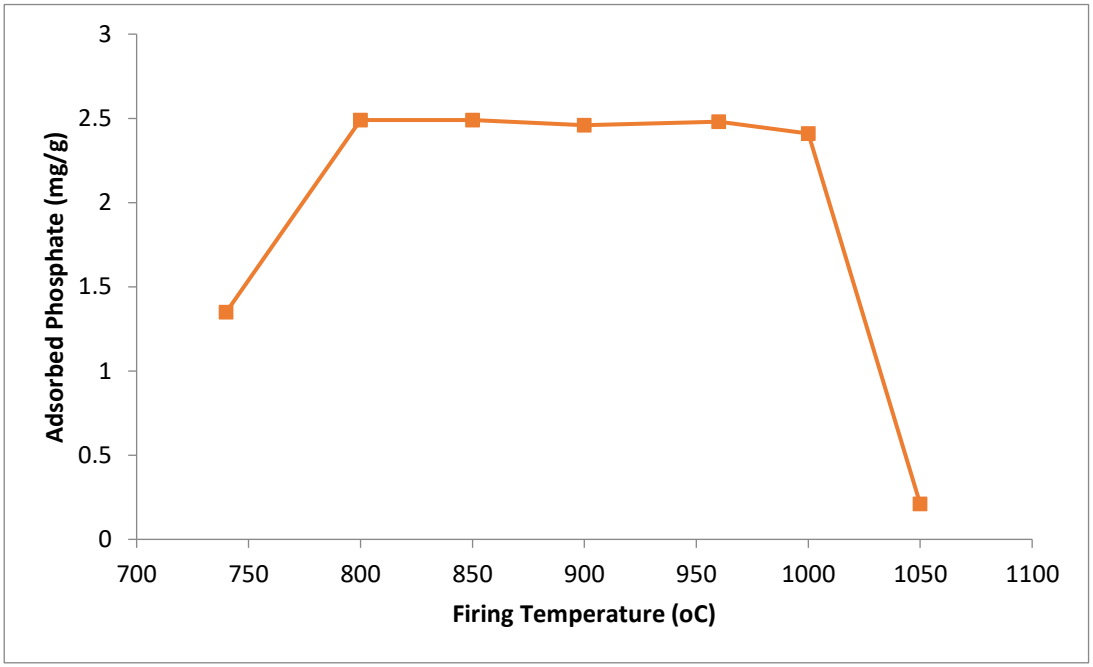

Figure 5.3: The effect of firing temperature on the adsorption of phosphate FCP using standard experimental conditions

The adsorption of phosphate increased from 1.35 to 2.49 mg/g as the firing temperature increased to 750 to 800^{o}C and remaining stable up to 960^{o}C before decreasing slightly to 2.41 mg/g at 1000^{o}C before declining sharply to 0.21 mg/g at 1050^{o}C.

The use of fired (calcined) materials for phosphate adsorption from wastewater has been reported: layered double hydroxides, Das (2006); alunite Ozacar (2003); dolomite Yuan *et al.* (2015), Karaca *et al.* (2006); palygorskite Chen *et al.* (2011). There has been limited research on the effect of firing temperature of clay for use as an adsorbent in water and wastewater treatment. A pivotal study in this area was the research conducted by Hauge *et al.* (1994) on defluoridation of drinking water which showed fluoride adsorption decreased with increasing firing temperature. Flouride adsorption using clay fired at 600^{o}C was found to be most effective, while those fired above 700^{o}C and above showed a decreased fluoride adsorption (Hague *et al.* 1994, Mohapatra *et al.* 2009). Tikariha and Sahu (2013) reported an increase in fluoride adsorption as firing temperature increased to 600^{o}C before declining when using clay as a low cost adsorbent for defluoridation of water. Another study

focusing on the removal of Cr(VI) using fired brick clay showed a decrease in the removal of Cr(VI) when firing temperature increased from 200^{o}C to 600^{o}C (Priyantha and Bandaranayaka 2011). These findings are contrary to results obtained in this study which showed an increase in the adsorption of phosphate with increase in firing temperature

Firing of clay generally reduces water trapped between the silicate sheets of the clay producing hard granules that, even when fully saturated with water, do not disintegrate easily (Ogutu and Williams 2009). During fluid bed drying occurring between 120^{o}C and 174^{o}C, which is the first stage of calcination, moisture content is reduced to 6% - 9% from 40% - 45% and further moisture reduction is achieved up to 0% in some cases when the temperature is between 460^{o}C and 800^{o}C. Sorption properties of clay are enhanced during firing as a result of the aggregation of clay particles creating a stable porous internal structure (Ogutu and Williams 2009). Although firing may reduce the exchange capacity of the clay, internal pores and surface binding can ensure the retention of the sorption properties. Heat treatment has been shown to cause the collapse of the interlayer in 2:1 Ca-montmorillonite through the incorporation of cations into the tetrahedral or unoccupied octahedral sheets when the firing temperature was between 200^{o}C and 400^{o}C (Bray *et al*. 1998). The physiochemical properties such as micromesopore volume, specific area and total surface acidity generally decrease with increasing temperature when the temperature exceeds 450^{o}C. Acidic binding has been shown to increase with increasing temperature particularly at the regions of dehydration and dehydroxylation occurring at 100^{0}C to 500^{o}C and 550^{o}C to 700^{o}C respectively (Noyan *et al.* 2006).

Decomposition of the silicate layer in the clay sheets and the collapse of the mesopore and micropore due to inter- and intraparticle sintering occurs when the temperature is increased causing a rapid decline in the specific surface area and specific micromesopore volume (Noyan *et al*. 2006). This could cause the sudden decline in the adsorption of phosphate using clay tiles fired at 1050^{o}C seen in this study.

5.4 Effect of Adsorbent Dosage on the Removal of Phosphates

The effect of dosage of FCP on the adsorption of phosphate from wastewater was investigated using different mass of FCP ranging from 0.5 g to 5 g; 150 ml of 50mg/L orthophosphate solution. The total amount of phosphate available for adsorption from this solution was 7.5 mg. This experiment did not test the maximum phosphate adsorption capacity of the FCP but was limited to the amount of phosphate available for adsorption; consequently the results of this experiment are discussed based on the amount of phosphate available for adsorption. The result of the experiment is presented in **Figure 5.4**.

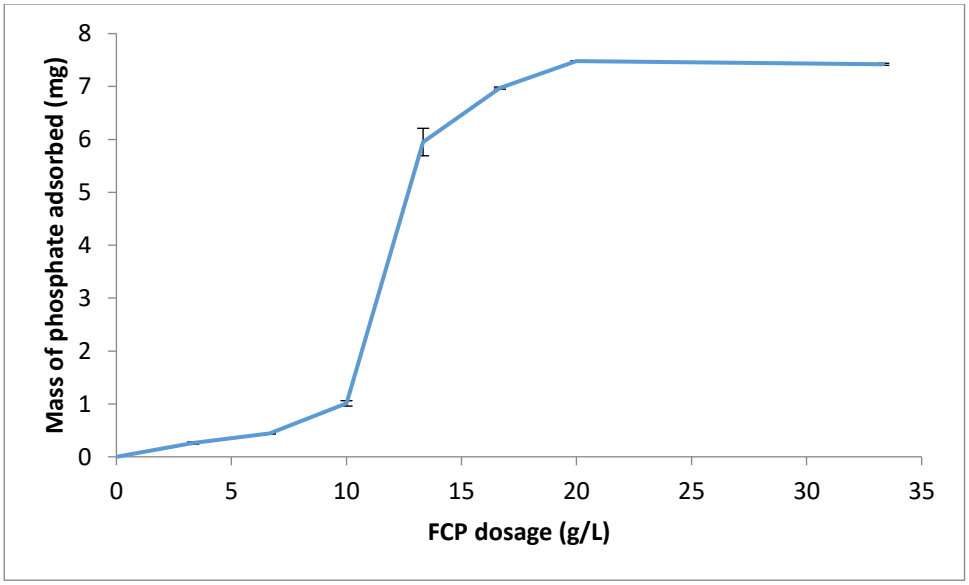

Figure 5.4: Effect of adsorbent dosage on the adsorption of phosphate by FCP using standard experimental conditions (n=3), standard error bars shown.

The adsorption of phosphate was observed to increase with an increase in dosage of FCP (**Figure 5.4)**; however, there was no change in the adsorption of phosphates between 20 and 33.33 g/L FCP. This could be attributed to the overlapping of active reaction sites as the mass of FCP increased. The increase in the dosage of FCP led to an increase in the removal efficiency of the FCP due to a greater surface area and consequently increased available binding sites for phosphates adsorption (Yadev *et al.* 2006; Yang *et al.* 2013).

As phosphate ions were taken out of solution, the rate of adsorption decreases due to the fact that although, there was still a large amount of active available reaction sites, there is a decrease in the amount of phosphate ions in solution hence

reducing the chance of phosphate ion encountering an available site to which would led to a decrease in the rate of adsorption as it progressed until the phosphate ions were completely removed.

An increase in the removal efficiency of phosphate due to an increase in the mass of adsorbent has reported by Kamiyango *et al.* (2009), Jia *et al.* (2013), Yoon *et al.* (2014), and Dey *et al*. (2014).

There was a decrease in the amount of phosphate adsorbed per unit FCP with an increase in dosage of FCP and this could be attributed to the prevalence of vacant or surplus adsorption sites and increased surface area available for adsorption (Albadarin *et al.* 2012; Ashekuzzaman and Jiang 2014). The decrease in adsorbed phosphate may also be due to the splitting effect of the concentration gradient between phosphate ions and FCP, where an increase in dosage of FCP led to a decrease in the amount of phosphate adsorbed per unit mass of FCP (Rathinam *et al.* 2010; Albadarin *et al.* 2012).

5.5 Effect of Contact Time on the Removal of Phosphate from Wastewater using FCP

5.5.1 Rate of Adsorption

An experiment was carried out to study the effect of contact time on the adsorption of phosphate by FCP. The aim of the experiment was to evaluate the effect of contact time on the removal of phosphate by FCP. The result of the experiment is presented in **Figure 5.5**.

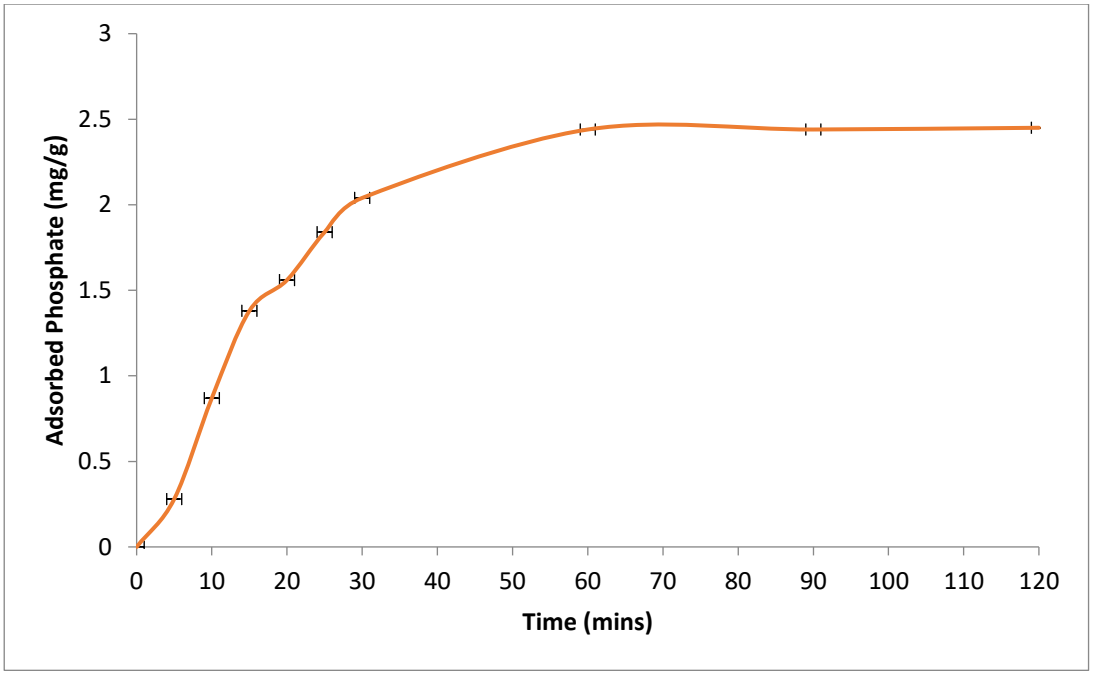

Figure 5.5: Effect of contact time on the adsorption of phosphate by FCP. This experiment was carried out using 3g clay tiles, 150 ml of 50 mg/l phosphate solution.

The kinetic profile of FCP displayed a fast uptake of phosphate in the first 30 minutes, and then plateauing as complete removal was obtained **(Figure 5.5)**. There was a fast initial adsorption period followed by a gradual uptake as the phosphate was removed from solution by FCP. This is consistent with the results obtained by Gu *et al.* (2013) who analysed removal of phosphorus and nitrogen using novel porous bricks incorporated with wastes and minerals. The method of pelletization used in this experiment provided a better performance in the removal of phosphate than conventional brick dust.

Diffusion is one of the major mechanisms for the transfer of solute onto a solid. The phosphate ions diffuse through the fluid film surrounding the tiles and through the pores to adsorption sites (Ragheb 2013). During the initial stage of the adsorption, the rate of adsorption is faster as there is a high concentration gradient between the fluid film and the available adsorption sites. The concentration gradient reduces as phosphate ions are taken out of solution thus reducing the rate of reaction until an equilibrium concentration (plateau value) is reached **(Figure 5.5)**.

The increased adsorption of phosphate with an increase in time results from a decline in the boundary layer resistance to mass transfer of phosphate in the bulk solution and an increase in the mobility of the hydrated phosphate ions (Kumar *et*

al. 2010). The results are consistent with findings reported from Sousa *et al* (2012) and Lalley *et al.* (2015).

5.6 Kinetic Models

The kinetics of the adsorption of phosphate from wastewater using FCP was examined to determine the rate order and adsorption mechanism using Pseudo-first, pseudo-second order, intraparticle diffusion, Elovich and Bangham's kinetic models.

5.6.1.1 Pseudo- First Order Kinetics

The pseudo-first order kinetic model explains the relationship between the rate the sorption sites of the adsorbents are occupied and the number of unoccupied sites. It is defined using the Lagergreen Equation as presented in **Equation 2.16**:

$$\ln (q_e - q_t) = \ln q_e - (k_1 t) \qquad \textbf{Equation 2.16} \text{ (Zhou } et\ al.\text{ 2013)}$$

Where

q_e and q_t is the amount of phosphate adsorbed at equilibrium and time t (mins)

k_1 is the equilibrium rate constant of adsorption (min^{-1}).

The linear plot of ln (qe-qt) against time **(Figure 5.6a)** was used to determine the rate constant k_1,

5.6.1.2 Pseudo Second Order Kinetics

The pseudo-second order kinetic is used to describe the dependency of the adsorption capacity of the adsorbent on time and can be calculated using the equilibrium adsorption capacity and rate constant. The pseudo-second order kinetic is expressed thus in **Equation 2.17**:

$$t/qt = 1/k_2 q_e^2 + t/q_e \qquad \textbf{Equation 2.17} \text{ (Zhou } et\ al.\text{ 2011)}$$

Where

q_t and q_e is the amount of phosphate (mg/g) adsorbed at equilibrium and time t (mins)

$k_2 q_e^2$ is the initial adsorption rate when $t \rightarrow 0$

And k_2 is the pseudo-second order rate constant (g/mg/min)

The linear plot of t/qt against time **(Figure 5.6b)** is used to determine q_e and k_2 using the slope and intercept respectively.

5.6.1.3 *Elovich Kinetic Model*

Elovich kinetic model has been used to chemisorption of gases onto heterogeneous surfaces and solid systems and it is now used to study the removal of pollutants from aqueous solutions (Yuan 2015). It is used to describe second order kinetic with the assumption that the solid surface has heterogeneous energy but do not propose any mechanism for adsorption (Mezenner and Bensmaili 2009). The Elovich kinetic model is represented as:

$$\frac{dq}{dt} = a_e^{-\alpha q}$$ **Equation 2.18** (Qiu *et al.* 2009)

Where q is the amount of amount of phosphate adsorbed at time t
a is the adsorption constant
α is the initial rate of adsorption (mg/g/min)

Integration of **Equation 2.18** assuming the boundary conditions of q= 0 at t= 0 and q= q at t= t yields

$$q = \alpha \ln(a\alpha) + \alpha \ln t$$ **Equation 2.19**

The linear form of this equation is expressed:

$$qt = \frac{ln\alpha b}{b} + \frac{1}{b} \ln t$$ **Equation 2.20 (Yakout and Elsherif 2010)**

Where α is the initial rate of adsorption (mg/g/min), and
b is related to the extent of surface coverage and activation energy for chemisorption (g/mg)

A plot of qt against ln t yields a straight line **(Figure 5.6c)** with α and b determined using the slope and intercept respectively.

5.6.1.4 *The Bangham's Kinetic Model (Pore Diffusion Model)*

The Bangham's kinetic model is used to evaluate the dominance of pore diffusion in the adsorption process (Subha and Namasivayam 2008). It is expressed as **Equation 2.21**:

$$\text{Log Log}\left[\frac{Co}{Co-qtM}\right] = \text{Log}\left[\frac{ko}{2.3.3V}\right] + \alpha \text{Log } t \qquad \textbf{Equation 2.21}$$

Where C_o is the initial concentration (mg/L)
V is the volume of the solution (ml)
M is the mass of the adsorbent (g/L)
qt is the amount of phosphate adsorbed at time t, and
k_o and α are constant

The plot of Log Log [C_o/ (C_o- Mqt)] against Log t **(Figure 5.6d)** yields a straight line and k_o and α were determined from the slope and intercept

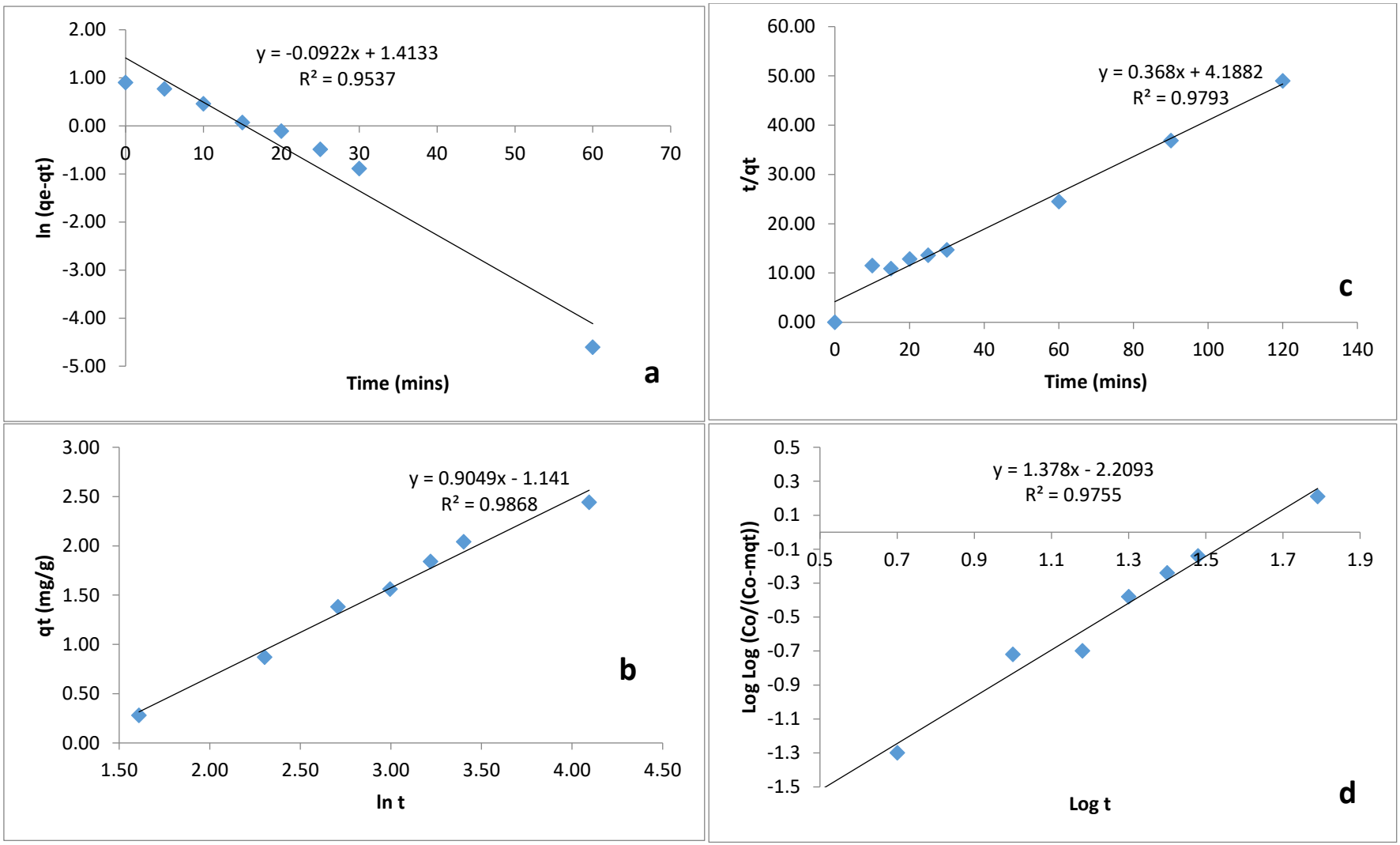

Figure 5.6: Kinetic model plot for the adsorption of phosphate using FCP: a) Pseudo-first order kinetic model; b) Pseudo-second order kinetic model; c) Elovich kinetic model; and d) Gangham's kinetic model

A pseudo-first order plot of ln (qe-qt) against t showed a linear relationship that fits the experimental data. The first order rate constant and the equilibrium adsorption capacity qe **(Table 5.1)** were calculated from the slope of the graph. The R^2 value for FCP was 0.98 showing a better fit than the pseudo second order kinetic model. The better fit shown by the pseudo first order model indicates that individual phosphate ions were adsorbed onto individual adsorption site on the surface of and within the tile which does not allows for the formation of binuclear bonding (Yaghi and Hartikainen 2013; Cheung 2001).

The pseudo-second order plot of t/qt also showed a strong linear relationship with R^2 value of 0.95 and the theoretical qe of FCP was not close to the experimental data **(Table 5.1)**. It could be assumed that each phosphate ion is adsorbed onto two adsorption sites on the surface of the tile which allows the formation of a stable binuclear bond. Another assumption of the pseudo second order kinetic is based on the chemisorption being the rate limiting step.

Table 5.1: Kinetic model adsorption parameters of adsorption of phosphate onto FCP. Adsorption conditions: initial concentration 50mg/l, pH 6.7, adsorbent dose 20g/l, room temperature

Kinetic Model	Parameter	FCP
	Q_e exp (mg/g)	13.24
Pseudo- first order	K_1 (/min)	0.02
	q_e (mg/g)	10.85
	R^2	0.9794
Pseudo- second order	k_2 (g/mg/min)	0.03
	q_e (mg/g)	2.72
	h (mg/g/min)	0.71
	R^2	0.9537
Elovich Model	α (mg/g/min)	0.32
	b (g/mg)	1.10
	R^2	0.9872
Bangham's model	k_o (mL/g/L)	0.41
	α	0.11
	R^2	0.9755

The applicability of Elovich equation to the kinetic data shows that Elovich equation can be used to describe properly the kinetics of phosphate adsorption on FCP (Mezenner and Bensmali 2009; Yakout and Elsherif 2010). The kinetic plot of the Elovich showed a strong linear relationship with R^2 value of 0.99 when FCP was

used, the kinetic parameters obtained from the Elovich equation are listed in **Table 5.1**. The correlation coefficient of Elovich kinetic model was better than all the kinetic models studied. This indicates that diffusion was a rate limiting step, and could be said that diffusion was not the only rate limiting step and other mechanisms are involved in the adsorption process (Singh and Majumder 2015).

The Bangham's kinetic showed a good linear relationship with R^2 values of 0.98 using FCP. The good linearity of the kinetic plot shows Bangham's Equation could be used to describe the kinetics of the adsorption, however, the better R^2 value of FCP (0.99) for the Elovich kinetic model indicates that although pore diffusion was involved in the adsorption of phosphate, it was not the only rate controlling step.

5.6.1.5 *Intra-particle Diffusion*

The adsorption mechanism of solute onto an adsorbent can be described using the intra particle diffusion theory proposed by Weber and Morris (1963), the model is expressed as **Equation 2.22**:

$$q_t = K_{di}\sqrt{t} + C_i \qquad \textbf{Equation 2.22} \text{ (Acelas } \textit{et al.} \text{ 2015)}$$

Where

K_{di} is the intra-particle diffusion rate constant (mg g^{-1} $mins^{-0.5}$)
C_i is the intercept
And *t* is time (mins)
The plot of the adsorbate uptake qt (mg/g) against the square root of time (minutes) $\sqrt{t}$ results in a linear relationship and K_{di} and C values were obtained from this plot.

A plot of the qt against $\sqrt{t}$ should yield a linear relationship if intra-particle diffusion is involved in the adsorption of phosphate by the clay tiles. A line passing through the origin indicates that intra-particle diffusion is the rate controlling step and the slope of the linear curve is the diffusion rate constant. When the line does not pass through the origin, it shows a degree of boundary layer control indicating that intra-particle diffusion is not the only rate controlling step and other kinetic models may be operating simultaneously to control the rate of reaction (Mezenner and Bensmaili 2009). The slope of the plot indicates the rate constant of intra-particle diffusion

while the intercept is proportional to the thickness of the boundary layer (Haung *et al.* 2014).

The model is based on a two phase uptake process: the mass transfer of phosphate molecules from the bulk phosphate solution to the clay surface and then the intra particle diffusion of phosphate molecules on the FCP (Zhou *et al*. 2013). The intra-particle diffusion of adsorption of phosphate by FCP is shown in **Figure 5.7**.

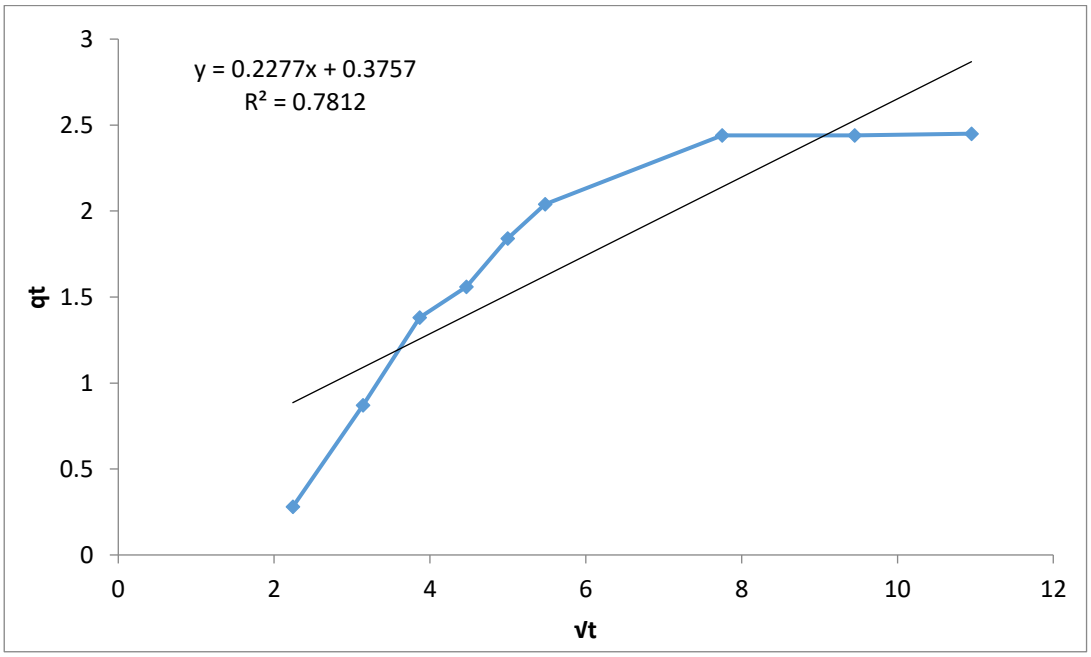

Figure 5.7: Intraparticle diffusion model plot of qt (mg/g) against t1/2 (mins) for the adsorption of 50mg/l phosphate solution using 3g FCP.

The plot in **Figure 5.7** show a multi-linear profile that do not pass through the origin and indicated a poor fit (R^2 = 0.78). The profile for FCP shows a multi-step process, where the initial section could be described as the area of fast uptake as a result of the boundary layer diffusion on the surface of the FCP involving the mass transfer of phosphate molecules from the aqueous solution to the clay surface. This is due to the initial concentration of the phosphate solution. The second stage of the profile shows a gradual adsorption of phosphate in which the rate of adsorption is limited by the intra-particle diffusion (Huang *et al.* 2014). The latter stage shows a decreasing adsorption as a result of the low residual phosphate concentration in the solution (Huang *et al.* 2014, Ifelebuegu 2012).

This profile indicates that other mechanisms could be involved in the adsorption process as the value of *C*, rate constant of intra-particle diffusion was 0.27. If the value of *C* was zero then the adsorption rate of the entire adsorption process would governed by intra-particle diffusion (Huang 2014).

5.7 Effect of pH on Phosphate Adsorption

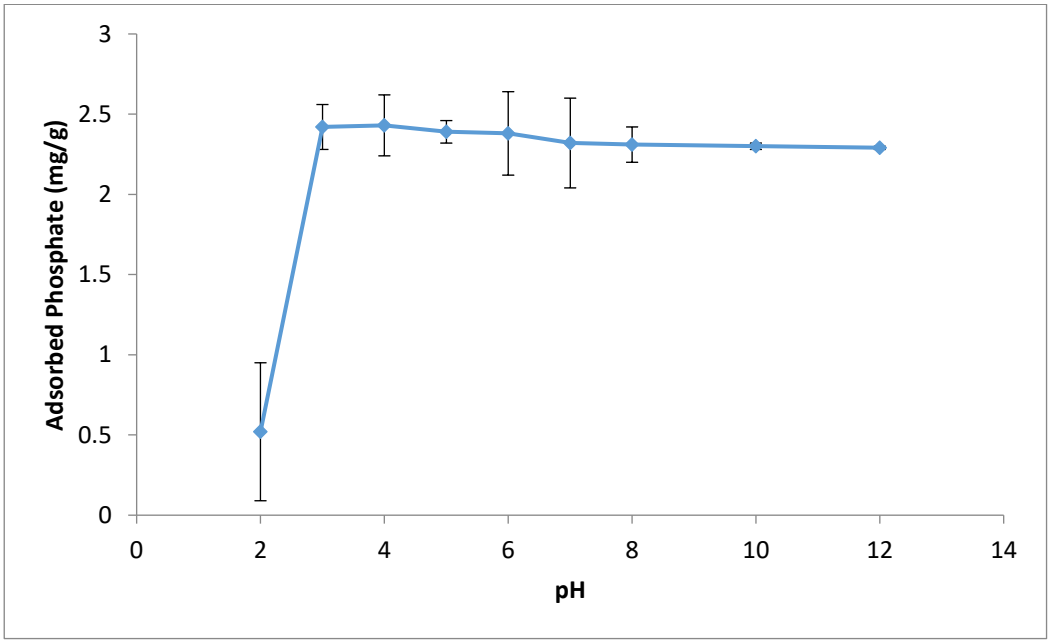

Figure 5.8: Effect of pH on the removal of phosphate by FCP using standard experimental conditions (n=3), standard error bars shown.

The effect of pH on phosphate adsorption was studied at pH between 2 and 12 using 150 ml of 50mg/l phosphate solution. It was observed that phosphate adsorption increased sharply when pH increased from 2 to 3, followed by a slight decline as pH increased to 12 **(Figure 5.8)**. The highest level of phosphate adsorption was achieved at pH 4. The results obtained were consistent with the study by Rout *et al.* (2014) on the mechanism for the adsorption of phosphate onto solid waste. Phosphate adsorption with other water-adsorbent interfaces is strongly dependent on pH (Das *et al.* 2006; Tian *et al.* 2009). The general trend reported for the effect of pH on phosphate adsorption follows the pattern described in **Figure 5.8**, however, it is suggested that phosphate adsorption can occur within two pH ranges (Kamiyango *et al.* 2009) although phosphate adsorption across three pH ranges have also been known to occur (Petrik 2005 cited in Taylor 2005:30). Haung *et al.* (2008) reported phosphate adsorption using red mud decreasing with

increasing pH, due to the alkaline properties of red mud at low pH resulting in greater adsorption of acidic ions. This contradicts the results of this study as 91% removal was obtained at pH 12. The high removal efficiency at pH 12 could be attributed to the effect of calcium ions on the adsorption process. The final pH of the solution was found to increase from 3 to 11.78 **(Figure 5.9)**

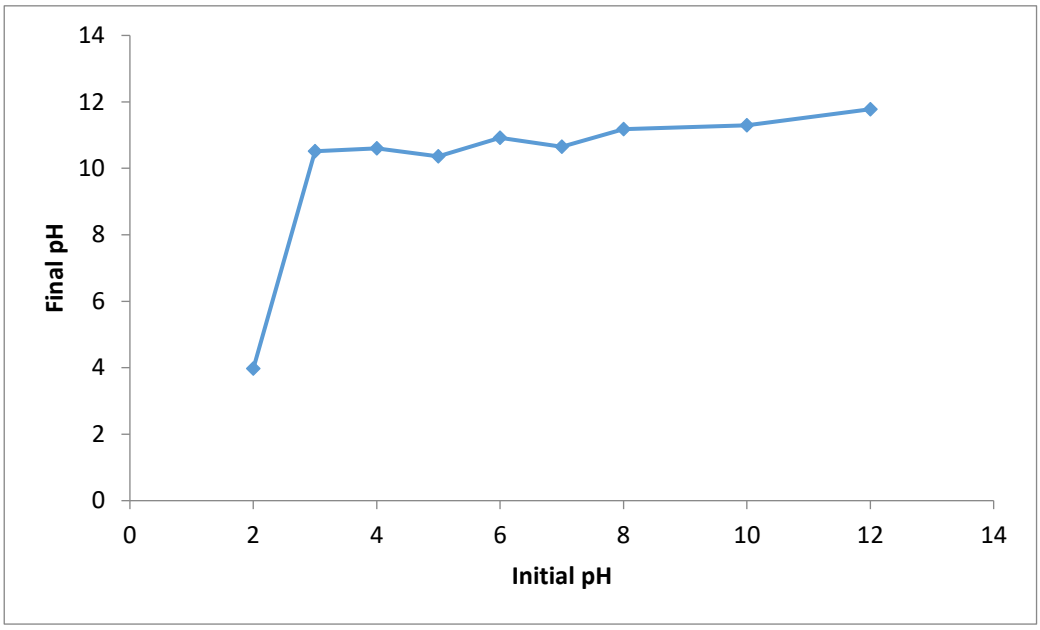

Figure 5.9: Final pH of phosphate solution at the end of contact using FCP.

An increase in the pH of the solution could also be due to the release of hydroxyl ions from the surface of the clay (Boujelben *et al.* 2008). Phosphate adsorption is found to generally decrease with increase in pH (Goldberg and Sposito 1985) and phosphate ions could be adsorbed when net negative surface charge exists. This could be attributed to the adsorption of protonated anions on negatively charged surface after the dissociation of the protons. These protons would react with the hydroxyls found on the surface of the FCP to form water which are the readily replaced by anions (Goldberg and Sposito 1985). The ligand exchange is used to describe this process. Ligand exchange refers to the adsorption mechanism that occurs when anions with specific affinity for metal ions in a hydroxylated mineral enter the coordination layer of its surface to adsorb disproportionately to its activity in an aqueous solution (Goldberg and Sposito 1985).

The increase in the pH could also be attributed to the increase in Ca^{2+} ions in the solution as a result of dissolution of Ca^{2+} from the surface of the clay tile. The

concentration of Ca^{2+} was found to increase from 6,277 mg/kg to 26,100 mg/kg at the end of contact.

Clay used in FCP predominantly contains oxides of metals such as Ca, Fe and Al; and nonmetals such as Si. These oxides play a role in phosphate adsorption as they are hydroxylated when in contact with water and positive or negative charged developed on the interface depending on the pH (Mall *et al.* 1996). The positive charged interface serves as bonding sites for phosphates adsorption.

The results obtained for the study indicate a region of high removal efficiency between pH 4 and 8. Different phosphate adsorption mechanisms are assumed to be responsible for phosphate uptake at different pH as phosphate can exist as $H_2PO_4^-$, PO_4^{3-} and HPO_4^{2-} depending on the pH of the solution (Das *et al.* 2006; Huang et al 2014). The high phosphate adsorption observed at pH 4 suggests the surface of the tiles served as an active adsorption site for the bonding of monovalent $H_2PO_4^-$, replacing hydroxyl ions (OH^-) on the tile surfaces as described by ligand exchange mechanism (Yoon *et al.* 2014). This could also be attributed to the accumulation of positive charges on the surface of the FCP which increased its attraction for negatively charged phosphate ions (Xue *et al*. 2009; Agyei *et al.* 2002; Goldberg and Sposito 1985). Another possible explanation is at lower pH, the FCP surface carries a more positive charge and thus attracting more negatively charged monovalent $H_2PO_4^-$ ions in solution (Chikratar 2006). As the pH increases, the surface of the FCP becomes more negatively charged resulting in the increased repulsion between the negatively charged phosphate ions and the FCP surface (Xue *et al.* 2009; Ou *et al*. 2007).

The surface charge of the FCP is dependent on the pH, at lower pH the surface is positively charged and at higher pH the surface is negatively charged. Surface charges on the FCP are produced as a result of the hydrolysis of the Si-OH or Al-OH bonds along the clay lattice (Ismadji *et al.* 2015). These charges could be negatively or positively charged depending on the pH of the solution and the structure of the silica.

The zero point of charge refers to the pH at which the total net charge of the surface of the clay is zero. The zero point charge of the clay tiles was 8.13 and was determined using the method described by Rivera-Utrilla *et al.* (2001) and is within

the range reported for smectite which is the predominant mineral found in the clay (Mnasri *et al.* 2014; Arfaoui *et al*. 2012). When the pH is less than pH_{zpc} the clay surface has a net positive charge and the propensity to attract anions increases. When pH is greater than pH_{zpc} the clay surface is negatively charged and the attraction of anions decreases. Phosphate adsorption in this study was found to be higher at pH lower than pH_{zpc}. This result is consistent with results reported by Moharami and Jalali (2013) and Kamiyango *et al.* (2009).

The presence of positive charged H^+ is another possible mechanism for phosphate adsorption at lower pH. These ions when in solution can induce the formation of protonated surfaces which supports the electrostatic attraction of phosphate species to the tile surface (Huang *et al* 2014).

Figure 5.10: pH range for phosphate adsorption by different species Source: Petrik Laboratories Inc. In Taylor (2005)

Phosphorus adsorption is believed to be dominated by different species at different pH **(Figure 5.10)**. Fe dominates phosphate adsorption at pH range of 5 and below while Al dominates between pH 5 and 6 while Ca is primarily responsible for adsorption at pH above 7 (Petrik 2005 cited in Taylor 2005:30). Calcium is believed to possess a higher ability to form complexes with phosphate hence precipitating it out in solution at pH between 8.5 and 10 (Nassef 2012). Increased phosphate removal with increasing pH was reported by Chen *et al.* (2013) using hydrothermally

modified oyster shell material, phosphate adsorption was found to be at its maximum at pH 11.

The result presented in this study show the highest phosphate adsorption occurred at pH 4 **(Figure 5.8)**, and it can be assumed that phosphate adsorption at this pH was controlled primarily by Fe^{3+} and has been reported to be the dominant species responsible for phosphate fixation at pH 5 and below (Li *et al.* 2014; Yoon *et al.* 2014; Boujelben 2008) **(Figure 5.10)**. Aluminium has also been reported to be responsible for phosphate adsorption at low pH (Tanada *et al*. 2003). Several studies have also shown that improved phosphate adsorption at pH between 4 and 5 can also be attributed to Al as shown in Figure 6.5.3. A study conducted by Altundogan and Tumen (2001) reported improved phosphate adsorption under acidic conditions with the maximum phosphate adsorption occurring at pH 4.5. Another study on the adsorption of phosphate using aluminium pillared bentonite reported a maximum phosphate adsorption at pH 3 (Yan et al 2010).

Phosphate adsorption at pH 2 was lower than other pH and this could be due to The prevalence of $H_2PO_4^-$ as the predominate form of phosphate ion at lower pH which has a weak interaction with the cationic group thereby leading to the decreased adsorption seen.

Aluminium could be assumed to be the most likely cation responsible for phosphate adsorption at pH between 5 and 7 shown in Figure 6.5.1.

5.8 Effect of Temperature on the adsorption of phosphate by FCP

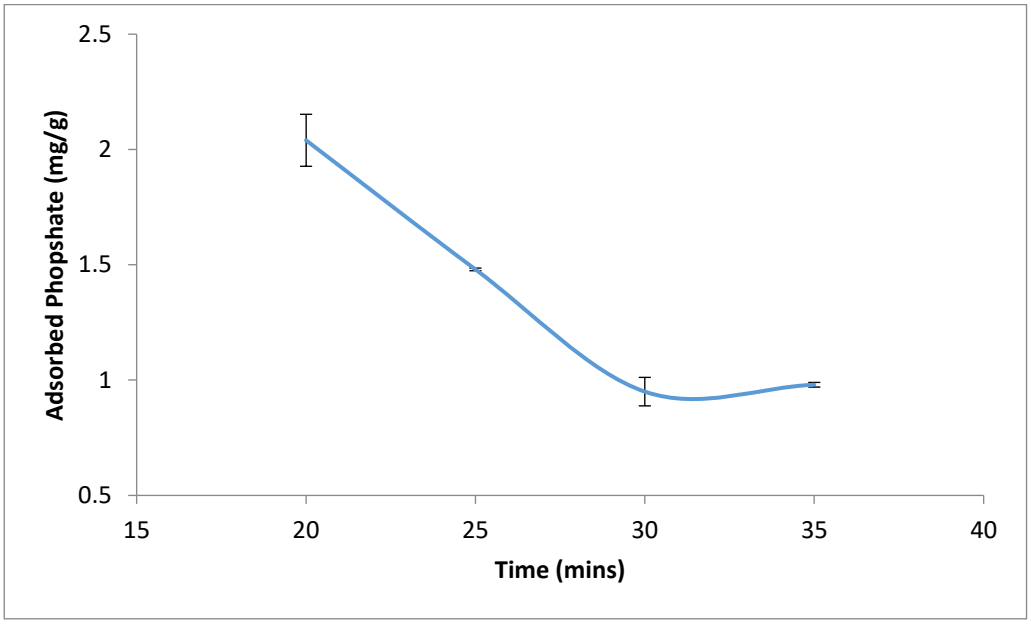

Figure 5.11: The effect of temperature on the removal of phosphate by brown clay tiles using standard experimental conditions (n=3) standard error bars shown.

Phosphate adsorption was found to decrease with increase in temperature **(Figure 5.11)** suggesting an exothermic reaction between the phosphate molecules and clay surface (Tian *et al.* 2009, Das *et al.* 2006). This indicates a low energy requirement for the adsorption of phosphate by FCP, i.e. phosphate adsorption is favoured at lower temperature The decrease in adsorption with increase in temperature could be also be attributed to an increase in the rate of desorption of the adsorbed phosphate from the surface of the FCP (Mall *et al*. 1996). An increase in the number of adsorption sites influenced by the disintegration of some of the internal bonds around the edge of the active sites of the FCP as a result of the exothermic nature of the adsorption could be responsible for the increased adsorption of phosphates at lower temperature observed in this study.

Adsorption reactions are normally thought to be endothermic reactions with the rate of adsorption increasing with increasing temperature (Zeng *et al.* 2004; Namasivayam and Prathap 2005; Huang *et al.* 2008); however, phosphate adsorption has also been shown to be exothermic in nature. Das *et al.* (2006) using double layered hydroxides to remove phosphate from aqueous solution; Kose and Kivanc (2011) using calcined waste eggshell and Yuan *et al.* (2015) using dolomite

mineral reported a decrease in phosphate adsorption with increasing temperature. These results are similar to those obtained in this study.

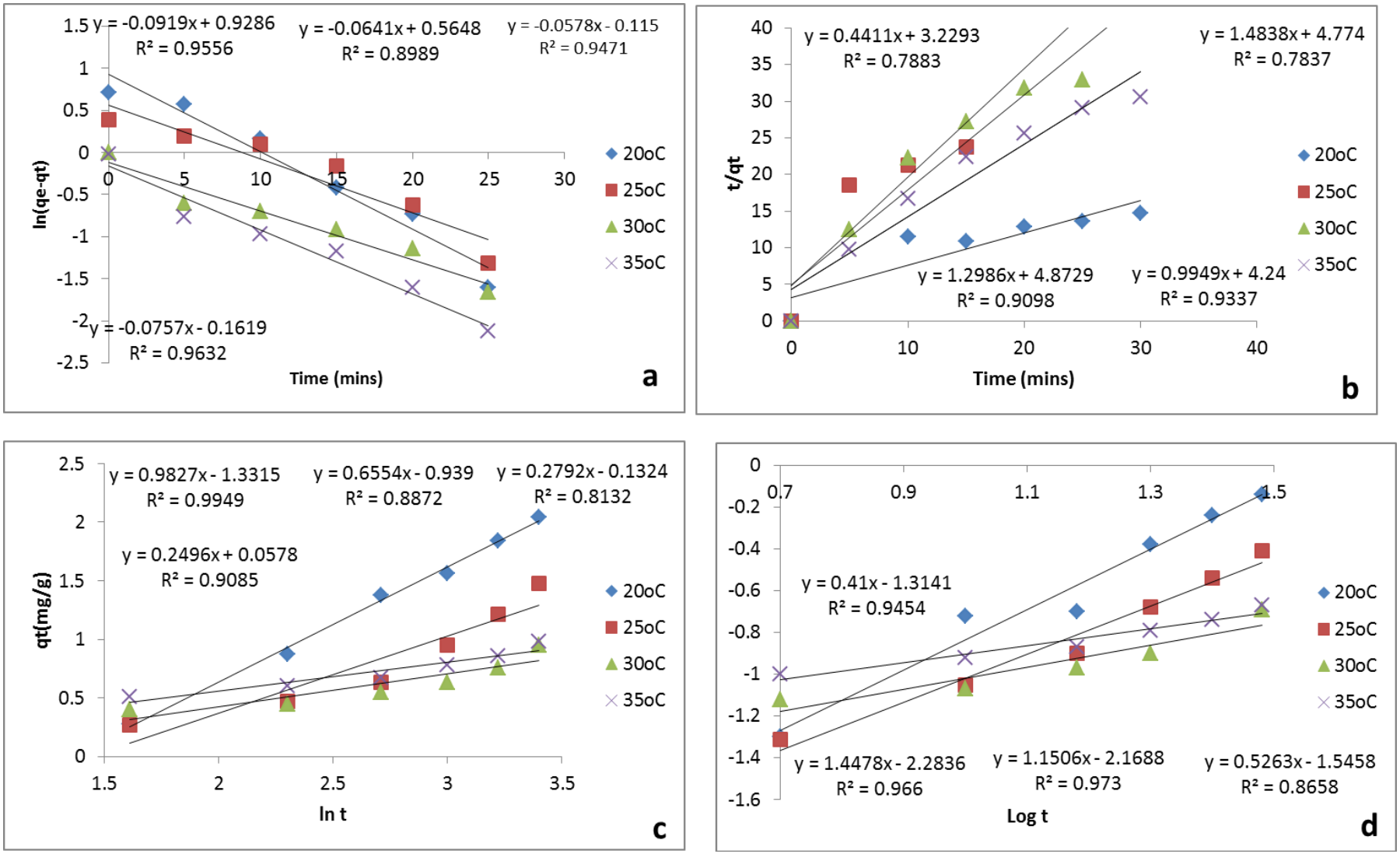

Figure 5.12: Kinetic model plot for the adsorption of phosphate using FCP: a) Pseudo-first order kinetic model; b) Pseudo-second order kinetic model; c) Elovich kinetic model; and d) Gangham's kinetic model.

5.8.1 Kinetic Model

The data obtained in **Section 5.6** were analysed using the kinetic models described earlier in **Section 5.4.2 (Figure 5.12)** and the kinetic parameters are presented in **Table 5.2.**

Table 5.2: Kinetic model adsorption parameters of adsorption of phosphate onto clay pellets at different temperature. Adsorption conditions: initial concentration 50mg/l, pH 6.7, adsorbent dose 20g/l

Kinetic Model	Parameter	20°C	25°C	30°C	35°C
	Q_e exp (mg/g)		13.24		
Pseudo- first order	K_1 (/min)	-0.006	-0.023	-0.031	-0.041
	q_e (mg/g)	52.00	15.60	17.30	13.32
	R^2	0.9556	0.8989	0.9471	0.9632
Pseudo- second order	k_2 (g/mg/min)	0.06	0.46	0.35	0.23
	q_e (mg/g)	2.27	0.67	0.77	1.00
	h (mg/g/min)	0.31	0.21	0.21	0.24
	R^2	0.7883	0.7837	0.9098	0.9227
Elovich Model	α (mg/g/min)	0.26	2.56	0.88	1.06
	b (g/mg)	1.02	1.53	3.58	4.01
	R^2	0.9949	0.8872	0.8132	0.9085
Bangham's model	k_o (mL/g/L)	73.47	54.58	29.24	26.03
	α	0.10	0.11	0.21	0.27
	R^2	0.966	0.973	0.8658	0.9454

The pseudo-first order kinetic plot showed a good fit for all temperature studied except 25 °C indicating the applicability of the pseudo-first order kinetic model to the study. The values of K_1 decreased from -0.006/min to -0.041/min as temperature increased from 20 to 35 °C confirming phosphate adsorption decreased with increase in temperature **(Table 5.2)**. Conformity to pseudo-first order kinetic model normally indicates the adsorption process is usually physisorption. This indicates a loose binding between the phosphate and FCP, probably due to electrostatic attraction between them, in which there is little perturbation in the electronic structure of phosphate and FCP. It also indicates electrons are not shared or exchanged between phosphate and the adsorbent.

The pseudo-second kinetic plot did not show a good fit using the experimental data. R^2 was between 0.79 and 0.93. The k_2 value was found to decrease from 0.41 g/mg/min to 0.23 g/mg/min when the temperature increased form 20°C to 35°C confirming the decrease in phosphate adsorption with increase in temperature. The initial rate of adsorption h also decreased from 0.31 (mg/g/min) to 0.21 mg/g/min when the temperature increased from 20°C

to 30°C. The poor fit of the pseudo-second order kinetic model to the adsorption data indicates the removal mechanism was not chemisorption.

The adsorption data from the study did not give a good correlation using the Elovich kinetic model indicating the model could not be used to de describe the result. The values of b increased from 1.02 g/mg at 20°C to 4.01 g/mg at 35°C indicating there were more available sites for phosphate adsorption (Yakout and Elsherif 2010). The fluctuation in the value of α as temperature increased could mean the rate of desorption was greater than adsorption resulting in the decrease in adsorption with increase in temperature. The R^2 values indicated diffusion could be a mechanism for adsorption, but it was not the rate limiting stem and other mechanisms were involved.

The Bangham's kinetic model showed a good correlation with R^2 values >0.9 except for 30°C. The good linearity shows the model can be used to describe the kinetics of phosphate adsorption using FCP. The k_o value decreased from 73.47 mL/g/L to 26.03 mL/g/L when the temperature increased form 20°C to 35°C and the value of α increased with increase in temperature.

The good correlation of the Bangham's kinetic model indicates that pore diffusion was a rate controlling step. As the pseudo-first order kinetic model also showed a good linearity, it could be said the adsorption mechanism was a physical process with pore diffusion as a rate limiting step.

5.8.2 Thermodynamic Parameters

The temperature dependence of the adsorption process is often associated with changes in the thermodynamic parameters. These parameters include Gibbs free energy (ΔG^o), enthalpy (ΔH^o) and entropy (ΔS^o) and are used to determine the spontaneous nature of the adsorption process and evaluate the applicability of the adsorbent (Huang *et al.* 2015). The parameters were determined using the following **Equations 3.14-3.16**:

$$\Delta G = -RT \ln(kd) \qquad \textbf{Equation 3.14}$$

$$\Delta G^o = (\Delta H^o) - (\Delta S^o) \qquad \textbf{Equation 3.15}$$

$$-RT \ln(kd) = (\Delta H^o) - T(\Delta S^o) \qquad \textbf{Equation 3.16}$$

Where

R is the universal gas constant (joules/mole/K)

T is temperature in Kelvin (K)

Kd (qe-CT) is the quantity of phosphate adsorbed on to the clay tile (1/g)

A plot of ln Kd against 1/T **(Figure 5.13)** using data obtained in **Figure 5.12a**, yielded a straight line graph showing a linear relationship between the logarithm of the rate constant and the inverse of temperature with ΔH^o and ΔS^o values calculated from the slope and intercept of the Van't Hoff plot and ΔG was calculated using **Equation 3.14** (Ifelebuegu 2012, Mezenner and Bensmaili 2009). The thermodynamic parameters for the adsorption of phosphate by FCP are shown in **Table 5.3**.

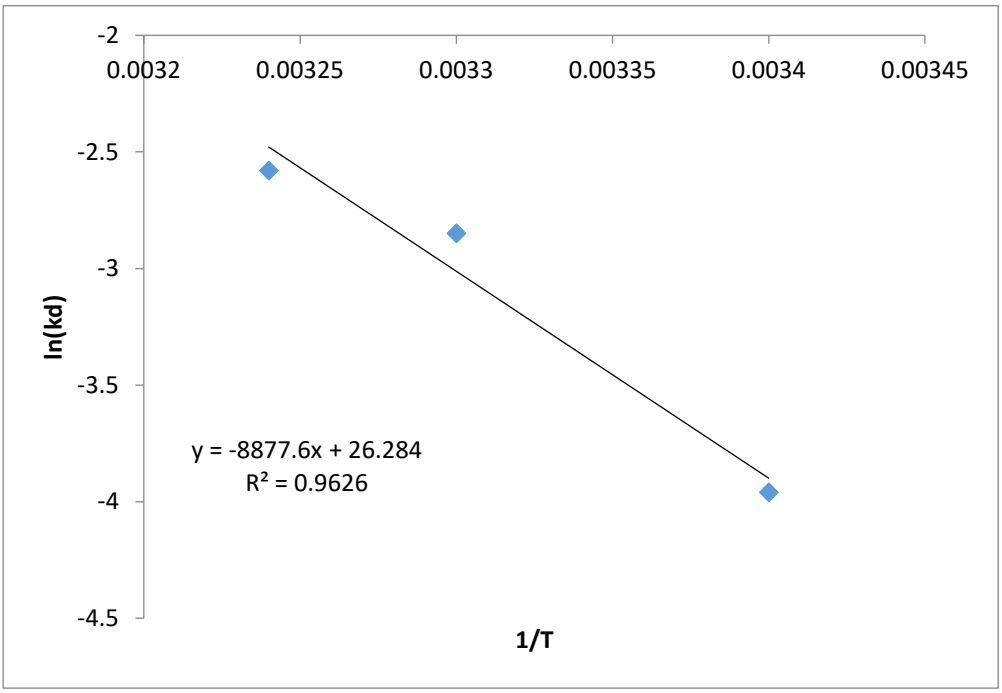

Figure 5.13: Van't Hoff plot for the adsorption of phosphate by FCP.

Table 5.3: Thermodynamic parameters for the adsorption of phosphate by FCP.

Temp (°C)	ΔG^o (KJ/mol)	ΔH^o (KJ)	ΔS^o (KJ/mol)
20	-16.5	-8.87	0.026
25	-16.63		
30	-16.76		
35	-16.89		

The value of ΔG^o obtained at all temperature studied was negative, this indicated the spontaneous nature of the adsorption of phosphate onto FCP and adsorption was a thermodynamically favourable process **(Table 5.3)**. The decrease in the ΔG^o from -16.5 KJ/mol to -16.89KJ/mol implied an increase in the spontaneity of the adsorption process at higher temperature confirming a decrease in adsorption as the temperature increased and was similar to those obtained by the use of mixed lanthanum/aluminum pillared montmorillonite for the adsorption of phosphate (Tian *et al* 2009). The values of ΔG^o suggests a physisorption process as values of ΔG^o for physisorption process are generally between -20 KJ/mol and 0 KJ/mol. The negative value of ΔH^o (-8.87KJ) confirmed the exothermic nature of the process. The positive value of ΔS^o indicated the increased randomness at the solid-solution interface during the adsorption of phosphate onto FCP and a good affinity of phosphate ions towards the FCP (Huang 2015). The negative value of the activation energy E_a (-0.22J/mol) indicated the absence of an energy barrier and confirmed the exothermic nature of the adsorption process.

5.9 Effect of initial concentration on the adsorption of phosphates by FCP

The effect of initial concentration on the adsorption of phosphates by clay tiles was studied using 200ml of 100, 250, 500, 750 and 1000mg/L phosphate solution and the total reaction time was 72 hours.

5.9.1 Effect of initial concentration on the adsorption of phosphate

The effect of initial concentration on phosphate adsorption was assessed by varying the concentration of ortho-phosphate solution while maintaining all other experimental conditions. The result from this experiment was also used to evaluate the adsorption isotherms. The removal efficiency of FCP was observed to increase as the initial concentration decreased **(Figure 5.14)**. However, complete phosphate removal was obtained using all concentrations of phosphate solution except when 750 mg/L and 1000 mg/L was used.

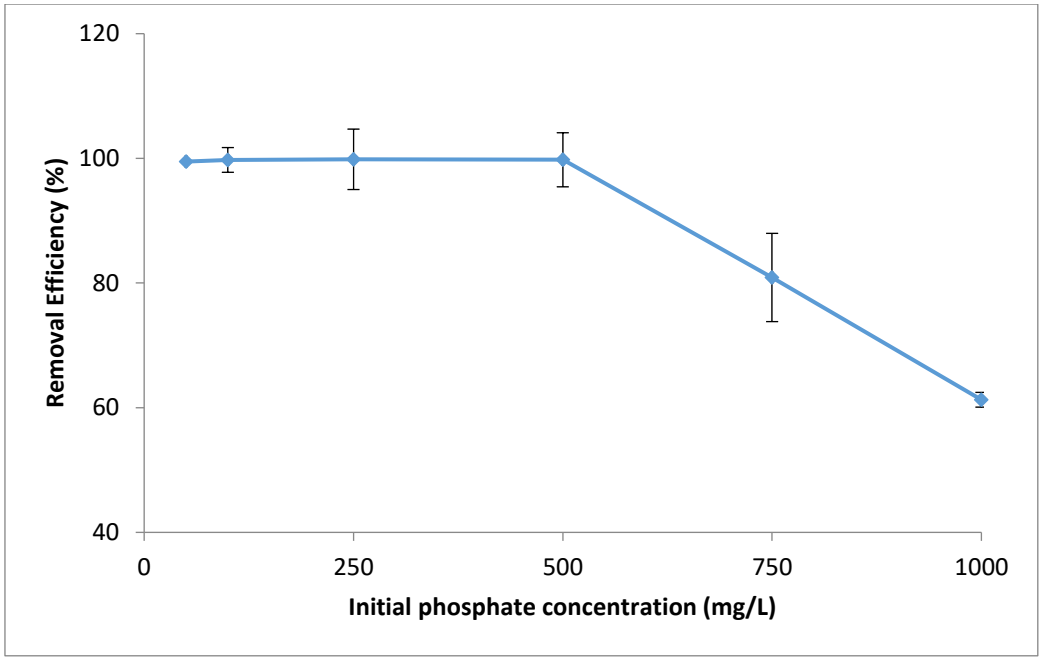

Figure 5.14: Effect of initial concentration on removal efficiency of clay pellets using 5g FCP and 200ml phosphate solution (n=3), standard error bars shown.

Adsorption saturation could not be reached under lower initial concentration due to the availability of more reaction sites when compared to the amount of phosphate molecules present in the solution (Rout *et al* 2014). This resulted in higher removal efficiency or complete removal obtained using lower initial concentration of phosphate solution. As the initial concentration increased, the amount of free active adsorption sites declined and were harder to find due to the fixed number of total available adsorption sites for any given mass of adsorbent (Das *et al.* 2006); thus there was increased competition between phosphate molecules for these available active sites at a higher concentration resulting in the reduced removal efficiency seen as the initial concentration increased.

The difference in the extent of phosphate adsorption could also be attributed to the fact that all the adsorption sites are initially vacant and the concentration gradient of the solute is relatively high. As the extent of adsorption decreases over time, the remaining vacant surface adsorption sites are difficult to occupy due to the repulsive forces that exist between the phosphate ions adsorbed to the surface of the FCP and the bulk solution (Mezenner and Bensmaili 2009).

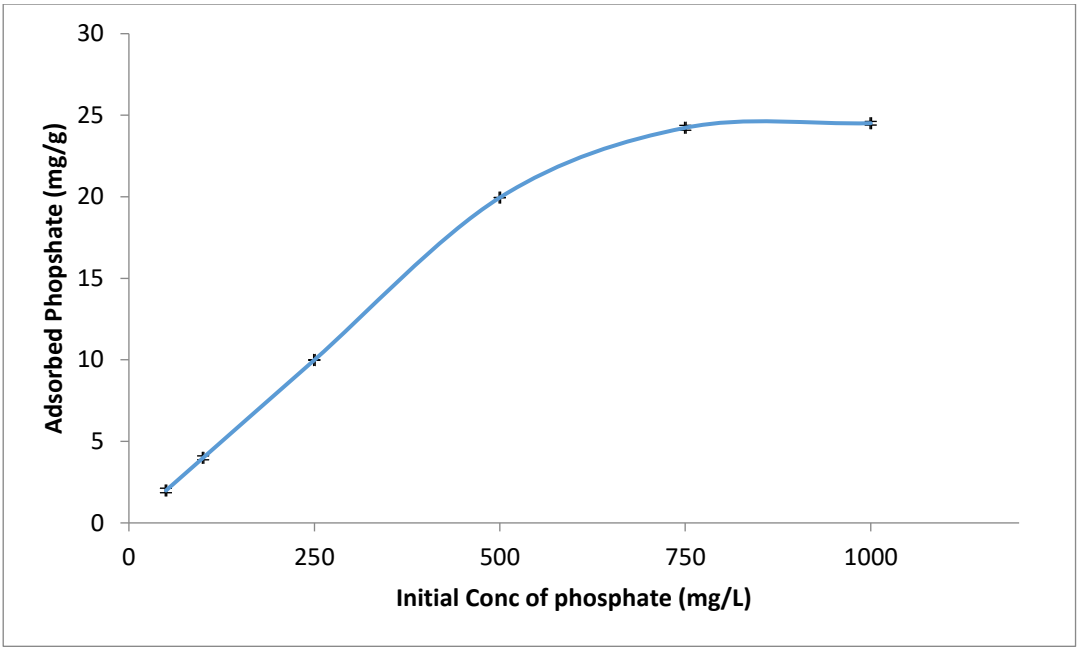

Figure 5.15: The effect of initial concentration on amount of phosphate adsorbed by FCP using 5g clay pellets and 200ml phosphate solution (n=3), standard error bars shown.

The amount of phosphate adsorbed by FCP was found to increase with increasing concentration **(Figure 5.15)**. This was due to an increase in the number of phosphate ions available for binding unto the active sites of the FCP surface resulting in a higher probability of collision between the phosphate ions and the surface of the FCP (Dawodu and Akpomie (2014). The increase in the phosphate ion concentration resulted in a corresponding increase in the generation of driving force required to lower the mass transfer resistance between the FCP and the phosphate solution (Albadarin *et al.* 2012, Hameed and El-Khaiary 2008).

Another possible explanation could be attributed to the fact that at lower concentration the ratio of phosphate ions to available surface area is large; consequently phosphate adsorption is dependent on the initial concentration of the solution (Arivoli *et al.* 2014). As the concentration increases, the ratio of available reaction sites to phosphate^{-} ions reduces causing adsorption of phosphate to be dependent on the amount of phosphate ions present.

5.9.2 Adsorption Isotherm

The adsorption data using FCP discussed in the **Section 5.9.1** were analyzed using Langmuir, Freundlich, Tempkin and Dubinin-Radushkeivich Isotherm models to determine the model that best fit the adsorption of phosphate onto FCP. Results are presented in **Figure 5.16.**

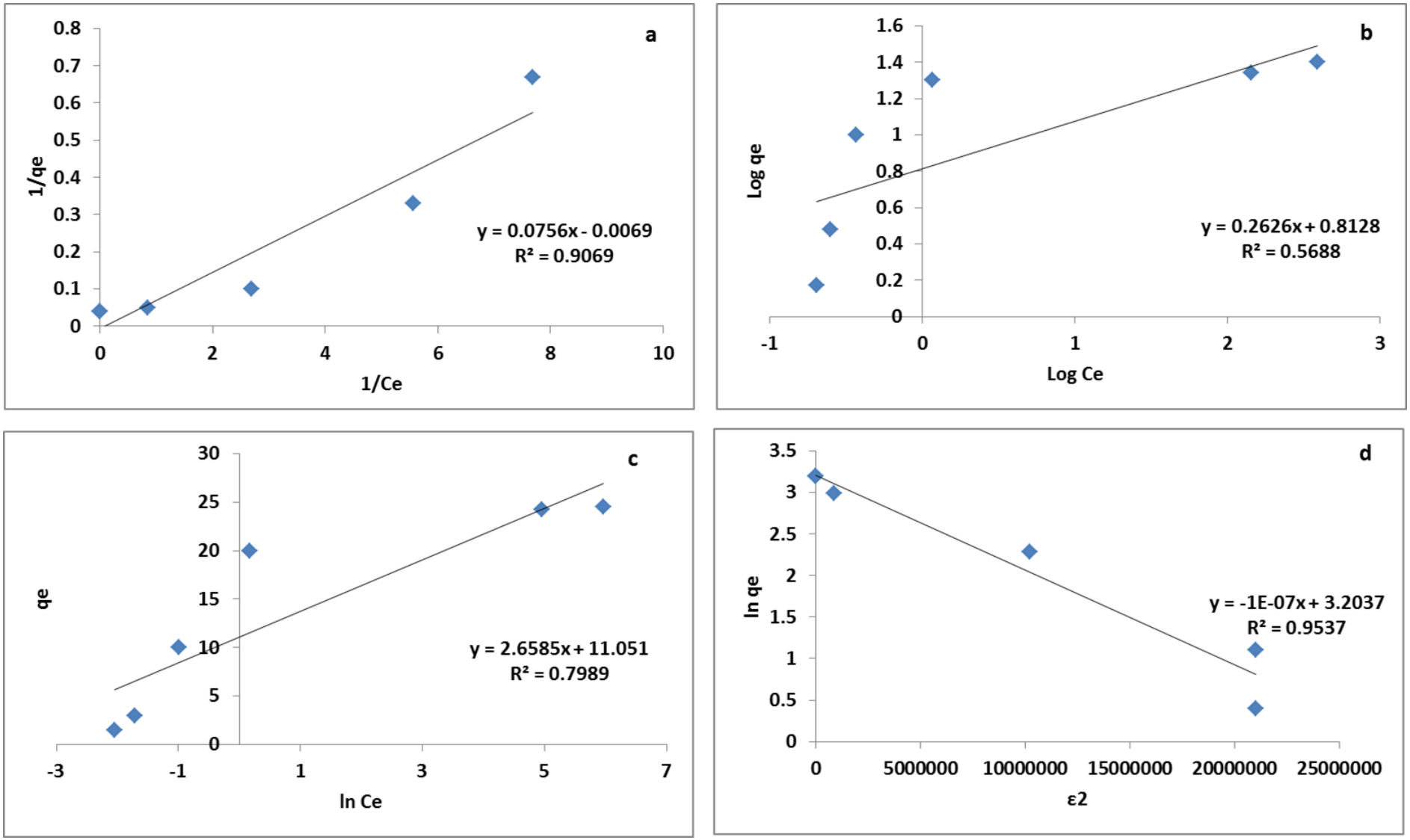

Figure 5.16: The adsorption isotherm plots for the adsorption of phosphate using FCP: a) Langmuir adsorption isotherm; b) Freundlich adsorption isotherm; c) Tempkin; and d) Dubinin-Radushkevich adsorption Isotherm

The maximum adsorption capacity, Q_m (13.23 mg/g) was determined from the slope of Langmuir isotherm **(Figure 5.16a).** K_L and R_L was determined as 0.09 L/mg and 0.02 respectively **(Table 5.4)**. Langmuir isotherm had a better fit than Freundlich and Tempkin models. This indicates a monolayer adsorption where phosphate ions are adsorbed on identical and equivalent localized sites on the FCP without lateral interaction between the adsorbed phosphates and the adjacent sites. The R_L value was less than 1 indicating phosphate adsorption using FCP was a favourable process. The Q_m implies a significant potential for phosphate removal from wastewater using FCP on an industrial scale and is similar to results obtained by Yan *et al*. (2014) on the removal of phosphate from etching wastewater using calcined alkaline residue. Q_m obtained using FCP (Q_m = 13.23 mg/g) was higher than those using brick dust (Q_m = 5.35 mg/g) in **Section 4.3.4.1,** this indicates FCP developed in this study showed a better performance that the conventional brick dust used in Chapter 4.

Dubinin-Radushkevich (D-R) isotherm model was employed to determine the nature of the adsorption of phosphate on FCP. The R^2 value of D-R isotherm was higher than Langmuir isotherm **(Figure 5.16d)**. The value of E is used to predict the type of adsorption, E value < 8 kJ/mol is classified as physical adsorption. The value of E in this study was 2.87kJ/mol indicating the adsorption was a physical process **(Table 5.4).** This confirms result of the kinetic study which showed the adsorption was physisorption. The E value obtained in this study is similar to result obtained by Kose and Kivanc (2011).

Freundlich isotherm model is used to determine the heterogeneity of the adsorption surface. The adsorption data did not fit the isotherm as the R^2 for Freundlich isotherm was lower than all the isotherms studied **(Figure 5.16b)**. Adsorption intensity n is used to describe the heterogeneity of the adsorption surface, a smaller 1/n value indicates a more heterogeneous surface and an n value between one and ten indicates a favourable process. The value of 1/n and n in this study was 0.26 and 3.81 respectively showing the surface was heterogeneous and adsorption was favourable **(Table 5.4)**.

Tempkin adsorption can be used to determine heat of sorption which could be used to describe the adsorption process. Tempkin isotherm did not give a good fit with

the experimental data **(Figure 5.16c).** A_T and *B* value were 1.08 L/mg and 35.58 J/mol respectively **(Table 5.4).** The positive value of *B* means the adsorption was exothermic confirming the result of the kinetic study.

Table 5.4: Adsorption isotherm constants for the adsorption of phosphate onto FCP

Adsorption Isotherm Model	Parameter	FCP
Langmuir Isotherm	Q_m (mg/g)	13.23
	K_L (L/mg)	0.09
	R_L	0.02
	R^2	0.9096
Freundlich Isotherm	k_f (mg/g)	6.50
	$\frac{1}{n}$	0.2626
	n	3.81
	R^2	0.5688
Temkin Isotherm	A_T (L/mg)	1.08
	b	68.50
	B (J/mol)	35.58
	R^2	0.7989
Dubinin-Radushkeivich Isotherm	B (mol^2/kJ^2)	0.06
	E (kJ/mol)	2.87
	R^2	0.9537

5.10 Effect of perforation

FCP showed an improved performance in the removal of phosphate when compared with conventional brick dust in wastewater treatment. Adsorption takes place on active sites on the adsorbent. These sites, however, are limited based on the amount and corresponding surface area of the adsorbent. An increase in the active sites of the adsorbent would consequently increase adsorption as there would be more active sites for the adsorption of phosphate. Perforation of the pellets could lead to an increase in the number of available active sites for adsorption thereby increasing phosphate adsorption.

To study the effect of perforation on the adsorption of phosphates, an experiment was designed to artificially increase the pores of the clay tile. RO water was added to the clay to improve manageability, after incorporating the water into the clay, it was spread using a squeegee unto metal grid described earlier in this chapter, and hair brush with different sized bristles and wire brush were rolled over it, creating

holes on the clay as it rolled along. The clay was left for air dry for 2 days and fired using the firing programme described in **Section 3.2.2**. The pellets produced using perforation with a hair brush was designated as HB pellets while those produced using wire brush was designated WB pellets. Results are presented in **Figure 5.17**.

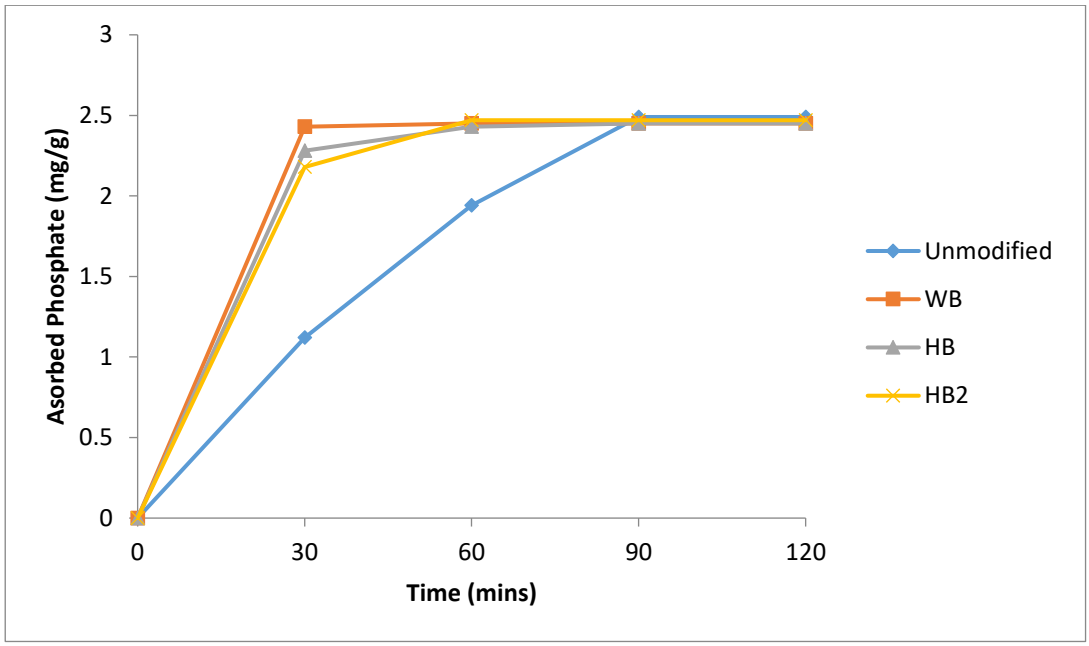

Figure 5.17: The effect of perforation on the adsorption of clay pellets using standard experimental conditions

There was an increase in the performance of the tiles with perforation and the performance increased with perforation **(Figure 5.17)**. Complete phosphate adsorption was achieved by the perforated pellets after 30 minutes; consequently there was the need to study the rate of reaction of the perforated pellets within 30 minutes **(Figure 5.18)**.

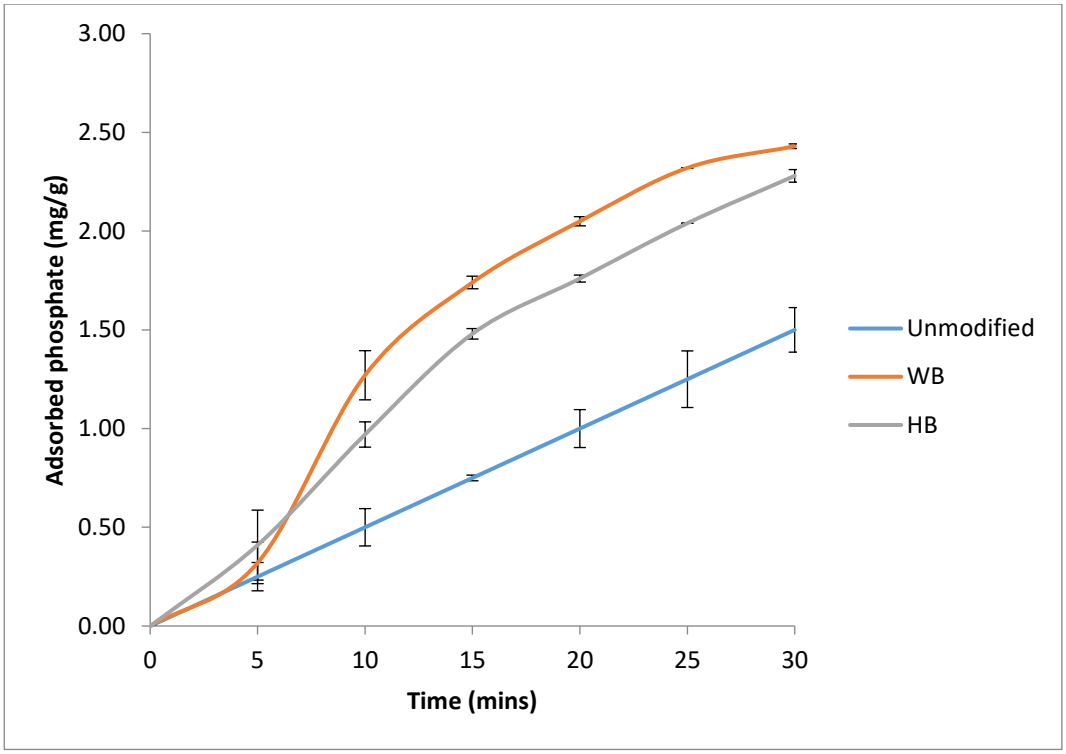

Figure 5.18: The effect of perforation on the performance of clay tiles within 30 minutes (n=3) standard error bars shown.

The performance of the tiles increased with increase in the perforation. The increase in the adsorption of phosphate from the solution could be due to the increase number of adsorption sites as a result of the increase in the size and quantity of the pores in the perforated clay. There is no study where an adsorbent was artificially perforated hence there was not data to compare this result.

The data obtained were analysed using the kinetic models described earlier in **Section 4.8 (Figure 5.19)** and the kinetic parameters are presented in **Table 5.5.**

Table 5.5: Kinetic model adsorption parameters of adsorption of phosphate onto perforated clay pellets at different temperature. Adsorption conditions: initial concentration 50mg/l, pH 6.7, adsorbent dose 20g/l

Kinetic Model	Parameter	Unmodified	Hair Brush Perforated	Wire Brush Perforated
Pseudo- first order	K_1 (/min)	-0.024	-0.028	-0.024
	q_e (mg/g)	18.73	8.26	11.24
	R^2	0.9519	0.9393	0.9627
Pseudo- second order	k_2 (g/mg/min)	0.062	0.074	0.06
	q_e (mg/g)	1.27	2.65	2.50
	h (mg/g/min)	0.10	0.52	0.38
	R^2	0.5626	0.5859	0.7979
Elovich Model	α (mg/g/min)	0.57	4.63	3.85
	b (g/mg)	2.22	0.84	0.95
	R^2	0.8574	0.9942	0.9921
Bangham's model	k_o (mL/g/L)	42.51	99.03	68.3
	α	7.29	10.69	7.8
	R^2	0.9633	0.9839	0.9983

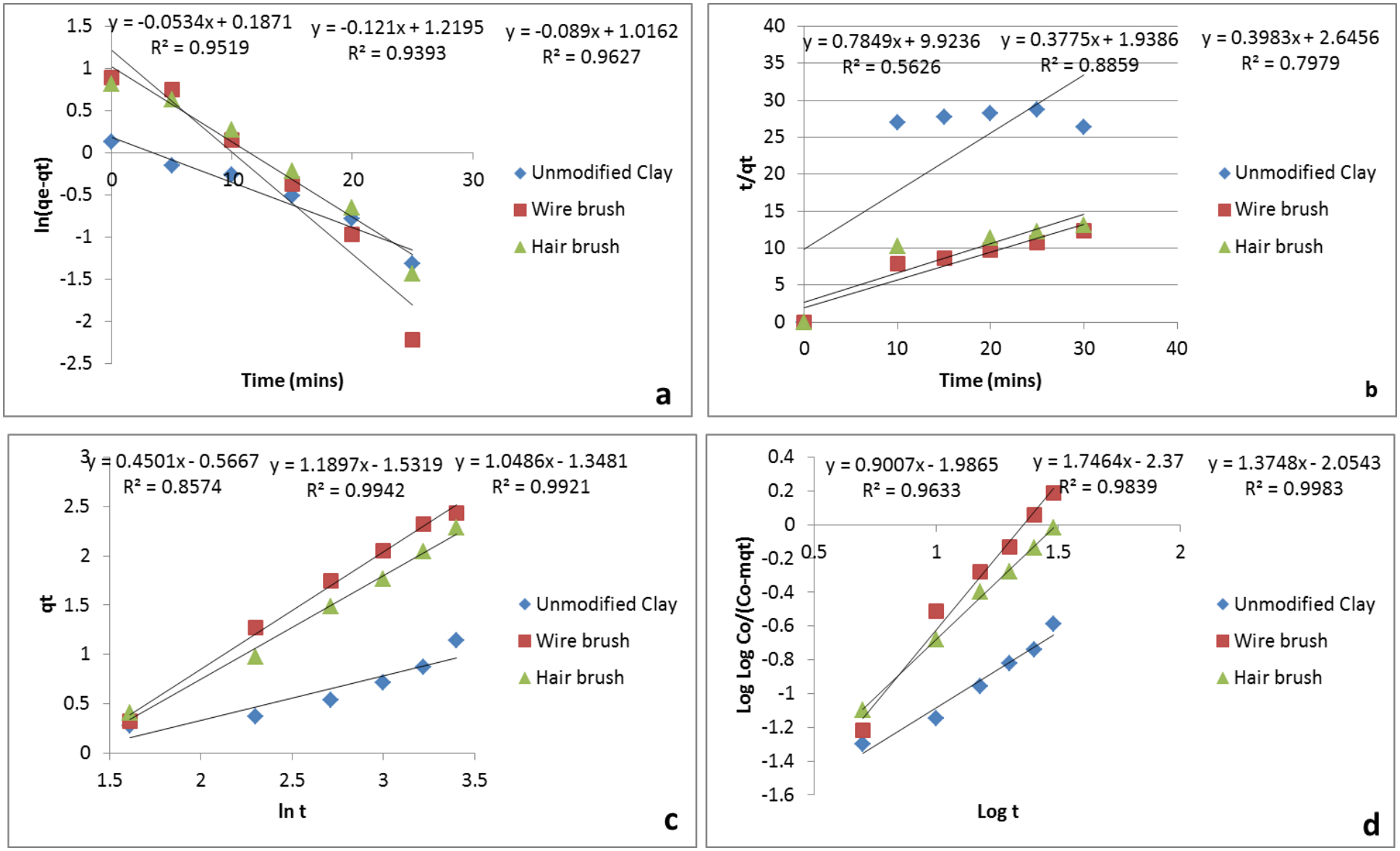

Figure 5.19: Kinetic model plot for the adsorption of phosphate using perforated FCP: a) Pseudo-first order kinetic model; b) Pseudo-second order kinetic model; c) Elovich kinetic model; and d) Bangham's kinetic model

The pseudo-first order kinetic plot showed a good correlation of the experimental data which shows the applicability of the adsorption data to the model. The R^2 value was >0.9 in all cases **(Figure 5.19a).** The k_1 value decreased from -0.024 t0 -0.028 when the pellets were perforated **(Table 5.5).** The better fit also showed each phosphate ion was adsorbed on individual sites on the pellet as explained in Section 5.4.2; and the mechanism for adsorption could be physisorption.

The pseudo-second-order kinetic model did not show a good correlation of the experimental data **(Figure 5.19b)**. The low correlation coefficient showed the model could not be used to describe the adsorption and the adsorption mechanism was not chemisorption.

The applicability of the Elovich kinetic model to the experimental data was indicated by the good linearity of the plot of qt against ln t **(Figure 5.19c).** The R^2 value of the HB and WB tiles were >0.99. The initial rate of adsorption α increased from 0.57 mg/g/min to 4.63 mg/g/min and 3.85 mg/g/min when HB and WB were used respectively, while the value of b reduced from 2.2 g/mg to 0.84 g/mg and 0.95 g/mg **(Table 5.5)**. This means the rate of adsorption was higher than desorption leading to increased adsorption when the perforated pellet was used (Yakout and Elsherif 2010).

The Bangham's kinetic model showed good linear relationship with the data indicating its applicability in describing the adsorption process (**Figure 5.19d)**. This means pore diffusion was a pore controlling step but as the Elovich and pseudo-first-order also showed good linearity particularly when using the perforated pellets, it could be said pore diffusion was not the only limiting step but other mechanisms were involved in the adsorption.

5.11 Summary and Conclusion

This study showed the potential of fired clay pellets for use for phosphate removal in wastewater treatment. Phosphate adsorption increased with increase in firing temperature from 750 ^oC to 800 ^oC before decreasing as the firing temperature increased from 1000 ^oC to 1050 ^oC. At 1050 ^oC, the adsorption capacity of the pellets had deteriorated due to the decomposition of the silicate layer in the clay sheets and the collapse of the mesopore and micropore due to sintering from

increased firing temperature. An earlier attempt to fire the pellets at 1200^{o}C resulted in the vitrification of the pellets.

Phosphate adsorption increased with increase in contact time and adsorbent dosage. Acidic pH favoured adsorption with pH 3-4 as optimum, adsorption declined slightly in neutral and alkaline pH but phosphate removal was greater than 90% at all pH except pH 2. Perforation of the pellets before firing increased phosphate adsorption.

Adsorption followed pseudo-first order rate kinetics and was spontaneous and exothermic (Gibbs free energy -16.5 kJ/mol, and enthalpy -8.87 kJ/mol). Adsorbed phosphate increased with increased in initial concentration of phosphate but removal efficiency decreased with increase in phosphate. The experimental data showed good correlation with Langmuir and Dubinin-Radushkeivich isotherm and Q_m derived from Langmuir isotherm was 13.23 mg/g. The adsorption was predominantly by physisorption supported by some diffusion. Perforation of the clay pellets improved the performance in the removal of phosphate. This study developed a method of palletization that provided better performance than conventional brick dust for the removal of phosphate in wastewater treatment.

Pellets used in this study have shown the potential for use in removal off phosphate in wastewater treatment. In a bid to further improve the performance of the pellets, the composition of the elements responsible for phosphate adsorption (Al, Ca, and Fe) will be modified in order to maximise the phosphate adsorption capacity of the pellets. The effect of modification of the elemental composition of the pellets will be explored further in the next chapter to determine the elemental composition that will ensure optimum adsorption.

6 Evaluation of the impact of compositional modification on the adsorptive properties of clay pellets

6.1 Introduction

An improvement in the removal of phosphate in water treatment was obtained using pellets developed in the preceding chapter. The maximum adsorption capacity increased to 13.23 mg/g when compared to 5.35 mg/g obtained using conventional brick dust. This improvement can be further enhanced through the modification of the pellets by varying the composition of the elements responsible for adsorption of phosphate.

Aluminium, calcium and iron are elements often credited with phosphate sorption and it is assumed that if these elements are present in any medium in a substantial amount, then that medium can be used as a substrate for phosphate removal (Fondu *et al.* 2010). Studies have been conducted using various low cost adsorbents containing considerable quantities of one or more of these elements for the removal of phosphates in wastewater treatment. These adsorbents include alunite (Ozacar 2006), zeolite (Jiang *et al.* 2013), LECA (Vohla *et al.* 2005; Johansson 1997), ochre (Littler *et al.* 2013), red mud (Huang *et al.* 2008), clay (Kamiyango *et al.* 2009) and fired clay pellets (Edet *et al*. 2016).

The modification of any adsorbent could be done through acid or heat treatment of the material, coating with metal salt or exchanging a layer in the adsorbent as obtained in pillaring. Pillaring is the interchanging of a layer in the structure of an absorbent mostly clay. Pillared clays are synthesised by exchanging Ca^{2+}, K^{+} or Na^{+} present in the clay with hydroxyl cations of Fe, Al, Ti (Baksh *et al.* 1992). The polycations of these multivalent metals act as “pillars” between the clay layers which give rise to modified clay known as pillared clays (PILCs) with high specific surface area and permanent porosity, and on calcination the resulting material have metal oxide pillars which prop open the clay sheets, exposing the internal surfaces of the clay layers (Shanableh and Elsergany 2013; Baksh *et al.* 1992). In principle, any metal oxide or salt that can form polynuclear species on hydrolysis can be inserted as pillars (Tian *et al*. 2009) and all layered clay of the phyllosilicate family and other layered clay can be used as host (Baksh *et al.* 1992).

Clays in the natural phase consist of aluminous silicates and in this phase, the cationic metal of Al^{3+}, Mn^{3+} and Fe^{3+} are available as hydroxides (Dable *et al.* 2008). Ion exchange has been proposed as a possible removal mechanism for phosphate adsorption by clays. It is assumed an exchange occurs between PO_4^{3-} and OH^- located on the positively charged surface of the clay (Tian *et al.* 2009). The ion exchange mechanism is represented by a simplified reaction as follows:

Clay-Metal ≡ OH^- + PO_4^{3-} ↔ Clay–Metal ≡ PO_4^{3-} + OH^- **(Equation 6.1)** Shanableh and Elsergany (2013).

The performance of adsorbents can be enhanced through modification of the adsorbent, and one of the methods of modification is the change in the composition of the adsorbent. The objective of this experiment was to explore ways of modifying the composition of the key elements of Al, Ca, and Fe within the parent clay to determine the extent and rate of adsorption in order to maximize phosphate adsorption. The modification of the clay was done through the addition of Aluminium sulphate ($Al_2(SO_4)_3$, Calcium carbonate ($CaCO_3$), Iron (III) chloride ($FeCl_3$) and Iron (II) sulphate ($FeSO_4$) as these elements have been known to be crucial in increasing the phosphate adsorption capacity and these salts have been used in conventional wastewater treatment for the removal of phosphate. The salts were added to clay before firing using the programme outlined in **Section 3.2.2**. SEM micrograph images of the modified FCP are presented in **Figure 6.1a-f.**

Figure 6.1: SEM micrographs of the modified fires clay pellets (a) AlMFCP before adsorption; (b) AlMFCP after adsorption; (c) CaMFCP before adsorption; (d) CaMFCP after adsorption; (e) FeMFCP before adsorption; (f) FeMFCP after adsorption

The SEM micrographs of the modified pellets **(Figure 6.1 a-f)** revealed surface morphology that was rough and irregular. The rough textured surfaces acted as adsorption sites for the uptake of phosphate. The micrographs obtained after

adsorption showed buildup of deposit with the deposit on FeMFCP showing a more even distribution.

6.2 Effect of $Al_2(SO_4)_3$ modification on the performance of fired clay

The effect of aluminium modification on the performance of FCP in the adsorption was investigated by the addition of Aluminium sulphate ($Al_2(SO_4)_3$). One of the commonly used salts for the precipitation of phosphate in WWTWs is Aluminium sulphate. 0.5, 1. 2.5, 5 and 10 g of $Al_2(SO_4)_3$ was added to 50 g of clay, equating to 0.04, 0.08, 0.2,0.4 and 0.8 g of Al respectively was added to the clay. The result of this study is presented in **Figure 6.2**.

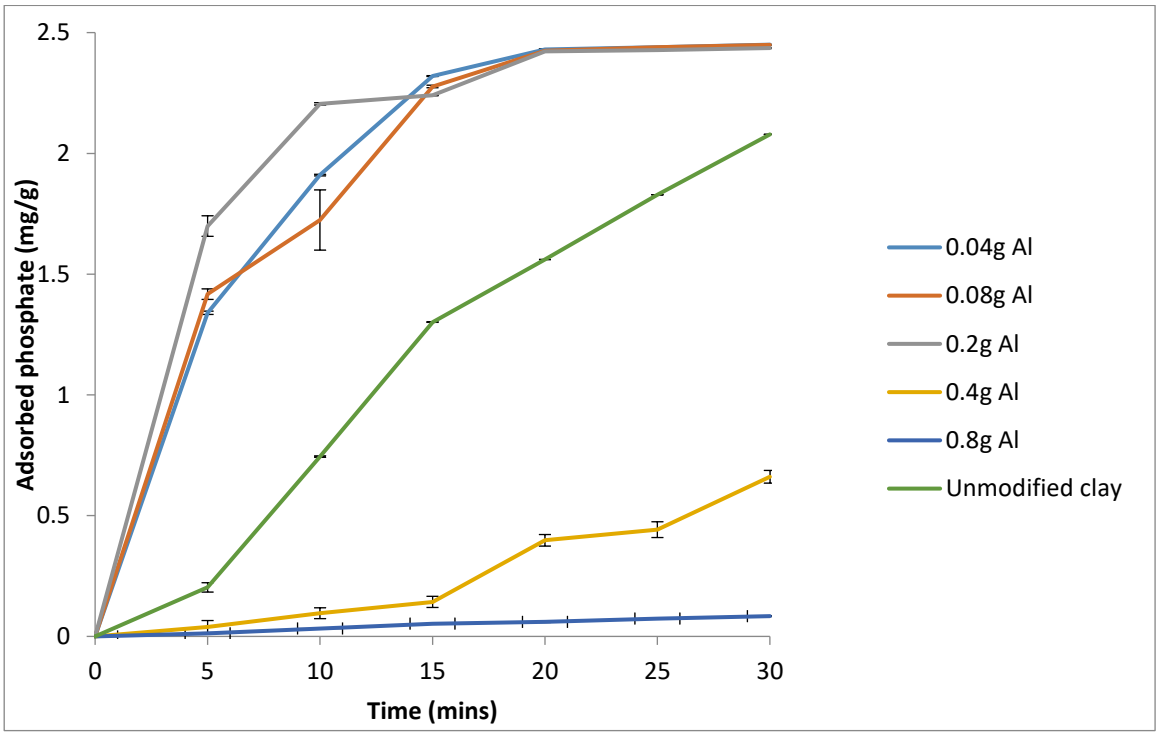

Figure 6.2: Effect of $Al_2(SO_4)_3$ modification on the adsorption of phosphate by FCP using standard experimental conditions (n=3); standard error bars shown.

Addition of $Al_2(SO_4)_3.16H_2O$ was shown to improve the performance of clay tile in the adsorption of phosphate from wastewater **(Figure 6.2)**. The increase in Al concentration was found to have a random effect on phosphate adsorption within the first 15 minutes of contact when Al concentration was between 0.04g and 0.2g. Phosphate adsorption was highest at 10 minutes (2.21 mgP/g pellet), when 0.2 g Al was added to the clay pellets. 0.04g Al, 0.08g Al and 0.2g Al all achieved complete

phosphate removal after 20 minutes of contact. Phosphate removal was shown to decrease as the concentration of Al increased beyond 0.2g Al/g pellet.

The basic reaction between aluminium and phosphate is represented as:

$$Al^{3+} + H_nPO_4^{n-3} \leftrightarrow AlPO_4\downarrow + nH^+ \qquad \textbf{Equation 6.2}$$

$$Al^{3+} + PO_4^{3-} \leftrightarrow AlPO_4\downarrow \qquad \textbf{Equation 6.3}$$

This basic reaction involves aluminium groups on the surface of the clay pellets and phosphate ions present in solution. Surface groups on the clay pellets will ionise when contact with water causing positive aluminium groups to develop due to the protonation of the aluminium surface groups. This protonation of the aluminium groups leads to profusion of positive charges on the pellets surface that reacts with phosphate ions in solution.

The reaction between aluminium sulphate and phosphate could be expressed as:

$$Al_2(SO_4)_3.16H_2O \rightarrow Al_2O_3 + 3SO_3 + 16H_2O \qquad \textbf{Equation 6.4}$$

$$Al_2O_3.2Al(OH)_3 + 3H + 3PO_4^{3-} \rightarrow Al_2O_3)_n.Al_2(OH)_3.AlPO_4 + H_2O \qquad \textbf{Equation 6.5}$$

The interaction of Al with phosphate is usually dependent on the density of the surface charges of the Al species (Boisvert *at al.* 1997). Lowered pH usually leads to increased cationic charges hence increased phosphate removal by Al (Boisvert *at al.* 1997). Phosphate removal by Al species is believed to occur largely through the complexation due to several interactions between Al and phosphates with the concentration of Al, phosphates and pH as major determinants. Optimum pH for adsorption by aluminium ions is between pH 4-6, as adsorption has been reported to decrease as the pH increases to 7 (Nassef 2012).

Phosphate removal from wastewater is believed to occur through three mechanisms.

One of the mechanisms is the adsorption of phosphate ions onto $Al(OH)_3$. It is believed that phosphate can be removed from solution by adsorption to $Al(OH)_3$ flocs formed system through outer sphere complexation. A higher Al/P ratio is usually required for the formation of sufficient flocs. The introduction of clay allows the flocs that carry a weak positive charge to adsorb on the surface of the negatively

charged clay platelets surface and flocculation and settlement of the $Al(OH)_3$ coated clay was faster.

The addition of clay has been reported to improve the chemical precipitation of phosphate from solution. Ozacar and Sengil (2003) reported an improvement in the precipitation of phosphate from solution using $Al_2(SO_4)_3.18H_2O$ when clay was injected into the system. The addition of aluminium in the form of $Al(NO_3)_3.9H_2O$ was reported to improve the performance of mesoporous silicates in the adsorption of phosphates (Shin *et al.* 2004). The addition of aluminium to the mesoporous silicates imparted a phosphate adsorbing capacity that was previously absent. These results are similar to those reported in this study.

An increase in the concentration of the Al^{3+} has been reported to reduce the adsorption of phosphate by mesoporous silicates (Shin *et al.* 2004). The study showed a decrease in Q_m from 862µmol/g to 619µmol/g when the amount of aluminium impregnated into the mesoporous silicates increased from 10% to 30%. It was opined that the addition of aluminium increased the number of active sites present but Al_{30}-SBA-15 had less active sites than Al_{10}-SBA-15 as a result of the poor pore structure of Al_{30}-SBA-15. The mesopore structure was believed to have been partially destroyed by the attack of the surplus Al on the silicate framework. The low P/Al ratio was also suggested to have contributed to the higher phosphate adsorption exhibited by Al_{10}-SBA-15. The P/Al ratio reduced from .231 in Al_{10}-SBA-15 to 0.0556 in Al_{30}-SBA-15 as the percentage of aluminium in the mesoporous silicate increased.

In order to eliminate the deficit attributed to low P/Al ratio during phosphate removal, Ozacar and Sengil (2003) suggested an increase in the concentration of clay within the system. In a study assessing the effect of clay injection on the precipitation of phosphate, an increase in the concentration of clay from 0mg/L to 20mg/L led to an increase in phosphate removal from 50% 83% using an AL/P ratio of 1.76. The addition of 150mg/L clay to the system increased phosphate removal to 95.8%.

It was hypothesised that phosphate was removed from the solution by adsorption to $Al(OH)_3$ flocs formed system through outer sphere complexation. A higher Al/P ratio is usually required for the formation of sufficient flocs. The introduction of clay allows the flocs that carry a weak positive charge to adsorb on the surface of the negatively charged clay platelets surface and flocculation and settlement of the

$Al(OH)_3$ coated clay was faster. Osalo *et al.* (2013) reported an improvement in the performance of bentonite from 90% to 97% when 10% of the mass of bentonite was replaced with Al_2O_3.

Another reason for the decrease in phosphate adsorption at higher concentration of Al could be due to the effect of sulphate ions on the uptake of phosphate from aqueous solutions. Sulphate ions have been reported to have a variable effect on the uptake of phosphate. Kamiyango *et al.* (2009) reported increasing sulphate concentration had no effect on the adsorption of phosphate using kaolintic clay. The addition of sulphuric acid to kaolin was reported to improve the performance of the clay to remove phosphate from 45% to 75% when the concentration of the acid increased from 2M to 4M (Onu *et al*. 2015). However, an increase in the concentration of the acid beyond 4M did not improve adsorption. The improved performance of the acid modified clay was not attributed to the presence of sulphate ions in the system but to an increased H^+ concentration which enhanced the adsorption of negatively charged phosphate ions. This is contrary to the results of this study as the increase in the concentration of sulphate had variable effect on the uptake of phosphate. An increase in the sulphate concentration in the clay pellets from 0.92g/g to 4.6g/g led to a decline in phosphate sorption from 97% to 3.36%, while phosphate removal was unaffected when the sulphate concentration was between 0.23g/g and 0.92g/g clay pellet.

The presence of SO_4^{2-} has been also reported to reduce the adsorption of phosphate by aluminium pillared clays (Tian *et al*. 2009). In that study, the addition of 0.5mmol/L SO_4^{2-} was found to reduce phosphate adsorption from 92.2% to 78%.

6.3 Phosphate Adsorption using Fired Calcium Modified Clay Pellets (CaFMCP)

The effect of calcium modification on the performance of FCP in the adsorption was investigated by the addition of ($CaCO_3$) which is commonly used for the precipitation of phosphate in WWTWs. 0.5, 1. 2.5, 5 and 10 g of $CaCO_3$ was added to 50 g of clay, resulting in 0.2, 0.4, 1, 2 and 4 g of Ca added to the clay. The result of this study is presented in **Figure 6.3.**

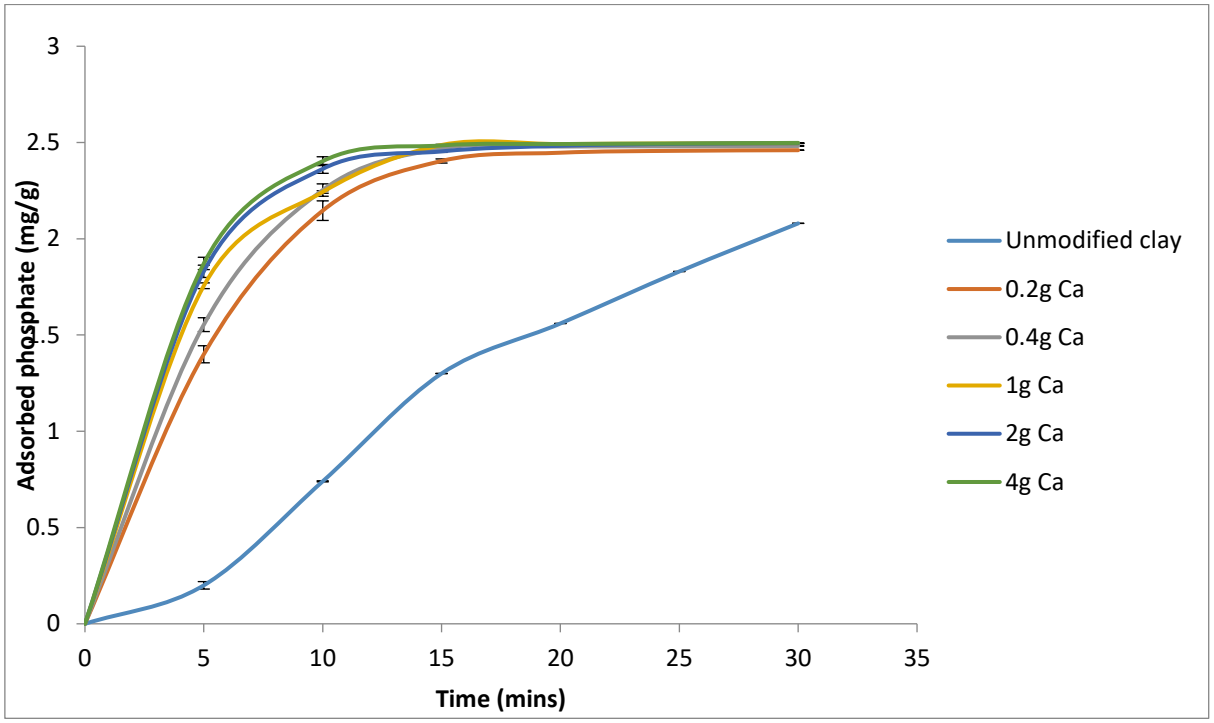

Figure 6.3: Effect of CaCO3 modification on the adsorption of phosphate by FCP using standard experimental conditions (n=3); standard error bars shown.

There was an improvement in the phosphate uptake by the $CaCO_3$ modified fired clay pellets (CaMFCP). The kinetic profile indicates complete phosphate removal was obtained within 30 minutes of contact **(Figure 6.3)**. All subsequent experiment was done using 30 minutes as the total contact time.

Phosphate adsorption was shown to increase with the addition of $CaCO_3$; these findings are consistent with those reported by Chen *et al.* (2009) on phosphate removal and recovery through crystallization of hydroxyapatite using xonotlite as seed crystal and Hosni *et al.* (2008) on the removal of phosphate by calcium hydroxide from synthetic wastewater. There was an increase in the phosphate adsorbing capacity of FCP as the concentration of Ca increased. This trend could be attributed to the presence of excess calcium ions in system and is consistent with results obtained by Kaminyango *et al.* (2009). They reported an increase in the removal efficiency of kaolinite for the removal of phosphate from aqueous solutions when the concentration of calcium ions increased.

CaMFCP showed a faster kinetic, achieving complete removal within 15 minutes of contact, than unmodified FCP. The time required for unmodified FCP to achieve was 60 minutes and this was four times more than the time required by CaMFCP **(Section 6.4.1)**. The faster kinetic exhibited by CaMFCP would mean a smaller

reactor volume would be required when CaMFCP was used for the removal of phosphate in wastewater treatment.

Phosphate adsorption has been shown to increase with increasing calcium ion concentration, this is due to the greater ability of calcium ions to form complexes with phosphate and precipitate it in the solution as the concentration of calcium ion increases (Nassef *et al.* 2012).

The displacement of Al^{3+} from the clay surface by Ca^{2+} and the subsequent interaction with OH^- to form metallic hydroxide imparts a positive charge to the tile surface allowing for PO_4^{3-} to bind with the positively charged surface. This interaction between the Ca^{2+} and the negatively charged clay surface is believed to occur through Coulombic interactions (Ren *et al.* 2012).

Another possible mechanism for phosphate removal was through the precipitation of calcium phosphate as apatite from the solution. Calcium carbonate decomposes into CaO when heated above 800^{o}C. The CaO could partially fuse with SiO_2 present in the clay to form $CaSiO_3$ represented by the following equations:

$$CaO + SiO_2 \rightarrow CaSiO_3$$ **Equation 6.6** (Yu *et al.* 2010)

$$5CaSiO_3 + SiO_2 + 5H_2O \rightarrow Ca_5(Si_6O_{18}H_2).4H_2O$$ **Equation 6.7** (Yu *et al.* 2010).

The formation of $CaSiO_3$ contributes to the active Ca^{2+} distribution within the clay lattice that could react with free phosphate ions (Chen *et al.* 2013). The reaction between Ca^{2+} and phosphate containing solution under neutral or alkaline conditions will most likely result in the precipitation of calcium phosphate as hydroxyl apatite (Littler *et al.* 2013) and could be represented by following equations:

$$Ca_5(Si_6O_{18}H_2).4H_2O + 3H_2PO_4^- \rightarrow Ca_5(PO_4)_3OH\downarrow + 6H_2SiO_3 + 2H_2O$$ **Equation 6.8**

$$5Ca^{2+} + 3HPO^{2-} + 4OH^- \rightarrow Ca_5(PO_4)_3OH\downarrow + 3H_2O$$ **Equation 6.9** (Chen *et al*. 2013)

The equilibrium dissolution of CaO would also increase the availability of free Ca^{2+} that acts as nuclei for the precipitation of phosphate (Kaasik *et al.* 2008).

The dissociation of $CaCO_3$ to CaO is believed to increase the pH of the solution, as final pH increased from 7 to 10.5 after 30 minutes of contact. At pH range of 8.5 – 10 the ability of Ca^{2+} to form complexes with phosphate and precipitate it out of solution increases (Nassef 2012). The effect of pH on the adsorption of phosphate by CaMFCP will be discussed in greater detail in **Section 6.5.4**.

6.4 Phosphate Adsorption Using Fired Iron Modified Clay Pellets

The addition of iron salts is commonly used to remove phosphate during wastewater treatment. Chemical precipitation through the addition of aluminium and iron salts has been widely used to supplement biological treatment for the removal of phosphate in wastewater treatment. The most commonly used Fe salts for the removal of phosphate are ferric chloride, ferric and ferrous sulphates (Nassef 2012).

The use of various Fe-based adsorbent has been widely reported to improve the adsorption of phosphate in wastewater treatment (Caravelli *et al.* 2010; Mezenner and Bensmaili 2009; Yaghi and Hartikainen 2013; Yoon *et al*. 2014). The objective of this section was to attempt to improve the phosphate adsorbing capacity of FCP by the addition of iron salt through the manipulation of the concentration of Fe in the clay.

6.4.1 $FeCl_3$ Modified Fired Clay Pellet

The addition of $Fecl_3$ to clay tiles had an adverse effect on the uptake of phosphate. Phosphate adsorption reduced as the concentration of Fe added to the clay increased **(Figure 6.4)**.

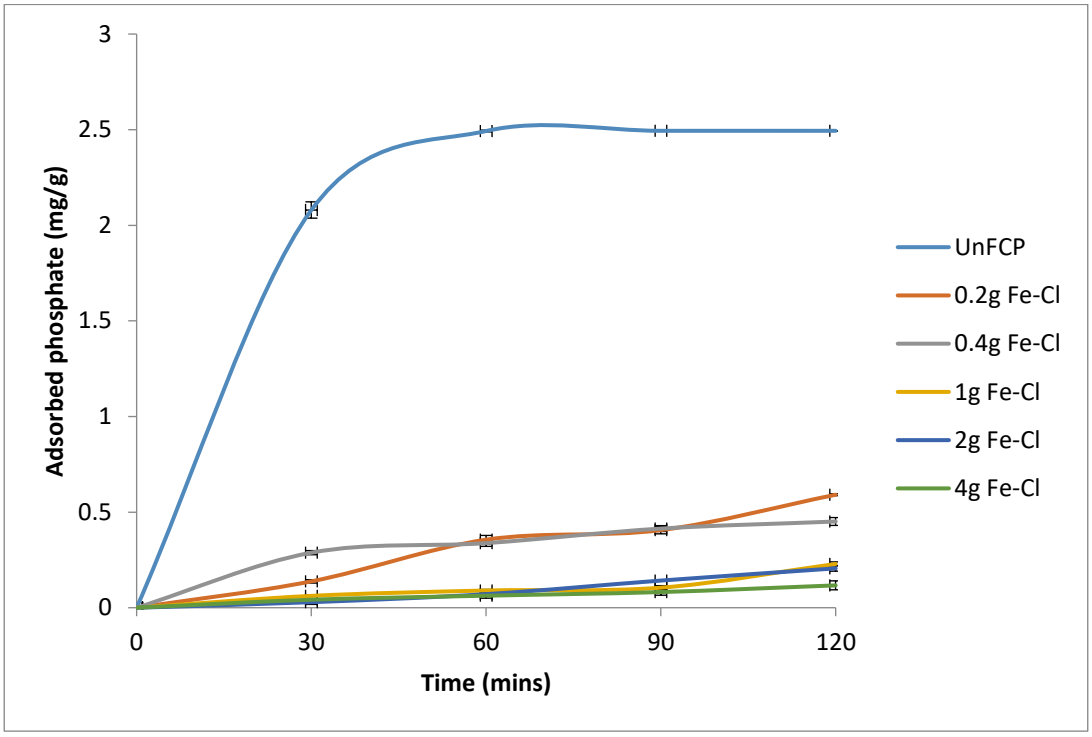

Figure 6.4: Effect of FeCl3 addition on the adsorption of phosphate by FCP using standard experimental conditions (n=3); standard error bars shown.

The negative effect of $FeCl_3$ addition could be attributed to the effect of chloride on the structure of the clay. It was observed during the addition of $FeCl_3$ that the consistency was not plastic but had a gritty feel during the preparation of the pellets. It is believed that the addition of $FeCl_3$ caused a collapse of the clay structure that is integral to the adsorptive properties attributed to clay.

The negative effect of the $FeCl_3$ addition could also be due to the impact of chloride on the adsorption of phosphate**.** The presence of chloride during phosphate adsorption has been shown to compete with phosphate ions for adsorption sites, thus reducing the removal of phosphate from solution (Chen *et al.* 2002; Zhao and Sengupta 1998). The possible ion exchange reaction can be described using the following equation:

$n[R^+ - Cl^-] + HPO_4^{3-} \rightarrow [Rn^{+n} - HPO_4^{3-}] + nCl^- + H^+$ **Equation 6.10** (Chen *et al.* 2002)

Where R represent the positively charged functional group of the ion exchanger and [ ] represent the solid phase.

The presence of Cl^- in the system would cause the reaction to be shifted to the left as Cl^- competes for available reaction sites leading to decreased phosphate removal (Chen *et al.* 2002).

However, the use of $FeCl_3$ has been reported in the removal of phosphate from wastewater. Fytianos *et al.* (1998) studied the modeling of phosphorus removal from aqueous and wastewater samples using ferric iron reported 63% phosphorus removal using 1:1 Fe:P ratio and complete removal when the Fe excess increased to 155% (Fe:P ratio of 2.55:1). Fe:P ratio of 5.24 has been reported in the removal of phosphate from wastewater. Fe:P ratio of 3 has been used to achieved a phosphate adsorption of more than 95% by ferric chloride (Zhou *et al.* 2008).

6.4.2 $FeSO_4$ modified fired clay pellets

The effect of iron modification on the performance of FCP in the adsorption was also investigated by the addition of $FeSO_4$ which also used for the precipitation of phosphate in WWTWs. 1, 2, 5, 10 and 20 g of $FeSO_4.7H_2O$ was added to 50 g of clay, equating to 0.2, 0.4, 1, 2 and 4 g of Fe added to the clay. The result of this study is presented in **Figure 6.5**.

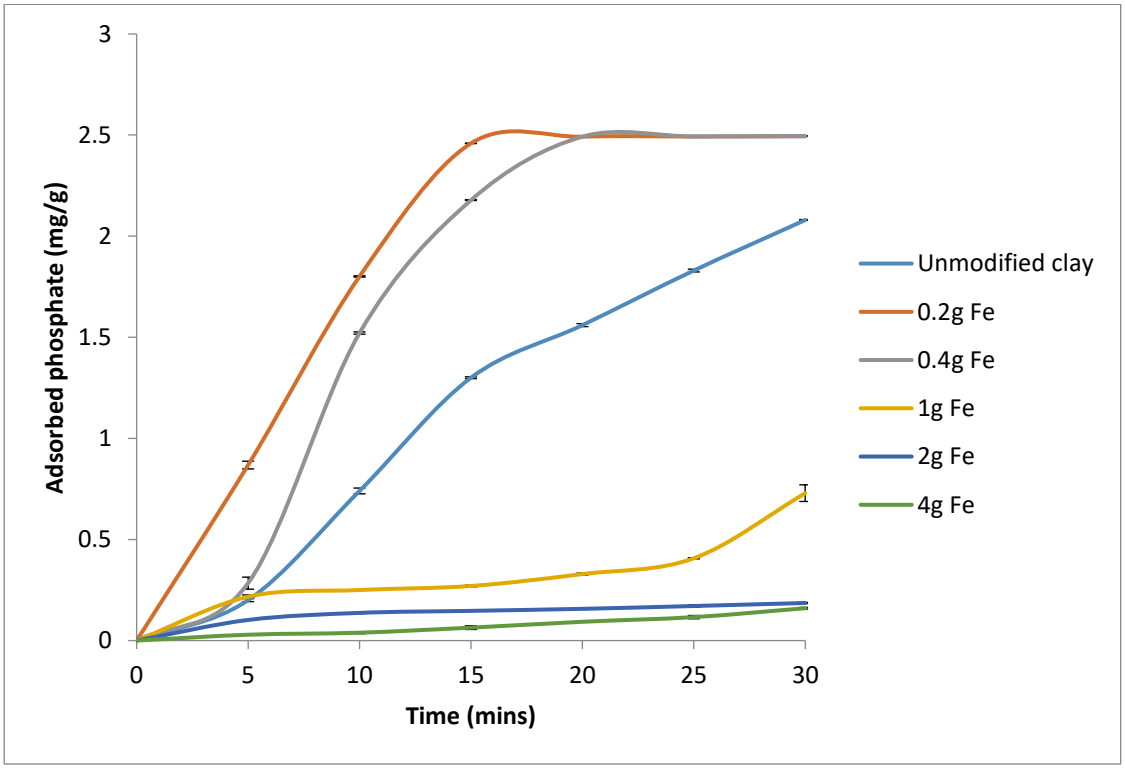

Figure 6.5: Effect of FeSO4 modification on the adsorption of phosphate by FCP using standard experimental conditions (n=3); standard error bars shown

The addition of $FeSO_4$ was shown to have a variable effect on the performance of FCP in the removal of phosphate **(Figure 6.5)**. The performance of FCP using lower concentrations of 0.2g and 0.4g Fe/g pellet was better than those obtained using higher Fe concentration of 1g, 2g and 4g Fe/g pellet. Phosphate adsorption generally decreased with increase in Fe concentration.

$FeSO_4.7H_2O$ decomposes on heating to produce iron (III) oxide, the reaction is expressed:

$$FeSO_4.7H_2O \rightarrow FeSO_4 + 7H_2O \qquad \textbf{Equation 6.11}$$

$$FeSO_4 \rightarrow Fe_2O_3 + SO_2 + SO_3 \qquad \textbf{Equation 6.12}$$

The presence of Fe^{3+} in the adsorbent could cause the rapid hydrolysis and precipitation of hydrous iron (III) (hydr)oxide with a reactive surface functional group and high surface area that could replace Al^{3+} on the FCP surface (Neethling *et al.* 2008). The iron (III) (hydr)oxide surface serves as the binding sites for the adsorption of phosphates. Ligand exchange with surface hydroxyl group is the initial process in the reaction with iron (III) (hydr)oxide and phosphates (Bastin *et al.* 1999; Yoon *et al*. 2014). Phosphate adsorption occurs when PO_4^{3-} replaces OH^- on the surface of the iron (III) (hydr)oxide (Yoon *et al.* 2014).

Stoichiometrically, 1 mole of Fe^{3+} is required to remove 1 mole of phosphate. However, during the precipitating process, a competing reaction of Fe^{3+} with hydroxyl ions to form hydroxides also occurs. This competing reaction of hydroxyl ions with phosphate ions for Fe^{3+} indicates that a higher stoichiometric mass ratio of Fe:P is required (de Haas *et al.* 2000; Yeoman *et al.*1988).

The reaction between Fe^{3+} and PO_4^{3-} can be summarized by the following equation

$$Fe^{3+} + PO_4^{3-} \rightarrow FePO_4\downarrow \qquad \textbf{Equation 6.13} \qquad \text{(Nassef 2012)}$$

$$Fe^{3+} + H_nPO_4^{3-n} \leftrightarrow FePO_4\downarrow + nH^+ \qquad \textbf{Equation 6.14} \qquad \text{(Martin 2010}$$

The use of ferric oxide has been reported to improve the adsorption of phosphate. Pan *et al.* (2009) reported an enhanced phosphate removal form waste effluents using polymer-based nanosized hydrated ferric oxides, while 80% phosphate removal was achieved using iron oxide tailings consisting mainly of magnetite (Fe_3O_4) (Zeng *et al.* 2004). The result of this study is in part similar to these studies.

Phosphate adsorption improved at lower concentration of Fe and decreased at higher concentration.

This decrease in phosphate adsorption with increase in Fe concentration could be attributed to the presence of sulphate within the system as the concentration of sulphate was about twice the concentration of Fe in the system. The effect of sulphate on the adsorption of phosphate has already been discussed in **Section 6.1**.

6.5 Effect of combined compositional modification clay pellets

The effect of compositional modification of FCP through the addition of $Al_2(SO_4)_3$ and other metal salts on the adsorption of phosphate was investigated by comparing the performance of single modification with the combination of two or more metal salt modification. The aim of this experiment was to determine if the contact time could be further reduced from 15 minutes obtained using modified clay pellets. It was believed that the combined effect of the elements as Al/Ca, Al/Fe, Ca/Fe or Al/Ca/Fe could improve the performance of the pellets beyond what was obtained using single element modification. The modifications investigated were; i) addition of $Al_2(SO_4)_3$ alone; ii) addition of $Al_2(SO_4)_3$ with $CaCO_3$; iii) addition of $Al_2(SO_4)_3$ with $FeSO_4$; and iv) addition of $Al_2(SO_4)_3$ with perforation of pellets. The modifications were repeated with $CaCO_3$ and $FeSO_4$ as the added salts. The results of this study are presented in **Figure 6.6**.

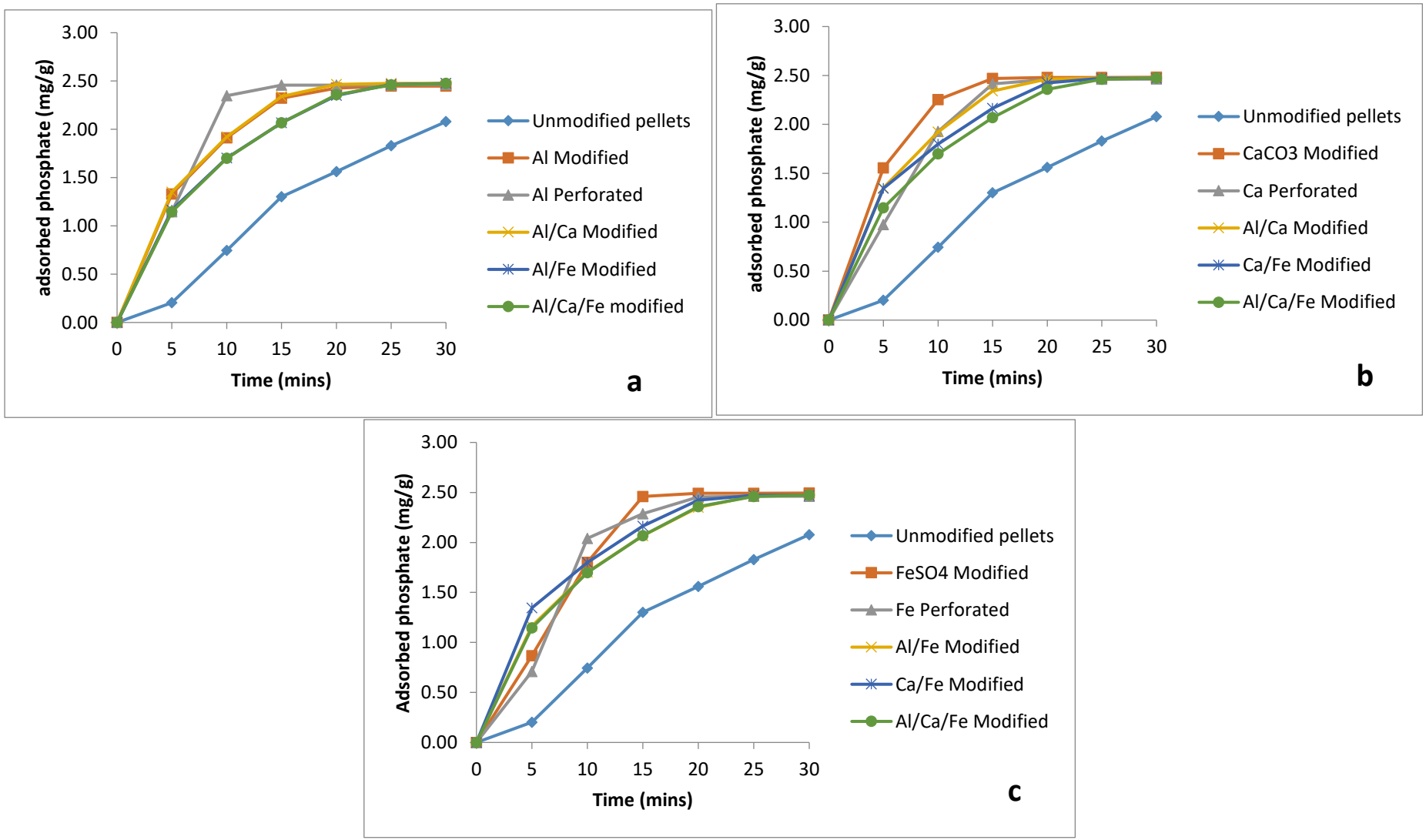

Figure 6.6: Effect of composition modification on the adsorption of phosphate by FCP: a) addition of Al2(SO4)3 and other modifications; b) addition of CaCO3 and other modifications; and c) addition of FeSO4 and other modifications.

The use of multi-element modification of clay to improve phosphate adsorption from wastewater has been reported (Tian *et al*. (2009) using lanthanum/aluminum pillared montmorillonite; Zhu *et al*. (2009) using hydroxyiron/aluminum montmorillonite complex; Cheng *et al*. (2010) using Zn-Al layered double hydroxides; Yan *et al*. (2010) using hydroxy-iron-aluminum pillared bentonites; Shanableh and Elsergany (2013) using Al-Fe-modified bentonite and Xu *et al*. (2016) using Ca-layered double hydroxides. Phosphate adsorption was shown to improve with the combination of different modification. Adsorption using $Al_2(SO_4)_3$ modified FCP followed the order Al perforated >Al modified = Al/Ca modified > Al/Fe modified = Al/Ca/Fe modified > unmodified pellets **(Figure 6.6a)**. Pellets modified with $CaCO_3$ exhibited an improvement in the performance and adsorption was in the order Ca modified > Ca perforated > Al/Ca modified > Ca/Fe modified > Al/Ca/Fe modified >unmodified pellets **(Figure 6.4.1b)**, while phosphate adsorption using pellets modified with $FeSO_4$ was Fe modified > Fe perforated > Ca/Fe modified > Al/Fe = Al/Ca/Fe modified > unmodified pellets **(Figure 6.4.1c)**. There was considerable improvement in the performance of the unmodified pellets at all treatments studied. Addition of $CaCO_3$ to $Al_2(SO_4)_3$ or $FeSO_4$ improved the performance of the pellets over the addition of $Al_2(SO_4)_3$ to $FeSO_4$.

Combinations of iron and aluminium modification to improve phosphate adsorption have been reported to have varying effect on adsorption. Yan *et al*. (2010) reported greater adsorption using Fe-bentonite than Al-bentonite of Fe-Al-bentonite. Adsorption followed the order Fe-bentonite > Al-bentonite > Fe-Al-bentonite. Zhu *et al*. (2009) reported an increase in the performance montmorillonite for phosphate adsorption when modified with hydroxyaluminum and hydroxyiron. The rate of adsorption was HyFeAl-$Mt_{0.5}$ > HyFeAl- $Mt_{0.2}$ > HyAl-Mt > HyFe-Mt. Yaghi and Hartikainen (2013) reported a better adsorption using Fe coated LECA than Al coated LECA, while Shanableh *et al*. (2016) reported a higher adsorption when Al^{3+} was combined with Fe^{3+} to modify bentonite. Bentonite modified with Fe^{3+} performed better than those modified with Al^{3+} alone. In this study, similar result was obtained using Al or Fe alone, but Fe showed faster rate of adsorption. The adsorption order for Shanableh *et al*. (2016) was Al/Fe> Fe > Al.

Phosphate adsorption mechanism of Calcium is usually dominated by precipitation of phosphates out of the solution through the formation of hydroxyapatite (Xu *et al*.

2016). Precipitation is initiated by the reaction of Ca with SiO_2 present in the clay to form $CaSiO_3$ which in turn contributes to the active Ca^{2+} pool within the clay Yu *et al.* 2010, Chen *et al.* 2013). The active Ca^{2+} in turn reacts with phosphate ions in solution to precipitate calcium phosphate as hydroxyapatite (Littler *et al*. 2013). The reactions are represented by **Equations 6.6 – 6.9**. Precipitation was thus considered as a possible mechanism for the adsorption of phosphate in this study.

Ligand exchange via inner-sphere or outer-sphere complexation is another mechanism responsible for the uptake of phosphate by Al/Fe oxides and clay minerals (Zhu *et al*. 2009, Yang *et al*. 2015). The anions such as phosphate forms a covalent bond with the metal cation on the surface of the adsorbent leading to the release of OH^- previously bonded to the surface of the adsorbent (Loganathan *et al*. 2014). The surface functional groups form strong inner-sphere complexes through a covalent bond between the ligand and metal ions (Wang *et al*. 2016) and is described using **Equations 6.15 – 6.16**

$$\equiv M\text{-}OH + H_2PO_4^- \leftrightarrow \equiv M - (H_2PO_4) + OH^- \qquad \textbf{Equation 6.15}$$

$$2 \equiv M\text{-}OH + HPO_4^{2-} \leftrightarrow M_2 - (HPO_4) + 2OH^- \qquad \textbf{Equation 6.16}$$

These inner–sphere complexes could be monodentate, bidentate or binuclear depending on the concentration of the phosphate solution, density and reactivity of the surface functional groups (Zhu *et al*. 2009). The outer-sphere complexes are formed via electrostatic attraction involving the retention of a water molecule between the ligand and exchange sites (Bradl 2004; Wang *et al*. 2016). The formation of outer-sphere complexes is represented by **Equations 6.17 and 6.18**:

$$\equiv M\text{-}OH_2^+ + H_{2+}PO_4^- \leftrightarrow \equiv M - (OH_2^+)\,(H_2PO_4^-) \qquad \textbf{Equation 6.17}$$

$$\equiv M - OH_2^+ + HPO_4^{2-} \leftrightarrow \equiv M - (OH_2^+)\,(HPO_4^{2-} \qquad \textbf{Equation 6.18}$$

An increase in the pH of the solution coupled with a decrease in phosphate concentration in the solution usually indicates the release of OH^- from the surface of the adsorbent signifying the adsorption of phosphate by the surface complex (Yang *et al.* 2006). This indicates ligand exchange may be a mechanism for the adsorption of phosphate within that system. There was an increase in the final pH

of the solution. The final pH of the solution from initial pH between 3 and 12 averaged 10.35 for AlMFCP; 10.34 for CaMFCP; and 9.40 for FeMFCP **(Figure 6.5.3.1)**. The increase in the final pH of the solution implies ligand exchange between phosphate in the solution and OH^- released form the surface of the pellets was a possible mechanism of phosphate adsorption by the pellets.

Phosphate adsorption is a complicated process due to the variation in the formation of phosphate-metal complexes and the different adsorption behaviour exhibited by different phosphate species on the same adsorbent. Hence, phosphate adsorption by the pellets could be a complicated interplay of precipitation, ion exchange and some ligand exchange.

Perforation was shown to improve the performance of the pellets in the adsorption of phosphate in every category; however this was not explored further as the test of structural integrity of perforated bricks was not within the scope of this study. Further research could be done using perforated bricks as the potential for phosphate adsorption in wastewater treatment was exhibited.

6.6 Adsorptive properties of modified fired clay pellets

6.6.1 Effect of contact time on the adsorption of phosphate using modified fired clay pellets

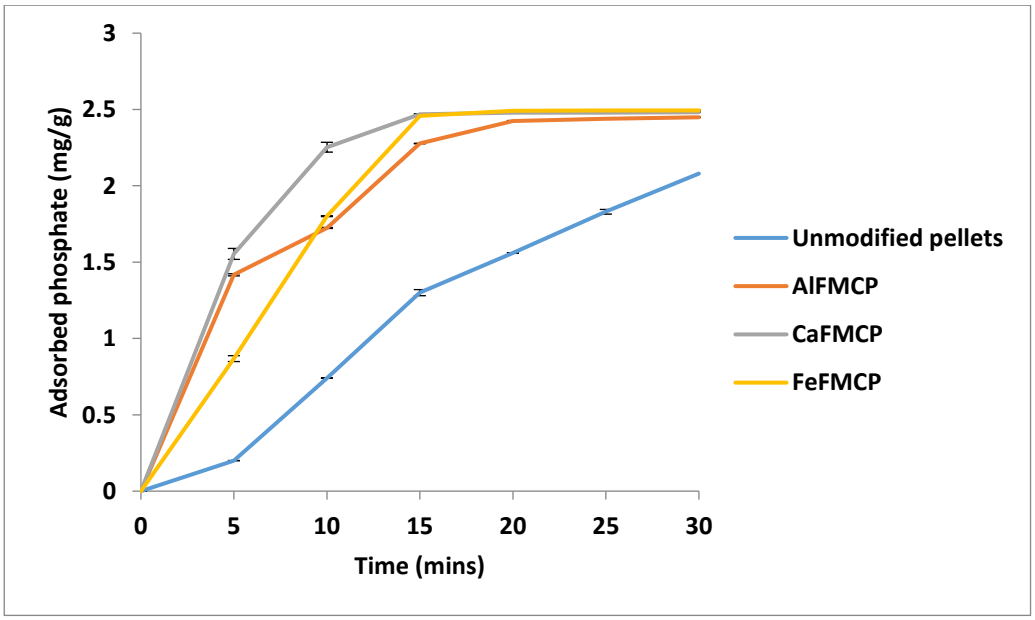

Figure 6.7: Effect on contact time on the adsorption of phosphate by modified clay pellets using standard experimental conditions (n=3); standard error bars shown.

Sorption of phosphate increased with increasing contact time. The kinetic profile showed a fast adsorption at the initial stage of the adsorption which slowed as it progressed **(Figure 6.7)**. Equilibrium concentration was achieved after 15 minutes of contact when CaFMCP and FeFMCP were used, and during 20 minutes when AlFMCP was used. During the first five minutes of adsorption, AlFMCP and CaFMCP showed an identical rate of adsorption. The overall rate of phosphate removal followed the order CaFMCP> FeFMCP> AlFMCP> unmodified pellets **(Figure 6.7)**. During the initial stages of adsorption, the concentration gradient between the available sorption sites on the pellet surface and the phosphate fluid film surrounding the pellets is large as a result the rate of adsorption is faster. As phosphate is taken out of the solution, the concentration gradient decreases leading to a decrease in the rate of adsorption during the later stages (Baraka *et al.* 2012).

Phosphate removal was greater than 90% within the first 15 minutes when modified clay pellets were used. Higher phosphate removal during the initial stages of adsorption has been reported. Boujelben *et al.* (2008) achieved an equilibrium concentration after 15 minutes using iron oxide coated crushed bricks; Hamdi and and Srasra (2012) reported an equilibrium concentration obtained within two hours when two types of Tunisian clay minerals were used. Similar result was also reported by Yan *et al.* (2010) using Al and Fe pillared bentonite. A short contact time is crucial in the application of an adsorbent in wastewater treatment, consequently it is essential that an adsorbent possess a rapid reaction with the phosphate ions (Kamiyango *et al.* 2011).

6.6.2 Effect of adsorbent dosage on the adsorption of phosphate using modified clay pellets

The effect of adsorbent dosage on the removal of phosphate using modified clay pellets was studied under standard experimental conditions stated in **Section 3.6.2**.

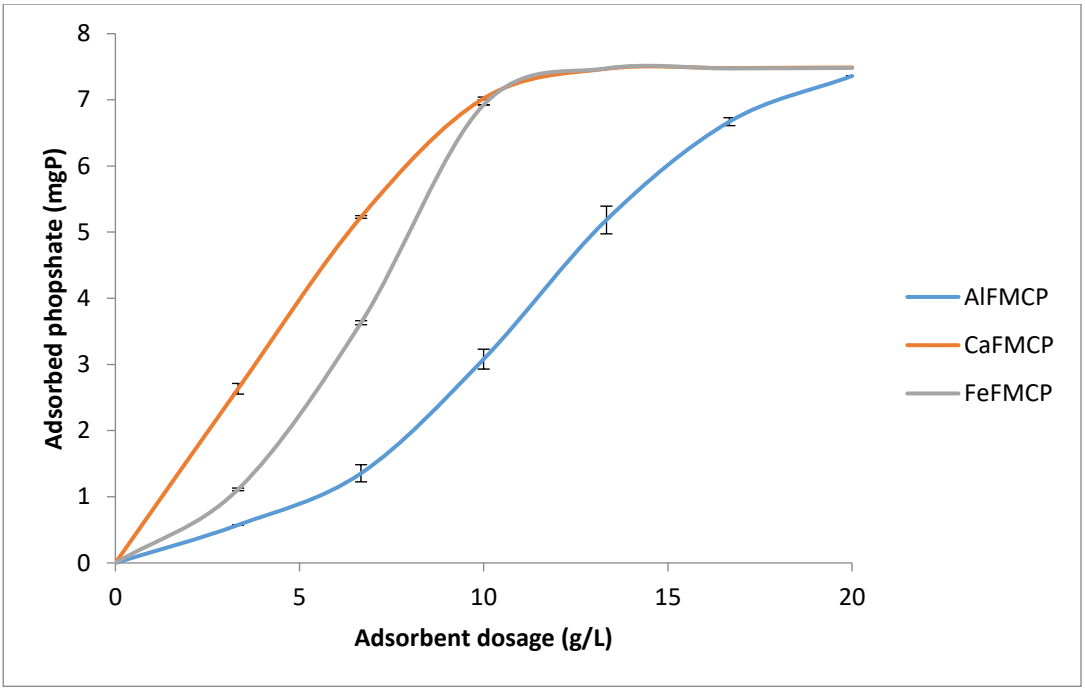

Figure 6.8: Effect of adsorbent dosage on the adsorption of phosphate by modified clay pellets using standard experimental conditions (n=3); standard error bars shown.

Sorption of phosphate increased with increasing dose of adsorbent **(Figure 6.8)**. Maximum phosphate removal was observed when 13.33 g/L of CaMFCP and FeMFCP was used; subsequent increase in adsorbent dosage did not result in any change. However, AlMFCP did not achieve maximum removal until 20 g/L of the pellets was used.

The increase in sorption is due to the increase in the quantity of active sites available for sorption of phosphate ions as the mass of the adsorbent increases. Similar trend was reported by Deng and Shi (2015) using mesoporous modified kaolin clay; and Ni *et al*. (2015) using red mud- polyaluminum chloride composite coagulant. The effect of adsorbent dosage on the adsorption of phosphate has been discussed extensively in **Section 5.3**.

6.6.3 Effect of pH on the adsorption of phosphate using modified clay pellets

The effect of pH on the adsorption phosphate on modified FCP was investigated at pH between pH 2 and 12, using 150 ml of 50 mg/L phosphate solution.

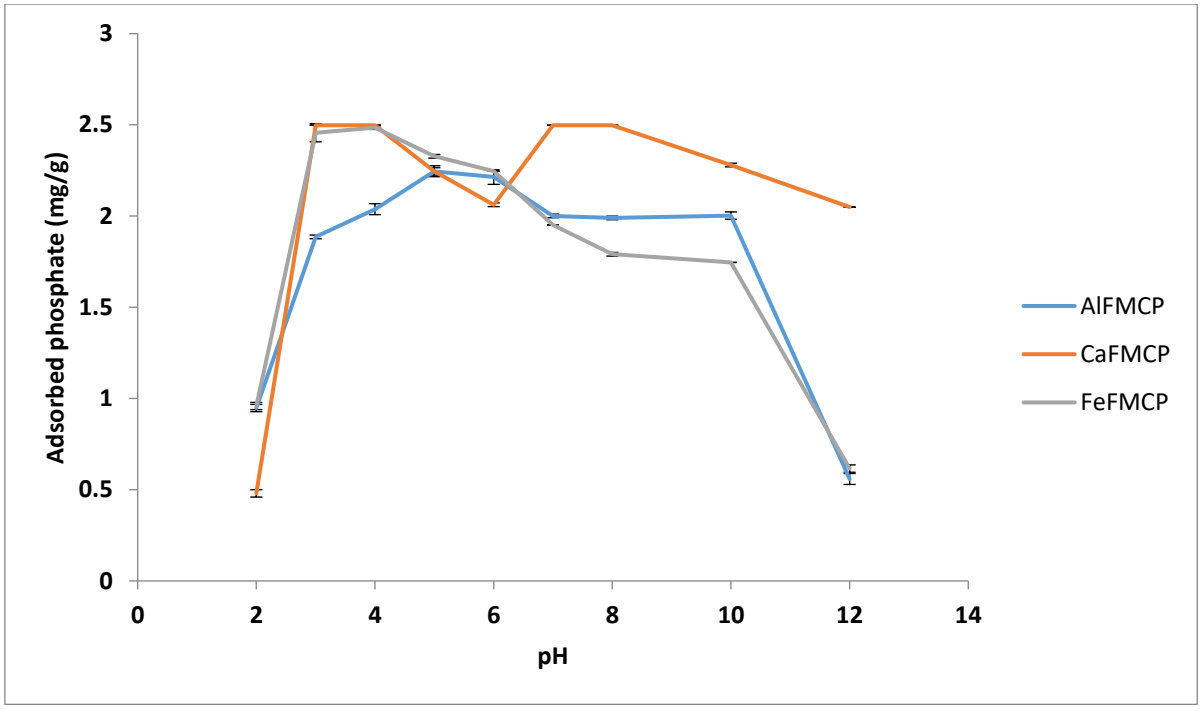

Figure 6.9: Effect of pH on the adsorption of phosphate by modified clay pellets using standard experimental conditions (n=3); standard error bars shown.

One of the crucial factors affecting the adsorption of anions at water-adsorbent interface is pH (Tian *et al*. 2009, Zamparas *et al*. 2012). Phosphate adsorption by modified clay pellets was observed to be affected by pH **(Figure 6.9).** Phosphate adsorption increased from 0.96 mg/g at pH 2 reaching a maximum of 2.25 mg/g between pH 5 and 6 before decreasing slightly to 2 mg/g between pH 7 and 10 and declining further to 0.56 mg/g at pH 12 using AlMFCP. Phosphate adsorption using CaMFCP increased from 0.48 mg/g at pH 2 to 2.5 mg/g between pH 3 and 4 and between pH 7 and 8 before decreasing to 2.04 mg/g as the pH increased to 12. Adsorption was greater than 80% at all pH studied using CaMFCP. There was a decrease in adsorption from 2.5 mg/g to 2.06 mg/g as the pH increased from pH 4 to 6, before increasing once more to 2.5 mg/g as the pH increased to 7.

A delay in phosphate adsorption or a phenomenon known as hysterersis was observed between pH 4 and 7 when CaMFCP was used. Several reasons have been postulated for this phenomenon. Jiang *et al*. (2014) suggested that phosphate adsorption was in a non-equilibrium state and was consequently dependent on the pH, ionic strength of the solution and adsorption function as affected by the characteristics of the adsorbent. It was also suggested the presence of H^+ and OH^-

in the solution as a result of pH could hinder adsorption. This however, does not explain the increase in adsorption as pH increased from pH 6 to pH 7.

Different species is thought to be responsible for phosphate adsorption at different pH **(Figure 5.10)**. Fe is believed to dominate adsorption at pH below 5, while Al is the dominant species responsible for phosphate adsorption at pH range between 5 and 6 and Ca is responsible for adsorption at pH above 7. Nassef (2012) reported optimum phosphate adsorption at pH between 4 and 6 using aluminium sulphate to precipitate phosphate from solution. Babatunde and Zhao (2010) reported a decrease in maximum phosphate adsorption capacity evaluated from the Langmuir isotherm from 31.9 mg/g at pH 4 to 10.9 mg/g at pH 9 when waste alum sludge was used to remove phosphate from aqueous solution. Ozacar (2003) reported a decrease in phosphate adsorption as pH increased from 5 to 8 when alunite was used for the adsorption of phosphate from aqueous solution. These studies show a pH range between 4 and 6 as optimum pH for phosphate adsorption with aluminium as the dominant species responsible for adsorption and these results are similar to those obtained in this study.

Phosphate adsorption increased with increasing pH from 2 to 10 with maximum adsorption at pH 10 using alginate calcium carbonate composite beads for the adsorption of phosphate ions (Mahmood *et al*. 2015). Optimum adsorption typically occurs at pH below 6. (Pawar *et al.* (2016) pH 6 using aluminium-pillared acid activated bentonite beads; Yan *et al.* (2010) pH 4 using Al-, Fe- and Al-Fe-modified bentonites; Shanableh and Elsergany (2013) pH 5 using Fe- and Al-Fe-modified bentonites; Hamdi and Srasra (2011) pH 5 using Tunisian clay; Yang *et al.* (2015) using calcined Kanuma clay; Jia *et al*. (2013) pH 5 using used bricks). These finding are similar to the results in this study using Al and Fe modified clay pellets. Optimum phosphate adsorption at pH higher than 6 has also been reported in literature, Moharami and Jalali (2013) reported high phosphate adsorption at pH 2 to 10 using Iranian clay, while Deng and Shi (2015) reported higher phosphate adsorption at pH 7 and 8 using Mg-Al hydrotalcite-loaded kaolin clay. The result obtained in this study using CaMFCP showed optimum adsorption could be attained at two pH ranges below and above pH 6. This result is silimar to that reported by Kamiyango *et al*. (2009) using kaolinite from Linthipe. Phosphate adsorption between pH range of 5 and 8 is crucial as this is the practical pH for wastewater treatment (Shanableh

and Elsergany 2013). Result of this study indicates CaMFCP and AlMFCP could be used in wastewater treatment; CaMFCP is more suitable due to the higher adsorption (2.5 mg/g) obtained within the pH range.

Ion exchange has also been suggested as one of the phosphate removal mechanisms using metal modified clay adsorbents (Shanableh *et al*. 2016) where OH^- on the surface of the adsorbent is replaced with PO_4^{3-}. The mechanism is represented as Equation 6.14:

Clay-Metal ≡ OH^- + PO_4^{3-} ↔ Clay–Metal ≡ PO_4^{3-} + OH^- **(Equation 6.14)** Shanableh and Elsergany (2013).

Increase in OH^- concentration of the solution associated with increase in metal-OH surface bonds usually indicates ion exchange as an adsorption mechanism in the removal of phosphate (Kasama *et al*. 2004, Yan *et al*. 2010, Shanableh *et al*. 2016). Decrease in phosphate adsorption with increasing pH can be attributed to competition between phosphate and OH^- and changes in the surface charges of the pellets. The surface charges of the pellets is produced by the hydrolysis of the Al-OH or Si-OH bonds along the clay lattice and is dependent on the pH of the solution (Ismadji *et al*. 2015). The pH at zero point of charge (pH_{zpc}) is an important factor in adsorption. The pellet surface will be positively charged at pH below pH_{zpc} and negatively charged a pH above pH_{zpc}. The pH_{zpc} was 8.54, 8.58 and 8.64 for AlMFCP, CaMFCP and FeMFCP respectively. Increased adsorption of phosphate would occur at lower pH resulting from increased attraction between the positively charged surface of the pellets and phosphate ion due to increased positive charges on the surface (Babatunde *et al*. 2009; Pawar *et al*. 2016). As the pH increases, the surface becomes increasingly negatively charged, hence attraction for phosphate ions decrease leading to lower adsorption due to increased competition between the OH^- and phosphate ions. Adsorption in this study was higher at pH lower than pH_{zpc}, and is consistent with results reported by Moharami and Jalali (2013). Increase in OH^- concentration with increase in pH is confirmed by the increase in pH of the solution after adsorption **(Figure 6.10).**

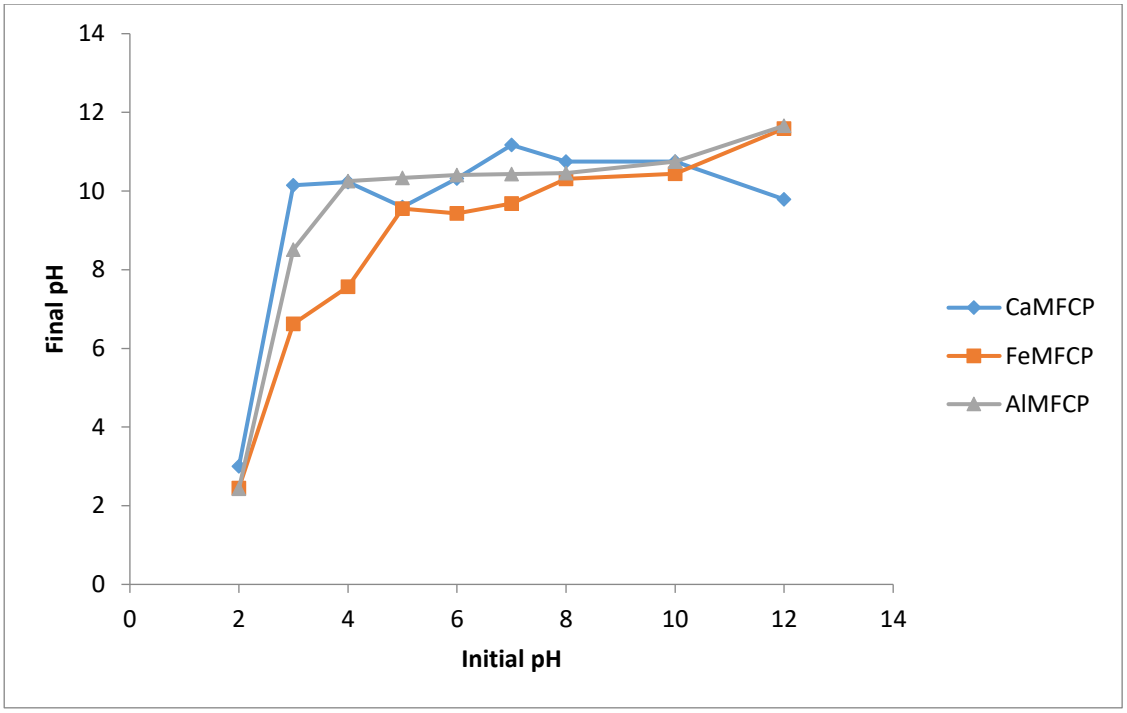

Figure 6.10: Final pH of phosphate solution at the end of contact using modified FCP.

Different phosphate species dominate at different pH **(Figure 6.11)**.

Some materials have been removed due to 3rd party copyright. The unabridged version can be viewed in Lancester Library - Coventry University.

Figure 6.11: Distribution of phosphate species in solution as a function of pH (Kamiyango et al. 2009).

$H_2PO_4^-$ and HPO_4^{2-} are the dominant species between pH 5 and 10, at pH below 7 $H_2PO_4^-$ is the dominant species, while HPO_4^{2-} tends to dominate in region of pH 7 - 12 and at pH over 12.5 PO_4^{3-} exists at higher concentration (Karageorgiou *et al*.

2007). Ligand exchange is one of the adsorption mechanisms for the adsorption of phosphate on clay minerals and Al/Fe oxides (Zhu *et al*. 2009). Protonation of metal oxides resulting in adequate adsorption sites for the uptake of phosphate occur at suitable pH (**Equation 6.19**):

$$\equiv M\text{-}OH + H^+ \rightarrow \equiv M\text{-}OH^+ \qquad \textbf{Equation 6.19}$$

Where M is a metal such as Al, Ca, Fe etc.

Phosphate exists as $H_2PO_4^-$ and HPO_4^{2-} at lower pH and is taken out of solution via phosphate-hydroxyl monodentate and proptonation of adsorbed phosphate and the process is represented as:

$$\equiv M\text{-}OH_2^+ + PO_4^{3-} + 2H^+ \rightarrow \equiv M\text{-}PO_4 - 2H + H_2O \qquad \textbf{Equation 6.20}$$

$$\equiv M\text{-}OH_2^+ + PO_4^{3-} + H^+ \rightarrow \equiv M\text{-}PO_4^{2-} - H + H_2O \qquad \textbf{Equation 6.21}$$

As the pH decreases further, the metal oxides and hydroxides becomes less stable and dissolves leading to a decrease in number of available sites for adsorption (Yang *et al*. 2015). This could be responsible for the low adsorption obtained for pH 2 in this study. At higher pH, HPO_4^{2-} and PO_4^{3-} are the dominant species and phosphate adsorption is as described in **Equations 6.22 and 6.23**:

$$\equiv M\text{-}OH_2^+ + PO_4^{3-} \rightarrow \equiv M\text{-}PO_4^{2-} + H_2O \qquad \textbf{Equation 6.22}$$

$$\equiv M\text{-}OH_2^+ + PO_4^{3-} + H^+ \rightarrow \equiv M\text{-}PO_4^{2-} - H + H_2O \qquad \textbf{Equation 6.23}$$

The increase in OH^- concentration as a result of continued increase in pH leads to deprotonation of oxides/hydroxides that could destroy the OH^- groups causing the materials to become more negatively charged (**Equation 6.24**).

$$\equiv M - OH \rightarrow \equiv M - O^- + H^+ \qquad \textbf{Equation 6.24}$$

This leads to decrease in phosphate adsorption due to electrostatic repulsion between the increasing negatively charged surface and phosphate ions (Yang *et al*. 2015). This could also be attributed to the decrease in adsorption reported in this study. Low adsorption at extreme pH obtained in this study is similar to those obtained by Yang *et al*. (2015) using calcined Kanuma clay and Yan *et al*. (2010)

using Al- bentonite and Fe-Al-bentonite. Low phosphate adsorption was at pH below 3 and above 10.

6.6.4 Effect of temperature

The effect of temperature on the adsorption of phosphate was studied at 20, 25, 30 and 35 ^{o}C and the result presented in **Figure 6.12**.

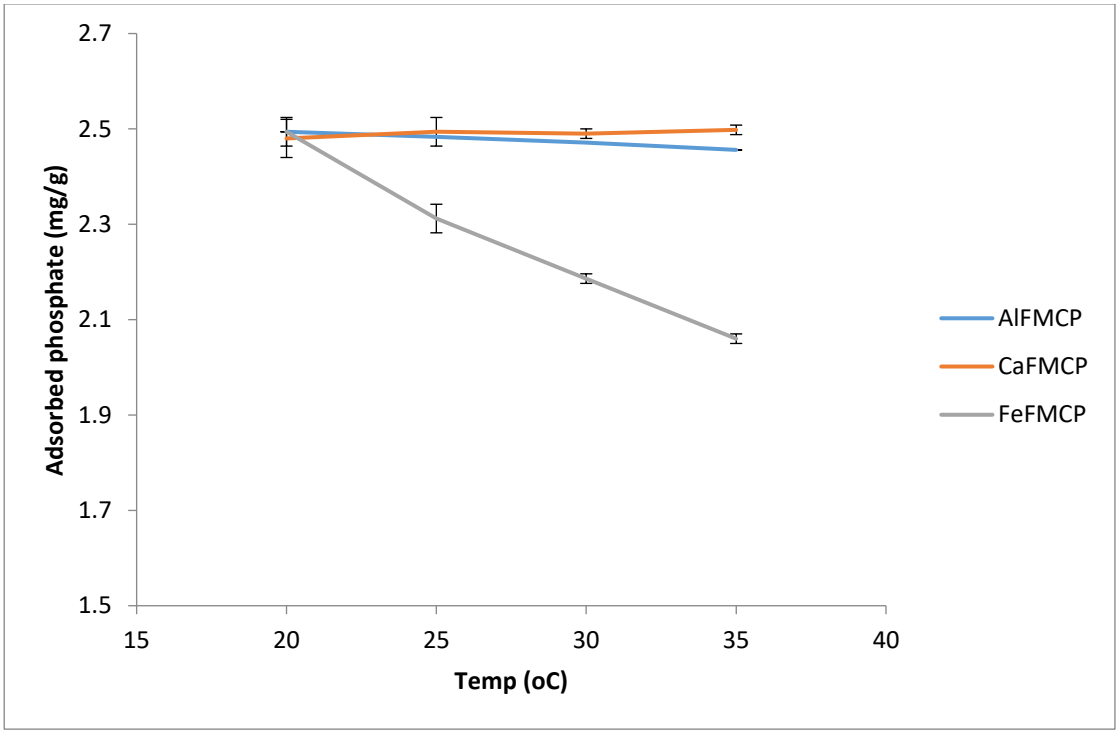

Figure 6.12: Effect of temperature on the adsorption of phosphate by modified clay pellets using standard experimental conditions (n=3); standard error bars shown.

Phosphate sorption declined with increase in temperature **(Figure 6.12)** indicating a low energy requirement for the adsorption of phosphate using Al and Fe modified clay pellets, CaMFCP was however, not effected by temperature. An increase in the number of adsorption sites influenced by the disintegration of some of the internal bonds around the edge of the active sites of the FCP as a result of the exothermic nature of the adsorption could be responsible for the increased adsorption of phosphates at lower temperature observed in this study. A decrease in phosphate adsorption with increase in temperature has been reported in literature. Das *et al.* (2006) using double layered hydroxides to remove phosphate from aqueous solution reported a decline in the adsorption of phosphate when temperature increased; this is similar to the trend reported in this study.

It has been suggested that effect of temperature on adsorption process is more pronounced on the position of the equilibrium rather that the rate of adsorption (Kamiyango *et al.* 2011). In this study, the rate of adsorption for AlMCFP and FeMCP was affected by temperature. The rate of adsorption was found to decrease as the temperature decreased.

Adsorption Kinetic Model

The data obtained from the investigation of the effect of temperature on the adsorption of phosphate using modified clay pellets were analysed using the kinetic models described in **Section 5.6 (Figure 6.13 - 6.15)** and the kinetic parameters are presented in **Table 6.1 - 6.3**.

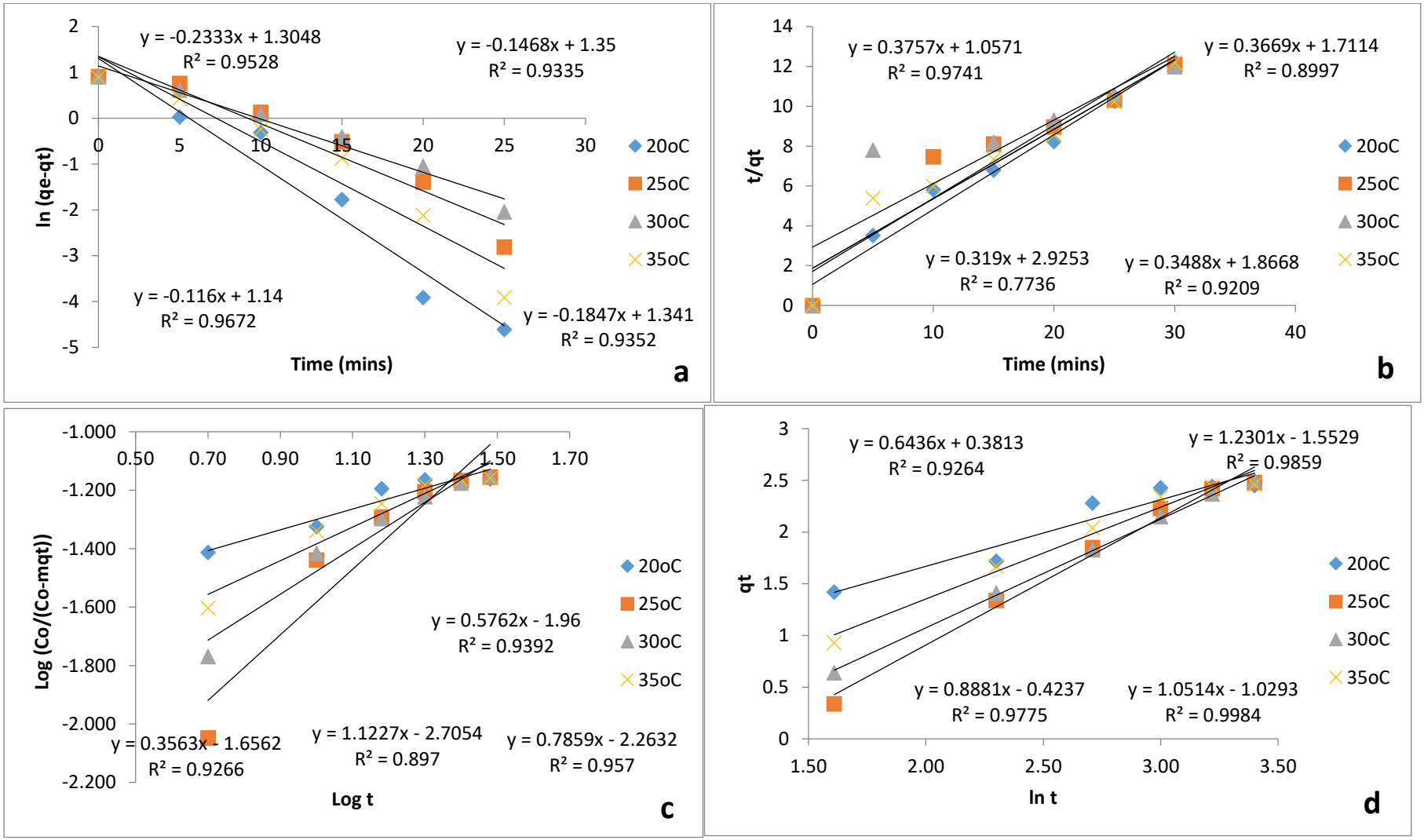

Figure 6.13: Kinetic model plot for the adsorption of phosphate using AlMFCP: a) Pseudo-first order kinetic model; b) Pseudo-second order kinetic model; c) Bangham's kinetic model; and d) Elovich kinetic model

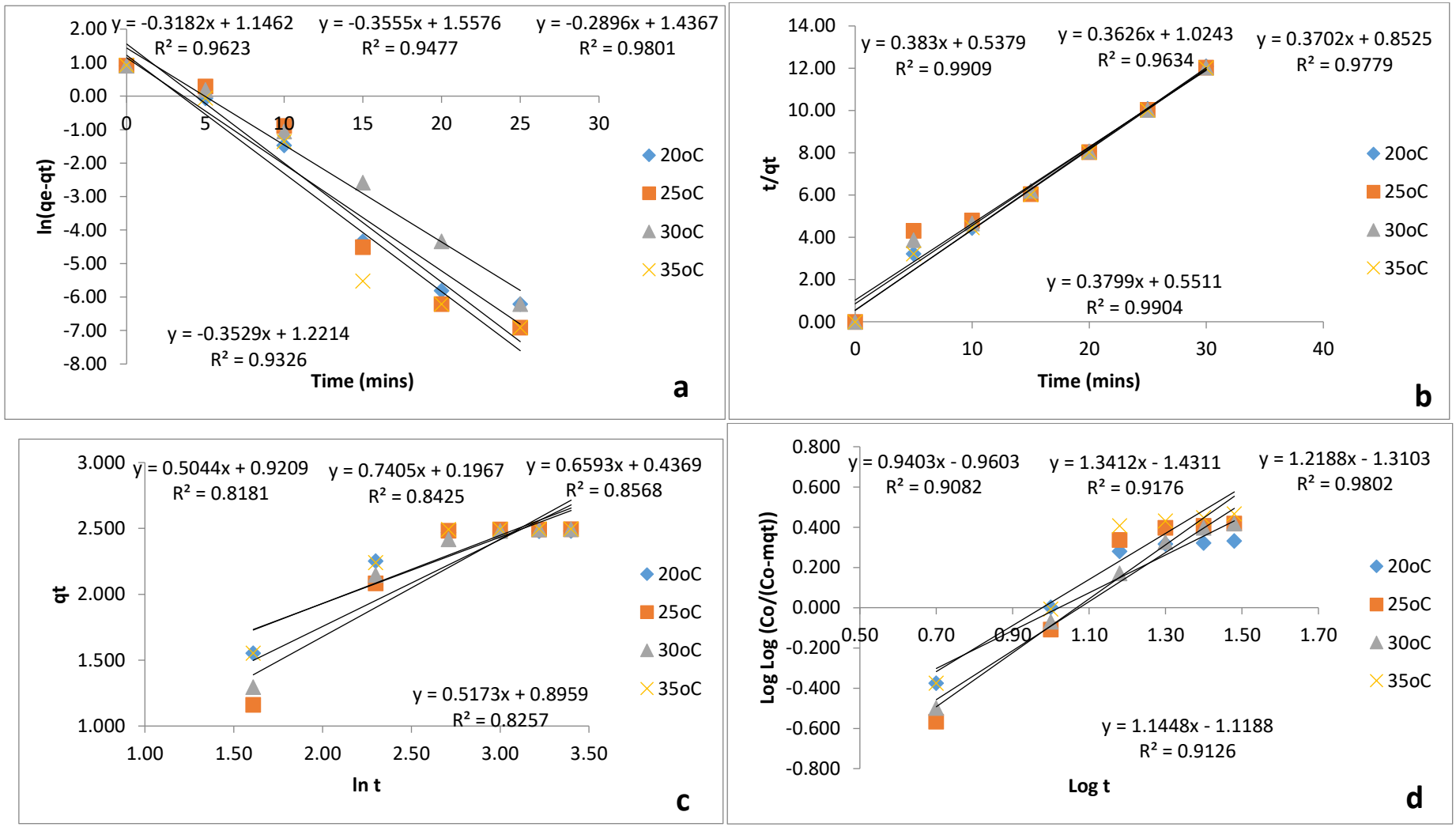

Figure 6.14: Kinetic model plot for the adsorption of phosphate using CaMFCP: a) Pseudo-first order kinetic model; b) Pseudo-second order kinetic model; c) Elovich kinetic model; and d) Bangham's kinetic model.

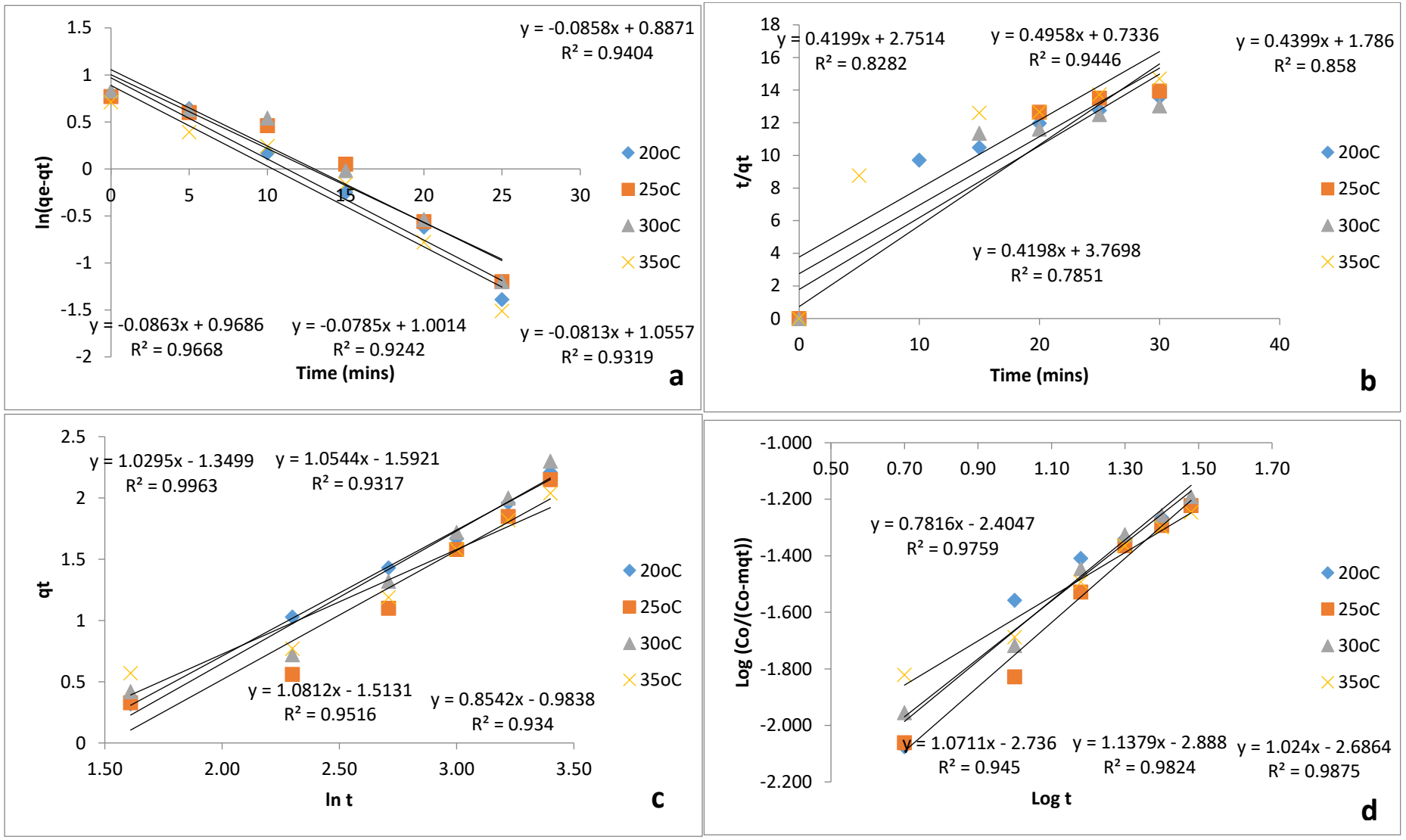

Figure 6.15: Kinetic model plot for the adsorption of phosphate using FeMFCP: a) Pseudo-first order kinetic model; b) Pseudo-second order kinetic model; c) Elovich kinetic model; and d) Bangham's kinetic model

Table 6.1: Kinetic model adsorption parameters of adsorption of phosphate onto AlMFCP at different temperature. Adsorption conditions: initial concentration 50mg/l, pH 6.7, adsorbent dose 20g/l

Kinetic model	Parameter	20°C	25°C	30°C	35°C
Pseudo-first order	k_1 (/min)	-0.05	-0.03	-0.028	-0.04
	R_2	0.9528	0.9335	0.9672	0.9352
Pseudo-second order	k_2 (g/mg/min)	0.13	0.08	0.03	0.07
	h (mg/g/min)	0.95	0.58	0.34	0.54
	R^2	0.9741	0.8997	0.7736	0.9209
Elovich	α (mg/g/min)	1.46	-0.64	-0.97	2.34
	b (g/mg)	1.55	0.81	0.95	1.13
	R^2	0.9264	0.9859	0.9984	0.9775
Bangham's	k_o (mL/g/L	39.23	229.12	105.50	65.10
	α	0.022	0.002	0.006	0.011
	R^2	0.9401	0.9916	0.9965	0.9947

Table 6.2: Kinetic model adsorption parameters of adsorption of phosphate onto CaMFCP at different temperature. Adsorption conditions: initial concentration 50mg/l, pH 6.7, adsorbent dose 20g/l

Kinetic model	Parameter	20°C	25°C	30°C	35°C
Pseudo-first order	k_1 (/min)	-0.076	-0.062	-0.056	-0.08
	R_2	0.9623	0.9477	0.9801	0.9326
Pseudo-second order	k_2 (g/mg/min)	0.273	0.128	0.161	0.262
	h (mg/g/min)	1.86	0.98	1.17	1.81
	R^2	0.9909	0.9634	0.9779	0.9904
Elovich	α (mg/g/min)	2.51	1.22	1.55	2.45
	b (g/mg)	1.98	1.35	1.52	1.93
	R^2	0.8181	0.8425	0.8568	0.8257
Bangham's	k_o (mL/g/L	150.54	378.93	285.86	241.08
	α	0.11	0.04	0.05	0.08
	R^2	0.9082	0.9176	0.9802	0.9126

The pseudo-first order kinetic plot showed a good fit for all three pellets types studied indicating the applicability of the pseudo-first order kinetic model to the study **(Figure 6.13a - 6.15a)**. The values of k_1 decreased with increase in temperature confirming phosphate adsorption decrease with increase in temperature **(Table 6.1 and 6.2)**. K_1 decreased from 0.05/min to 0.028/mins, 0.076/min to 0.056/min when temperature increased form 20°C to 30°C for AlMFCP and CaMFCP respectively. The value of K_1 decreased from 0.002/min to 0.04/min using FeMFCP when the

temperature increased from 25°C to 35°C. Conformity to pseudo-first order kinetic model normally indicates physiosorption.

The pseudo-second kinetic plot showed a good fit using the experimental data for CaMFCP, R^2 was greater than 0.96 for all the temperatures studied **(Figure 6.14b)**. The adsorption rate constant k_2 value was found to increase from 0.128 g/mg/min to 0.262 g/mg/min when the temperature increased form 25°C to 35°C confirming the increase in phosphate adsorption using CaMFCP with increase in temperature. The initial rate of adsorption (h) also increased from 0.98 (mg/g/min) to 1.81 mg/g/min when the temperature increased from 25°C to 30°C **(Table 6.2)**. The pseudo-second order kinetics could be used to describe the adsorption of phosphate on CaMFCP. Good fit to pseudo-second order model indicates the adsorption of phosphate by CaMFCP occurred primarily via chemisorption and this suggests that each phosphate molecule was attached to two active sites on the adsorbent and the adsorption process was irreversible.

Table 6.3: Kinetic model adsorption parameters of adsorption of phosphate onto FeMFCP at different temperature. Adsorption conditions: initial concentration 50mg/l, pH 6.7, adsorbent dose 20g/l

Kinetic model	Parameter	20°C	25°C	30°C	35°C
Pseudo-first order	k_1 (/min)	-0.02	-0.002	-0.03	-0.04
	R_2	0.9668	0.9242	0.9319	0.9404
Pseudo-second order	k_2 (g/mg/min)	0.06	0.34	0.11	0.05
	h (mg/g/min)	0.36	1.36	0.56	0.27
	R^2	0.8282	0.9446	0.858	0.7851
Elovich	α (mg/g/min)	0.26	0.20	0.22	0.37
	b (g/mg)	0.97	0.95	0.92	1.17
	R^2	0.9963	0.9317	0.9516	0.934
Bangham's	k_o (mL/g/L	203.45	237.28	182.54	104.46
	α	0.002	0.001	0.002	0.004
	R^2	0.945	0.9824	0.9875	0.9759

The pseudo-second order kinetic plot did not show a good fit for AlMFCP and FeMFCP **(Figure 6.13b and 6.15b)**. The R^2 values for AlMFCP ranged 0.7736 at 30°C to 0.9741. The R^2 of the plot for 25°C and 35°C was 0.8997 and 0.9209 respectively. The R^2 for FeMFCP ranged from 0.7851 to 0.9446 for 35°C and 25°C respectively. The adsorption rate constant (k_2) values for AlMFCP and FeMFCP decreased with increase in temperature from 0.13 g/mg/min to 0.07 g/mg/min and

from 0.34 g/mg/min to 0.05 g/mg/min when the temperature increase from 20ºC to 35ºC and from 25ºC to 35ºC for AlMFCP and FeMFCP respectively **(Table 6.1 and 6.3)**. The inconsistency in the kinetic parameters of the pseudo-second order kinetic model suggests the adsorption mechanism for AlMFCP and FeMFCP were complicated with interactions of different processes.

The adsorption data from the study gave a good fit using AlMFCP and FeMFCP for the Elovich kinetic model, The R^2 was greater than 0.92 for all temperatures studied, indicating the model could be used to describe the results **(Figures 6.13d and 6.15c)**. The adsorption data for CaMFCP did not give a good fit, R^2 values were between 0.81 and 0.86 **(Figure 6.14c)**. The values of b for adsorption using AlMFCP increased from 1.55 g/mg at 20ºC to 1.13 g/mg at 35ºC **(Table 6.1)**, CaMFCP decreased from 1.98 g/mg to 1.93 g/mg and FeMFCP increased from 0.97 g/mg to 1.17 g/mg as the temperature increased from 20ºC to 35ºC respectively **(Table 6.2 and 6.3)**. An increase in the value of b indicates there were more available sites for phosphate adsorption, while a decrease signifies a decrease in the number of sites available for adsorption (Yakout and Elsherif 2010). The initial rate of adsorption (α) did not follow any specific trend; there were fluctuations in the values of α across the temperatures and type of pellets **(Table 6.1 - 6.3)**. The fluctuation in the value of α as temperature increased could mean the rate of desorption was greater than adsorption resulting in the decrease in adsorption with increase in temperature. The R^2 values indicated diffusion could be a mechanism for adsorption, but it was not a rate limiting step and other mechanisms were involved.

The Bangham's kinetic model showed a good correlation with R^2 values >0.9 at all temperature for all pellet types **(Figure 6.13c and 6.14d- 6.15d)**. The good linearity shows the model can be used to describe the kinetics of phosphate adsorption using modified clay pellets. The kinetic constants derived from the Bangham's equation are listed in **Table 6.1 - 6.3**, and was observed the value of k_o and α varied as a function of temperature. The value of k_o generally decreased as the temperature increased from 25ºC to 35ºC. k_o decreased from 229.12 mL/g/L to 65.1 mL/g/L using AlMFCP when the temperature increased from 25ºC to 35ºC **(Table 6.1)**. The value of k_o decreased from 378.93mL/g/L to 241.08mL/g/L and 237.28 mL/g/L to 104.46 mL/g/L when the temperature increased from 25ºC to 35ºC using CaMFCP and

FeMFCP **(Table 6.2 and 6.3)**. The value of α generally decreased when the temperature increased from 20^{o}C to 35^{o}C using AlMFCP and CaMFCP, and increased as the temperature increased using FeMFCP.

The good correlation of the Bangham's kinetic model indicates that pore diffusion could be a rate controlling step. As the pseudo-first order kinetic model also showed a good linearity and there were variations in the trend of all kinetic models studied as a function of temperature, it could be said the adsorption mechanism for AlMFCP and FeMFCP was predominantly physisoprtion but complicated with interactions of different mechanisms.

The pseudo-second order kinetic model showed a better fit for CaMFCP than pseudo-first order kinetic model. A good fit to the pseudo-second order usually indicates chemisorption involving valency forces through exchange or sharing of electrons between CaMFCP and phosphate could be a rate limiting step. This suggests that each phosphate molecules was attached to two adjacent active sites on the CaMFCP and the process was irreversible. The Bangham's diffusion model also showed a good fit for CaMFCP, this indicates that pore diffusion was involved in the uptake of phosphate by CamFCP. The multistep process of the model signifies that pore diffusion was not the only rate limiting step for the uptake of phosphate by CaMFCP and could be concluded that the adsorption of phosphate by CaMFCP was a chemical process coupled with some physical diffusion process.

The pseudo-first order kinetic model showed a better fit for AlMFCP and FeMFCP suggesting physisorption as a mechanism for the adsorption of phosphate using these pellets. The pellets also showed a good fit to Bangham's pore diffusion model. This suggests the adsorption of phosphate using AlMFCP and FeMFCP involved an electrostatic attraction between the phosphate and the pellets supported by physical diffusion processes **(See Section 5.6.1)**.

6.6.4.1 Intra-particle Diffusion

The adsorption mechanism of phosphate onto modified FCP was investigated using intra-particle diffusion theory described in **Section 5.6.1.5**. A plot of the qt against √t **(Figure 6.16)** should yield a linear relationship if intra-particle diffusion is involved in the adsorption of phosphate by FCP. A line passing through the origin indicates intra-particle diffusion was the rate controlling step and the slope of the linear curve

is the diffusion rate constant. When the line does not pass through the origin, it shows a degree of boundary layer control indicating that intra-particle diffusion was not the only rate controlling step and other kinetic models may have been operating simultaneously to control the rate of reaction (Mezenner and Bensmaili 2009). The slope of the plot indicated the rate constant of intra-particle diffusion while the intercept was proportional to the thickness of the boundary layer (Haung *et al.* 2014).

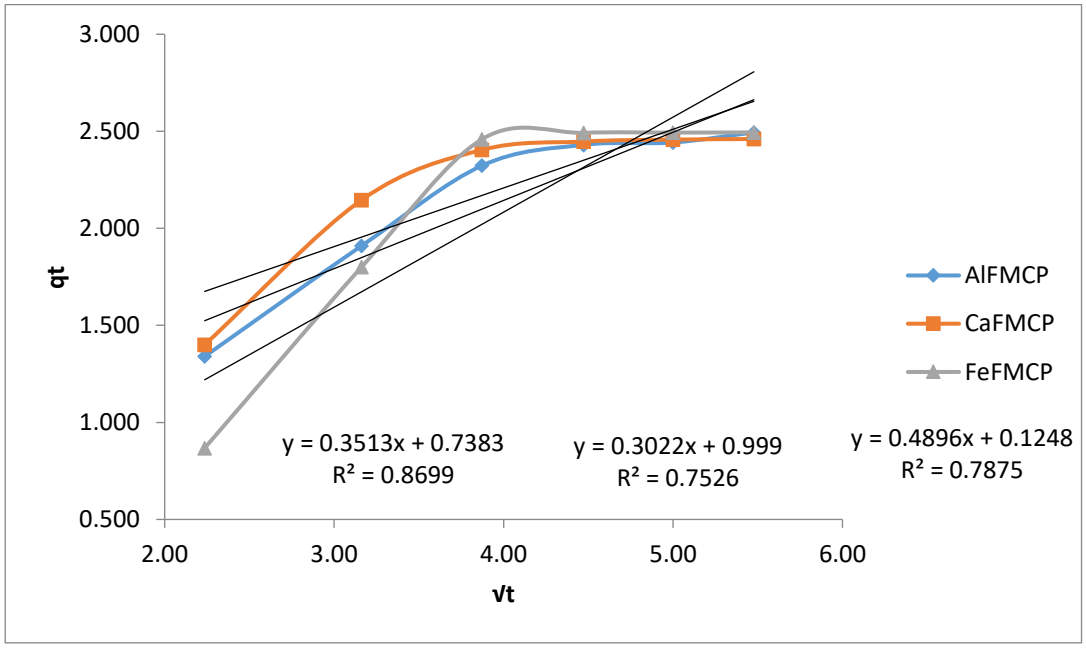

Figure 6.16: Intraparticle diffusion model plot of qt (mg/g) against √t (mins) for the adsorption of 50mg/l phosphate solution using 3g FCP.

The plot in **Figure 6.16** show a multi-linear profile that do not pass through the origin and indicated a poor fit (R^2 = 0.86 AlMFCP; 0.75 CaMFCP and 0.79 FeMFCP). There was some degree of boundary layer control in the adsorption of phosphate using modified FCP as the plots did not pass through the origin. The profile for modified FCP showed multi-step processes, where the initial sections could be described as the area of fast uptake as a result of the boundary layer diffusion on the surface of the modified FCP. This involved the mass transfer of phosphate molecules from the aqueous solution to the pellet surface influenced by the initial concentration of the phosphate solution. The second stage of the profile indicated a gradual adsorption of phosphate in which the rate of adsorption is limited by the intra-particle diffusion (Huang *et al.* 2014). The latter stages showed a decreasing adsorption as a result of the low residual phosphate concentration in the solution (Huang *et al.* 2014, Ifelebuegu 2012).

This profile indicates that other mechanisms were involved in the adsorption process as the value of intercept *C*, was 0.74, 1 and 0.12 for AlMFCP, CaMFCP and FeMFCP respectively. If the value of *C* was zero then the adsorption rate of the entire adsorption process would governed by intra-particle diffusion (Huang 2014).

6.6.4.2 Thermodynamic parameters

The temperature dependence of the adsorption process is often associated with changes in the thermodynamic parameters. These parameters Gibbs free energy (ΔG^o), enthalpy (ΔH^o) and entropy (ΔS^o) were determined using **Equations 3.14-3.16**.

A plot of ln Kd against 1/T **(Figure 6.17)** using data obtained in **Figure 6.13a- 6.15a**, yielded a straight line graph showing a linear relationship between the logarithm of the rate constant and the inverse of temperature with ΔH^o and ΔS^o values calculated from the slope and intercept of the Van't Hoff plot while ΔG^o was calculated using **Equation 3.14** (Ifelebuegu 2012, Mezenner and Bensmaili 2009). The thermodynamic parameters for the adsorption of phosphate by modified FCP are shown in **Table 6.4 and 6.5**.

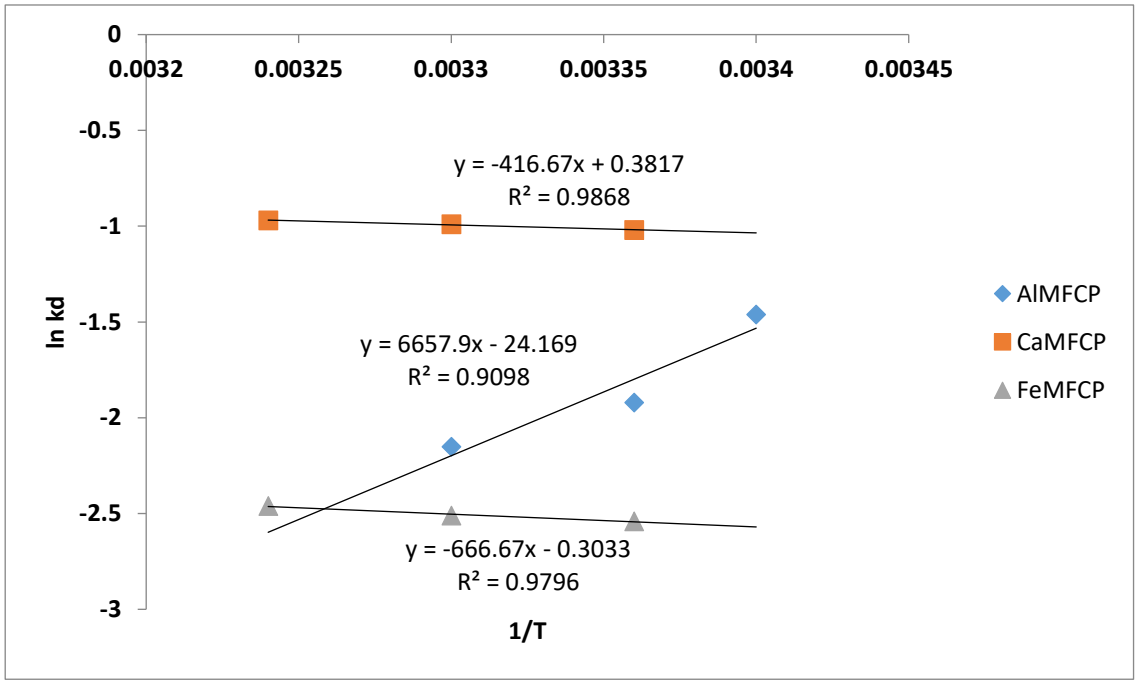

Figure 6.17: Van't Hoff plot for the adsorption of phosphate by modified FCP.

Table 6.4: Gibbs free energy (ΔG°) for the adsorption of phosphate using modified FCP

	ΔG° (KJ/mol)		
Temp (°C)	**$Al_2(SO_4)_3$**	**$CaCO_3$**	**$FeSo_4$**
20	-0.378	-0.529	-0.579
25	-0.498	-0.531	-0.578
30	-0.618	-0.533	-0.576
35	-0.738	-0.535	-0.575

Table 6.5: Thermodynamic parameters for the adsorption of phosphate by modified FCP.

	$Al_2(SO_4)_3$	**$CaCO_3$**	**$FeSo_4$**
ΔH° (KJ/mol)	6.66	-0.417	-0.667
ΔS° (KJ/mol/K)	-0.024	3.82×10^{-4}	3.03×10^{-4}
E_a (J/mol)	0.20	-3.33×10^{-3}	0.003
A	1.11	0.59	1.79

The values of ΔG^o obtained for all pellets type at all temperatures studied were negative, this indicated the spontaneous nature of the adsorption of phosphate onto FCP and adsorption was a thermodynamically favourable process **(Table 6.4)**. The decrease in ΔG^o as temperature increased suggests an increase in the spontaneity of the adsorption process at higher temperature and is similar to the trend reported by Tian *et al* (2009) on the use of mixed lanthanum/aluminum pillared montmorillonite for the adsorption of phosphate. The decrease in ΔG^o contradicts the result of the effect of temperature **(Figure 6.12)** as increased spontaneity should increase adsorption. The values of ΔG^o suggests a physisorption process as values of ΔG^o for physisorption process are generally between -20 KJ/mol and 0 KJ/mol. However, due to the inconsistencies with the results and trends in this study, the adsorption mechanism could be said to be complicated with an interaction of different processes. The negative value of ΔH^o (-0.42 kJ for CaMFCP and -0.67 kJ for FeMFCP) confirmed the exothermic nature of the process **(Table 6.5)**. The positive value of ΔS^o (3.82×10^{-4} for CaMFCP and 3.03×10^{-4} for FeMFCP) indicated the increased randomness at the solid-solution interface during the adsorption of phosphate onto FCP and a good affinity of phosphate ions towards the FCP (Huang 2015). This is consistent with the higher adsorption capacity reported for these pellets **(Table 6.6).** The negative value of the activation energy E_a (-3.33×10^{-3} J/mol) for CaMFCP indicated the absence of an energy barrier, while the low

activation energy E_a of 0.2 J/mol and 0.003 J/mol for AlMFCP and FeMFCP respectively signified a low energy barrier for the adsorption of phosphate using AlMFCP and FeMFCP.

The results of the thermodynamic study confirm the absence of a single process being predominantly responsible as the adsorption mechanism using the modified pellets as an adsorbent for wastewater treatment.

6.6.5 Effect of initial concentration

The effect of the initial concentration of phosphate solution using modified fired clay pellets was investigated by varying the concentration of the phosphate solution from 50 mg/L to 1000 mg/L while maintaining other experimental conditions. Complete phosphate removal was achieved for all phosphate concentrations studied except 750 mg/L and 1000 mg/L **(Figure 6.18)**. This result was also used to evaluate the adsorption isotherms.

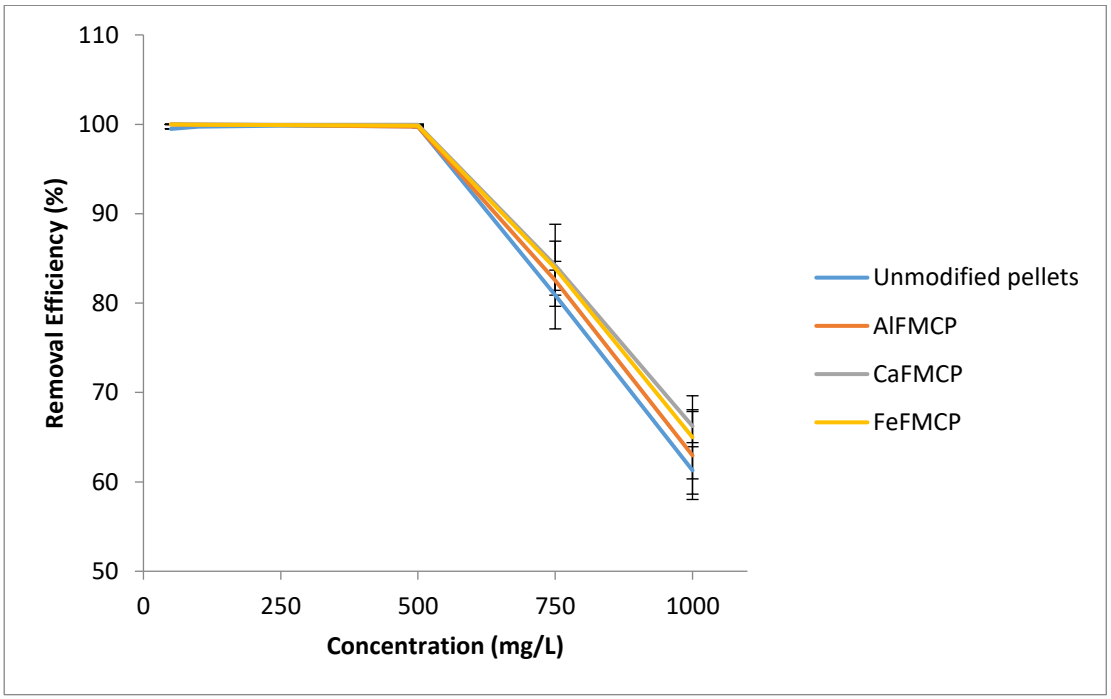

Figure 6.18: Effect of initial concentration on removal efficiency of clay pellets using 5g FCP and 200ml phosphate solution (n=3), standard error bars shown.

Removal efficiency decreased as the concentration of the phosphate solution increased from 500 mg/L to 1000 mg/L **(Figure 6.18)**. The time curve for adsorption was smooth and continuous which suggests the probability of the development of a monolayer coverage on FCP surface (Das *et al*. 20006). At lower concentration, the

ratio of available active sites on the surface of the pellets to total phosphate ions present in the solution is high; hence phosphate ions are sorbed on the active sites and taken out of solution (Teka and Enyew 2014; Das *et al.* 2006). An increase in the concentration of the phosphate solution reduces the ratio of available active sites to total phosphate ions present; making available active sites harder to find due to the fixed number of available active sites for any given mass of adsorbent. The decline in the ratio increases competition for available sites between the phosphate molecules thus leading to a reduction in the removal efficiency seen at higher concentration.

Complete phosphate removal achieved at lower concentration is due the availability of excess active sites in relation to phosphate ions present in the solution, consequently adsorption saturation was not achieved at the lower concentrations (Rout *et al.* 2014).

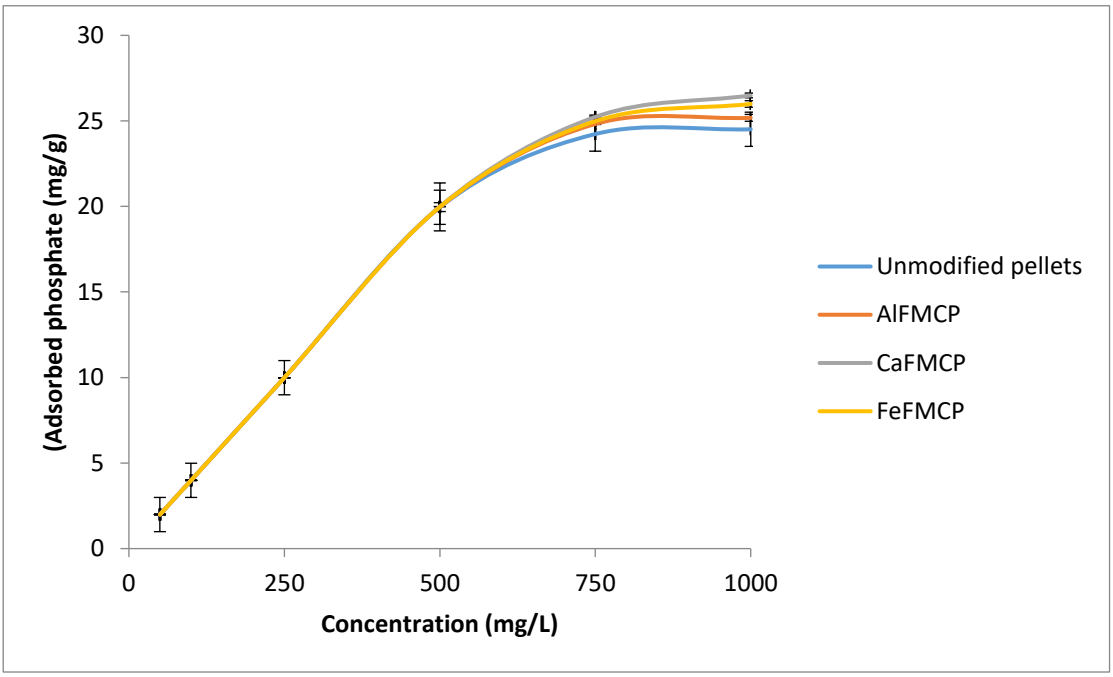

Figure 6.19: The effect of initial concentration on amount of phosphate adsorbed by FCP using 5g clay tiles and 200ml phosphate solution (n=3), standard error bars shown.

The amount of phosphate adsorbed per unit mass of the clay pellets increased with increase in concentration **(Figure 6.19)**. This is due to the increase in the amount of phosphate ions available as the concentration increases leading to an increase in the probability of collision between the phosphate ions and the active sites on the

surface of modified FCP. A higher concentration of phosphate also increases the concentration gradient between the phosphate solution and the solid phase resulting in an increase in the amount of phosphate taken out of solution (Nawar *et al*. 2015).

The generation of the driving force required to reduce the mass transfer resistance between the phosphate solution and modified FCP increases as the amount of phosphate ions available for adsorption increases at higher concentration. This corresponding increase in the generation of the driving force consequently results in an increase in the amount of phosphate taken out of the solution (Albadarin *et al.* 2012, Hameed and El-Khaiary 2008).

6.6.6 Adsorption Isotherms

The adsorption data using FCP discussed in the previous section were analyzed using Langmuir, Freundlich, Tempkin and Dubinin-Radushkeivich Isotherm models described in **Section 2.7.2** to determine the model that best fit the adsorption of phosphate onto modified FCP.

The Langmuir isotherm parameters Q_m, K_L and R_L obtained using **Equation 2.24 and Equation 2.25** were calculated from the slope and intercept of a plot of $1/q_e$ against 1/Ce **(Figures 6.20a – 6.22a)**.

The Freundlich isotherm parameters K_f, 1/n and n obtained using **Equation 2.27** were calculated from the slope and intercept of a plot of Log qe against Log Ce **(Figures 6.20b – 6.22b)**.

The Tempkin isotherm parameters A_T, *b*, *B* obtained using **Equations 2.29 – 2.32** were calculated from the slope and intercept of the plot of qt against ln t **(6.20c - 6.22c)**.

Dubinin-Radushkevich (D-R) adsorption isotherm model is usually applied to distinguish the physical and chemical adsorption using the mean free energy E. E (kJ/mol) is the energy required to remove a molecule of adsorbate from its location in the sorption site to infinity (Foo and Hameed 2010). The D-R isotherm parameters *B* and E obtained using **Equations 2.33- 2.35** were calculated from the slope and intercept of the plot of ln qe against ε^2 **(Figures 6.20d - 6.22d)**.

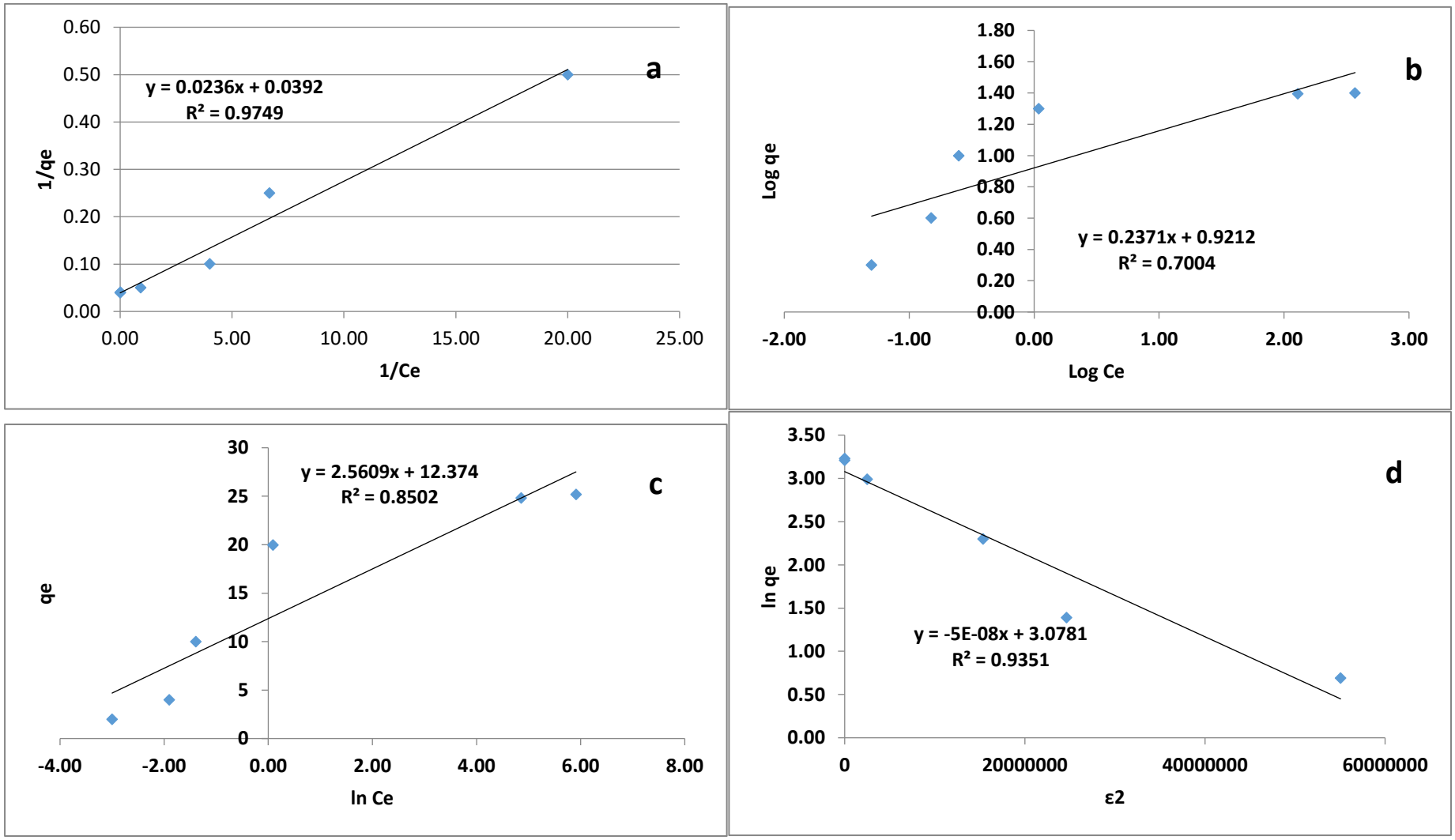

Figure 6.20: The adsorption isotherm plots for the adsorption of phosphate using AlMFCP: a) Langmuir adsorption isotherm; b) Freundlich adsorption isotherm; c) Tempkin; and d) Dubinin-Radushkevich adsorption Isotherm.

The adsorption isotherm plots for the adsorption of phosphate using AlMFCP are shown in **Figure 6.20**. The Langmuir isotherm showed the best fit (R^2 = 0.9749) of all the isotherms studied **(Figure 6.20a)**. K_L and R_L was determined as 0.6L/mg and 0.03 respectively **(Table 6.6)**. The R_L value was less than 1 signifying the adsorption of phosphate using ALMFCP was a favourable process. The maximum adsorption capacity Q_m was 42.37 mg/g was greater than 13.23 mg/g reported for FCP **(Section 5.7.1)**, this implies a significant potential for the industrial application of AlMFCP for the removal of phosphates from wastewater. The Q_m is similar to those reported in literature. Cheng *et al*. (2009) reported Q_m of 44.11 mg/g using zinc-aluminum layered double hydroxides to remove phosphate from sewage sludge filtrate. Hamdi and Srasra (2012) obtained 42.19 mg/g when a Tunisian Smectite clay was used to remove phosphate ions from aqueous solution.

The nature of the adsorption of phosphate on AlMFCP was determined using D-R isotherm model. The R^2 value of the D-R isotherm was 0.9351 **(Figure 6.20d)**. The value of E is used to predict the nature of the adsorption process. E values less than 8 kJ/mol usually indicate a physical adsorption, while values between 8 and 16 kJ/mol indicate a chemical adsorption (Kose and Kivanc 2011). The value of E for the adsorption of phosphate on AlMFCP was 2.7 kJ/mol **(Table 6.6)**, this indicates adsorption was a physical process.

Freundlich isotherm model is used to describe the heterogeneity of the adsorption surface. The adsorption data for the adsorption of phosphate did not give a good fit for Freundlich isotherm with an R^2 of 0.7004 **(Figure 6.20b)**. Adsorption intensity n is used to describe the heterogeneity of the adsorption surface, a smaller 1/n value indicates a more heterogeneous surface and an n value between one and ten indicates a favourable process (Nawar *et al.* 2015). The value of n and 1/n for this study was 4.22 and 0.24 respectively **(Table 6.6)**, indicating the adsorption was favourable and the surface of AlMFCP was heterogeneous.

Tempkin isotherm model is used to evaluate the heat of sorption which could be used to describe the adsorption process. Tempkin isotherm did not give a good fit with the data for the adsorption of phosphate on AlMFCP **(Figure 6.20c)**. A_T and *B* value was 1.07 L/mg and 36.80 J/mol respectively **(Table 6.6)**. The positive value of *B* means the adsorption was exothermic confirming the result of the kinetic study.

Table 6.6: Adsorption isotherm parameters for the adsorption of phosphate onto modified FCP

Adsorption Isotherm Model	Parameter	AlMFCP	CaMFCP	FeMFCP
Langmuir Isotherm	Q_m (mg/g)	42.37	70.42	52.91
	K_L (L/mg)	0.60	0.69	0.52
	R_L	0.03	0.03	0.04
	R^2	0.9749	0.9895	0.9668
Freundlich Isotherm	k_f (mg/g)	8.34	10.04	8.80
	$\frac{1}{n}$	0.2371	0.2049	0.2311
	n	4.22	4.85	4.33
	R^2	0.7004	0.6332	0.695
Temkin Isotherm	A_T (L/mg)	1.07	1.13	1.08
	b	66.23	130.26	78.37
	B (J/mol)	36.80	18.71	31.10
	R^2	0.8502	0.8074	0.8557
Dubinin-Radushkeivich Isotherm	B (mol^2/kJ^2)	0.07	0.06	0.07
	E (kJ/mol)	2.70	2.86	2.70
	R^2	0.9351	0.9797	0.9429

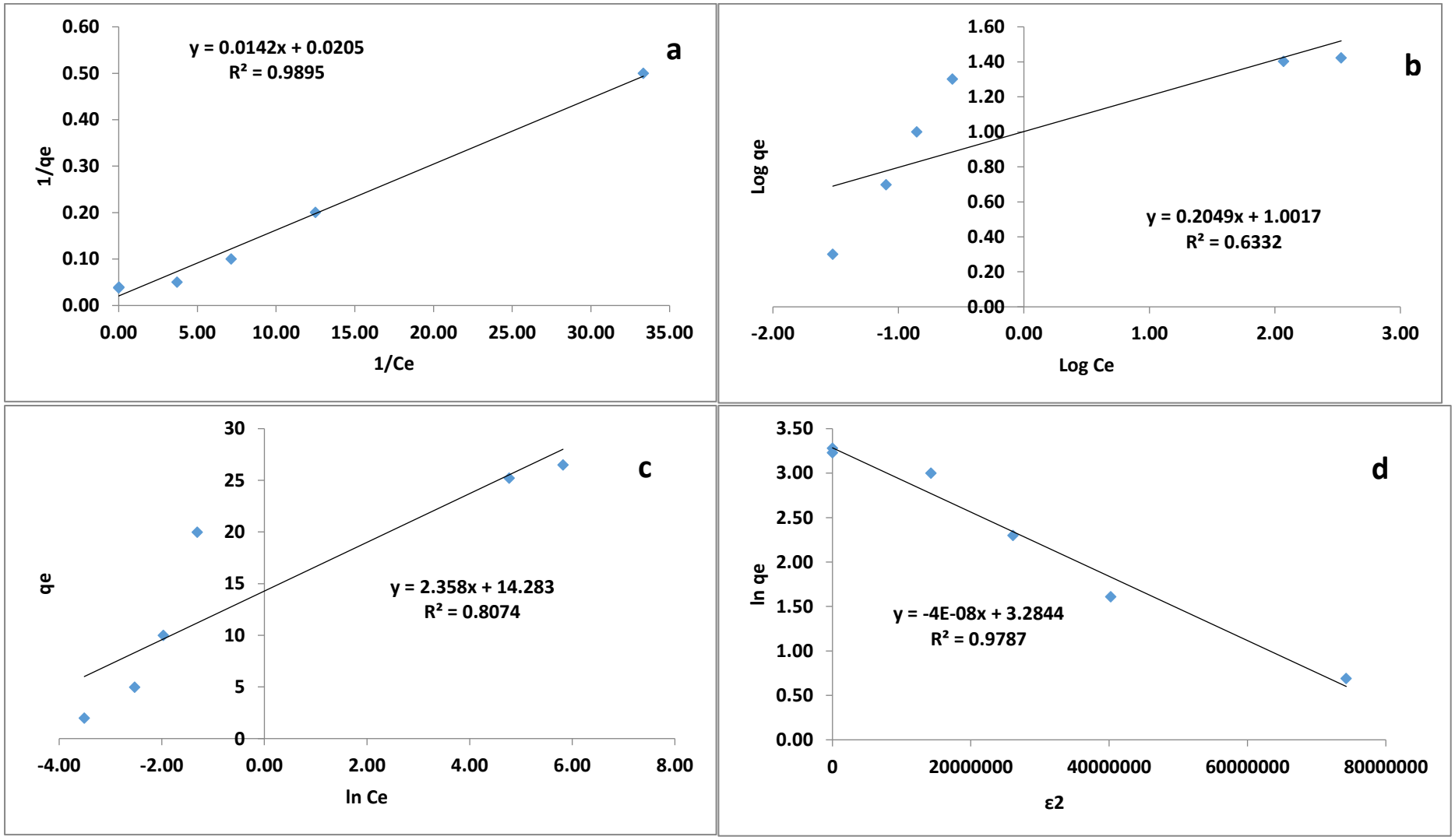

Figure 6.21: The adsorption isotherm plots for the adsorption of phosphate using CaMFCP: a) Langmuir adsorption isotherm; b) Freundlich adsorption isotherm; c) Tempkin; and d) Dubinin-Radushkevich adsorption Isotherm

The adsorption isotherm plots for the adsorption of phosphate from wastewater using CaMFCP are shown in **Figure 6.21**. The Langmuir isotherm showed the best fit (R^2 = 0.9895) with the experimental data **(Figure 6.20a)**. K_L and R_L were estimated from the slope of the plot as 0.69 L/mg and 0.03 respectively **(Table 6.6)**. R_L also known as separation factor is a dimensionless constant used in predicting the affinity between the adsorbent and adsorbate (Al-Fatlawi and Neamah 2015). The adsorption of phosphate using CaMFCP was a favourable process as the R_L value was less than 1. R_L values between zero and one signifies a favourable process. The Langmuir affinity constant K_L was 0.69 L/mg, indicating a high affinity of CaMFCP towards phosphate ions (Pawar *et al*. 2016). The maximum adsorption capacity Q_m was 70.42 mg/g **(Table 6.6)** this is higher than 13.23 mg/g obtained using FCP **(Section 5.7.1)** indicating a better performance by CaMFCP. The maximum adsorption capacity demonstrates that that CaMFCP has a significant potential for use on an industrial scale in removing phosphate from wastewater. The Q_m is similar to those reported by Huang (2014) 69.8 - 79.6 mg/g using $La(OH)_3$-modified exfoliated vermiculites as phosphate adsorbent.

The experimental data did not give a good fit using Freundlich isotherm model with R^2 = 0.6332 **(Figure 6.21b)** and could not be used to describe the adsorption. Adsorption intensity n is used to describe the heterogeneity of the adsorption surface, a smaller 1/n value indicates a more heterogeneous surface and an n value between one and ten indicates a favourable process (Nawar *et al.* 2015). The degree of linearity between the adsorption and solution concentration is also evaluated using n. An n value of one signifies a linear adsorption, n values less than one indicates a chemical process, while n values greater than one shows adsorption is a physical process (Al-Fatlawi and Neamah 2015). The value of n and 1/n for this study was 4.85 and 0.2 respectively **(Table 6.6)**, indicating the adsorption was favourable and the surface of CaMFCP was heterogeneous and adsorption was a physical process.

The nature of the adsorption of phosphate on CaMFCP was determined using D-R isotherm model. The R^2 value of the D-R isotherm was 0.9797 **(Figure 6.5.6.2d)**. The value of E is used to predict the nature of the adsorption process. E value less than 8 kJ/mol usually indicates a physical adsorption, while values between 8 and 16 kJ/mol indicate a chemical adsorption (Kose and Kivanc 2011). The value of E

for the adsorption of phosphate on CaMFCP was 2.86 kJ/mol **(Table 6.6)**, this indicates adsorption of phosphate using CaMFCP was a physical process.

Tempkin isotherm model is used to evaluate the heat of sorption which could be used to describe the adsorption process. Tempkin isotherm did not give a good fit with the data (R^2 = 0.8074) for the adsorption of phosphate on CaMFCP **(Figure 6.21c)**. A_T and *B* value was 1.13 L/mg and 18.71 J/mol respectively **(Table 6.6)**. The positive value of *B* means the adsorption was exothermic confirming the result of the kinetic study.

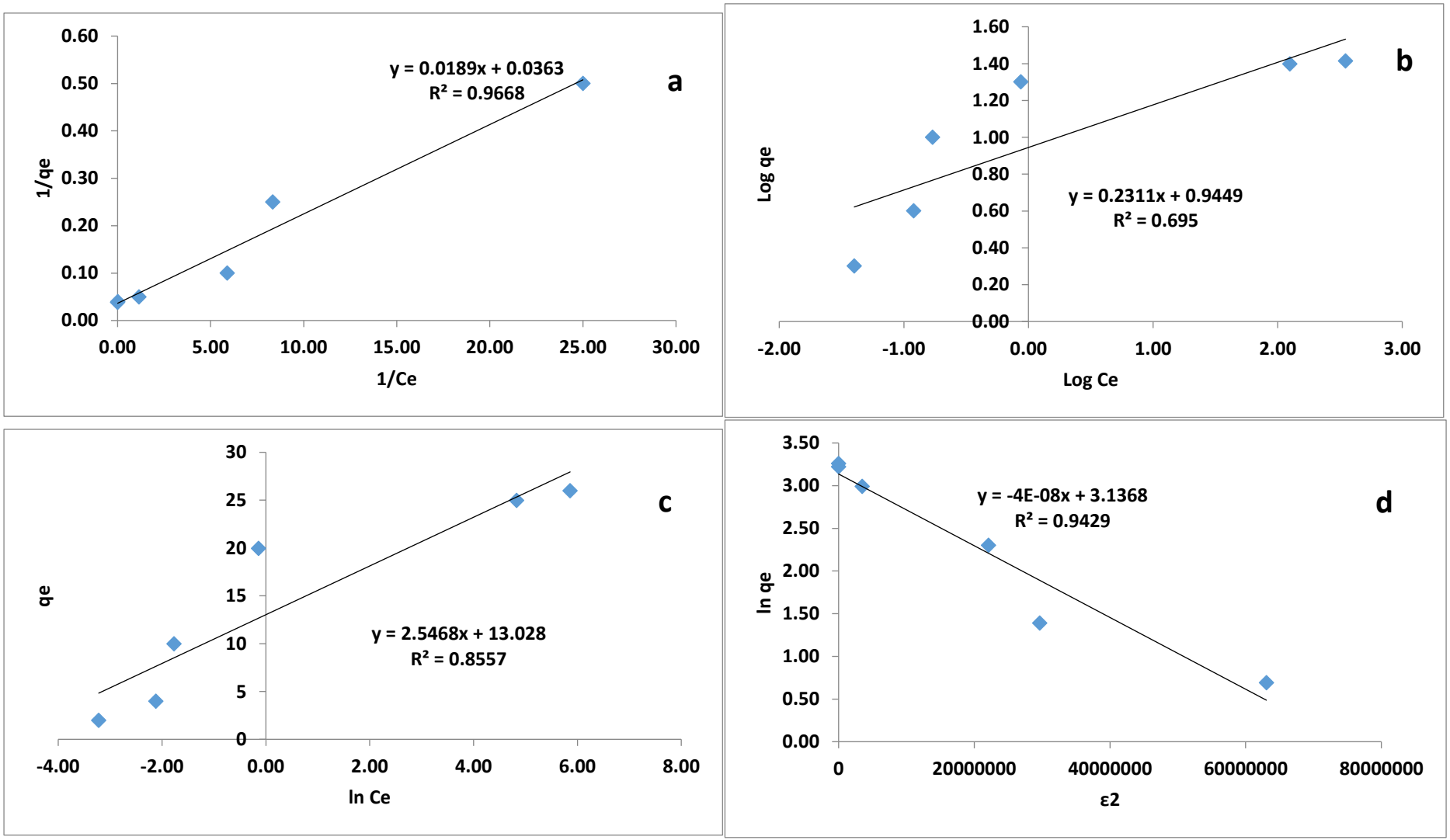

Figure 6.22: The adsorption isotherm plots for the adsorption of phosphate using FeMFCP: a) Langmuir adsorption isotherm; b) Freundlich adsorption isotherm; c) Tempkin; and d) Dubinin-Radushkevich adsorption Isotherm

The adsorption isotherm plots for the adsorption of phosphate using FeMFCP are shown in **Figure 6.22**. The Langmuir isotherm showed the best fit (R^2 = 0.9668) of all the isotherms studied **(Figure 6.22a)** similar to those shown by AlMFCP and CaMFCP discussed earlier in this section. R_L and K_L was determined as 0.04 and 0.52L/mg respectively **(Table 6.6)**. The R_L value was less than 1 signifying the adsorption of phosphate using FeMFCP was a favourable process. The maximum adsorption capacity Q_m was 52.91 mg/g was also higher than the value obtained using FCP **(Section 5.7.1)**, implying a significant potential for the industrial application of FeMFCP for the removal of phosphates from wastewater. The Q_m is similar to those reported by Vyshak and Jayalekshmi (2014), who obtained a Q_m of 52.63 mg/g using Kuttanad clay for the purification of phosphate contaminated water.

The nature of the adsorption of phosphate on FeMFCP was determined using D-R isotherm model. The R^2 value of the D-R isotherm was 0.9429 **(Figure 6.22d)**. E is used to predict the nature of the adsorption process, E value less than 8 kJ/mol usually indicates a physical adsorption, while values between 8 and 16 kJ/mol indicate a chemical adsorption (Kose and Kivanc 2011). The value of E for the adsorption of phosphate on FeMFCP was 2.7 kJ/mol **(Table 6.6)**, this indicates adsorption was a physical process.

Freundlich isotherm model is used to describe the heterogeneity of the adsorption surface. The adsorption data for the adsorption of phosphate did not give a good fit for Freundlich isotherm with an R^2 of 0.695 **(Figure 6.22b)**. K_f obtained from Freundlich isotherm was 8.8 mg/g and is similar the value reported by Pawar *et al*. (2016) using alginate immobilized aluminium-pillared acid activated bentonite beads. Adsorption intensity, n is used to describe the heterogeneity of the adsorption surface, a smaller 1/n value indicates a more heterogeneous surface and n value between one and ten indicates a favourable process (Nawar *et al.* 2015). The value of n and 1/n for this study was 4.33 and 0.23 respectively **(Table 6.6)**, indicating the adsorption was favourable and the surface of FeMFCP was heterogeneous.

Tempkin isotherm model is used to evaluate the heat of sorption which could be used to describe the adsorption process. Tempkin isotherm did not give a good fit with the data (R^2 = 0.8557) for the adsorption of phosphate on FeMFCP **(Figure 6.22c)**. A_T and *B* value was 1.08 L/mg and 31.10 J/mol respectively **(Table 6.6)**. The positive

value of *B* means the adsorption was exothermic confirming the result of the kinetic study.

6.7 Conclusion

This study has shown the potential for the use of modified clay pellets as a material for phosphate removal in wastewater treatment. The increase in the amount of phosphate adsorbed was shown to increase sharply as the concentration increased. This is a good characteristic of materials that could have industrial application for use in wastewater treatment. High phosphate adsorption rate at lower concentration will allow the treatment of large volume of wastewater before the pellets could be replaced or regenerated (Hamdi and Srasra 2012). Typical influent phosphate concentration in wastewater is 10 mg/L, lower than the concentration used in this study. There was a decrease in the contact time required for complete removal of phosphate. The maximum adsorption capacity was 42.37 mg/g, 70.42 mg/g and 52.91 mg/g for AlMFCP, CaMFCP and FeMFCP respectively. The modified pellets show a faster kinetic that was up to five times faster than FCP signifying that the modified pellets will require a reactor that was five times smaller in size than was required for FCP.

Performance using pellets with combined modification was not better than those with single modification. All three pellets showed good correlation with pseudo-first order and Bangham's kinetic model but there were variations in kinetic parameters as a function of temperature. This indicates physisorption as the dominant adsorption mechanism supported by some pore diffusion for AlMFCP and FeMFCP but the dominant mechanism for adsorption using CaMFCP was chemisorption supported by some physical diffusion processes. Acidic pH favoured adsorption using FeMFCP, and slightly acidic pH for AlMFCP while adsorption using CaMFCP was favoured at acidic and neutral pH. This means CaMFCP can be used in wastewater treatment without the need to adjust the pH, thereby reducing operational cost. The adsorption capacities of the pellets were in order CMFCP > FeMFCP > AlMFCP. The Langmuir affinity constant were also in the order CMFCP > FeMFCP > AlMFCP, signifying CaMFCP had a higher affinity for phosphate ions than AlMFCP and FeMFCP, consequently, CaMFCP was chosen for use in the column experiment and subsequent greenhouse trial.

7 Adsorption performance of a fixed bed column for the removal of phosphate using calcium carbonate modified clay pellets (CaMFCP)

7.1 Introduction

Phosphate is known to cause eutrophication of aquatic bodies which results in long-term and short term problems in the affected water bodies. One of the major effects of eutrophication is the proliferation of algae and other aquatic plants which leads to fish kill as a result of loss of deep water oxygen (Smith 2003, Smith and Schindler, Nyenje *et al.* 2010). Phosphate in municipal wastewater originate from anthropogenic sources domestic use of detergent, commercial and industrial use of phosphate as a raw material (Hammer and Hammer 2008, Kamiyango *et al* 2009, Miranzadeh *et al.* 2012). It is therefore essential to achieve low phosphate levels during wastewater treatment before discharge.

Chemical precipitation is an effective method, often results in high phosphate removal levels for phosphate removal in wastewater treatment plant (WWTWs.) The simplicity of the process makes it an attractive option in wastewater treatment (Clark *et al*. 1997). The major drawback of the chemical precipitation is the huge cost associated with chemical precipitation and sludge handling (Bertenza *et al*. 2013). The use of adsorbent for phosphate removal will provide an advantage of low cost and the reusability of the adsorbent over the commonly used precipitation (Chen *et al.* 2013).

The preceding chapter showed the potential of modified clay pellets for use in wastewater treatment using batch studies. Fixed bed column experiment is a more efficient method in studying adsorption process for industrial application in wastewater treatment (Gupta and Babu 2010). Fixed bed column experiment is usually used to provide more realistic laboratory result as it simulates the conditions obtained in wastewater treatment plants, compared to short-termed batch experiments which can lead to over estimation of adsorption capacities (Rout *et al.* 2014). Parameters that aid in design of adsorption column include flow rate, bed height, and column diameter and adsorbate concentration. Determination of breakthrough time for adsorption and other adsorption parameters allows for effective use of the column (Gupta and Babu 2010). The use of bricks or fired clay in fixed bed study for the adsorption of phosphate from wastewater has not been extensively studied. This study investigated the use of

Calcium modified fired clay pellets (CaMFCP) in a fixed bed column study. CaMFCP was chosen as the adsorbent for this study and the subsequent greenhouse experiment based on its performance in the previous chapter **(See Chapter 6)**. The breakthrough times and effect of adsorption parameters of flow rate, bed height, and column diameter and adsorbate concentration were investigated. The data obtained were analysed using Thomas, Adam-Bohart and Yoon-Nelson models to determine adsorption performance.

The fixed bed column experiment was conducted following the procedure described in **Section 3.7** and the performance parameters of the column are shown in **Table 7.1.**

Table 7.1: Fixed bed performance parameters of CaMFCP for the adsorption of phosphate

Parameter	Co (mg/L)	D (cm)	Q (ml/min)	H (cm)	t_b (Days)	t_{total} (Days)	P_{total} (mg)	q_{total} (mg)	Veff (l)	Removal Efficiency (%)	EBCT (mins)	Ur (kg/m^3)
Co	10	6	2.49	10	68	101	3611.76	1946.27	361.18	53.89	47.39	0.76
	20	6	2.49	10	57	80	5721.60	3069.71	286.08	53.65	56.02	1.05
	50	6	2.49	10	36	61	10906.80	4837.83	218.14	44.36	53.68	1.71
Bed Height	20	5	2.50	10	36	57	4104.00	1941.80	205.20	47.31	16.87	0.78
	20	5	2.50	20	46	82	5904.00	2535.62	295.20	42.95	33.74	1.06
	20	5	2.50	30	64	103	7416.00	3533.76	370.80	47.66	50.63	1.21
Flow Rate	20	4	1.70	10	68	93	4553.28	2621.36	227.66	57.57	34.84	0.71
	20	4	2.00	10	54	80	4608.00	2469.20	230.40	53.59	29.62	0.69
	20	4	2.60	10	47	68	5091.84	2646.86	254.59	51.98	22.78	0.58
Column Diameter	20	2.5	2.39	10	22	36	2471.04	1069.20	123.55	43.27	1.75	0.26
	20	5	2.39	10	47	68	4667.52	2527.09	233.38	54.14	17.58	0.81
	20	6	2.39	10	55	78	5353.92	2902.10	267.70	54.21	56.02	1.10

7.1.1 Effect of influent phosphate concentration

The effect of influent phosphate concentration on the performance of CaMFCP was investigated using varying concentrations of phosphate from 10 – 50 mg/L, bed height of 10 cm and column diameter of 6 cm. The results showed breakthrough time decreased with an increase in influent concentration as the active sites on CaMFCP were quickly saturated as there was increase in the amount of phosphate present at higher concentration **(Table 7.1)**. The adsorbent usage rate also increased with increasing influent concentration while the throughput volume of solution treated increased with a decrease in influent concentration. The decrease in the throughput volume was as a result of lower concentration gradient brought about by a slower transport of phosphate molecules due to a decrease in the mass transfer coefficient. The breakthrough curves obtained from the study evaluating the effect of influent phosphate concentration showed the steepness of the curves increased with increase

in influent phosphate concentration **(Figure 7.1).** The increase in steepness indicated a relative decrease in the mass transfer zone as influent phosphate concentration increased.

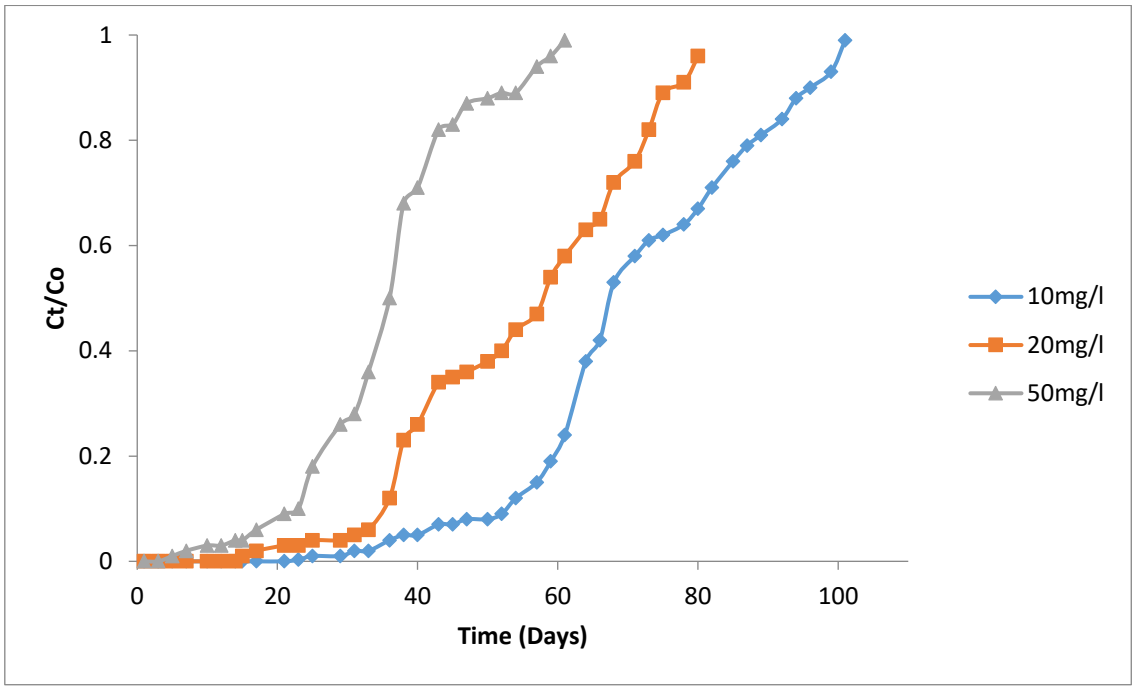

Figure 7.1: Effect of influent phosphate concentration on the experimental breakthrough curves (bed height 10 cm; column diameter 6 cm; temperature 25oC ±2 oC; pH 6.5)

The amount of phosphate adsorbed by the column increased with increasing concentration. This is as a result of a higher concentration gradient obtained as influent phosphate concentration increases which cause a faster movement of phosphate molecules (Woumfo *et al.* 2015). A higher influent phosphate concentration also provided a greater driving force that enabled the transfer process overcome the mass transfer resistance leading to an increase of phosphate adsorbed (Nur *et al.* 2014; Rout *et al.* 2014). A higher driving force for mass transfer due to increased influent phosphate concentration caused the adsorbent to achieve saturation at a faster rate leading to a decrease in the exhaustion time and length of the adsorption zone. On the other hand, the longer exhaustion time exhibited by the column with a lower influent phosphate concentration was due to a lower driving force as a result of reduced mass transfer coefficient (Rout *et al.* 2014).

7.1.2 Effect of bed height

The effect of bed depth on the performance of CaMFCP for the removal of phosphate in a fixed bed study was investigated using varying bed depth between 10 and 30 cm.

The influent phosphate concentration was 20 mg/l and column diameter was 5 cm. An increase in bed depth increased the mass of adsorbent in the column providing a larger service area for the adsorption of phosphate. The results showed breakthrough time increased from 36 to 64 days with increase in bed depth **(Table 7.1)**. The throughput volume of solution (V_{eff}) treated was shown to increase as the bed depth increased. This increase could be due to an increased contact time between the CaMFCP and phosphate ions as evidenced by the increasing EBCT with increasing bed depth. The increase in the throughput volume was also due to the increase in the availability of adsorption sites as the mass of the adsorbent increased with bed height. The adsorbent usage rate also increased with increase in bed depth. The slope of the breakthrough curve was more gradual as the bed depth increased **(Figure 7.2)** indicating the presence of an expanded mass transfer zone as bed depth increased. An increase in the mass of CaMFCP in the column created a longer distance for the mass transfer zone to move from the entrance of the bed towards the exit thus increasing the breakthrough time. Phosphate adsorption by the column was also shown to increase as a result of the expanded mass transfer zone, q_{total} increased from 1941.80 to 3533.76 mg as the bed depth increased from 10 cm to 30 cm. Yan *et al.* (2014) reported a similar increase in value of qe from 54.45 to 78.08 mg/g when the bed height 15 to 25 cm when using calcined alkaline residue for the removal of phosphate from etching wastewater. The decrease in the slope of the breakthrough curve with increased bed depth also increased the contact time resulting in a longer exhaustion time from 57 to 103 days and higher phosphate removal efficiency as the bed height increased from 10 cm to 30 cm **(Figure 7.2)**. Similar increase in exhaustion time from 310 to 700 minutes was reported obtained by Yan *et al.* (2014) when bed height increased from 15 to 25 cm.

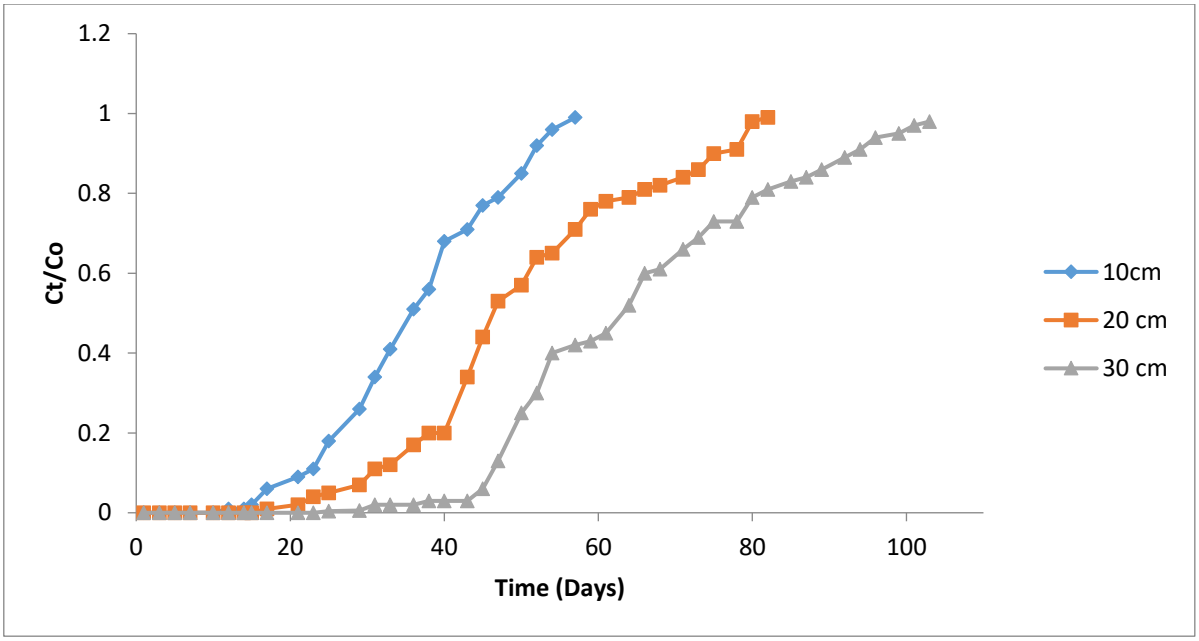

Figure 7.2: Effect of bed height on the experimental breakthrough curves (initial phosphate concentration 20 mg/l; column diameter 5 cm; temperature 25oC ±2 oC; pH 6.5)

The amount of phosphate adsorbed was also shown to increase with an increase in bed depth. The increase in the amount of phosphate adsorbed is evident in the decreased steepness of the breakthrough curve **(Figure 7.2)** associated with the longer EBCT as bed height increased. This increase in phosphate adsorption could be attributed to the increase in surface area of the adsorbent which provided more available binding sites for the adsorption of phosphate ions (Gupta and Babu 2010).

7.1.3 Effect of adsorbate flow rate

The effect of phosphate solution flow rate on the performance of CaMFCP for the removal of phosphate in a fixed bed study was investigated using varying flow rate between 1.7 and 2.6 ml/min. The influent phosphate concentration was 20 mg/l and column diameter was 4 cm and bed height was 10 cm.

The result showed a decrease in the breakthrough time from 68 to 47 days **(Table 7.1)**. The decrease in the breakthrough time as a result of the exchange of more phosphate ions with the adsorption sites on CaMFCP within a shorter time (Li *et al*. 2013). The EBCT decreased from 34.84 to 22.78 minutes as the flow rate increased. The slope of the breakthrough curve was steeper as the flow rate increased **(Figure 7.3)** indicating the presence of an extended mass transfer zone as the flow rate decreased. An increase in the flow rate resulted in the quick movement of the mass transfer zone along the column causing an early saturation of the columns at higher

flow rate. The decrease in the steepness of the breakthrough curve with decrease in flow rate resulted in higher contact time and subsequent increase in exhaustion time from 68 to 93 days when the flow rate decreased from 2.6 ml/min to 1.7 ml/min. The higher contact time at lower flow rate between the phosphate ions and CaMFCP resulted in higher removal efficiency as the flow rate decreased. Lower phosphate removal efficiency at higher flow rate could also be as a result in the reduction in the external mass film resistance at the surface of CaMFCP when the flow rate increased, leading to decreased contact time and subsequent removal efficiency (Han *et al*. 2009; Woumfo *et al*. 2015). The through put volume of solution (V_{eff}) treated was shown to increase from 227.66 to 254 litres as the flow rate increased, while the adsorbent rate usage decreased from 0.71 to 0.58 kg/m^3.

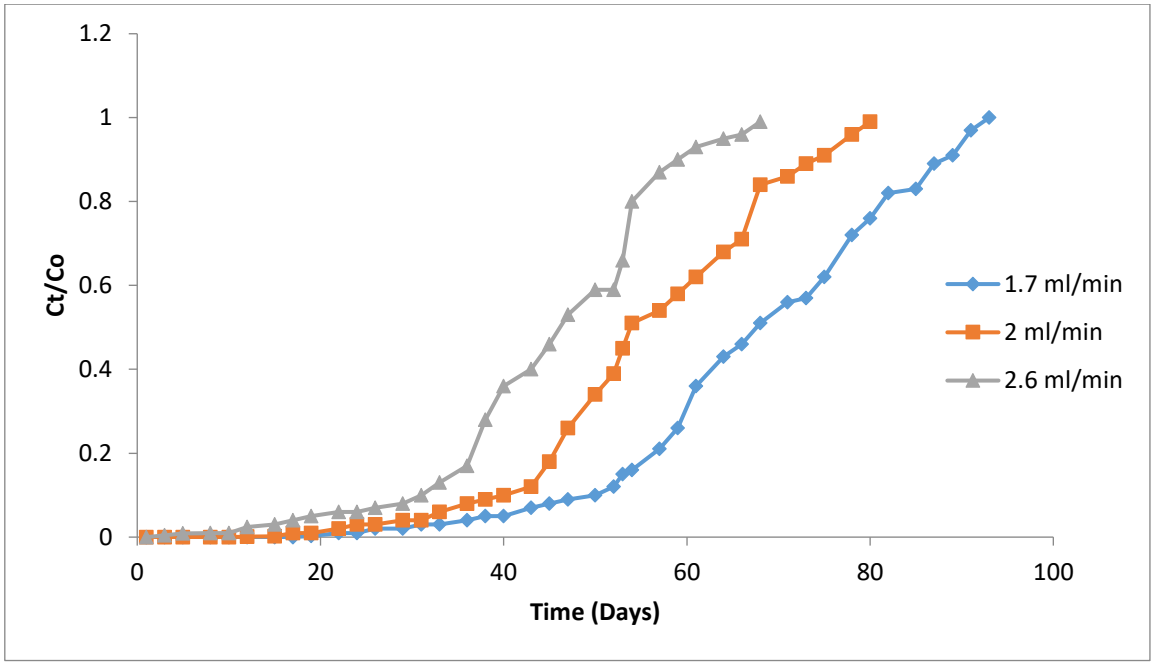

Figure 7.3: Effect of adsorbate flow rate on the experimental breakthrough curves (initial phosphate concentration 20 mg/l; column diameter 4 cm; bed height 10 cm; temperature 25oC ±2 oC; pH 6.5)

However, the amount of phosphate passing through the column increased with increasing flow rate leading to an increase in the amount of phosphate adsorbed by the column as the flow rate increased **(Table 7.1)**. The amount of phosphate adsorbed by the columns was shown to increase from 2621 to 2646 mg as the flow rate increased. The result of this study contradicts those reported by Xu *et al*. (2009) on the adsorption of phosphate from aqueous solution onto modified wheat residue. In that study, adsorbed phosphate was reported to decrease from 67.4 to 64.4 mg/g when the flow rate increased from 1 to 10 ml/min. It is suggested that an increase in

the EBCT with increase in flow rate does not allow for sufficient interaction between the adsorbate in solution and adsorbent (Sun *et al.* 2014). However, an increase in flow rate led to a corresponding increase in the volume of solution passing through the column **(Table 7.1)**, consequently increasing the P_{total} available for adsorption. This increase in P_{total} could result in the increase in the q_{total} obtained in this study.

7.1.4 Effect of column diameter

The effect of column diameter on the performance of CaMFCP for the removal of phosphate in a fixed bed study was investigated using varying diameter of the column between 2.5 and 6 cm. The influent phosphate concentration was 20 mg/l, flow rate was 2.39 ml/min and bed height was 10 cm.

An increase in the diameter of the column led to an increase in the mass of CaMFCP in the column from 32.57g to 208.52g. The breakthrough time was shown to increase from 22 to 55 days as the column diameter increased from 2.5 cm to 6 cm. Exhaustion time was also reported to increase from 36 to 78 days, which led to a subsequent increase in the through put volume (V_{eff}) from 123.55 litres using column diameter of 2.5 cm to 267.70 litres when a column with diameter of 6 cm was used. This increase in V_{eff} as a result of an increase in the mass of CaMFCP present in the column led to an increase in the quantity of active sites available for adsorption. The adsorbent usage rate was shown to increase with increase in column diameter. The slope of the breakthrough curve was steeper as the column diameter decreased **(Figure 7.4)** indicating the expansion of the mass transfer zone as the column diameter increased. The decrease in the steepness of the breakthrough curve also indicated a higher contact time between the phosphate ions and CaMFCP as EBCT was reported to increase from 1.75 minutes to 56.02 minutes. This increase in contact time resulted in a longer exhaustion time from 36 to 78 days and subsequent higher removal efficiency of 54.21% reported using 6cm column diameter **(Table 7.1)**.

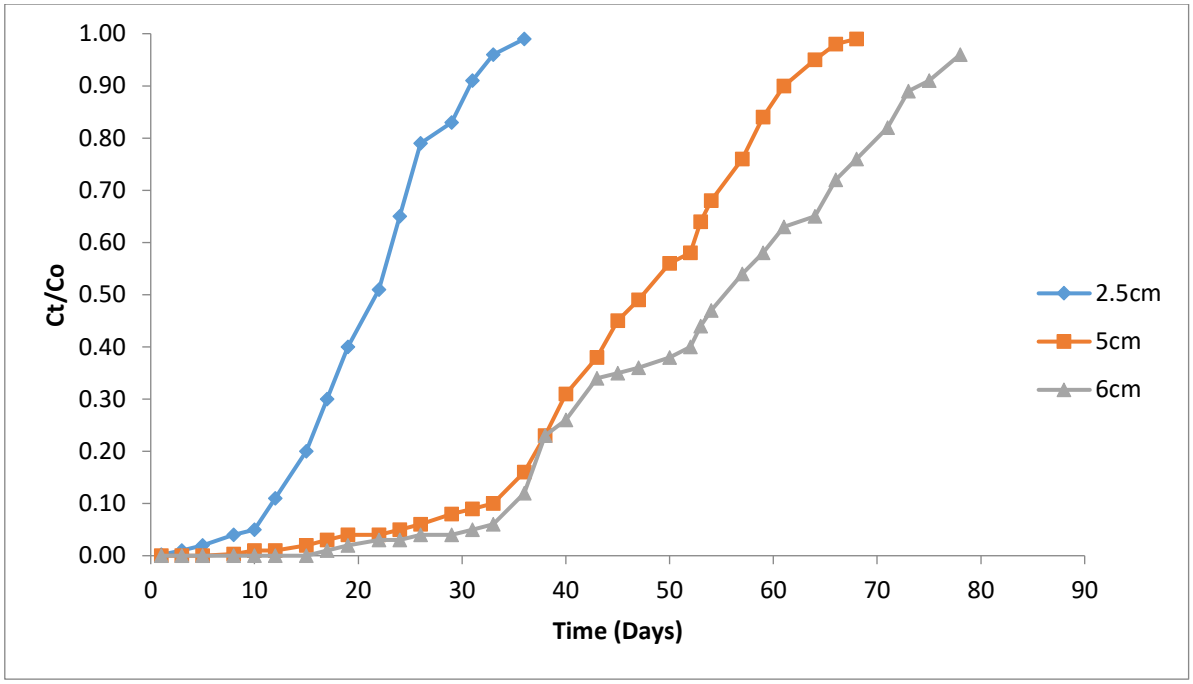

Figure 7.4: Effect of column diameter on the experimental breakthrough curves (initial phosphate concentration 20 mg/l; flow rate 2.39 ml/min; bed height 10 cm; temperature 25oC ±2 oC; pH 6.5)

The amount of phosphate adsorbed was also shown to increase with an increase in bed depth. The increase in the amount of phosphate adsorbed is evident in the decreased steepness of the breakthrough curve **(Figure 7.4)** associated with the longer EBCT as column diameter increased. This increase in phosphate adsorption could be attributed to the increase in surface area of the adsorbent which provided more available binding sites for the adsorption of phosphate ions (Gupta and Babu 2010).

7.2 Modelling of fixed bed adsorption data

The prediction of the concentration-time profile from the breakthrough curve is essential when used in full scale wastewater treatment. This prediction is assisted by the successful design of the fixed bed adsorption column. To predict and analyse the dynamics of phosphate adsorption onto CaMFCP, Bed Depth Service Time (BDST), Thomas, Yoon-Nelson and Adams-Bohart models were applied to the experimental data for C_t/C_o ratio from 0.04 to 0.6 reported in **Section 7.2**.

7.2.1 Bed Depth Service Time (BSDT)

The Bed Depth Service Time (BSDT) is the commonly used model in predicting the performance of adsorption columns with known bed depths. The constants obtained from the model are used to scale up height of adsorption bed for a given influent

concentration and flow rates. The model is based on the assumption that the adsorption rate is dependent on the surface interaction between the adsorbate and unused adsorbent (Rout *et al.* 2014). The design criterion is based on the prediction of service time of the bed where the service time is the time required to remove a specific amount of adsorbate by the adsorbent before the regeneration of the adsorbent is needed. The model states that there is an existing linear relationship between bed height (H) and service time (t) and is represented as:

$$\mathbf{t = \frac{No}{CoV}H - \frac{1}{KbdCo}\ln[\frac{Co}{Cb} - 1]}$$ **Equation 7.1 (Hutchins 1973)**

where V is the linear velocity (cm^3/h), t is time (days), H is the bed height (cm), N_o is the adsorption capacity of the bed (mg/g) and K_{BD} is the BDST rate constant (L/mg/h) C_o is the influent phosphate concentration (mg/L) and C_b is the desired phosphate concentration (mg/L).

Assuming t=0

$$\mathbf{H_o = \frac{V}{KBDNo}\ln(\frac{Co}{Cb}) - 1}$$ **Equation 7.2 (Mohan and Sreelakshmi 2008)**

Where H_o is the minimum height required to produce the effluent concentration C_b. H_o is also known as the critical bed depth.

Equation 7.2 can also be expressed as

t = aH x b

where **a = slope =** $\mathbf{\frac{No}{CoV}}$ **Equation 7.3 (Mohan and Sreelakshmi 2008)**

and **b = intercept =** $\mathbf{\frac{1}{KaCo}\ln\left(\frac{Co}{Cb} - 1\right)}$ **Equation 7.4 (Mohan and Sreelakshmi 2008)**

A plot of t against H yielded a straight line and N_o and K_{BD} evaluated from the slope and intercept respectively **(Figure 7.5)**.

The model fitting was done by linear regression analysis and predicted curves obtained at various experimental conditions. The BDST plots for 10%, 50% breakthroughs and exhaustion are shown in **Figure 7.5**. The N_o, K_{BD} and R^2 values are given in **Table 7.2**.

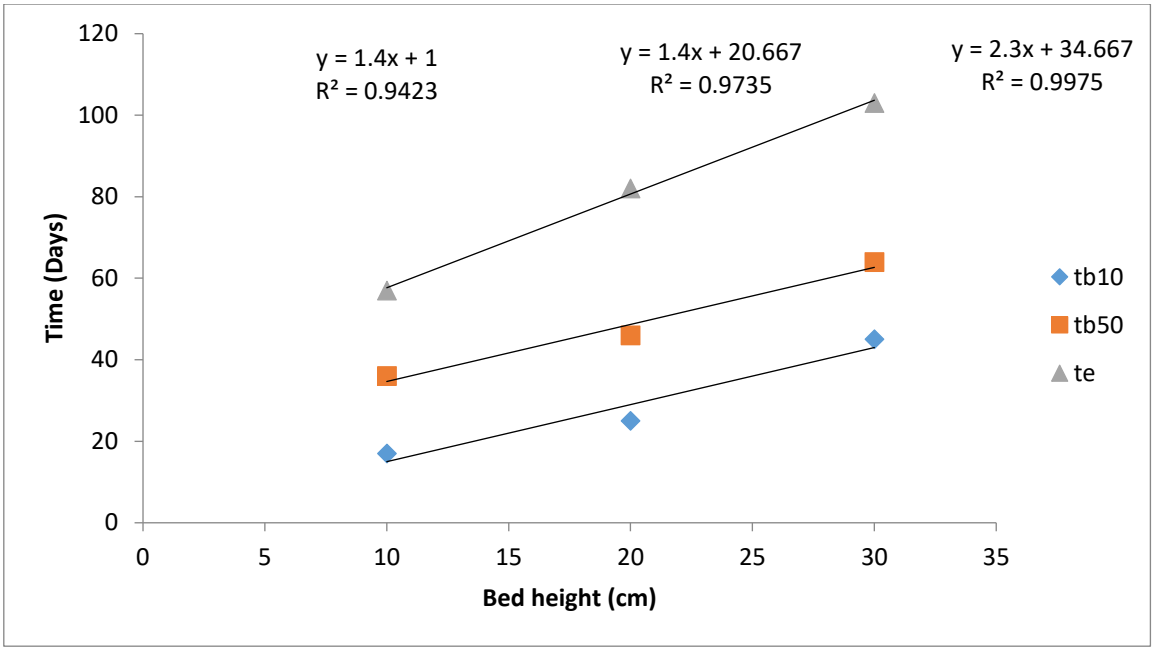

Figure 7.5: BDST plot for different bed height (flow rate 2.5 ml/min; influent phosphate concentration 20 mg/L)

There was an increase in the slope of the breakthrough with a corresponding increase in the adsorption capacity (N_o) of the columns from 4200 mgP/g to 6900 mgP/g **(Table 7.2)**.

Table 7.2: BDST parameters for adsorption of phosphate onto CaMFCP

Parameter	N_o (mg/L)	k_{BD} (L/mg min)	R^2
t_{b10}	4200	0.11	0.9423
t_{b50}	4200	7.26×10^{-5}	0.9735
t_e	6900	7.98×10^{-6}	0.9975

The BDST constant k_{BD} is used to show the rate of transfer of adsorbate from the liquid phase onto the solid phase. High k_{BD} values allow breakthrough to be avoided even when a shorter bed is used while low k_{BD} values would require deeper bed to avoid breakthrough (Jahangiri-rad *et al.* 2014). This is confirmed by the increase in the critical bed depth, which was determined as 7.1 cm, 14.76 cm and 15.07 cm with K_{BD} of 0.11 L/mg min, 7.26×10^{-5} L/mg min and 7.98×10^{-6} L/mg min for 10%, 50% breakthroughs and exhaustion respectively. This suggested that application of CaMFCP in a bed with a short depth could be used effectively while avoiding breakthrough.

Adsorption capacity obtained using BDST was lower than the total capacity of the adsorbent. The increase in the adsorption capacity from 4200 to 6900 mg/L when the bed depth increased from 10 to 20 cm corresponded with an increase in the contact time as the bed height increased allowing more phosphate ions to adsorb onto CaMFCP. Similar trend has been reported in several studies. Sun *et al.* (2014) reported an increase in the adsorption capacity of calcined Mg_3-Fe layered double hydroxides from 1104.95 mg/L to 1742.05 mg/L for the adsorption of phosphates when the breakthrough increased from 10% to 60%. The low adsorption capacity exhibited at lower breakthroughs suggests the availability of unused active sites for adsorption of phosphate ions as the column remained unsaturated. The high R^2 values (>0.94) indicate the applicability of BDST model for the adsorption of phosphate using CaMFCP.

Extrapolation of 50% breakthrough did not pass through the origin at t =0, which shows the adsorption of phosphate ions onto CaMFCP involves several processes as discussed in **Section 6.5**. Diffusion of adsorbate into the adsorbent is believed to be one of the mechanisms involved in the adsorption of phosphates from solution. A good R^2 obtained from the Elovich kinetic model usually indicates diffusion as a rate limiting step, but there were fluctuations in the values of kinetic parameters as a function of temperature **(Section 6.5.4.1)**. Other kinetic models studied also showed these fluctuations in kinetic parameters indicating one process was not the dominant adsorption mechanism but the adsorption was a result of the interaction of several processes.

7.2.2 Thomas model

Thomas model is widely used to describe the adsorption rate constant, adsorption process and maximum solid phase concentration of adsorbate on adsorbent in a fixed bed column. It is based on the assumption that the adsorption follows second rate reaction kinetics, Langmuir kinetics of adsorption and desorption and there is no axial dispersion. The model is expressed as:

$$\frac{Ct}{Co} = \frac{1}{1+\exp[\frac{KTH}{Q}(qoM - CoV)]}$$ **Equation 7.5**

Where K_{TH} is the Thomas model rate constant (ml/h/mg), q_o is maximum solid phase concentration of the solute (mg/g), V is the effluent volume (L), m is the mass of adsorbent (g) and Q is the volumetric flow rate (ml/h).

The linearised form of the model is expressed as:

$$\ln\left[\frac{Co}{Ct} - 1\right] = \frac{kTHqom}{Q} \quad - k_{TH}C_o t \qquad \textbf{Equation 7.6 (Lim and Aris 2014)}$$

Where k_{TH} is the Thomas kinetic constant (ml/h/mg), q_o is the maximum solid phase concentration (mg/g), C_o is the influent phosphate concentration, Q is the volumetric flow rate (ml/hr) and t is the total flow time. The values of K_{TH} and q_o were obtained from the plot of $\ln(C_o/C_t - 1)$ against time **(Figure 7.6)**.

The model fitting was done by linear regression analysis and predicted curves obtained at various experimental conditions.

The Thomas model (Thomas 1944; Woumfo *et al.* 2015) assumes the flow of phosphate solution through the column follows plug flow behaviour. The model is based on the assumption that phosphate ions migrate from the solution to a film surrounding the pellets before diffusing to the surface of the pellets followed by adsorption on the active sites (Han *et al.* 2009). K_{TH} and q_o obtained using **Equation 7.6** are shown in **Table 7.3**.

Table 7.3: Parameters of Adams-Bohart and Thomas models for the adsorption of phosphate by fired clay pellets under different experimental conditions.

					Adams -Bohart model			Thomas model		
Parameter	Co (mg/l)	D (cm)	Q (ml/min)	H (cm)	K_{AB} x10^{-3} (l/mg/hr)	No (mg/l)	R^2	K_{TH} (ml/h/mg)	qo (mg/g)	R^2
Initial Conc	10	6	2.49	10	7.54	419.30	0.9644	0.69	0.1	0.9393
	20	6	2.49	10	3.89	679.52	0.8861	0.28	0.25	0.937
	50	6	2.49	10	2.37	1070.20	0.9866	0.11	1.02	0.9639
Bed Height	20	5	2.50	10	5.46	797.50	0.9788	0.27	0.40	0.9931
	20	5	2.50	20	4.91	516.90	0.9866	0.32	0.28	0.9821
	20	5	2.50	30	4.46	433.63	0.7881	0.38	0.18	0.8696
Flow Rate	20	4	1.70	10	3.78	1280.48	0.9793	0.35	0.25	0.9853
	20	4	2.00	10	4.76	1205.99	0.9774	0.35	0.36	0.9839
	20	4	2.60	10	4.24	1388.07	0.9707	0.27	0.55	0.9757
Column Diameter	20	2.5	2.39	10	9.07	1461.28	0.9577	0.25	4.15	0.981
	20	5	2.39	10	4.62	1004.21	0.9795	0.29	0.46	0.9821
	20	6	2.39	10	4.22	643.78	0.9187	0.29	0.25	0.952

The results shown in **Table 7.3** indicated the Thomas kinetic constant (K_{TH}) decreased from 0.69 ml/h/mg to 0.11 ml/h/mg when influent concentration increased form 10 mg/l to 50 mg/l while the maximum solid phase concentration of phosphate (q_o) increased from 0.10 mg/g to 1.02 mg/g as influent concentration Increased. This is due to the concentration gradient acting as the driving force for the adsorption of phosphate onto CaMFCP. A higher phosphate concentration as the influent concentration increased resulted in a greater driving force which led to a higher q_o value as the concentration increased. This trend is similar to those reported by Li *et al.* (2013) on phosphate removal using nanosized FeOOH modified anion resin; Sun *et al.* (2014) on phosphate adsorption using calcined Mg_3-Fe layered double hydroxides and Yan *et al.* (2014) using calcined alkaline waste residue.

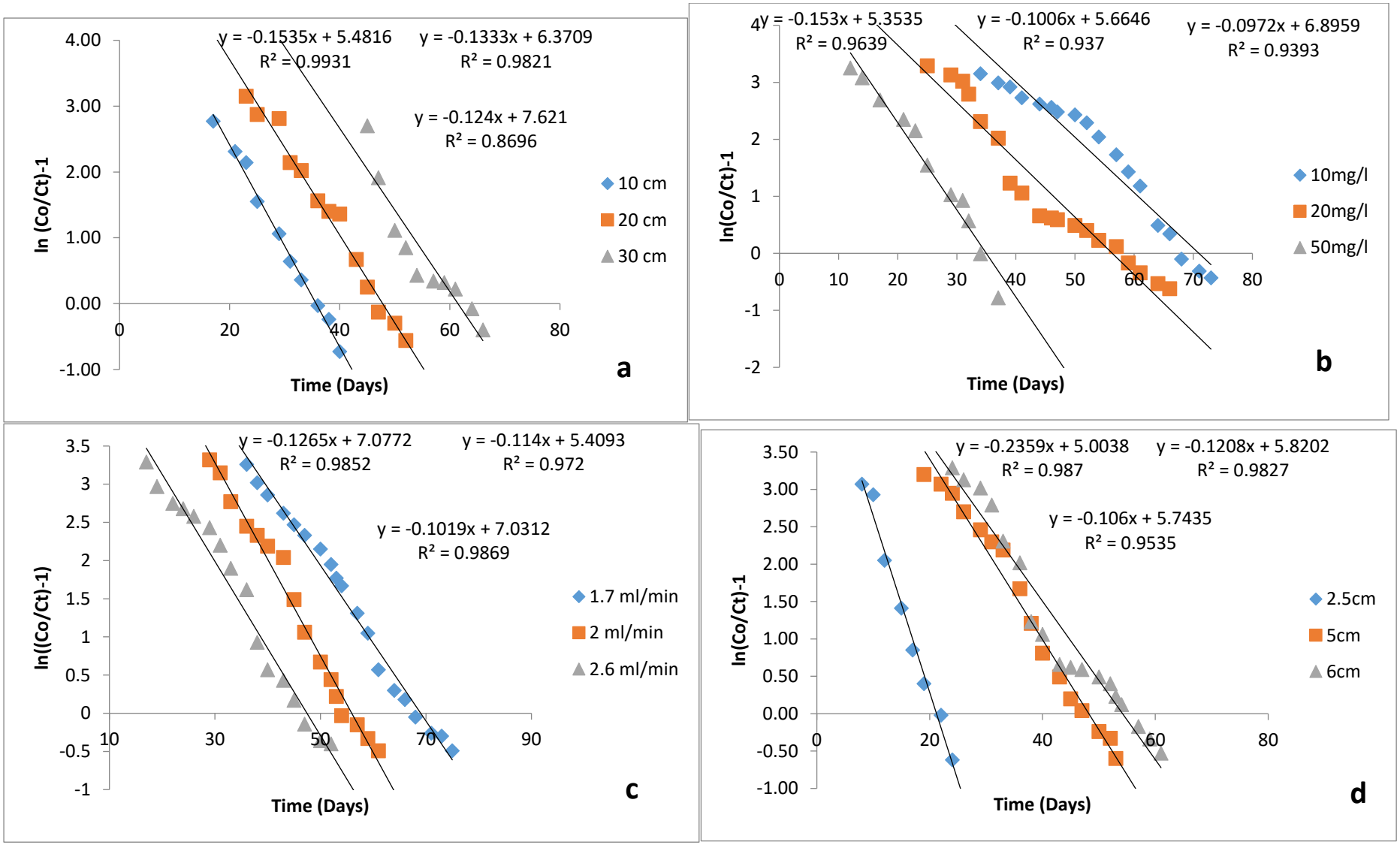

Figure 7.6: Thomas plot for the adsorption of phosphate on CaMFCP: Effect of (a) bed height; (b) influent phosphate concentration; (c) flow rate; and (d) column diameter.

The Thomas kinetic rate constant (K_{TH}) increased with an increase in bed height and column diameter. K_{TH} increased from 0.27 to 0.38 ml/h/mg as the bed height increased from 10 to 30 cm and from 0.25 to 0.29 ml/h/mg as the column diameter increased from 2.5 cm to 6 cm. The maximum solid phase concentration q_o decreased with increase in bed height and column diameter from 0.40 to 0.18 mg/g as the bed height increased from 10 to 30 cm and also decreased from 4.15 to 0.25 mg/g as column diameter increased from 2.5 to 6 cm. The increase in flow rate resulted in a decrease of the Thomas kinetic rate constant. (K_{TH}). The Thomas kinetic rate constant decreased from 0.35 to 0.27 ml/h/mg as the flow rate increased from 1.7 to 2.6 mL/min. However, q_o was shown to increase with an increase in flow rate from 0.25 to 0.55 mg/g as the flow rate increased from 1.7 to 2.6 mL/min. The value of q_o increased noticeably from 0.10 to 1.02 mg/g, but the value of K_{TH} decreased as the initial influent concentration increased from 10 to 50 mg/L. The good fit of the Thomas model to the experimental data shows could be suitably used to describe the adsorption of phosphate onto CaMFCP where pore or film diffusion was not a rate limiting step.

7.2.3 Yoon-Nelson Model

Yoon-Nelson model is commonly used to predict the exhaustion time and behaviour of the adsorption process for a given adsorbate concentration. It is based on the assumption that the rate of decrease in the probability of adsorption of adsorbate molecules is directly proportional to the adsorbate molecule adsorption and the adsorbate breakthrough on the adsorbent (Kavak and Ozturk 2004; Nwabanne and Igbokwe 2012). The model is expressed as:

$$\frac{Ct}{Co} = \frac{(\exp(Kynt) - \tau Kyn)}{1 + (\exp(Kynt) - \tau Kyn)} \qquad \textbf{Equation 7.7}$$

Where is K_{YN} is the Yoon-Nelson constant (L/h) and τ is the time required for 50% breakthrough. A linearised form of the equation for a one component system is expressed as

$$ln\frac{Ct}{Co - Ct} = Kynt - \tau Kyn \qquad \textbf{Equation 7.8}$$

Where K_{YN} is the Yoon-Nelson constant (ml/min); and τ is the time required for 50% breakthrough (mins) and are obtained from the plot of $\ln[C_t/(C_o-C_t)]$ against t **(Figure 7.7)**.

The model fitting was done by linear regression analysis and predicted curves obtained at various experimental conditions. The values of K_{YN} and τ are shown in **Table 7.4**.

Table 7.4: Parameters of Yoon-Nelson model for the adsorption of phosphate by fired clay pellets under different experimental conditions.

					Yoon-Nelson model		
Parameter	**Co (mg/l)**	**D (cm)**	**Q (ml/min)**	**H (cm)**	**K_{YN} (ml/min)**	**τ (days)**	**R^2**
Initial Conc	10	6	2.49	10	0.097	71	0.9393
	20	6	2.49	10	0.102	56	0.9366
	50	6	2.49	10	0.153	35	0.9647
Bed Height	20	5	2.50	10	0.154	36	0.9931
	20	5	2.50	20	0.130	48	0.9862
	20	5	2.50	30	0.112	56	0.8076
Flow Rate	20	4	1.70	10	0.101	69	0.9869
	20	4	2.00	10	0.126	56	0.9852
	20	4	2.60	10	0.114	47	0.972
Column Diameter	20	2.5	2.39	10	0.234	21	0.987
	20	5	2.39	10	0.120	48	0.9827
	20	6	2.39	10	0.110	56	0.9595

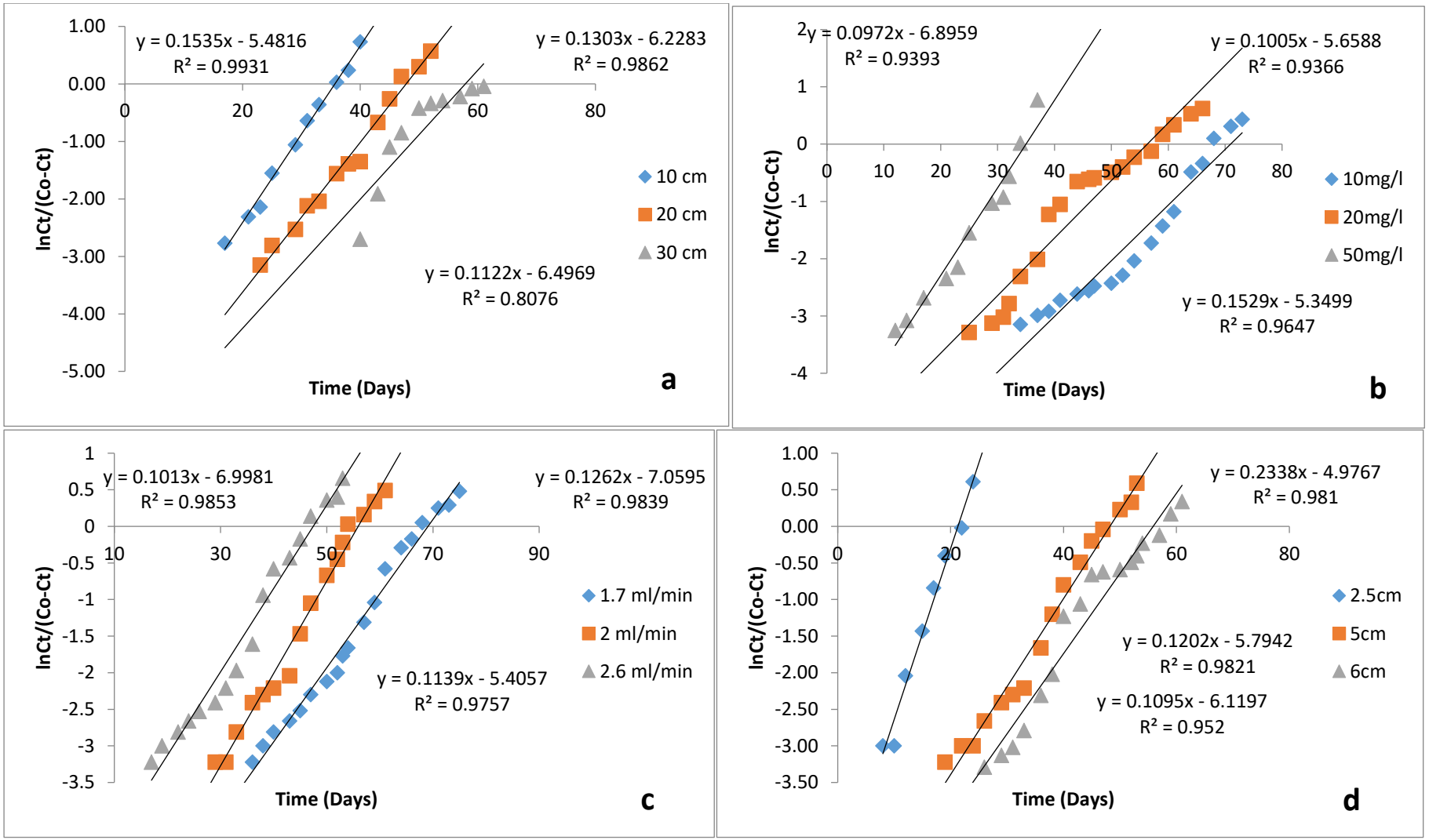

Figure 7.7: Yoon-Nelson plot for the adsorption of phosphate on CaMFCP: Effect of (a) bed height; (b) influent phosphate concentration; (c) flow rate; and (d) column diameter

The Yoon-Nelson kinetic rate constant (K_{YN}) was found to increase from 0.097 to 0.153 ml/min as influent concentration increased from 10 mg/l to 50 mg/l while the time required to achieve 50% breakthrough (τ) was found to decrease from 71 to 35 days as the influent concentration increased **(Table 7.4)**. K_{YN} increased from 0.101 to 0.126 ml/min as the flow rate increased from 1.7 ml/min to 2 ml/min before decreasing to 0.114 ml/min as the flow rate increased to 2.6 ml/min, while the time required to achieve 50% breakthrough (τ) decreased from 69 to 47 days when the flow rate increased from 1.7 ml/min to 2.6 ml/min. This is as a result of an increase in the amount of phosphate ions available for adsorption as a result of increased concentration and higher flow rate leading a faster saturation of the adsorption sites and consequently a shorter breakthrough time. A similar trend has been reported in studies by Chen *et al.* (2012) using modified corn stalk for hexavalent chromium adsorption from aqueous solution; and Rout *et al.* (2014) using a mixture of red soil and ground burnt patties to remove phosphate from aqueous solution.

On the contrary, the value of K_{YN} decreased from 0.154 to 0.112 ml/min while τ increased from 36 to 56 days as the bed height increased from 20 to 30 cm. Also, K_{YN} decreased from 0.234 ml/min to 0.11 ml/min while τ increased from 21 to 56 days as the column diameter increased from 2.5 cm to 6 cm. The increase in the breakthrough time as the bed height and column diameter increased is due to a higher number of available adsorption sites leading to a longer retention time. The effluent adsorbate concentration ratio increases more rapidly as the bed height increases with a smaller bed height corresponding to a less amount of phosphate ions adsorbed the column and time required to saturate the column (Babu and Gupta 2005). Higher breakthrough time (τ) usually corresponds to greater adsorption by the column. A high K_{YN} value indicates a smaller MTZ with greater mass transfer coefficient and lower mass transfer resistance between the phosphate molecules and CaMFCP leading to ease of adsorption. This ease of adsorption could be attributed to the decrease in τ with an increase in K_{YN} and vice versa reported in this study.

The overall good fit of the experimental data to Yoon and Nelson model shows the model can be used to predict the breakthrough curve and characteristic parameters for the adsorption of phosphate using CaMFCP.

7.2.4 Adams-Bohart Model

The Adams-Bohart model is used to describe the initial stage of operation of a breakthrough curve. It is based on the theory of surface reaction where it is assumed the rate of adsorption is proportional to the residual capacity of the adsorbent and the concentration of the adsorbing species (Han *et al.* 2009, Lim and Aris 2014). The linear form of Adams-Bohart equation is expressed as

$$\ln\left[\frac{Ct}{Co}\right] = KabCot - KabNa\left(\frac{H}{Uo}\right) \qquad \textbf{Equation 7.9}$$

where K_{AB} is the Adam-Bohart constant representing the mass transfer coefficient (l/mg/min), N_a is the saturation concentration (mg/l), U_o is the superficial velocity (cm/min), H is the bed height (cm) and t is the total flow time (days). The parameters were derived from the plot of ln C_t/C_o against time **(Figure 7.8).**

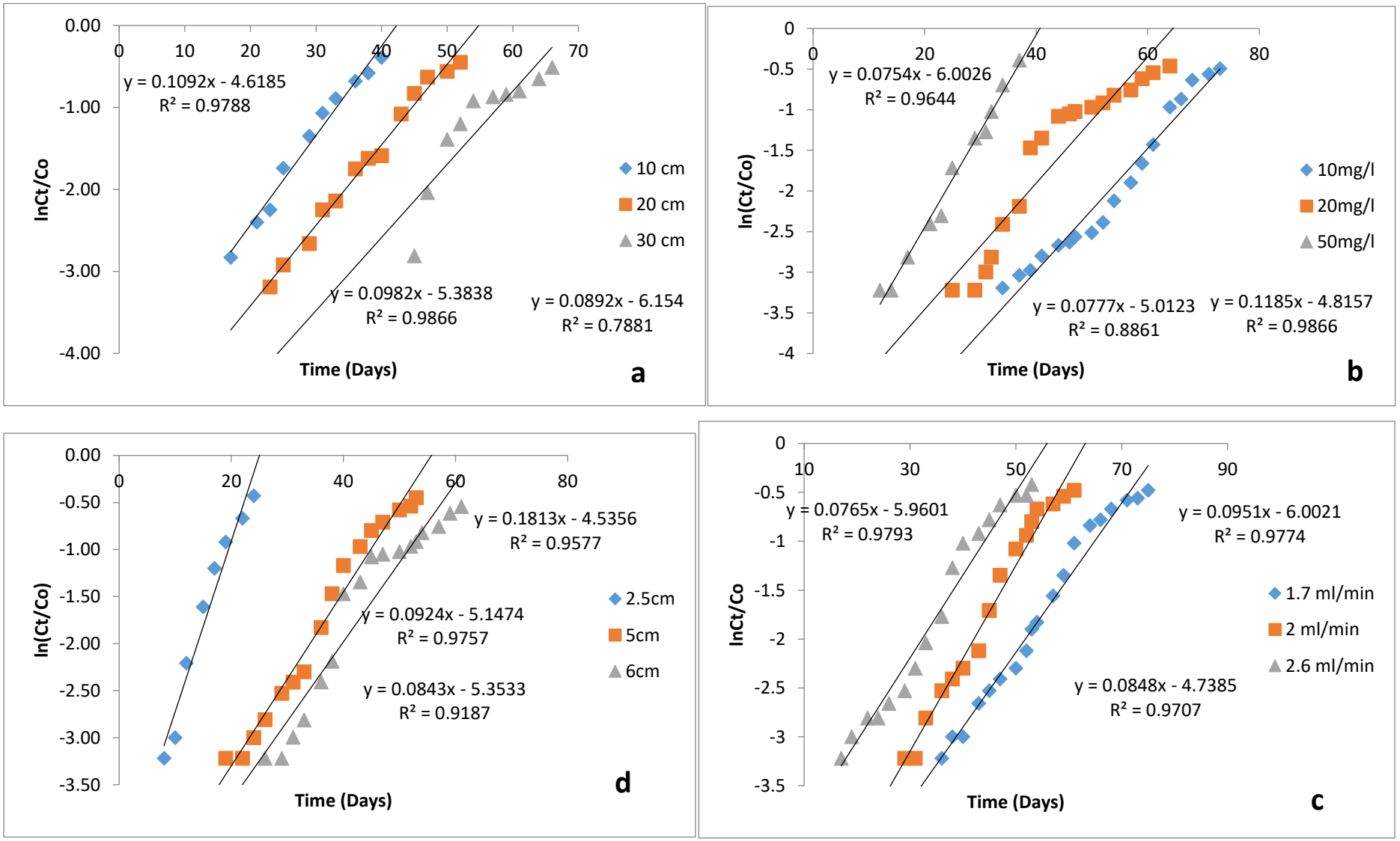

Figure 7.8: Adams-Bohart plot for the adsorption of phosphate on CaMFCP: Effect of (a) bed height; (b) influent phosphate concentration; (c) flow rate; and (d) column diameter.

Mass transfer coefficient (K_{AB}) decreased with increase in influent concentration while the saturation concentration (N_a) increased with increasing influent concentration **(Table 7.3)**. K_{AB} decreased from 7.54 $x10^{-3}$ L/mg/min to 2.37 $x10^{-3}$ L/mg/hr, while saturation concentration (N_a) increased from 419.30 to 1070.20 mg/L as influent phosphate concentration increased from 10 mg/L to 50 mg/L. Low K_{AB} value indicates smaller resistance to phosphate adsorption and higher phosphate ion concentration resulted in a reduction to the mass transfer resistance. The decrease in K_{AB} with increasing influent concentration suggests the role of external mass transfer on the kinetics of the system during the initial stages of adsorption (Han *et al.* 2009).

The mass transfer coefficient (K_{AB}) and saturation concentration decreased with increase in bed height and column diameter. K_{AB} decreased from 5.46 $x10^{-3}$ L/mg/hr to 4.46 $x10^{-3}$ L/mg/hr while the saturation concentration decreased from 797.50 to 433.63 mg/L when the bed height increased from 10 cm to 30 cm. The increase in the diameter of the column also resulted in a decrease in K_{AB} from 2.52 $x10^{-4}$ to 5.40 $x10^{-5}$ L/mg/min and a decrease in the saturation concentration (N_o) from 1461.28 to 643.78 mg/L as the column diameter increased from 2.5 cm to 6 cm.

On the other hand, the flow rate had a variable effect on the K_{AB} and N_o. The K_{AB} increased from 3.78 to 4.76 L/mg/hr as the flow rate increased from 1.7 to 2 ml/min before reducing to 4.24 L/mg/hr as the flow rate increased to 2.6 ml/min. Similarly, N_o decreased from 1280.48 to 1205.99 mg/L before increasing to 1388.07 mg/L as the flow rate increased from 1.7 ml/min to 2.6 ml/min. This trend is inconsistent with that reported in a study by Woumfo *et al*. (2015) on phosphate removal from aqueous solution using an andosol-bagasse mixture. In that study, K_{AB} increased from 3.30 $x10^{-3}$ L/mg/min to 8.20 $x10^{-3}$ L/mg/min while N_o decreased from 1049.91 mg/L to 691.5 mg/L when the flow rate increased from 4 ml/min to 8 ml/min.

Reaction and mass transfer in a liquid/solid system occurs across a film at the liquid/solid interphase. The dominance of mass transfer is affected by the condition of the system. Mass transfer dominates as the adsorption mechanism at low flow rate while reaction between the analyte in solution and the solid phase is dominant at higher flow rate. An increase in the mass transfer resistance with increase in bed height usually indicates the dominance of external mass transfer as the adsorption

mechanism; this was not the case in this study. The variable trend on the effect of flow rate and the decrease of mass transfer resistance with increase in bed height indicates mass transfer was not the dominant adsorption mechanism for adsorption by the columns confirming results from **Sections 6.5** and **7.3.1** that several mechanisms were involved in the uptake of phosphate using CaMFCP.

7.3 Up scaling models

Up scaling of data obtained from **Section 7.2** were done using EBCT and BDST model discussed in **Section 7.3.1**. The up scaling calculation was carried out using data obtained from columns with the following parameters from **Section 7.2:** 10 mg/L influent phosphate concentration, 10 cm and 20 cm bed height, and 6cm column diameter designated as Column 1, Column 2, Column 3 and Column 4 respectively, and data for Moreton WWTW (Littler 2012) as shown in **Table 7.4.**

Table 7.5: Moreton WWTW Data (Littler 2012)

Dry Weather Flow (DWF) m^2/day	Population Equivalent (p.e)	Total phosphorus load (kg/day)	Average influent phosphorus concentration (mg/L)
1086	**4157**	**10.4**	**9.6**

The area flow rate of Column 1 was 53.21 L/hr/m^2 would require an area of 84.84 m^2 to maintain the area flow rate. Using an influent concentration of 9.6 mg/L, an operational time of 68 days and 63.2 tonnes of CaMFCP would be required. The data for other columns are presented in **Table 7.5**.

Table 7.6: Scaling up data

Column	Column 1	Column 2	Column 3	Column 4
Diameter (m)	10.33	7.43	12.06	10.69
Height (m)	20	20	20	20
Area flow rate (L/hr/m^2)	532.14	937.5	93.75	51.07
Surface Area (m^2)	85.04	48.27	48.27	88.29
Operational lifespan (days)	68	36	46	55
Adsorbent mass (tonnes)	63.20	30.50	66.60	65.60
Tonnage usage (tonnes/hour)	0.93	0.85	1.45	1.20

Column 2 was the most efficient column and would require 30.5 tonnes of CaMFCP with a filter bed lifespan of 36 days. The annual demolition waste produced in England and Scotland is approximately 31.8 million tonnes per annum (Mtpa) out of which the concrete and ceramic waste constitute 65.8% amounting to approximately 21 million tonnes annually (CRWP 2007). The construction waste generated would be sufficient for use for a year round treatment of wastewater at this treatment works. However, considering this is a small WWTW, the large scale implementation of this technology is not very feasible.

7.3.1 Up scaling using Empty Bed Contact Time (EBCT)

The empty bed contact time plot of the columns with different bed height against adsorbent usage rate is given in **Figure 7.9**.

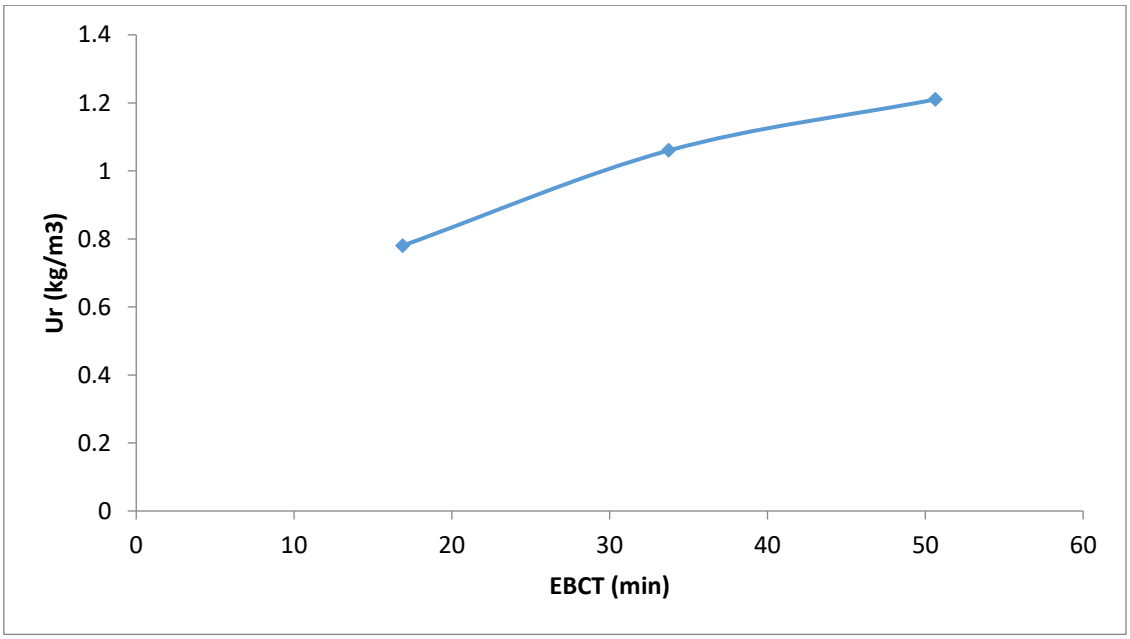

Figure 7.9: EBCT plot for columns of different bed heights (10, 20 and 30 cm; influent concentration 20 mg/L; column diameter 5 cm; flow rate 2.5 ml/min)

The EBCT was shown to increase as the usage rate increase. Typically EBCT increases with a decrease in usage rate. It is believed that the portion of the column above the mass transfer zone does not participate in adsorption. This is due to the as the mass transfer zone moves up the column, the adsorption capacity of materials at the top of the column is already diminished due to leaching of ions responsible for adsorption. This is substantiated by the fact that volume of solution treated using 20 cm column volume was 30% more than 10 cm column despite the adsorbent was 50%

more than the 10 cm column, suggesting tall column might not be very efficient for the removal of phosphate using CaMFCP.

10 cm column has the lowest usage rate of 0.78 kg/m^3 with an EBCT of 16.87 minutes, while the 30 cm column has a usage rate and EBCT of 1.21 kg/m^3 and 50.63 minutes respectively **(Table 7.1).** This suggests a 300% increase in EBCT would result in a 156% in usage rate implying and increase in the filter size would not yield a corresponding increase in the adsorbent usage rate.

Using EBCT of 16.87 minutes, a filter size of 85.34 m^3 containing 0.44 tonne of pellets would be required to treat wastewater at Moreton WWTW daily. The filter would be able to treat 339618.36 m^3 of water which is equivalent to 312 days' worth of wastewater, giving a new adsorbent usage rate of 0.0014 tonne/day. This however, may be an overestimation of the lifespan and performance of the column.

7.3.2 Up scaling using Bed Depth Service Time (BDST)

Using the principle discussed in **Section 7.3.1**, a column with an area of 43.35 m^2 would be required to treat the daily volume of water at Moreton WWTW with an area flow rate of 937.5 L/hr/m^2 assuming the bed depth as 20 m and service time of the column as 68 days. This would give a column with diameter of 7.43 m and volume of 867.16 m^3 holding 25.79 tonnes of clay pellets. These values suggest BDST might not be suitable for the design of the column and EBCT model could be a better alternative or other plant options may be applied for the use of CaMFCP.

7.4 Summary and Conclusion

Fixed bed column test was carried out under different conditions to investigate the adsorption of phosphate using CaMFCP. Effect of influent phosphate conditions, bed height, flow rate and column diameter was investigated. All columns were allowed to run till exhaustion. Effluents were sampled regularly to measure the concentration of phosphate and the column stopped when effluent phosphate concentration equaled influent phosphate concentration.

The column with column diameter of 2 cm, bed height of 10 cm and influent phosphate concentration of 20 mg/L showed the shortest retention time of 1.75 minutes, followed by the column with a bed height of 10 cm, column diameter of 5 cm and influent phosphate concentration of 20 mg/L while the longest retention time was 56.02

minutes exhibited by the columns with bed height of 10 cm, influent phosphate concentration of 20 mg/L, and column diameter of 6 cm. The total volume of solution treated by the columns were found to increase with an increase in bed height and column diameter but decreased with an increase in influent phosphate concentration and flow rate. The increase in the total volume of solution treated did not however, correspond with the increase in the amount of pellet used. For instance, there was a 50% increase in the amount of pellets used by the column with a bed height of 20 cm over the column with bed height of 10 cm but only a 30% in volume of solution treated. The amount of phosphate available for adsorption and adsorbed increased as the different parameters increased.

Phosphate- enriched materials obtained from this study could be used sustainably rather than go to landfill. The phosphate sorbed to these pellets could be recycled and one of the options would be for use in agriculture. A minimum of 2400 mg of phosphate was adsorbed by the column in this study; this phosphate could ensure a “green” approach to agriculture with the phosphate sorbing materials having an additional benefit for use as a liming material or in improving soil structure.

The next chapter will investigate the availability of phosphate sorbed to CaMFCP to plants as a form of a slow release fertilizer.

8 Calcium-modified fired clay pellet as an adsorbent for the removal of phosphate from waste water and its potential for a slow release fertilizer

8.1 Introduction

Phosphate in wastewater is a source of pollution as elevated levels lead to euthrophication of aquatic bodies (Smith and Schindler 2009). The Urban Wastewater Treatment Directive mandates effluent concentration of 1-2 mg/L for wastewater treatment works (WWTWs).

Conventional method for the removal of phosphate involves chemical precipitation using iron, aluminium and calcium salts (Clark *et al*. 1997). Chemical precipitation has a major disadvantage of being an expensive treatment option. Adsorption on to low cost adsorbent is viewed as an alternative low cost option for phosphate removal from wastewater (Jia *et al*. 2013). Sorption of phosphate on to suitable materials consists of the chemical, physical and biological processes involved in the retention of phosphate on these materials (Zhu *et al* 1997; Hylander *et al*. 2006). These phosphate enriched materials could be reused by effectively recycling adsorbed phosphate in agricultural production rather than sent to landfill.

Recycled bricks and other clay adsorbents have been effectively used for the adsorption of phosphate (Johansson 1997; Zhu *et al*. 2003; Kamiyango *et al*. 2009; Jia *et al*. 2013). Phosphate enriched materials have been used as a fertilizer source to provide phosphate for agricultural production.

The objective of this study was to investigate the potential of the use of phosphate sorbed to Calcium modified fired clay pellets discussed in Chapter Seven as an effective fertilizer source for the production of ryegrass.

8.2 Soil analysis

8.2.1 Soil pH

The pH of the soil decreased from 6.5 before planting to 6.12, this decrease could be attributed to a decrease in the concentration of Ca in the soil and relative increase in the concentration of Fe due to the leaching of Fe from the soil post-planting **(Figures 8.1- 8.2).**

8.2.2 Analysis of elemental content

An analysis of the elemental content of the soil (Ca, Al, Fe, Mg, and P) was conducted to determine the concentration of Al, Ca, Fe, Mg and P in the soil before and after planting. The results are presented in **Figures 8.1- 8.2.**

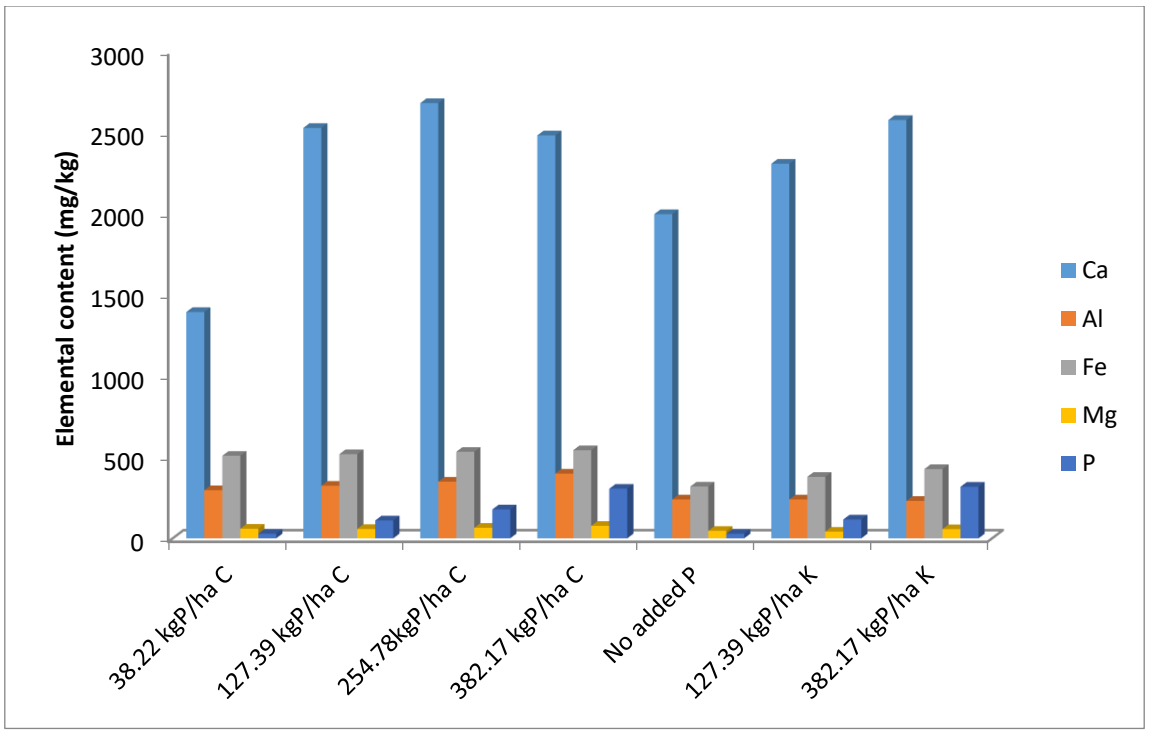

Figure 8.1: Concentration of elements in the soil pre-planting

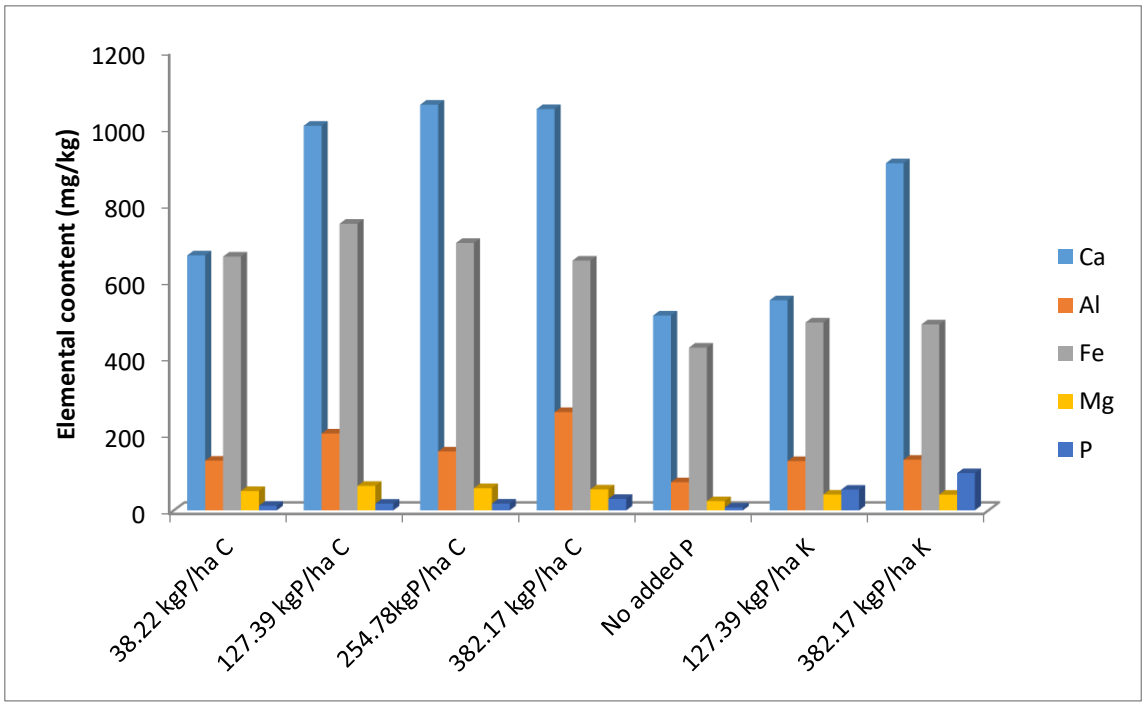

Figure 8.2: Concentration of elements in the soil post-planting

There was a general increase in the concentration of elements pre-planting with an increase in the concentration of added phosphate (P) in the form of phosphate sorbed to CaMFCP (PSC). This is as a result of the increase in the mass of added material as the concentration of P increased. The mass of added material increased from 0.87 to 8.65g as application rate of phosphate increased from 38.22 to 382.17 kgP/ha. Ca concentration increased from 1395 to 2482 mg/kg while the concentration of Al increased from 297 to 399 mg/kg when the as application rate of phosphate increased from 38.22 to 382.17 kgP/ha. Similarly, the concentration of Fe increased from 509 to 544 mg/ kg while that of Mg increased from 59 to 77 mg/kg under the same conditions **(Figure 8.1)**.

The concentration of the elements decreased post-planting except for Fe. The concentration of Fe increased from 509 to 665.5 mg/kg when the application rate of phosphate was 38.22 kgP/ha. This increase in concentration of Fe could be as a result of the release of Fe from the clay added to the soil. The concentration of Ca declined from 2482 to 1049 mg/g while the concentration of Al and Mg decreased from 399 to 259 mg/kg and 77 to 55 mg/kg respectively when the application rate of phosphate was 38.22 kgP/ha. Similar trend was also reported for all the levels of added phosphate **(Figure 8.2).**

The pots with P added in the form of KH_2PO_4 also exhibited a similar trend, the concentration of Ca decreased from 2577 mg/kg pre-planting to 908 mg/kg post-planting when 382.17 kgP/ha of phosphate was applied. The concentration of Al and Mg also decreased from 231 to 134 mg/kg and from 57 to 41 mg/kg respectively under the same conditions.

8.3 Growth parameters

8.3.1 Germination rate

The effect of application rate of phosphate on the germination rate of ryegrass was investigated and results are presented in **Figure 8.3**.

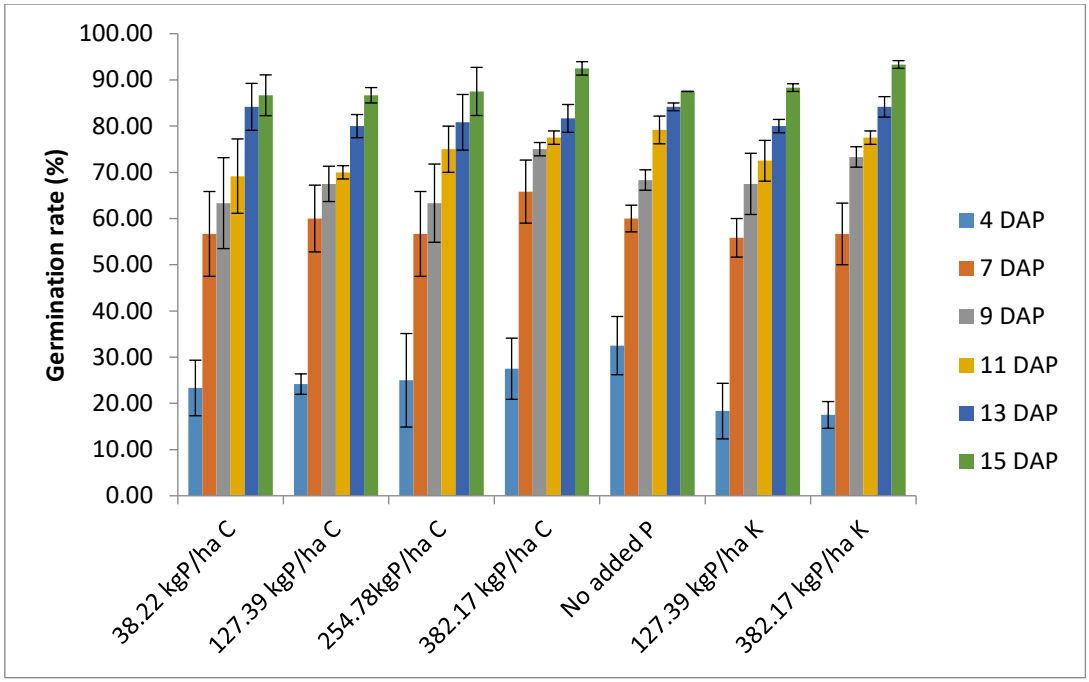

Figure 8.3: Germination rate of ryegrass as a function of added phosphate sorbed to CaMFCP (n=3), standard error bars shown

Germination rate was found to typically increase with increase in added P in the form of PSC. Germination rate was shown to increase from 23% to 27.5% at 4 days after planting (DAP) as P application rate increased from 38.22 to 382.17 kgP/ha. Germination rate was found to increase from 69% to 77.4 % and from 86.67% to 92.5% at 11 DAP and 15 DAP when the application rate of P increased from 38.22 to 382.17 kgP/ha.

The germination rate did not show a consistent trend with the pots with added P in the form of KH_2PO_4. The germination rate decreased from 18.33% to 17.5 % at 4 DAP while it increased from 55.83% to 56.67% and from 88.33 to 93.3% at 7DAP and 15DAP respectively when the application rate of P increased from 254.78 to 382.17 kgP/ha. The germination rates also increased from 80% to 84.17% at 13 DAP.

There was an increase in the germination rate with increasing P levels applied. Germination increased from 86.67% to 92.50% when the application rate of P increased from 32.22 to 382.17 kgP/ha using PSC; and from 88.33 % to 93.33% when the amount of KH_2PO_4 applied increased from 127.39 to 382.17 kgP/ha. The germination rate obtained using PSC was comparable to those obtained using KH_2PO_4. Germination rate was 86.67% and 88.33% using 127.39 kgP/ha; and was 92.50% and 93.33% when PSC and KH_2PO_4 respectively was used.

p value = 4.28 E-39 <0.05 =α or (F= 229.99 >3.08= F-crit) was obtained for pot with 127.39 kgP/ha applied and p value = 7.99E-40 < 0.05 = α or (F= 239.15 >3.08 = F-crit) for pots with 382.17 kgP/ha applied. The p values < 0.05 suggests a significant difference between the germination rate of ryegrass using added P in the form of PSC and KH_2PO_4.

The difference in germination rate was not attributed to the difference in the amount of added P but is believed to be as a result of the sowing depth of the seed. As germination usually occurs near the soil surface, burying the seeds in the soil could have resulted in the low initial germination rate observed in this study. High germination rates are often observed in ryegrass and 100% germination has been reported (Nnadi 2009). The average germination rate of 85% obtained in this study could be attributed to error during sowing.

8.3.2 Plant height

The effect of P application on the growth of ryegrass was studied as a function of the height of ryegrass. The height was measured weekly during each four week growing cycle. The result is presented in Figures **8.4a-d**.

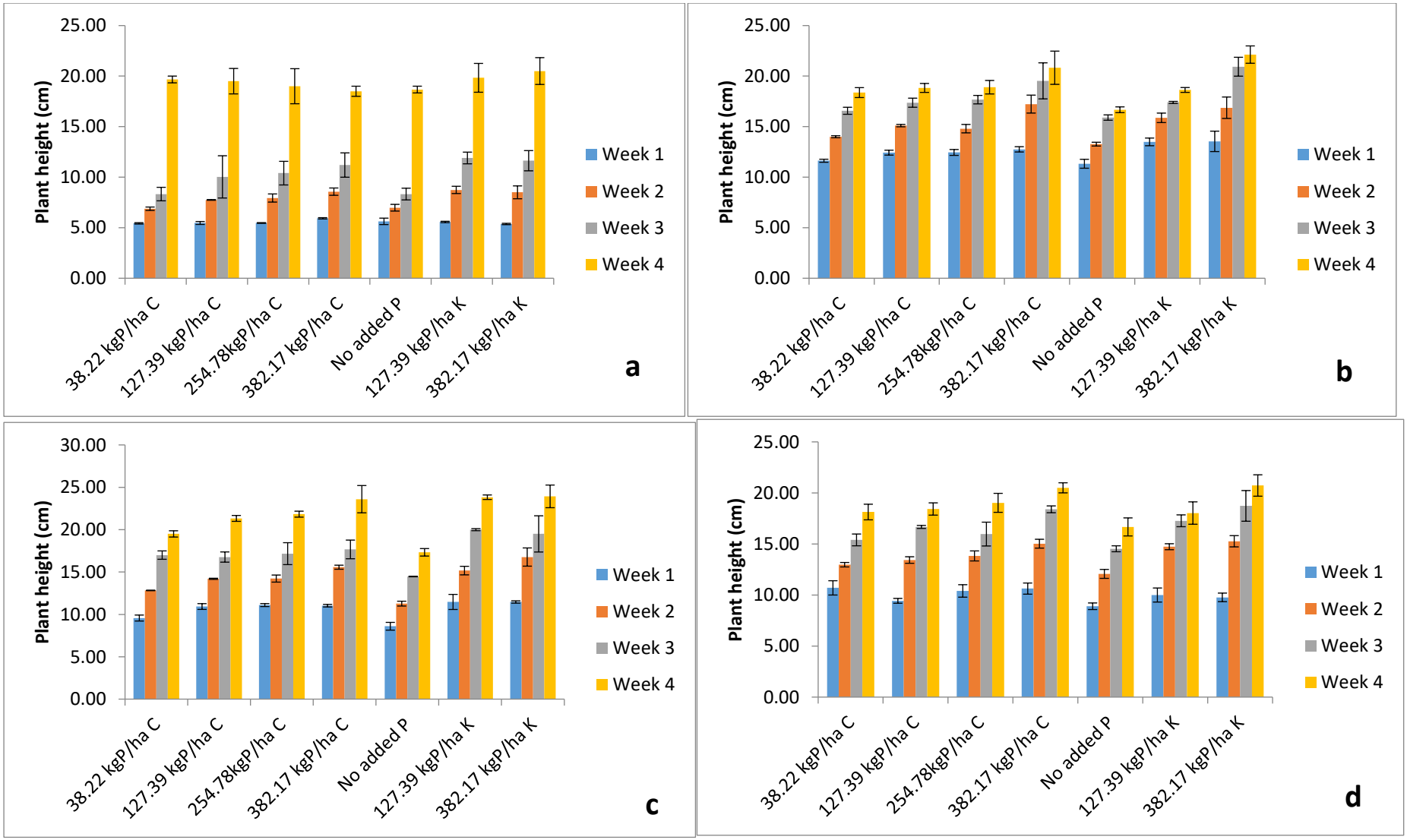

Figure 8.4: Plant height of ryegrass: a) 1st growing cycle; b) 2nd growing cycle; c) 3rd growing cycle and d) 4th growing cycle; (n=3) standard error bars shown

Plant height typically increased along each crop cycle as time progressed and also increased with increase in amount of added P. Plant height increased from 5.43cm in week 1 to 19.67 cm in week 4 during the first crop cycle when the P application rate was 38.22 kgP/ha **(Figure 8.4a)**. The initial growth rate of ryegrass was slow as evidenced in the plant height **(Figure 8.4a)**. The slow growth at the initial stages could be attributed to the establishment level of the crop. A more proportionate growth rate was observed at weekly intervals during subsequent crop cycles for all treatment levels as plants became more established. The rate of growth between harvest and the first weekly reading after harvest during the second to the fourth crop cycles was greater than the rate of growth between germination and the first weekly reading of the first crop cycle.

The third crop cycle showed the highest growth rate. Plant height at the end of the fourth week was between 19.5 cm for the pot with 38.22 kgP/ha applied and 23 cm for the pot with application rate of 382.17 kgP/ha.

Plant height increased with increasing phosphate levels applied. Plant height increased from 18.37 cm to 20.83 cm by the end of the second cropping cycle when P level increased form 32.22 kgP/ha to 382.17 kgP/ha when P was added in the form of PSC. During the same period, plant height in pots with added KH_2PO_4 increased form 18.62 cm to 22.13 cm when added P levels was 127.39 kgP/ha and 382.17 kgP/ha respectively.

Plant height increased from 18.13 cm to 20.50 cm using PSC as the added P levels increased form 38.22 kgP/ha to 382.17kgP/ha by the end of the fourth cropping cycle. Plant height also increased from 18.03 cm to 20.73cm when the P level increased from 127.39 kgP/ha to 382.17 kgP/ha when added as KH_2PO_4 during the same period.

There was comparable results obtained using both forms of phosphate. Plant height was higher using PSC when 127.39 kgP/ha was applied during the second cropping cycle. A higher pant height of 22.13 cm was obtained using 382.17 kgP/ha in the form of KH_2PO_4 during the same period.

The same pattern was obtained during the fourth cropping cycle. Plant height using PSC was 18.43 cm and 18.03 cm using KH_2PO_4 when 127.39 kgP/ha was applied. While the

plant height was 20.50 cm and 20.73 cm when 382.17 kgP/ha was applied in the form of PSC and KH_2PO_4 respectively.

p value = 2.01 E-34 <0.05 =α or (F= 292.5 >3.13= F-crit) was obtained for pots with 127.39 kgP/ha applied and p value = 2.63 E-31 < 0.05 = α or (F= 231.07 >3.12 = F-crit) for pots with 382.17 kgP/ha applied. The p values < 0.05 suggests a significant difference between the plant height of ryegrass using added phosphate in the form of phosphate PSC and added in the form of KH_2PO_4.

Overall, plant height increased with increasing P levels using both forms of phosphate was applied and showed similar results when the two forms of P applied were compared.

8.3.3 Effect of phosphate application on the wet matter (WM) yield of ryegrass

The effect of application of phosphate on the yield of ryegrass was investigated as a function of the fresh biomass yield. The fresh weight of the grass was measured after harvesting every four weeks, where the grass blades were cut 1cm above the soil. The wet matter (WM) yield of ryegrass is presented in **Figure 8.5**.

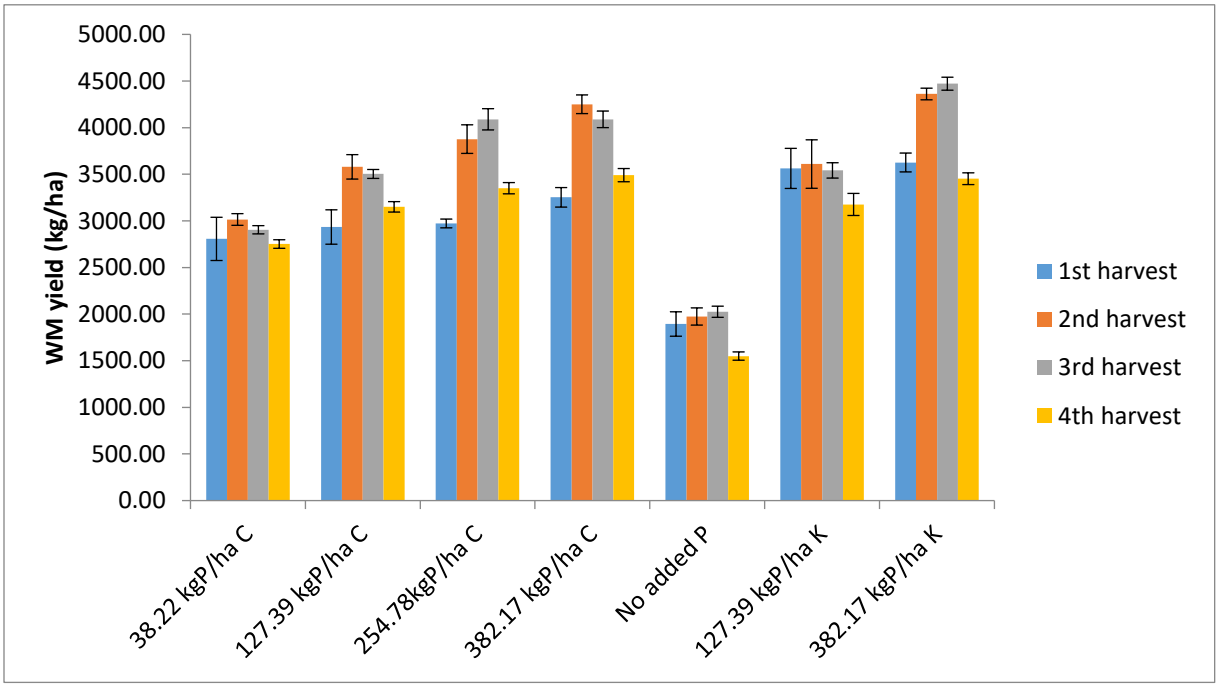

Figure 8.5: Effect of phosphate application on the wet matter yield (WM) of ryegrass, (n=3) standard error bars shown

WM yield increased with increase in rate of P application **(Figure 8.5)**. WM yield for pots with P in the form of PSC increased from 2806.79 to 3252.65 kg/ha when the rate of P application increased from 38.22 to 382.17 kgP/ha during the first crop cycle and from 2751.59 to 3490.45 kg/ha during the fourth crop cycle as the rate of P application increased from 38.22 to 382.17 kgP/ha. Similar trend was observed during all four harvest cycles. The ryegrass yield from the pot with no added P decreased from 1893.84 kg/ha to1549.89 kg/ha. Highest WM yield was obtained after the second cycle for the pots with P application rate of 38.33 and 127.39 kgP/ha, while highest yield was obtained after the third crop cycle when 254.78 and 382.17 kgP/ha of P in the form of PSC was applied. The application of P in the form of KH_2PO_4 increased WM yield from 3562.63 to 3626.33 kgP/ha during the first crop cycle and from 3176.22 to 3452.23 kg/ha during the fourth crop cycle as the rate of application increased from 127.29 to 382.17 kgP/ha.

Yield from the second harvest was greater than yield from the first harvest in all cases for pots with P added in the form of PSC. Similar trend was also observed in the crops where P was applied in the form of KH_2PO_4, this increase could be due to the fact that the grass was not fully established during the first crop cycle.

WM yield was highest at the end of the second cropping cycle for all pots with P added in the form of PSC except pots with P level of 254.78 kgP/ha. While highest yield was obtained at the end of the second cropping cycle for pots with P level of 127.39 kgP/ha; and at the end of the third cropping cycle for pots with P level of 382.17 kgP/ha added in the form of kH_2PO_4. WM yield of ryegrass from pots with P added in the form of PSC was comparable to yield from pots with P added as KH_2PO_4. WM yield of 3150.74 kg/ha and 3176.22 kg/ha was obtained with P level of 127.39 kgP/ha in the form of P added as PSC and KH_2PO_4. The WM yield of pots with P in the form of PSC (3490.45 kg/ha) was higher than those obtained from pots with added KH_2PO_4 (3452.23kg/ha) when 382.17 kgP/ha was applied.

P value = 9.7 E-07 <0.05 =α or (F=17.04 > 3.13 = F-crit) was obtained from the pots with P level of 127.39 kgP/ha and p value = 3.24 E-09 <0.05 =α or (F=26.37 > 3.13 = F-crit was obtained from pots with 382.17 kgP/ha applied. The p values < 0.05 suggests a

significant difference between the WM yield of rye grass using added P in the form of PSC and added in the form of KH_2PO_4.

8.3.4 Effect of phosphate application on the dry matter (DM) yield of ryegrass

The effect of application of P on the yield of ryegrass was investigated as a function of its dry biomass yield. The DM weight of the grass was measured after oven-drying harvested grass blades at 55^{o}C for 3 days. The DM yield of ryegrass is presented in **Figure 8.6**.

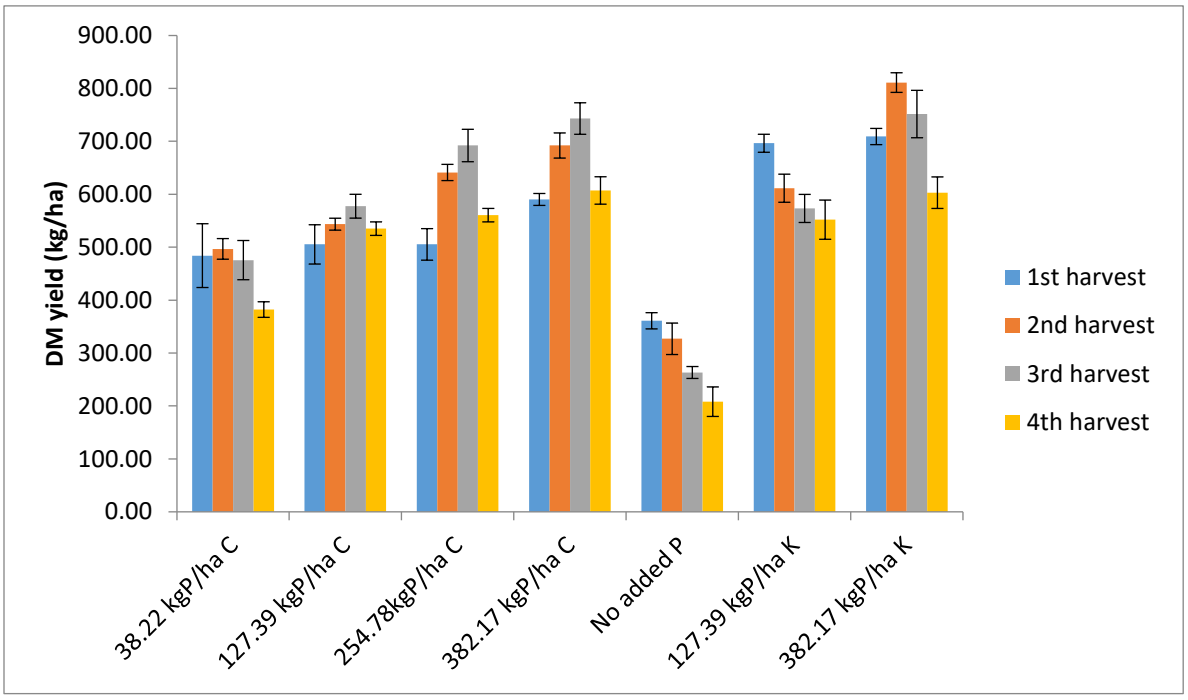

Figure 8.6: Effect of phosphate application on the dry matter yield (DM) of ryegrass, (n=3) standard error bars shown

DM yield was found to generally increase with increase in the rate of P application **(Figure 8.6)**. DM yield increased from 696.39 to 709.13 kg/ha during the first crop cycle and from 552 to 602.97 kg/ha during the fourth crop cycle as the P application rate increased from 38.22 kgP/ha to 382.17 kgP/ha when P in the form of PSC was applied. Similar trend has been reported, Robinson and Eilers (1996) obtained an increase in yield of ryegrass from 3.5 to 4.8 lb/A (3.9 to 5.38 kg/ha) when the application rate of phosphate increased from 20 to 358.67 lb/A (22.52 to 358.67 kgP/ha). Sarir *et al*. (2009) also reported an increase in DM yield of ryegrass from 1.3 to 2.7 g/pot as P application rate increased from 0 to 100

kgP/ha. Hylander and Siman (2001) reported an increase in DM yield of barley as the rate of application of P increased form 0.2 µmol/pot to 2.3 µmol/pot using P sorbed to LECA.

DM yield of the pots with no added P decreased from 360.93 kg/ha at the end of the first cropping cycle to 208.07 kg/ha at the end of the fourth cropping cycle. A decline in the DM yield was obtained when 127.39 kgP/ha was added to the pots in the form of KH_2PO_4. DM yield decreased from 696.39 kg/ha at the end of the first cropping cycle to 552.02 kg/ha at the end of the fourth cropping cycle. While the pots with 382.17 kgP/ha added in the form of KH_2PO_4 showed an increase in DM yield from 709.13 kg/ha at the end of the first cropping cycle to 751.59 kg/ha at the end of the second cropping cycle before decreasing to 602.97 kg/ha at the end of the fourth cropping cycle.

The pots with P added as KH_2PO_4 showed a better DM yield than pots with P added in the form of PSC. The DM yield of pots with P added in the form of PSC was 505.31, 641.19, 692.14 and 560.51kg/ha, while those with P added as KH_2PO_4 were 590.23, 692.14, 743.10 and 607.22 kg/ha for the first, second, third and fourth cropping cycle respectively when 127.39 kgP/ha was applied. Similarly, DM yield was 696.39, 611.46, 573.25 and 552.02 kg/ha for pots with P added in the form of PSC; and 709.13, 811.04, 751.59 and 602.97 for pots with P added as KH_2PO_4 at the end of the first, second, third and fourth cropping cycle respectively when 382.17 kgP/ha was applied.

p value = 7.91 E-14 <0.05 =α or (F=48.21 > 3.13 = F-crit) was obtained from the pots that had 127.39 kgP/ha applied and p value = 4.73 E-13 <0.05 =α or (F=44.04 > 3.13 = F-crit was obtained from pots that had 382.17 kgP/ha applied. The p values < 0.05 suggests a significant difference between the DM yield of rye grass using added phosphate in the form of PSC and added in the form of KH_2PO_4.

The response of ryegrass to different P levels varied along the crop cycle. Maximum DM yield was obtained during the third crop cycle for all levels of phosphate applied except when 38.22 kgP/ha was applied. DM yield increased from 505.31 kg/ha during the first crop cycle to 577.49 kg/ha during the third crop cycle before reducing to 535.03 kg/ha using 127.39 kgp/ha in the form of PSC. DM yield using 382.17 kgP/ha in the form of PSC also increased from 590.23 kg/ha during the first crop cycle to 743.1 kg/ha during the third

crop cycle before reducing to 607.22 kg/ha by the end of the fourth crop cycle. DM yield using 38.22kgP/ha in the form of PFC increased to a highest yield of 496.82 kg/ha during the second crop cycle from 484.08 kg/ha obtained during the first crop cycle before declining to 382.17 kg/ha by the end of the fourth crop cycle. The results presented in **Figures 8.5** and **8.6** show application of P as PSC could produce three harvest of ryegrass without the need for the application of supplementary phosphate. The increase in yield along the crop cycle could suggest the slow mineralization of phosphate with relation to time (Correa and Da Silva 2016).

8.3.5 Fertilizer Effectiveness of Applied Phosphate

The fertilizer effectiveness of the applied P was described as the relative effectiveness (RE%) of P sorbed on CaMFCP (PSC) in increasing ryegrass dry matter yield in relation to the yield with standard fertilizer - KH_2PO_4 (Hylander *et al*. 2006).

The relative effectiveness is determined as

$$\text{RE (\%)} = \left[\frac{(\textit{yield with PSC})-(\textit{yield with control})}{(\textit{yield with KH2PO4})-\textit{yield with control}}\right]*100 \quad \textbf{Equation 8.1}$$

The relative effectiveness of PSC is presented in **Figure 8.7**.

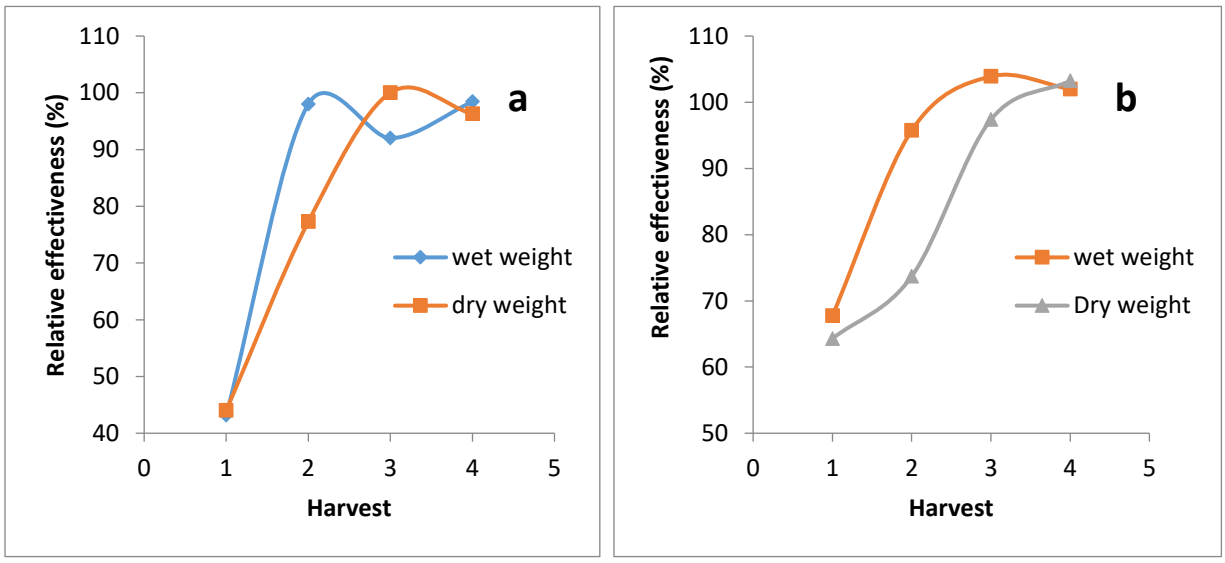

Figure 8.7: Relative effectiveness of phosphate sorbed to CaMFCP; application rate: a) 127.39 kgP/ha; b) 382.17 kgP/ha

Relative effectiveness of PSC increased along the crop cycle. Low relative effectiveness of 43.18 and 44 % for WM and DM yield respectively was obtained at first harvest when 127.39 khgP/ha was applied while the 67.74 and 64.29% for wet and dry wet respectively as the relative effectiveness of applying 382.17 kgP/ha. This could be as a result of the plants not being fully established during the first crop cycle. With progression of the crop cycle, the performance of PSC improved and 100% effectiveness in DM yield using 382.17 kgP/ha was achieved and over 100 % during the fourth cycle. This shows the performance of PSC in increasing the yield of ryegrass equaled that KH_2PO_4 when used as a fertilizer source. The figures obtained during the first cycle are higher to those obtained by Hylander *et al*. (2006) using phosphate sorbed to different media as a phosphate fertilizer for the production of barley. In that study, the highest relative effectiveness of 76% was obtained using crystalline steel-works furnace slag as phosphate fertilizer.

8.3.6 Yield Response

One of the measures of functional relationships between application rate of fertilizer and yield response is the quadratic yield response model and this accounts for more variability and is a more biologically acceptable model for the analysis of relationships between application rate of fertilizer and yield response (Morrison *et al.* 1980 cited in Pawlett *et al.* 2015).

The quadratic yield response model is based on the assumption that yield (t/ha) is related to the rate of fertilizer application (kgP/ha) and is represented as

$$y = a + bx - cx^2 \qquad \textbf{Equation 8.2}$$

where a, b and c are the regression coefficients, y is the yield of ryegrass (t/ha) and *x* is the rate of p applied (kgP/ha)

The first order differential is expressed as:

$$\frac{dy}{dx} = b - 2cx \qquad \textbf{Equation 8.3}$$

Equating to zero, the fertilizer rate at the maximum of yield response is derived as **Equations 8.4 and 8.5** as follows:

$$\frac{dy}{dx} = b - 2cx = 0 \qquad \textbf{Equation 8.4}$$

$$\Rightarrow x_{max} = \frac{b}{2c} \qquad \textbf{Equation 8.5}$$

When the differential is equated to the price ratio (R_P) defined as the ratio of the price of phosphate fertilizer P_p (£/kg) to the price of ryegrass P_r (£/t), the most economical rate of phosphate application (P_{MERP}) can be identified as expressed in **Equations 8.6 and 8.7**:

$$\frac{dy}{dx} = b - 2cx = R_P = \frac{Pp}{Pr} \qquad \textbf{Equation 8.6}$$

$$\Rightarrow P_{MERP} = \frac{b - Rp}{2c} \qquad \textbf{Equation 8.7}$$

The polynomial relationship between phosphate fertilizer application rate and yield response of applied phosphate is shown in **Figure 8.8**.

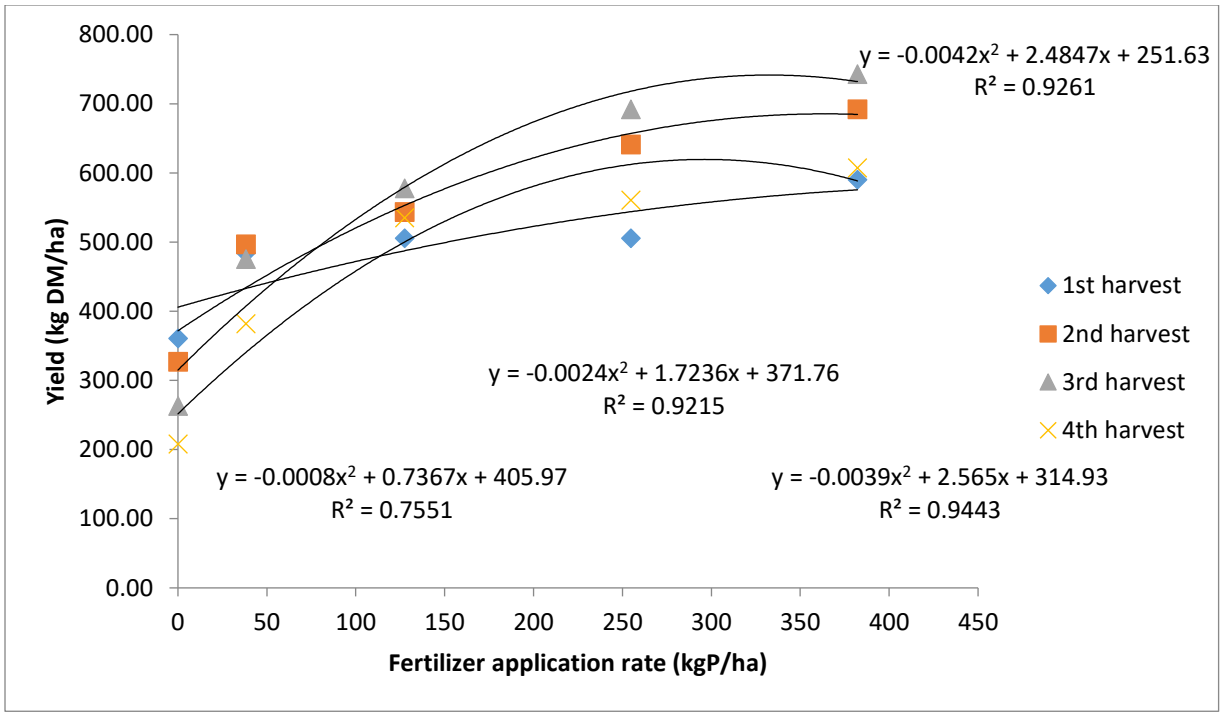

Figure 8.8: Quadratic yield response curve for phosphate application of ryegrass.

Yield produced from the pots with 38.22 and 127.39 kgP/ha in the form of PSC were respectively were significantly less (p = 0.02 and 0.04) than those obtained using higher application rates **(Table 8.1)**. Adjusted R^2 values for yields obtained using 254.78 and 382.17 kgP/ha were not acceptable; hence the results are not reported.

Table 8.1: Polynomial coefficient between yield response and fertilizer application rate of phosphate (kgP/ha)

Phosphate application rate (kgP/ha)	Polynomial equation	R^2 (adjusted)	p
O	-52.227 + 420.38	0.9866	0.0008
38.22	$-26.53x^2 + 99.99x + 408.72$	0.7043	0.02
127.39	$-20.168x^2 + 113.15x + 408.72$	0.969	0.04
254.78		0.1132	0.04
382.17		-0.49978	0.01

The negative coefficients of the square terms suggest a decrease in the yield of ryegrass above certain level of phosphate application under the prevailing conditions. This could justify the use of quadratic functions to describe the response curve of ryegrass to phosphate application. The fertilizer rate at the maximum of yield response (x_{max}) was estimated at 2.82 kgP/ha while the most economical rate of phosphate application (P_{MERP}) was estimated at 2.81 kgP/ha.

8.4 Summary and conclusion

Concentration of Al, Ca,Fe, Mg, and phosphate present in the soil before planting, increased with increase in the application rate of phosphate due to an increase in the amount of material added to provide the required phosphate level. Concentration of Al, Ca, Mg and Fe reduced during the planting period while the concentration of Fe increased. This increase in concentration of Fe could be as a result of the release of Fe from the added clay.

Phosphate application rates used in this study were 0. 38.22, 127.39, 254.78 and 382.17 kgP/ha for phosphate applied in the form of PSC, and 127.39 and 382.17 kgP/ha for phosphate applied in the form of KH_2PO_4. Yield of ryegrass increased for all application rates up to a maximum by the third cropping cycle. The yield also increased with increase in application rate of phosphate with 382.17 kgP/ha producing the highest yield. The performance of pots with P added in the form of PSC was similar to pots with P added in the form of KH_2PO_4 when germination rate, plant height and WM yield were considered while pots with added KH_2PO_4 showed a better DM yield than pots with P added in the form of PSC. Relative effectiveness of phosphate in the form of PSC increased from 44% during the first crop cycle to a maximum of 100% during the third cycle before declining to 96% by the end of the fourth crop cycle when 127.39 kgP/ha of phosphate in the form of PSC was used. 382.17 kgP/ha phosphate in the form of PSC showed an increase in relative effectiveness from 64 to 103% from the first to the fourth crop cycle. This shows the potential for the use of phosphate sorbed to CaMFCP as a source of phosphate for ryegrass.

X_{max} was estimated at 2.82 kgP/ha, which is 13 times less than the lowest application rate of phosphate used in this study. This implies application rate above x_{max} (2.82 kgP/ha)

may not result in any yield benefit. Growth parameters of germination rate, plant height, fresh and dry matter yield were all significantly more as the application rate of phosphate increased.

Quadratic response curve could be used to describe the yield of ryegrass as the values of the squared term were negative, however, the adjusted R^2 values for 254.78 and 382.17 kgP/ha were not acceptable.

9 Summary, Conclusion and Recommendation for Further Research

9.1 Chapter 5 Summary

This chapter reported the results of the kinetic test showed equilibrium in adsorption of phosphate using brick dust occurred within 60 minutes using adsorbent dosage of 33.33 g/L and adsorption increased with contact time from 0.27 to 0.59 mg/g. The profile showed a typical fast initial uptake associated with vacant adsorption sites at the start of the experiment. Removal efficiency increased with brick dosage but decrease with amount of phosphate adsorbed per unit mass of brick dust, 33.33 g/L achieved highest phosphate removal. Adsorption was affected by temperature as it decreased from 0.59 mg/g at 20^{o}C to 0.47 mg/g at 35^{o}C. This indicated adsorption was exothermic. Variation in kinetic properties as a function of temperature indicated the adsorption mechanism of phosphate using brick dust was a complicated process with interaction of different mechanisms but tending to physisorption as the dominant mechanism. Gibbs free energy value of -0.59 to -0.61 kJ/mol and enthalpy value of -0.139 J/mol indicated adsorption was spontaneous and exothermic while positive entropy value of 1.53 x10^{-3} showed a good affinity of phosphate towards brick dust and activation energy of 0.012 J/mol indicated a relatively low energy barrier. Adsorption of phosphates per unit mass of brick dust increased with increase in concentration as a result of an increase in the rate of collision between phosphate ions and the surface of the brick dust, while a decrease in the removal efficiency showed greater competition between phosphate ions and available adsorption sites. Q_m derived from Langmuir isotherm was 5.35 mg/g, R_L value of 0.04 indicated adsorption was a favourable process. Experimental data showed a good fit to Langmuir and Tempkin isotherms. The Dubinin-Radushkeivich E value of 1.35 J/mol indicated physisorption and the positive value of B (1.89 J/mol) from Temkin isotherm confirmed the exothermic nature of adsorption. The result showed the potential of brick dust for the adsorption of phosphate. However, the issues associated with suspended solid from the dust necessitated the further development of brick based adsorbent material to address the problem.

9.2 Chapter 6 Summary

This chapter reported the adsorption of phosphate using fired clay pellets increased from 0.25 to 2.49 mg/g as firing temperature increased from 540^{o}C to 800^{o}C. Optimum firing temperature was 850^{o}C with adsorption declining when the pellets were fired at 1050^{o}C. The decline in phosphate adsorption at a firing temperature of 1050^{o}C was attributed to collapse of the pores due to sintering. Adsorption increased from 0.26 to 7.48 mgP as dosage increased from 3.33 to 33.33 g/L. A characteristic kinetic profile was obtained as a function of contact time. Phosphate adsorption was affected by pH, and optimum adsorption occurred at pH 3. Phosphate adsorption was higher at pH lower that 8.13 which was the pH_{zpc}. High phosphate removal was obtained at neutral pH indicating the applicability of FCP for use in wastewater treatment without the need for pH adjustment. Phosphate adsorption decreased from 2.04 to 0.98 mg/ as temperature increased from 20 to 35^{o}C indicating an exothermic reaction. The adsorption data showed a good fit with pseudo-first order and Bangham's kinetic models indicating adsorption was physisorption supported by some diffusion. Gibbs free energy values of -16.5 to -16.89 kJ/mol and enthalpy value of -8.87 confirmed the exothermic nature of adsorption and indicated adsorption was spontaneous. The positive value of entropy 0.026 kJ/mol indicated a good affinity for phosphate ions toward FCP. The negative value of activation energy (-0.22 J/mol) indicated the absence of an energy barrier also confirming the exothermic nature of the adsorption. Adsorption increased with an increase in phosphate concentration. Q_m derived from the Langmuir isotherm was 13.23 mg/g and R_L of 0.02 indicated adsorption of phosphates onto FCP was favourable. The adsorption data did not show a good fit with Freundlich isotherm, the positive B value from Temkin isotherm confirmed exothermic adsorption confirming the results from the kinetic study. Perforation of the pellets improved the performance of the pellets and the rate of adsorption increased with perforation. The pellets were modified in further study to investigate the effect of the elemental composition. The method of pelletization provided a better performance than the conventional brick dust used by most researchers.

9.3 Chapter 7 Summary

This chapter reported the results obtained from the modification of the clay pellets by the addition of metal salts. Addition of $Al_2(SO_4)_3$, $CaCO_3$ and $FeSO_4$ improved phosphate adsorption. Increase in the concentration of CaCO3 increased phosphate adsorption while an increase in $Al_2(SO_4)_3$ and $FeSO_4$ concentration decreased phosphate adsorption probably due to the increase in the concentration of sulphate within the pellets. Phosphate adsorption increased with an increase in contact time, phosphate concentration and adsorbent dosage. Combining modification did not substantially improve adsorption; hence experiments on determining the adsorptive properties of modified clay were carried out on the single modification pellets. Adsorption using FeMFCP and CaMFCP was favoured at acidic pH, with optimum adsorption at pH 3-4 for FeMFCP and pH 3-4 and 7-8 for CaMFCP. Adsorption using AlMFCP was favoured at slightly acidic pH with optimium adsorption at pH 5-6. The results show CaMFCP could be employed in wastewater treatment as high adsorption was obtained at neutral pH. Temperature affected adsorption using FeMFCP and AlMFCP while adsorption using CaMFCP was unaffected by temperature. All three pellets types showed good fit to pseudo-first order kinetics and the rate of reaction (k_1) decreased with an increase in temperature for CaMFCP. Phosphate adsorption using CaMFCP showed a good fit to the pseudo-second order kinetic model. Elovich and Bangham's kinetic models did not show good fit with the experimental data for CaMFCP. AlMFCP showed a good fit to Bangham's model. FEMFCP did not show a good fit with pseudo-second order but showed better fit for Bangham's and Elovich kinetic models. Gibbs free energy was negative for all pellet types at all temperature and indicated spontaneous nature of adsorption and the values indicated adsorption was physisorption. The variations in kinetic parameters as a function of temperature suggested adsorption mechanism was predominatly physisorption supported by other mechanisms. Langmuir isotherm showed the best fit for all the isotherms studied, Q_m derived from Langmuir was 42.37, 70.42 and 52.91 mg/g for AlMFCP, CaMFCP and FeMFCP respectively, R_L values of less than 1, and n values were between 1 and 10 which indicated adsorption was favourable. Adsorption and Langmuir affinity constant were in the order CMFCP > FeMFCP > AlMFCP signifying

CaMFCP had higher affinity for phosphate and was used for the fixed bed column study and greenhouse trial.

9.4 Chapter 8 Summary

The slope of the breakthrough curve decreased with increase in bed height and column diameter but increase with an increase in phosphate concentration and flow rate. EBCT increased with an increase in phosphate concentration, bed height and column diameter but decreased with an increase in flow rate. Throughput volume increased with an increase in bed height and column diameter but decreased with an increase in phosphate concentration. The amount of phosphate adsorbed by the column increased with an increase in the adsorption parameters. An increase in the mass transfer resistance with an increase in bed height usually indicates the dominance of external mass transfer as the adsorption mechanism; this was not the case in this study confirming results from previous that several mechanisms were involved in the uptake of phosphate using CaMFCP. The overall good fit of the experimental data to Yoon and Nelson model indicated the model could be used to predict the breakthrough curve and characteristic parameters for the adsorption of phosphate using CaMFCP and the Thomas model could be used to describe adsorption of phosphate onto CaMFCP as pore or film diffusion were not rate limiting steps. The results from the modelling confirmed adsorption was not controlled by any single mechanism. The results from the modelling also indicated CaMFCP could have potential application in a full scale treatment.

9.5 Chapter 9 Summary

Phosphate application rates used in this study were 0. 38.22, 127.39, 254.78 and 382.17 kgP/ha for phosphate applied in the form of PFC, and 127.39 and 382.17 kgP/ha for phosphate applied in the form of KH_2PO_4. The yield of ryegrass increased for all application rates up to a maximum by the third cropping cycle. The yield also increased with increase in the application rate of phosphate with 382.17 kgP/ha producing the highest yield. Relative effectiveness of phosphate in the form of PFC increased from 44% during the first crop cycle to a maximum of 100% during the third cycle before declining to 96% by the end of the fourth crop cycle when 127.39 kgP/ha of phosphate in the form of PSC was used. 382.17 kgP/ha phosphate in the form of PSC showed an increase in

relative effectiveness from 64 to 103% from the first to the fourth crop cycle. This indicated a performance that was equal or better that those obtained using artificial fertilizer. This showed the potential for the use of phosphate sorbed to CaMFCP as a source of phosphate for ryegrass.

X_{max} was estimated at 2.82 kgP/ha, which is 13 times less than the lowest application rate of phosphate used in this study. This implies application rate above x_{max} may not result in any yield benefit. Growth parameters of germination rate, plant height, fresh and dry matter yield were all significantly more as the application rate of phosphate increased.

The results indicate phosphate sorbed to CaPMFCP has the potential for .for use as a slow release fertilizer

9.6 Conclusion

Fired clay pellets were investigated as adsorbent for the removal of phosphate from wastewater and the potential for the spent adsorbent to be reused as a slow release fertilizer for plant in agricultural processes. The results obtained demonstrated that fired clay pellets could be applied in wastewater treatment for the effective removal of phosphate. The mechanism of adsorption was not governed by any single process. However, results suggest that adsorption may be influenced by physisorption with elements of chemisorption and pore diffusion. pH played a major role in adsorption and CaMFCP could be used for the removal of phosphate from wastewater in large scale plants at neutral pH without the need for pH adjustment. Decrease in adsorption with an increase in temperature is advantageous as there would be no additional energy cost as adsorption could be carried out at prevailing environmental temperature.

9.6.1 Contribution to Knowledge

The following can be claimed as addition to knowledge in this field:

- A fired brick like material suitable for use in the removal of phosphate from wastewater treatment was developed and firing temperature for the pellets was optimised.

- A method of pelletization was developed which provided a better performance than the conventional brick dust employed.
- The mechanisms of removal of phosphate from wastewater by fired clay pellets were postulated.
- Industrial scale application of the fired clay pellets was modified and simulated.
- The potential application of the spent adsorbent as a slow release fertilizer was demonstrated and confirmed.

9.7 Areas for Further Research

The structural integrity of the pellets was not tested; the effect of $CaCO_3$ addition on strength could be researched further. The elemental composition of the combined modification could be altered to investigate the extent of adsorption. Multiple elemental modifications were only carried out at the optimum concentration for the individual elements.

References

Acelas, N. Y., Martin, B. D., López, D., and Jefferson, B. (2015) 'Selective Removal of Phosphate from Wastewater using Hydrated Metal Oxides Dispersed within Anionic Exchange Media'*. Chemosphere* 119 (0), 1353-1360

Agarry, S., Owabor, C., and Ajani, A. (2013) 'Modified Plantain Peel as Cellulose-Based Low-Cost Adsorbent for the Removal of 2, 6-Dichlorophenol from Aqueous Solution: Adsorption Isotherms, Kinetic Modeling, and Thermodynamic Studies'*. Chemical Engineering Communications* 200 (8), 1121-1147

Agyei, N. M., Strydom, C. A., and Potgieter, J. H. (2002) 'The Removal of Phosphate Ions from Aqueous Solution by Fly Ash, Slag, Ordinary Portland Cement and Related Blends'*. Cement and Concrete Research* 32 (12), 1889-1897

Aksu, Z. and Gönen, F. (2004) 'Biosorption of Phenol by Immobilized Activated Sludge in a Continuous Packed Bed: Prediction of Breakthrough Curves'*. Process Biochemistry* 39 (5), 599-613

Aksu, I., Bazilevskaya, E., and Karpyn, Z. T. (2015) 'Swelling of Clay Minerals in Unconsolidated Porous Media and its Impact on Permeability'*. Georesj* 7, 1-13

Al-Anber, M. A. (2011) *Thermodynamics Approach in the Adsorption of Heavy Metals*.: INTECH Open Access Publisher

Al- Fatlawi, A. H., Neamah, M. M. (2015) 'Batch Experiment and Adsorption Isotherm of Phosphate Removal by using Drinking Water Treatment Sludge and Red Mud'. *International Journal of Research in Science and Technology* 2 (3) 557-571

Albadarin, A. B., Mangwandi, C., Al-Muhtaseb, A. H., Walker, G. M., Allen, S. J., and Ahmad, M. N. M. (2012) 'Kinetic and Thermodynamics of Chromium Ions Adsorption Onto Low-Cost Dolomite Adsorbent'*. Chemical Engineering Journal* 179 (0), 193-202

Altundoğan, H. S. and Tümen, F. (2002) 'Removal of Phosphates from Aqueous Solutions by using Bauxite. I: Effect of pH on the Adsorption of various Phosphates'*. Journal of Chemical Technology and Biotechnology* 77 (1), 77-85

Aivalioti, M., Pothoulaki, D., Papoulias, P., and Gidarakos, E. (2012) ‘Removal of BTEX, MTBE and TAME from Aqueous Solutions by Adsorption onto Raw and Thermally Treated Lignite’. *Journal of Hazardous Materials* 207-208, 136-146

Anirudhan, T.S., Suchithra, P.S., Rijith, S. (2008) ‘Amine–Modified Polyacrylamide–Bentonite Composite for the Adsorption of Humic Acid in Aqueous Solutions’. *Colloids and Surfaces* A 326, 147–156

Antwi, J. Y. (2009) *The use of recycled red brick to adsorb phosphate from solution*. Unpublished Masters thesis. Coventry: Coventry University

Appel, C., Ma, L. Q., Dean Rhue, R., and Kennelley, E. (2003) 'Point of Zero Charge Determination in Soils and Minerals Via Traditional Methods and Detection of Electroacoustic Mobility'*. Geoderma* 113 (1–2), 77-93

Arai, Y. and Sparks, D. (2007) 'Phosphate Reaction Dynamics in Soils and Soil Components: A Multiscale Approach'*. Advances in Agronomy* 94, 135-179

Arfaoui, S., Hamdi, N., Frini-Srasra, N., and Srasra, E. (2012) 'Determination of Point of Zero Charge of PILCS with Single and Mixed Oxide Pillars Prepared from Tunisian-Smectite'*. Geochemistry International* 50 (5), 447-454

Arias, C., Del Bubba, M., and Brix, H. (2001) 'Phosphorus Removal by Sands for use as Media in Subsurface Flow Constructed Reed Beds'*. Water Research* 35 (5), 1159-1168

Arivoli, S., Marimuthu, V., and Judith, T. R. (2014) 'Equilibrium and Thermodynamics Studies on the Removal of Iron (III) Onto Activated Pistia Stratiotes Leaves Nano Carbon'*. Research & Reviews: Journal of Chemistry* 3 (1), 15-22

Ashekuzzaman, S. and Jiang, J. (2014) 'Study on the sorption–desorption–regeneration Performance of Ca-, mg-and CaMg-Based Layered Double Hydroxides for Removing Phosphate from Water'*. Chemical Engineering Journal* 246, 97-105

Babatunde, A. and Zhao, Y. (2010) 'Equilibrium and Kinetic Analysis of Phosphorus Adsorption from Aqueous Solution using Waste Alum Sludge'*. Journal of Hazardous Materials* 184 (1), 746-752

Babatunde, A., Zhao, Y., Burke, A., Morris, M., and Hanrahan, J. (2009) 'Characterization of Aluminium-Based Water Treatment Residual for Potential Phosphorus Removal in Engineered Wetlands'*. Environmental Pollution* 157 (10), 2830-2836

Babu, B. and Gupta, S. (2005) 'Modeling and Simulation of Fixed Bed Adsorption Column: Effect of Velocity Variation'*. I-Manager's Journal on Future Engineering and Technology* 1 (1), 60

Baker, M. J., Blowes, D. W., and Ptacek, C. J. (1998) 'Laboratory Development of Permeable Reactive Mixtures for the Removal of Phosphorus from Onsite Wastewater Disposal Systems'*. Environmental Science and Technology* 32 (15), 2308-2316

Baksh, M. S., Kikkinides, E. S., and Yang, R. Y. (1992) 'Characterization of Physisorption of a New Class of Microporous Adsorbents: Pillared Clays'*. Industrial and Engineering Chemistry Research* 31 (9), 2181-2189

Balomenou, G., Stath, P., Enotiadis, A., Gournis, D., Deligiannakis, Y. (2008) 'Physicochemical Study of Amino-Functionalized Organosilicon Cubes Intercalated in Montmorillonite Clay: H-Binding and Metal Uptake'. *Journal of Colloid and Interface Science* 325, 74–83

Balouch, A., Kolachi, M., Talpur, F. N., Khan, H., and Bhanger, M. I. (2013) 'Sorption Kinetics, Isotherm and Thermodynamic Modeling of Defluoridation of Ground Water using Natural Adsorbents'. *American Journal of Analytical Chemistry* 4, 221-228

Barrow, N. J. (1986) 'Reaction of Anions and Cations with Variable-Charge Soils'*. Advances in Agronomy* 38 (0), 183-230

Bastin, O., Janssens, F., Dufey, J., and Peeters, A. (1999) 'Phosphorus Removal by a Synthetic Iron oxide–gypsum Compound'*. Ecological Engineering* 12 (3–4), 339-351

Baraka, A.M., El-Tayieb, M.M., Shafai, M.E., Mohammed, N.Y. (2012) 'Sorptive Removal of Phospahte from Wastewater using Activated Red Mud'. *Australian Journal of Basic and Applied Science* 6(10) 500-510

Bauer, P. J., Szogi, A. A., and Vanotti, M. B. (2007) 'Agronomic Effectiveness of Calcium Phosphate Recovered from Liquid Swine Manure'*. Agronomy Journal* 99 (5), 1352-1356

Bertanza, G., Pedrazzani, R., Manili, L., and Menoni, L. (2013) 'Bio-P Release in the Final Clarifiers of a Large WWTP with Co-Precipitation: Key Factors and Troubleshooting'. *Chemical Engineering Journal* 230 (0), 195-201

Big Ceramic Store (n.d.) *Clay: The Drying and Firing Process* [online] available from < http://www.bigceramicstore.com/info/ceramics/tips/tip31_clay_drying_firing.html> [9 January 2015]

Blaney, L. M., Cinar, S., and SenGupta, A. K. (2007) 'Hybrid Anion Exchanger for Trace Phosphate Removal from Water and Wastewater'. *Water Research* 41 (7), 1603-1613

Bøen, A., Haraldsen, T. K., and Krogstad, T. (2013) 'Large Differences in Soil Phosphorus Solubility after the Application of Compost and Biosolids at High Rates'. *Acta Agriculturae Scandinavica, Section B–Soil & Plant Science* 63 (6) 473 – 482.

Boisvert, J., To, T. C., Berrak, A., and Jolicoeur, C. (1997) 'Phosphate Adsorption in Flocculation Processes of Aluminium Sulphate and Poly-Aluminium-Silicate-Sulphate'. *Water Research* 31 (8), 1939-1946

Boujelben, N., Bouzid, J., Elouear, Z., Feki, M., Jamoussi, F., and Montiel, A. (2008) 'Phosphorus Removal from Aqueous Solution using Iron Coated Natural and Engineered Sorbents'. *Journal of Hazardous Materials* 151 (1), 103-110

Boujelben, N., Bouhamed, F., Elouaer, Z., Bouzid, J., Feki, M. (2013) 'Removal of phosphorus ions from Aqueous Solutions using Manganese-Oxide-Coated Sand and Brick'. *Desalination and Water Treatment* 52 (10-12) 2282-2292 https://doi.org/10.1080/19443994.2013.822324

Bradl, H. B. (2004) 'Adsorption of Heavy Metal Ions on Soils and Soils Constituents'. *Journal of Colloid and Interface Science* 277 (1), 1-18

Bray, H. J., Redfern, S. A., and Clark, S. M. (1998) 'The Kinetics of Dehydration in Ca-Montmorillonite: An in Situ X-Ray Diffraction Study'. *Mineralogical Magazine* 62 (5), 647-656

Brix, H. and Arias, C. A. (2005) 'The use of Vertical Flow Constructed Wetlands for on-Site Treatment of Domestic Wastewater: New Danish Guidelines'. *Ecological Engineering* 25 (5), 491-500

Brogowski, Z. and Renman, G. (2004) 'Characterization of Opoka as a Basis for its use in Wastewater Treatment'. *Polish Journal of Environmental Studies* 13 (1), 15-20

Caravelli, A. H., Contreras, E. M., and Zaritzky, N. E. (2010) 'Phosphorous Removal in Batch Systems using Ferric Chloride in the Presence of Activated Sludges'. *Journal of Hazardous Materials* 177 (1), 199-208

Cazes, J. (2004) *Analytical Instrumentation Handbook* 3rd ed.: CRC Press

Cecen, F. and Aktas, O. (2012) *Activated Carbon for Water and Wastewater Treatment: Integration of Adsorption and Biological Treatment*. Weinheim: Wiley-VCH.

Chen, J. P., Chua, M., and Zhang, B. (2002) 'Effects of Competitive Ions, Humic Acid, and pH on Removal of Ammonium and Phosphorous from the Synthetic Industrial Effluent by Ion Exchange Resins'. *Waste Management* 22 (7), 711-719

Chen, J., Cai, Y., Clark, M., and Yu, Y. (2013) 'Equilibrium and Kinetic Studies of Phosphate Removal from Solution Onto A Hydrothermally Modified Oyster Shell Material'. *PloS One* 8 (4), e60243

Chen, S., Yue, Q., Gao, B., Li, Q., Xu, X., and Fu, K. (2012) 'Adsorption of Hexavalent Chromium from Aqueous Solution by Modified Corn Stalk: A Fixed-Bed Column Study'*. Bioresource Technology* 113, 114-120

Chen, H., Zhao, J., Zhong, A., and Jin, Y. (2011) 'Removal Capacity and Adsorption Mechanism of Heat-Treated Palygorskite Clay for Methylene Blue'*. Chemical Engineering Journal* 174 (1), 143-150

Chen, X., Kong, H., Wu, D., Wang, X., and Lin, Y. (2009) 'Phosphate Removal and Recovery through Crystallization of Hydroxyapatite using Xonotlite as Seed Crystal'*. Journal of Environmental Sciences* 21 (5), 575-580

Cheng, X., Huang, X., Wang, X., and Sun, D. (2010) 'Influence of Calcination on the Adsorptive Removal of Phosphate by Zn–Al Layered Double Hydroxides from Excess Sludge Liquor'*. Journal of Hazardous Materials* 177 (1–3), 516-523

Cheng, X., Huang, X., Wang, X., Zhao, B., Chen, A., and Sun, D. (2009) 'Phosphate Adsorption from Sewage Sludge Filtrate using zinc–aluminum Layered Double Hydroxides'*. Journal of Hazardous Materials* 169 (1–3), 958-964

Cheung, C. W., Porter, J. F., and Mckay, G. (2001) 'Sorption Kinetic Analysis for the Removal of Cadmium Ions from Effluents using Bone Char'*. Water Research* 35 (3), 605-612

Cheung, K. and Venkitachalam, T. (2000) 'Improving Phosphate Removal of Sand Infiltration System using Alkaline Fly Ash'*. Chemosphere* 41 (1), 243-249

Chitrakar, R., Tezuka, S., Sonoda, A., Sakane, K., Ooi, K., and Hirotsu, T. (2006) 'Selective Adsorption of Phosphate from Seawater and Wastewater by Amorphous Zirconium Hydroxide'*. Journal of Colloid and Interface Science* 297 (2), 426-433

Chmielewská, E., Hodossyová, R., and Bujdoš, M. (2013) 'Kinetic and Thermodynamic Studies for Phosphate Removal using Natural Adsorption Materials.'*. Polish Journal of Environmental Studies* 22 (5) 1307-1316

Chu, K. (2004) 'Improved Fixed Bed Models for Metal Biosorption'*. Chemical Engineering Journal* 97 (2), 233-239

Chuang, S. and Ouyang, C. (2000) 'The Biomass Fractions of Heterotrophs and Phosphate-Accumulating Organisms in a Nitrogen and Phosphorus Removal System'*. Water Research* 34 (8), 2283-2290

Çılgı, G. K. and Cetişli, H. (2009) 'Thermal Decomposition Kinetics of Aluminum Sulfate Hydrate'*. Journal of Thermal Analysis and Calorimetry* 98 (3), 855-861

Clark, T., Stephenson, T., and Pearce, P. A. (1997) 'Phosphorus Removal by Chemical Precipitation in a Biological Aerated Filter'*. Water Research* 31 (10), 2557-2563

Coma, M., Verawaty, M., Pijuan, M., Yuan, Z., and Bond, P. L. (2012) 'Enhancing Aerobic Granulation for Biological Nutrient Removal from Domestic Wastewater'*. Bioresource Technology* 103 (1), 101-108

Conley, D. J., Paerl, H. W., Howarth, R. W., Boesch, D. F., Seitzinger, S. P., Havens, K. E., Lancelot, C., and Likens, G. E. (2009) 'Controlling Eutrophication: Nitrogen and Phosphorus'*. Science* 323 (5917), 1014-1015

Cornell, R. M. and Schwertmann U. (1993) *The Iron oxides* Weinheim, WileyVCH, 664.

Corrêa, R. S. and Silva, D. J. d. (2016) 'Effectiveness of Five Biosolids as Nitrogen Sources to Produce Single and Cumulative Ryegrass Harvests in Two Australian Soils'. *Revista Brasileira De Ciência do Solo* 40

Cucarella, V., Zaleski, T., Mazurek, R., and Renman, G. (2008) 'Effect of Reactive Substrates used for the Removal of Phosphorus from Wastewater on the Fertility of Acid Soils'. *Bioresource Technology* 99 (10), 4308-4314

CRWP (2009) *Overview of Demolition Waste in the UK* [online] available from < http://www.wrap.org.uk/sites/files/wrap/CRWP-Demolition-Report-2009.pdf> [16 June 2014]

Dable, P., Adjoumani, Y., Yao, B., and Ado, G. (2008) 'Wastewater Dephosphorization using Crude Clays'. *International Journal of Environmental Science & Technology* 5 (1), 35-42

Dąbrowski, A. (2001) 'Adsorption—from Theory to Practice'. *Advances in Colloid and Interface Science* 93 (1), 135-224

Dada, A., Ojediran, J., and Olalekan, A. P. (2013) 'Sorption of from Aqueous Solution Unto Modified Rice Husk: Isotherms Studies'. *Advances in Physical Chemistry* 2013

Dada, A., Olalekan, A., Olatunya, A., and Dada, O. (2012) 'Langmuir, Freundlich, Temkin and Dubinin-Radushkevich Isotherms Studies of Equilibrium Sorption of Zn^{2+} unto Phosphoric Acid Modified Rice Husk'. *J Appl Chem* 3, 38-45

Dakovic, A., Kragovic, M., Rottinghaus, G., Ledoux, D.R., Butkeraitis, P., Vojislavljevic, D.Z., Zaric, S.D., Stamenic, L. (2012) 'Preparation and Characterization of Zinc-Exchanged Montmorillonite and its Effectiveness as Aflatoxin B1 Adsorbent'. *Materials Chemistry and Physics* 137, 213–220

Das, J., Patra, B. S., Baliarsingh, N., and Parida, K. M. (2006) 'Adsorption of Phosphate by Layered Double Hydroxides in Aqueous Solutions'. *Applied Clay Science* 32 (3–4), 252-260

Dawodu, F. A. and Akpomie, K. G. (2014) 'Kinetic, Equilibrium, and Thermodynamic Studies on the Adsorption of Cadmium (II) Ions using "Aloji Kaolinite" Mineral.'. *Pac.J.Sci.Technol.* 15, 268-276

De-Bashan, L. E. and Bashan, Y. (2004) 'Recent Advances in Removing Phosphorus from Wastewater and its Future use as Fertilizer (1997–2003)'. *Water Research* 38 (19), 4222-4246

De Haas, D., Wentzel, M., and Ekama, G. (2000) 'The use of Simultaneous Chemical Precipitation in Modified Activated Sludge Systems Exhibiting Biological Excess Phosphate Removal. Part 1: Literature Review: The use of Simultaneous Chemical Precipitation in Modified Activated Sludge Systems Exhibiting Biological Excess Phosphate Removal'. *Water SA* 26 (4), 439-452

Deng, L. and Shi, Z. (2015) 'Synthesis and Characterization of a Novel Mg–Al Hydrotalcite-Loaded Kaolin Clay and its Adsorption Properties for Phosphate in Aqueous Solution'. *Journal of Alloys and Compounds* 637, 188-196

Dehou, S. C., Wartel, M., Recourt, P., Revel, B., and Boughriet, A. (2012) 'Acid Treatment of Crushed Brick (from Central African Republic) and its Ability (After FeOOH Coating) to Adsorb Ferrous Ions from Aqueous Solutions'. *Open Materials Science Journal* 6, 50-59

Dehou, S. C., Wartel, M., Recourt, P., Revel, B., Mabingui, J., Montiel, A., and Boughriet, A. (2012) 'Physicochemical, Crystalline and Morphological Characteristics of Bricks used for Ground Waters Purification in Bangui Region (Central African Republic)'. *Applied Clay Science* 59–60 (0), 69-75

Dey, A., Singh, R., and Purkait, M. K. (2014) 'Cobalt Ferrite Nanoparticles Aggregated Schwertmannite: A Novel Adsorbent for the Efficient Removal of Arsenic'. *Journal of Water Process Engineering* 3 (0), 1-9

Donohue, I., Styles, D., Coxon, C., and Irvine, K. (2005) 'Importance of Spatial and Temporal Patterns for Assessment of Risk of Diffuse Nutrient Emissions to Surface Waters'. *Journal of Hydrology* 304 (1), 183-192

Drinan, J.E., and Spellman, F.R. (2013) *Water and Wastewater Treatment: A Guide for Non-engineering Professionals.* 2nd ed., Boca Raton: CRC Press

Drizo, A., Frost, C. A., Grace, J., and Smith, K. A. (1999) *Physico-Chemical Screening of Phosphate-Removing Substrates for use in Constructed Wetland Systems* [online] . available from <http://www.sciencedirect.com/science/article/pii/S0043135499000822>

Ebeling, J. M., Sibrell, P. L., Ogden, S. R., and Summerfelt, S. T. (2003) 'Evaluation of Chemical coagulation–flocculation Aids for the Removal of Suspended Solids and Phosphorus from Intensive Recirculating Aquaculture Effluent Discharge'. *Aquacultural Engineering* 29 (1–2), 23-42

Edet, U. A., Bateman, M. J., Ifelebuegu, A. I., Wood, A. (2016) 'The Adsorptive Properties of Fired Clay Pellets for the Removal of Phosphate in Wastewater Treatment'. in The IRED (ed.) *Proceedings of the Fourth International Conference on Advances in Bio-Informatics, Bio-Technology and Environmental Engineering*, 'ABBE 2016'. held 17-18 March 2016 at Birmingham UK. Institute of Research Engineers and Doctors, 1, 15-21

Edzwald, J. K., Toensing, D. C., and Leung, M. C. (1976) 'Phosphate Adsorption Reactions with Clay Minerals'. *Environmental Science & Technology* 10 (5), 485-490

Egnér H, Riehm H, Domingo WR (1960) Untersuchungen über die chemische Bodenanalyse als Grundlage für die Beurteilung des Nährstoffzustandes der Böden. II. Chemische Extraktionsmethoden zur Phosphor- und Kaliumbestimmung. K Lantbrukshögsk Ann 26:199–215: In **Hylander, L. D. and Simán, G. (2001)** 'Plant Availability of Phosphorus Sorbed to Potential Wastewater Treatment Materials'. *Biology and Fertility of Soils* 34 (1), 42-48

Elser, J. J. (2012) 'Phosphorus: A Limiting Nutrient for Humanity?'. *Current Opinion in Biotechnology* 23 (6), 833-838

El-Sergany, M., & Shanableh, A. (2012) 'Phosphorus Removal using Al-Modified Bentonite Clay-Effect of Particle Size'. *Asia Pacific Conference on Environmental Science and Technology Advances in Biomedical Engineering*, 6, 323– 329.

Eslinger, E. and Pevear, D. R. (1988) *Clay Minerals for Petroleum Geologists and Engineers*.: Society of Economic Paleontologists and Mineralogis ts

Farahbakhshazad, N. and Morrison, G. M. (2003) 'Phosphorus Removal in a Vertical Upflow Constructed Wetland System'. *Water Science and Technology* 48(5) 43-50

Feng, S., Zhang, N., Liu, H., Du, X., and Liu, Y. (2012) 'Comprehensive Analysis of Heavy Metals in Sediments Contaminated by Different Pollutants'. *Journal of Environmental Engineering* 138 (4), 483-489

Firsching, F. H. and Brune, S. N. (1991) 'Solubility Products of the Trivalent Rare-Earth Phosphates'. *Journal of Chemical and Engineering Data* 36 (1), 93-95

Fondu, L., Decoster, M., De Bo, I., and Van Hulle, S. (2010) 'Phosphate Sorption Capacities of Different Substrates in View of Application in Water Treatment Systems for Ponds'

Foo, K. Y. and Hameed, B. H. (2010) 'Insights into the Modeling of Adsorption Isotherm Systems'*. Chemical Engineering Journal* 156 (1), 2-10

Fytianos, K., Voudrias, E., and Raikos, N. (1998) 'Modelling of Phosphorus Removal from Aqueous and Wastewater Samples using Ferric Iron'*. Environmental Pollution* 101 (1), 123-130

Gan, F., Zhou, J., Wang, H., Du, C., and Chen, X. (2009) 'Removal of Phosphate from Aqueous Solution by Thermally Treated Natural Palygorskite'*. Water Research* 43 (11), 2907-2915

Goldberg, S. and Sposito, G. (1985) 'On the Mechanism of Specific Phosphate Adsorption by Hydroxylated Mineral Surfaces: A Review'*. Communications in Soil Science & Plant Analysis* 16 (8), 801-821

Grim, R. E. (1962) 'Clay Mineralogy: The Clay Mineral Composition of Soils and Clays is Providing an Understanding of their Properties'*. Science (New York, N.Y.)* 135 (3507), 890-898

Gu, D., Zhu, X., Vongsay, T., Huang, M., Song, L., and He, Y. (2013) 'Phosphorus and Nitrogen Removal using Novel Porous Bricks Incorporated with Wastes and Minerals'*. Polish Journal of Environmental Studies* 22 (5), 1349-1356

Guggenheim, S. and Martin, R. (1995) 'Definition of Clay and Clay Mineral: Joint Report of the AIPEA Nomenclature and CMS Nomenclature Committees'*. Clays and Clay Minerals* 43 (2), 255-256

Gupta, S. and Babu, B. (2010) 'Experimental, Kinetic, Equilibrium and Regeneration Studies for Adsorption of Cr (VI) from Aqueous Solutions using Low Cost Adsorbent (Activated Fly ash)'*. Desalination and Water Treatment* 20 (1-3), 168-178

Gupta, V., Carrott, P., Ribeiro Carrott, M., and Suhas (2009) 'Low-Cost Adsorbents: Growing Approach to Wastewater treatment—a Review'*. Critical Reviews in Environmental Science and Technology* 39 (10), 783-842

Gurang, I.R (2005) *Phosphate Removal from Wastewater Using Recycled Aggregates* Unpublished MSc Thesis. Coventry: Coventry University

Gustafsson, J. P., Renman, A., Renman, G., and Poll, K. (2008) 'Phosphate Removal by Mineral-Based Sorbents used in Filters for Small-Scale Wastewater Treatment'*. Water Research* 42 (1), 189-197

Haghseresht, F., Wang, S., and Do, D. D. (2009) 'A Novel Lanthanum-Modified Bentonite, Phoslock, for Phosphate Removal from Wastewaters'*. Applied Clay Science* 46 (4), 369-375

Hamdi, N. and Srasra, E. (2012) 'Removal of Phosphate Ions from Aqueous Solution using Tunisian Clays Minerals and Synthetic Zeolite'*. Journal of Environmental Sciences* 24 (4), 617-623

Hameed, B. H. and El-Khaiary, M. I. (2008) 'Malachite Green Adsorption by Rattan Sawdust: Isotherm, Kinetic and Mechanism Modeling'*. Journal of Hazardous Materials* 159 (2-3), 574-579

Hameed, B., Tan, I., and Ahmad, A. (2008) 'Adsorption Isotherm, Kinetic Modeling and Mechanism of 2, 4, 6-Trichlorophenol on Coconut Husk-Based Activated Carbon'*. Chemical Engineering Journal* 144 (2), 235-244

Hammer, M. J., Hammer, M. J. (2008) *Water and Wastewater Technology*. 6th ed., Upper Saddle River, NJ : Pearson Prentice Hall

Han, R., Wang, Y., Zhao, X., Wang, Y., Xie, F., Cheng, J., and Tang, M. (2009) 'Adsorption of Methylene Blue by Phoenix Tree Leaf Powder in a Fixed-Bed Column: Experiments and Prediction of Breakthrough Curves'*. Desalination* 245 (1-3), 284-297

Hascoet, M. and Florentz, M. (1985) 'Influence of Nitrates on Biological Phosphorus Removal from Wastewater.'*. Water S. A.* 11 (1), 1-8

Hauge, S., Østerberg, R., Bjorvatn, K., and Selvig, K. (1994) 'Defluoridation of Drinking Water with Pottery: Effect of Firing Temperature'*. European Journal of Oral Sciences* 102 (6), 329-333

Heisler, J., Glibert, P. M., Burkholder, J. M., Anderson, D. M., Cochlan, W., Dennison, W. C., Dortch, Q., Gobler, C. J., Heil, C. A., Humphries, E., Lewitus, A., Magnien, R., Marshall, H. G., Sellner, K., Stockwell, D. A., Stoecker, D. K., and Suddleson, M. (2008) 'Eutrophication and Harmful Algal Blooms: A Scientific Consensus'*. Harmful Algae* 8 (1), 3-13

Hernandez, J., de-Bashan, L. E., and Bashan, Y. (2006) 'Starvation Enhances Phosphorus Removal from Wastewater by the Microalga Chlorella Spp. Co-Immobilized with Azospirillum Brasilense'*. Enzyme and Microbial Technology* 38 (1–2), 190-198

Hilton, J., O'Hare, M., Bowes, M. J., and Jones, J. I. (2006) 'How Green is My River? A New Paradigm of Eutrophication in Rivers'*. Science of the Total Environment* 365 (1), 66-83

Ho, Y. S. and McKay, G. (1999) 'Pseudo-Second Order Model for Sorption Processes'*. Process Biochemistry* 34 (5), 451-465

Hosni, K., Moussa, S. B., Chachi, A., and Amor, M. B. (2008) 'The Removal of PO 4 3− by Calcium Hydroxide from Synthetic Wastewater: Optimisation of the Operating Conditions'*. Desalination* 223 (1), 337-343

Huang, W., Wang, S., Zhu, Z., Li, L., Yao, X., Rudolph, V., and Haghseresht, F. (2008) 'Phosphate Removal from Wastewater using Red Mud'*. Journal of Hazardous Materials* 158 (1), 35-42

Huang, W., Chen, J., He, F., Tang, J., Li, D., Zhu, Y., and Zhang, Y. (2015) 'Effective Phosphate Adsorption by Zr/Al-Pillared Montmorillonite: Insight into Equilibrium, Kinetics and Thermodynamics'*. Applied Clay Science* 104, 252-260

Huang, W., Li, D., Liu, Z., Tao, Q., Zhu, Y., Yang, J., and Zhang, Y. (2014) 'Kinetics, Isotherm, Thermodynamic, and Adsorption Mechanism Studies of La(OH)3-Modified Exfoliated Vermiculites as Highly Efficient Phosphate Adsorbents'*. Chemical Engineering Journal* 236 (0), 191-201

Huang, W., Zhu, R., He, F., Li, D., Zhu, Y., and Zhang, Y. (2013) 'Enhanced Phosphate Removal from Aqueous Solution by Ferric-Modified Laterites: Equilibrium, Kinetics and Thermodynamic Studies'*. Chemical Engineering Journal* 228 (0), 679-687

Huang, W., Wang, S., Zhu, Z., Li, L., Yao, X., Rudolph, V., and Haghseresht, F. (2008) 'Phosphate Removal from Wastewater using Red Mud'*. Journal of Hazardous Materials* 158 (1), 35-42

Husband, J. A., Slattery, L., Garrett, J., Corsoro, F., Smithers, C., and Phipps, S. (2012) 'Full-Scale Operating Experience of Deep Bed Denitrification Filter Achieving <3 mg/l Total Nitrogen and <0.18 mg/l Total Phosphorus'*. Water Science and Technology* 65 (3), 519-524

Hussain, S., Aziz, H. A., Isa, M. H., Ahmad, A., Van Leeuwen, J., Zou, L., Beecham, S., and Umar, M. (2011) 'Orthophosphate Removal from Domestic Wastewater using Limestone and Granular Activated Carbon'*. Desalination* 271 (1), 265-272

Hutchins R. A. (1973) 'New Method Simplifies Design of Activated Carbon System – Water Bed Depth Service Time Analysis'. *Journal of Chemical Engineering* 81 133-138

Hutson, N. D. and Yang, R. T. (1997) 'Theoretical Basis for the Dubinin-Radushkevitch (DR) Adsorption Isotherm Equation'*. Adsorption* 3 (3), 189-195

Hylander, L. D., Kietlińska, A., Renman, G., and Simán, G. (2006) 'Phosphorus Retention in Filter Materials for Wastewater Treatment and its Subsequent Suitability for Plant Production'*. Bioresource Technology* 97 (7), 914-921

Hylander, L. D. and Simán, G. (2001) 'Plant Availability of Phosphorus Sorbed to Potential Wastewater Treatment Materials'*. Biology and Fertility of Soils* 34 (1), 42-48

Ifelebuegu, A. O. (2012) 'Removal of Steriod Hormones by Activated Carbon adsorption—kinetic and Thermodynamic Studies'*. Journal of Environmental Protection* 2012

Ijagbemi, C.O., Baek, M.H., Kim, D.S. (2009) 'Montmorillonite Surface Properties and Sorption Characteristics for Heavy Metal Removal from Aqueous Solutions. *Journal of Hazardous Materials* 166, 538–546

Ismadji, S., Soetaredjo, F. E., and Ayucitra, A. (2015) *Clay Materials for Environmental Remediation*.: Springer

Jahangiri-Rad, M., Jamshidi, A., Rafiee, M., and Nabizadeh, R. (2014) 'Adsorption Performance of Packed Bed Column for Nitrate Removal using PAN-Oxime-Nano Fe_2O_3'*. Journal of Environmental Health Science and Engineering* 12 (1), 1

Jarvie, H. P., Neal, C., and Withers, P. J. A. (2006) 'Sewage-Effluent Phosphorus: A Greater Risk to River Eutrophication than Agricultural Phosphorus?'*. Science of the Total Environment* 360 (1–3), 246-253

Jia, C., Dai, Y., Chang, J., Wu, C., Wu, Z., and Liang, W. (2013) 'Adsorption Characteristics of used Brick for Phosphorus Removal from Phosphate Solution'*. Desalination and Water Treatment* 51 (28-30) 1-6

Jiang, C., Jia, L., He, Y., Zhang, B., Kirumba, G., and Xie, J. (2013) 'Adsorptive Removal of Phosphorus from Aqueous Solution using Sponge Iron and Zeolite'*. Journal of Colloid and Interface Science*

Jiang, S. Y. N., Su, L. C., Ruan, H. D., Zhang, G. F., Lai, S. Y., Lee, C. H., Yu, C. F., Wu, Z., Chen, X., He, S. (2014) 'Adsorption of Phosphorus by Modified Clay Mineral Waste Material Relating to Removal of It from Aquatic System' *International Journal of Environmental Monitoring and Analysis* 2 (1) 36-44

Johansson W. L. (2006) 'Substrates for Phosphorus removal—Potential Benefits for on-Site Wastewater Treatment?'*. Water Research* 40 (1), 23-36

Johansson, L. (1997) 'The use of Leca (Light Expanded Clay Aggregrates) for the Removal of Phosphorus from Wastewater'*. Water Science and Technology* 35 (5), 87-93

Johansson, L. and Gustafsson, J. P. (2000) 'Phosphate Removal using Blast Furnace Slags and Opoka-Mechanisms'*. Water Research* 34 (1), 259-265

Kaasik, A., Vohla, C., Mõtlep, R., Mander, Ü., and Kirsimäe, K. (2008) 'Hydrated Calcareous Oil-Shale Ash as Potential Filter Media for Phosphorus Removal in Constructed Wetlands'*. Water Research* 42 (4–5), 1315-1323

Kahraman, S., Yalcin, P., and Kahraman, H. (2012) 'The Evaluation of low-cost Biosorbents for Removal of an Azo Dye from Aqueous Solution'*. Water and Environment Journal* 26 (3), 399-404

Kamiyango, M., Sajidu, S., and Masamba, W. (2011) 'Removal of Phosphate Ions from Aqueous Solutions using Bauxite obtained from Mulanje, Malawi'*. African Journal of Biotechnology* 10 (56), 11972-11982

Kamiyango, M. W., Masamba, W. R. L., Sajidu, S. M. I., and Fabiano, E. (2009) 'Phosphate Removal from Aqueous Solutions using Kaolinite obtained from Linthipe, Malawi'*. Physics and Chemistry of the Earth, Parts A/B/C* 34 (13–16), 850-856

Karaca, S., Gürses, A., Ejder, M., and Açıkyıldız, M. (2004) 'Kinetic Modeling of Liquid-Phase Adsorption of Phosphate on Dolomite'*. Journal of Colloid and Interface Science* 277 (2), 257-263

Karageorgiou, K., Paschalis, M., and Anastassakis, G. N. (2007) 'Removal of Phosphate Species from Solution by Adsorption onto Calcite used as Natural Adsorbent'*. Journal of Hazardous Materials* 139 (3), 447-452

Karunanithi, R., Szogi, A. A., Bolan, N., Naidu, R., Loganathan, P., Hunt, P. G., Vanotti, M. B., Saint, C. P., Ok, Y. S., and Krishnamoorthy, S. (2015) 'Phosphorus Recovery and Reuse from Waste Streams'. in *Advances in Agronomy*. ed. by Anon: Elsevier, 173-250

Kasama, T., Watanabe, Y., Yamada, H., and Murakami, T. (2004) 'Sorption of Phosphates on Al-Pillared Smectites and Mica at Acidic to Neutral pH'*. Applied Clay Science* 25 (3–4), 167-177

Kavak, D. and Öztürk, N. (2004) 'Adsorption of Boron from Aqueous Solution by Sepirolite: II Column Studies'. *II Illuslrararasi Bor Sempozyumu* 23 (25), 495-500

Khawmee, K., Suddhiprakarn, A., Kheoruenromne, I., Singh, B. (2013) 'Surface Charge Properties of Kaolinite from Thai soils'. *Geoderma* 192, 120–131

Khitous, M., Salem, Z., and Halliche, D. (2016) 'Removal of Phosphate from Industrial Wastewater using Uncalcined MgAl-NO3 Layered Double Hydroxide: Batch Study and Modeling'*. Desalination and Water Treatment* 57 (34), 15920-15931

Kitano, Y., Okumura, M., and Idogaki, M. (1978) 'Uptake of Phosphate Ions by Calcium Carbonate'*. Geochem.J* 12, 29-37

Kling, H.J., Mugidde, R., and Hecky, R.E. (2001) 'Recent Changes in the Phytoplankton Community of Lake Victoria in Response to Eutrphication'. *The Great Lakes of the World (GLOW): Food-Web, Health and Integrity* Backuys, Leiden 47 – 65.

Koehler, A. (2008) 'Water use in LCA: Managing the planet's Freshwater Resources'*. The International Journal of Life Cycle Assessment* 13 (6), 451-455

Köse, T. E. and Kıvanç, B. (2011) 'Adsorption of Phosphate from Aqueous Solutions using Calcined Waste Eggshell'*. Chemical Engineering Journal* 178 (0), 34-39

Kosmulski, M. (2009) 'PH-Dependent Surface Charging and Points of Zero Charge. IV. Update and New Approach'*. Journal of Colloid and Interface Science* 337 (2), 439-448

Krejčová, A., Černohorský, T., and Pouzar, M. (2007) 'Determination of Metal Impurities in Pure Hydroxides and Salts by Inductively Coupled Plasma Optical Emission Spectrometry'. *Analytica Chimica Acta* 582 (2) 208-213.

Kumar, P., Sudha, S., Chand, S., and Srivastava, V. C. (2010) 'Phosphate Removal from Aqueous Solution using Coir-Pith Activated Carbon'. *Separation Science and Technology* 45 (10), 1463-1470

Kummu, M., Ward, P. J., de Moel, H., and Varis, O. (2010) 'Is Physical Water Scarcity a New Phenomenon? Global Assessment of Water Shortage Over the Last Two Millennia'. *Environmental Research Letters* 5 (3), 034006

Kurzbaum, E. and Bar Shalom, O. (2016) 'The Potential of Phosphate Removal from Dairy Wastewater and Municipal Wastewater Effluents using a Lanthanum-Modified Bentonite'. *Applied Clay Science* 123, 182-186

Kvarnström, M. E., Morel, C. A., and Krogstad, T. (2004) 'Plant-Availability of Phosphorus in Filter Substrates Derived from Small-Scale Wastewater Treatment Systems'. *Ecological Engineering* 22 (1), 1-15

Lalley, J., Han, C., Mohan, G. R., Dionysiou, D. D., Speth, T. F., Garland, J., and Nadagouda, M. N. (2015) 'Phosphate Removal using Modified Bayoxide® E33 Adsorption Media'. *Environmental Science: Water Research & Technology*

Lewis Jr., W. M. and Wurtsbaugh, W. A. (2008) 'Control of Lacustrine Phytoplankton by Nutrients: Erosion of the Phosphorus Paradigm'. *International Review of Hydrobiology* 93 (4-5), 446-465

Li, G., Gao, S., Zhang, G., and Zhang, X. (2014) 'Enhanced Adsorption of Phosphate from Aqueous Solution by Nanostructured Iron(III)–copper(II) Binary Oxides'. *Chemical Engineering Journal* 235 (0), 124-131

Li, N., Ren, J., Zhao, L., and Wang, Z. (2013) 'Fixed Bed Adsorption Study on Phosphate Removal using Nanosized FeOOH-Modified Anion Resin'. *Journal of Nanomaterials* 2013, 7

Li, Y., Liu, C., Luan, Z., Peng, X., Zhu, C., Chen, Z., Zhang, Z., Fan, J., and Jia, Z. (2006) 'Phosphate Removal from Aqueous Solutions using Raw and Activated Red Mud and Fly Ash'. *Journal of Hazardous Materials* 137 (1), 374-383

Lim, A. P. and Aris, A. Z. (2014) 'Continuous Fixed-Bed Column Study and Adsorption Modeling: Removal of Cadmium (II) and Lead (II) Ions in Aqueous Solution by Dead Calcareous Skeletons'. *Biochemical Engineering Journal* 87, 50-61

Littler J. (2012) *Removal of Phosphorus from Water using Acid Mine Drainage Solids and Pellets Made Thereof.* Unpublished PhD Thesis. Cardiff: Cardiff University.

Littler, J., Geroni, J. N., Sapsford, D. J., Coulton, R., and Griffiths, A. J. (2013) 'Mechanisms of Phosphorus Removal by Cement-Bound Ochre Pellets'. *Chemosphere* 90 (4), 1533-1538

Loganathan, P., Vigneswaran, S., Kandasamy, J., and Bolan, N. S. (2014) 'Removal and Recovery of Phosphate from Water using Sorption'. *Critical Reviews in Environmental Science and Technology* 44 (8), 847-907

Mahmood, T., Saddique, M. T., Naeem, A., Westerhoff, P., Mustafa, S., and Alum, A. (2011) 'Comparison of Different Methods for the Point of Zero Charge Determination of NiO'. *Industrial & Engineering Chemistry Research* 50 (17), 10017-10023

Mahmood, Z., Nasir, S., Jamil, N., Sheikh, A., and Akram, A. (2015) 'Adsorption Studies of Phosphate Ions on Alginate-Calcium Carbonate Composite Beads'*. African Journal of Environmental Science and Technology* 9 (3), 274-281

Mainstone, C. P. and Parr, W. (2002) 'Phosphorus in Rivers — Ecology and Management'*. Science of the Total Environment* 282–283 (0), 25-47

Malakootian, M., Nouri, J., and Hossaini, H. (2009) 'Removal of Heavy Metals from Paint industry's Wastewater using Leca as an Available Adsorbent'*. International Journal of Environmental Science & Technology* 6 (2), 183-190

Malkoc, E. and Nuhoglu, Y. (2006a) 'Removal of Ni(II) Ions from Aqueous Solutions using Waste of Tea Factory: Adsorption on a Fixed-Bed Column'*. Journal of Hazardous Materials* 135 (1–3), 328-336

Malkoc, E. and Nuhoglu, Y. (2006b) 'Fixed Bed Studies for the Sorption of Chromium(VI) Onto Tea Factory Waste'*. Chemical Engineering Science* 61 (13), 4363-4372

Mall, I., Upadhyay, S., and Sharma, Y. (1996) 'A Review on Economical Treatment of Wastewaters and Effluents by Adsorption'*. International Journal of Environmental Studies* 51 (2), 77-124

Mallikarjun, S. and Mise, S. R. (2013) 'A Batch Study of Phosphate Adsorption Characteristics on Clay Soil'*. International Journal of Research in Engineering and Technology, eISSN*, 2319-1163

Martín, M., Gargallo, S., Hernández-Crespo, C., and Oliver, N. (2013) 'Phosphorus and Nitrogen Removal from Tertiary Treated Urban Wastewaters by a Vertical Flow Constructed Wetland'*. Ecological Engineering* 61, Part A (0), 34-42

Masters, G. M., Ela, W. P. (2014) *Introduction to Environmental Engineering and Science*. 3rd ed., Pearson new international ed.. edn. Harlow, Essex: Harlow, Essex : Pearson

Mateus, D. M. R. and Pinho, H. J. O. (2010) 'Phosphorus Removal by Expanded Clay-Six Years of Pilot-Scale Constructed Wetlands Experience'*. Water Environment Research* 82 (2), 128-137

Mateus, D. M. R., Vaz, M. M. N., and Pinho, H. J. O. (2012) 'Fragmented Limestone Wastes as a Constructed Wetland Substrate for Phosphorus Removal'*. Ecological Engineering* 41 (0), 65-69

Melnyk, P., Norman, J., and Wasserlauf, M. (eds.) (1974) *Proceedings of Rare Earth Resources Conference, 11th. NTIS, Springfield, Cleveland, OH, USA*. 'Lanthanum Precipitation. Alternative Method for Removing Phosphates from Waste Water' 4-13

Merzouki, M., Delgenès, J. -., Bernet, N., Moletta, R., and Benlemlih, M. (1999) 'Polyphosphate-Accumulating and Denitrifying Bacteria Isolated from Anaerobic-Anoxic and Anaerobic-Aerobic Sequencing Batch Reactors'*. Current Microbiology* 38 (1), 9-17

Mezenner, N. Y. and Bensmaili, A. (2009) 'Kinetics and Thermodynamic Study of Phosphate Adsorption on Iron Hydroxide-Eggshell Waste'*. Chemical Engineering Journal* 147 (2–3), 87-96

Miranzadeh, M., Rabbani, D., and Dehqan, S. (2012) 'Electrocoagulation Process for Removal of Adenosine-5'-Monophosphate and Sodium Hexamethaphosphate from the Synthetic Wastewater'*. International Journal of Physical Sciences* 7 (10), 1571-1577

Miró, M., Estela, J. M., and Cerdà, V. (2003) 'Application of Flowing Stream Techniques to Water Analysis. Part I. Ionic Species: Dissolved Inorganic Carbon, Nutrients and Related Compounds'*. Talanta* 60 (5) 867-886.

Mnasri, S., Hamdi, N., Frini-Srasra, N., and Srasra, E. (2014) 'Acid–base Properties of Pillared Interlayered Clays with Single and Mixed Zr–Al Oxide Pillars Prepared from Tunisian-Interstratified illite–smectite'*. Arabian Journal of Chemistry*

Moges, G., Zewge, F., and Socher, M. (1996) 'Preliminary Investigations on the Defluoridation of Water using Fired Clay Chips'*. Journal of African Earth Sciences* 22 (4), 479-482

Mohan, S. and Sreelakshmi, G. (2008) 'Fixed Bed Column Study for Heavy Metal Removal using Phosphate Treated Rice Husk'*. Journal of Hazardous Materials* 153 (1), 75-82

Mohapatra, M., Anand, S., Mishra, B. K., Giles, D. E., and Singh, P. (2009) 'Review of Fluoride Removal from Drinking Water'*. Journal of Environmental Management* 91 (1), 67-77

Moharami, S. and Jalali, M. (2014) 'Phosphorus Leaching from a Sandy Soil in the Presence of Modified and Un-Modified Adsorbents'*. Environmental Monitoring and Assessment* 186 (10), 6565-6576

Moharami, S. and Jalali, M. (2013) 'Removal of Phosphorus from Aqueous Solution by Iranian Natural Adsorbents'*. Chemical Engineering Journal* 223, 328-339

Monclús, H., Sipma, J., Ferrero, G., Rodriguez-Roda, I., and Comas, J. (2010) 'Biological Nutrient Removal in an MBR Treating Municipal Wastewater with Special Focus on Biological Phosphorus Removal'*. Bioresource Technology* 101 (11), 3984-3991

Mor, S., Chhoden, K., and Ravindra, K. (2016) 'Application of Agro-Waste Rice Husk Ash for the Removal of Phosphate from the Wastewater'*. Journal of Cleaner Production* 129, 673-680

Morrison, J., Jackson, M.V., Sparrow, P.E. (1980) 'The Response of Perennial Ryegrass to Fertilizer Nitrogen in Relation to Climate and Soil. Report of the Joint ADAS/GRI Grassland Manuring Trial GM20'. Grassland Research Institute Technical Report No. 27 Hurley, Berkshire Grassland Research Institute

Morse, G. K., Brett, S. W., Guy, J. A., and Lester, J. N. (1998) 'Review: Phosphorus Removal and Recovery Technologies'*. Science of the Total Environment* 212 (1), 69-81

Murray, H. H. (2006) 'Structure and Composition of the Clay Minerals and their Physical and Chemical Properties'*. Developments in Clay Science* 2, 7-31

Namasivayam, C. and Prathap, K. (2005) 'Recycling Fe (III)/Cr (III) Hydroxide, an Industrial Solid Waste for the Removal of Phosphate from Water'*. Journal of Hazardous Materials* 123 (1), 127-134

Namasivayam, C. and Sangeetha, D. (2004) *Equilibrium and Kinetic Studies of Adsorption of Phosphate Onto ZnCl2 Activated Coir Pith Carbon* [online] . available from <http://www.sciencedirect.com/science/article/pii/S0021979704007180>

Nassef, E. (2012) 'Removal of Phosphates from Industrial Waste Water by Chemical Precipitation'. *IRACST- Engineering Science and Technology: An International Journal* 2 (3), 409-413

Nawar, N., Ahmad, M. E., El Said, W. M. Moalla, S. M. N. (2015) 'Adsorptive Removal of Phosphorus from Wastewater using Drinking Water Treatment-Alum Sludge (DWT-AS) as Low Cost Adsorbent' *American Journal of Chemistry and Application* 2 (6) 79-85

Ni, F., He, J., Wang, Y., and Luan, Z. (2015) 'Preparation and Characterization of a Cost-Effective Red mud/polyaluminum Chloride Composite Coagulant for Enhanced Phosphate Removal from Aqueous Solutions'*. Journal of Water Process Engineering* 6, 158-165

Ning, P., Bart, H., Li, B., Lu, X., and Zhang, Y. (2008) 'Phosphate Removal from Wastewater by Model-La(III) Zeolite Adsorbents'. *Journal of Environmental Science* 20 (6), 670-674

Nkansah, M. A., Christy, A. A., Barth, T., and Francis, G. W. (2012) 'The use of Lightweight Expanded Clay Aggregate (LECA) as Sorbent for PAHs Removal from Water'. *Journal of Hazardous Materials* 217, 360-365

Nnadi, E. O. (2009) . *An Evaluation of Modified Pervious Pavements for Water Harvesting for Irrigation Purposes*. Unpublished PhD Thesis. Coventry: Coventry University

Nourmoradi, H., Nikaeen, M., Pourzamani, H., and Nejad, M. (2013) 'Comparison of the Efficiencies of Modified Clay with Polyethylene Glycol and Tetradecyl Trimethyl Ammonium Bromide for BTEX Removal'. *International Journal of Environmental Health Engineering* 2 1 (7): 1-8.

Nourmoradi, H. and Nikaeen, M. (2012) 'Removal of Benzene, Toluene, Ethylbenzene and Xylene (BTEX) from Aqueous Solutions by Montmorillonite Modified with Nonionic Surfactant: Equilibrium, Kinetic and Thermodynamic Study'. *Chemical Engineering Journal* 191, 341-348

Noyan, H., Önal, M., and Sarikaya, Y. (2006) 'The Effect of Heating on the Surface Area, Porosity and Surface Acidity of a Bentonite'. *Clays and Clay Minerals* 54 (3), 375-381

Nur, T., Loganathan, P., Nguyen, T., Vigneswaran, S., Singh, G., and Kandasamy, J. (2014) 'Batch and Column Adsorption and Desorption of Fluoride using Hydrous Ferric Oxide: Solution Chemistry and Modeling'. *Chemical Engineering Journal* 247, 93-102

Nwabanne, J. and Igbokwe, P. (2012) 'Adsorption Performance of Packed Bed Column for the Removal of Lead (II) using Oil Palm Fibre'. *International Journal of Applied Science and Technology* 2 (5)

Nyenje, P. M., Foppen, J. W., Uhlenbrook, S., Kulabako, R., and Muwanga, A. (2010) 'Eutrophication and Nutrient Release in Urban Areas of Sub-Saharan Africa — A Review'. *Science of the Total Environment* 408 (3), 447-455

OECD (1984) *OECD Guideline for Testing Toxicity of Chemicals "Earthworm, Acute Toxicity Test"* [online] available from <http://www.oecd-ilibrary.org/docserver/download/9720701e.pdf?expires=1388831151&id=id&accname=guest&checksum=DB1566E097EB126904ADA496B974E10C> (29 December 2013).

Oehmen, A., Lemos, P. C., Carvalho, G., Yuan, Z., Keller, J., Blackall, L. L., and Reis, M. A. M. (2007) 'Advances in Enhanced Biological Phosphorus Removal: From Micro to Macro Scale'. *Water Research* 41 (11), 2271-2300

Ogutu, R. A., Williams, K. A., and Pierzynski, G. M. (2009) 'Phosphate Sorption of Calcined Materials used as Components of Soilless Root Media Characterized in Laboratory Studies'. *Hortscience* 44 (2), 431-437

Omoike, A. I. and vanLoon, G. W. (1999) 'Removal of Phosphorus and Organic Matter Removal by Alum during Wastewater Treatment'. *Water Research* 33 (17), 3617-3627

Onu, M. A., Okafor, J. O., Abdusalami, S., and Mohammad, Y. S. (2015) 'Development of Optimum Conditions for Modification of Kpautagi Clay for Application in Petroleum Refinery Wastewater Treatment'. *Leonardo Electronic Journal of Practices and Technologies* 1 (14), 131-137

Osalo, T. P., Merufinia, E., and Saatlo, M. E. (2013) 'Phosphorus Removal from Aqueous Solutions by Bentonite: Effect of Al2O3 Addition'. *Journal of Civil Engineering and Urbanism* 3 (5), 317-322

Ou, E., Zhou, J., Mao, S., Wang, J., Xia, F., and Min, L. (2007) 'Highly Efficient Removal of Phosphate by Lanthanum-Doped Mesoporous SiO2'. *Colloids and Surfaces A: Physicochemical and Engineering Aspects* 308 (1–3), 47-53

Özacar, M. (2006) 'Contact Time Optimization of Two-Stage Batch Adsorber Design using Second-Order Kinetic Model for the Adsorption of Phosphate Onto Alunite'. *Journal of Hazardous Materials* 137 (1), 218-225

Özacar, M. (2003) 'Adsorption of Phosphate from Aqueous Solution Onto Alunite'. *Chemosphere* 51 (4), 321-327

Özacar, M. and Şengil, İ. A. (2003) 'Enhancing Phosphate Removal from Wastewater by using Polyelectrolytes and Clay Injection'. *Journal of Hazardous Materials* 100 (1–3), 131-146

Paerl, H. W. (2009) 'Controlling Eutrophication Along the freshwater–marine Continuum: Dual Nutrient (N and P) Reductions are Essential'. *Estuaries and Coasts* 32 (4), 593-601

Palma, P., Alvarenga, P., Palma, V. L., Fernandes, R. M., Soares, A. M. V. M., and Barbosa, I. R. (2010) 'Assessment of Anthropogenic Sources of Water Pollution using Multivariate Statistical Techniques: A Case Study of the Alqueva's Reservoir, Portugal'. *Environmental Monitoring and Assessment* 165 (1-4), 539-552

Pan, B., Wu, J., Pan, B., Lv, L., Zhang, W., Xiao, L., Wang, X., Tao, X., and Zheng, S. (2009) 'Development of Polymer-Based Nanosized Hydrated Ferric Oxides (HFOs) for Enhanced Phosphate Removal from Waste Effluents'. *Water Research* 43 (17), 4421-4429

Pawar, R. R., Gupta, P., Lalhmunsiama, Bajaj, H. C., and Lee, S. (2016) 'Al-Intercalated Acid Activated Bentonite Beads for the Removal of Aqueous Phosphate'. *Science of the Total Environment* 572, 1222-1230

Pawlett, M., Deeks, L. K., and Sakrabani, R. (2015) 'Nutrient Potential of Biosolids and Urea Derived Organo-Mineral Fertilisers in a Field Scale Experiment using Ryegrass (Lolium Perenne L.)'. *Field Crops Research* 175, 56-63

Peach, B.N and Horne, J. (1881) 'The Glaciation of Caithness' Read Before the Royal Physical Society of Edinburgh 20th April 1881 In: The Pamphlet Collection of Sir Robert Stout: Volume 22 [online] available from <http://nzetc.victoria.ac.nz/tm/scholarly/tei-Stout22-t6-body-d1-d4-d1.html> (01 November 2013).

Postel, S. L. (1998) 'Water for Food Production: Will there be enough in 2025?'. *Bioscience* 48 (8), 629-637

Pratt, C., Shilton, A., Haverkamp, R., and Pratt, S. (2011) 'Chemical Techniques for Pretreating and Regenerating Active Slag Filters for Improved Phosphorus Removal'. *Environmental Technology* 32 (10), 1053-1062

Pratt, C., Shilton, A., Pratt, S., Haverkamp, R. G., and Bolan, N. S. (2007) 'Phosphorus Removal Mechanisms in Active Slag Filters Treating Waste Stabilization Pond Effluent'. *Environmental Science and Technology* 41 (9), 3296-3301

Prieto, A., Schrader, S., and Moeder, M. (2010) 'Determination of Organic Priority Pollutants and Emerging Compounds in Wastewater and Snow Samples using Multiresidue Protocols on the Basis of Microextraction by Packed Sorbents Coupled to Large Volume Injection Gas chromatography–mass Spectrometry Analysis'. *Journal of Chromatography A* 1217 (38), 6002-6011

Priyantha, N. and Bandaranayaka, A. (2011) 'Investigation of Kinetics of Cr(VI)–fired Brick Clay Interaction'. *Journal of Hazardous Materials* 188 (1–3), 193-197

Putra, E.K., Pranowo, R., Sunarso, J., Indraswati, N., Ismadji, S. (2009) 'Performance of Activated Carbon and Bentonite for Adsorption of Amoxicillin from Wastewater: Mechanisms, Isotherms and Kinetics'. *Water Resources* 43, 2419–2430

Qiu, H., Lv, L., Pan, B., Zhang, Q., Zhang, W., and Zhang, Q. (2009) 'Critical Review in Adsorption Kinetic Models'. *Journal of Zhejiang University-Science A* 10 (5), 716-724

Ragheb, S. M. (2013) 'Phosphate Removal from Aqueous Solution using Slag and Fly Ash'. *HBRC Journal* 9 (3), 270-275

Rahni, S. Y., Mirghaffari, N., Rezaei, B., and Ghaziaskar, H. S. (2014) 'Removal of Phosphate from Aqueous Solutions using a New Modified Bentonite-Derived Hydrogel'. *Water, Air, & Soil Pollution* 225 (4), 1-12

Rajan, S., Perrott, K., and Saunders, W. (1974) 'Identification of Phosphate-reactive Sites of Hydrous Alumina from Proton Consumption during Phosphate Adsorption at Constant pH Values'. *European Journal of Soil Science* 25 (4), 438-447

Rathinam, A., Maharshi, B., Janardhanan, S. K., Jonnalagadda, R. R., and Nair, B. U. (2010) 'Biosorption of Cadmium Metal Ion from Simulated Wastewaters using Hypnea Valentiae Biomass: A Kinetic and Thermodynamic Study'. *Bioresource Technology* 101 (5), 1466-1470

Recht, H., Ghassemi, M., and Kleber, E. (1970) *Proceedings of the 5th International Water Pollution Research* 'Precipitation of Phosphates from Water and Waste Water using Lanthanum Salts' *Pergamon*, 1-17

Reitzel, K., Andersen, F. Ø., Egemose, S., and Jensen, H. S. (2013) 'Phosphate Adsorption by Lanthanum Modified Bentonite Clay in Fresh and Brackish Water'. *Water Research* 47 (8), 2787-2796

Ren, H., Zhu, M., and Haraguchi, K. (2012) 'Effects of Counter Ions of Clay Platelets on the Swelling Behavior of Nanocomposite Gels'. *Journal of Colloid and Interface Science* 375 (1), 134-141

Rentz, J. A., Turner, I. P., and Ullman, J. L. (2009) 'Removal of Phosphorus from Solution using Biogenic Iron Oxides'. *Water Research* 43 (7), 2029-2035

Rijsberman, F. R. (2006) 'Water Scarcity: Fact Or Fiction?'. *Agricultural Water Management* 80 (1–3), 5-22

Rivera-Utrilla, J., Bautista-Toledo, I., Ferro-García, M. A., and Moreno-Castilla, C. (2001) 'Activated Carbon Surface Modifications by Adsorption of Bacteria and their Effect on Aqueous Lead Adsorption'. *Journal of Chemical Technology and Biotechnology* 76 (12), 1209-1215

Robinson, D. L., Eliers, T. L. (1996) 'Annual Ryegrass Yield Response and Return to Phosphorus and Potassium Fertilization'. *Better Crops* 80 (4) 28-31 [online] available from < http://www.ipni.net/publication/bettercrops.nsf/0/9BD2EE01B699F14385257D2E004D68E2/$FILE/BC-1996-4%20p28.pdf> (28 September 2016).

Rout, P. R., Bhunia, P., and Dash, R. R. (2014) 'Modeling Isotherms, Kinetics and Understanding the Mechanism of Phosphate Adsorption onto a Solid Waste: Ground Burnt Patties'. *Journal of Environmental Chemical Engineering* 2 (3), 1331-1342

Sarir, M., Sharif, M., Pulford, I., Flowers, T., and Ahmad, I. (2009) 'Response of Ryegrass to Phosphate in the Reclamation of Coal Mine Soil'*. Sarhad J.Agric* 25 (2), 203-207

Seida, Y. and Nakano, Y. (2002) 'Removal of Phosphate by Layered Double Hydroxides Containing Iron'*. Water Research* 36 (5), 1306-1312

Selvaraju, N. and Pushpavanam, S. (2009) 'Adsorption Characteristics on Sand and Brick Beds'*. Chemical Engineering Journal* 147 (2–3), 130-138

Shanableh, A., Enshasi, G., and Elsergany, M. (2016) 'Phosphorous Adsorption using Al3 /Fe3 -Modified Bentonite adsorbents—effect of Al3 and Fe3 Combinations'*. Desalination and Water Treatment* 57 (33), 15628-15634

Shanableh, A. M. and Elsergany, M. M. (2013) 'Removal of Phosphate from Water using Six Al-, Fe-, and Al-Fe-Modified Bentonite Adsorbents'*. Journal of Environmental Science and Health, Part A* 48 (2), 223-231

Shin, E. W., Han, J. S., Jang, M., Min, S., Park, J. K., Rowell, R. M. (2004) 'Phosphate Adsorption on Aluminum-Impregnated Mesoporous Silicates: Surface Structure and Behaviour of Adsorbents' *Environmental Science and Technology* 38 (3) 912-917

Singh, S., Srivastava, V. C., and Mall, I. D. (2009) 'Fixed-Bed Study for Adsorptive Removal of Furfural by Activated Carbon'*. Colloids and Surfaces A: Physicochemical and Engineering Aspects* 332 (1), 50-56

Smith, V. H. (2003) 'Eutrophication of Freshwater and Coastal Marine Ecosystems: A Global Problem'*. Environmental Science and Pollution Research* 10 (2), 126-139

Smith, V. H. and Schindler, D. W. (2009) 'Eutrophication Science: Where do we Go from here?'*. Trends in Ecology & Evolution* 24 (4), 201-207

Sousa, A. F. d., Braga, T. P., Gomes, E. C. C., Valentini, A., and Longhinotti, E. (2012) 'Adsorption of Phosphate using Mesoporous Spheres Containing Iron and Aluminum Oxide'*. Chemical Engineering Journal* 210 (0), 143-149

Subha, R. and Namasivayam, C. (2008) 'Modeling of Adsorption Isotherms and Kinetics of 2, 4, 6-Trichlorophenol Onto Microporous ZnCl2 Activated Coir Pith Carbon'*. J.Environ.Eng.Manage* 18 (4), 275-280

Sugashini, S., Begum, S., and Meera, K. (2012) 'Column Adsorption Studies for the Removal of Cr (VI) Ions by Ethylamine Modified Chitosan Carbonized Rice Husk Composite Beads with Modelling and Optimization'*. Journal of Chemistry* 2013

Sun, X., Imai, T., Sekine, M., Higuchi, T., Yamamoto, K., Kanno, A., and Nakazono, S. (2014) 'Adsorption of Phosphate using Calcined mg-3-Fe Layered Double Hydroxides in a Fixed-Bed Column Study'*. Journal of Industrial and Engineering Chemistry* 20 (5), 3623-3630

Tam, N. F. Y., Wong, Y. S., and Wong, M. H. (2009) 'Novel Technology in Pollutant Removal at Source and Bioremediation'*. Ocean and Coastal Management* 52 (7), 368-373

Tanada, S., Kabayama, M., Kawasaki, N., Sakiyama, T., Nakamura, T., Araki, M., and Tamura, T. (2003) 'Removal of Phosphate by Aluminum Oxide Hydroxide'*. Journal of Colloid and Interface Science* 257 (1), 135-140

Taylor, Y. (2005) *Removal of Phosphate from wastewater using Bricks.* Unpublished Masters thesis. Coventry: Coventry University

Teka, T. and Enyew, S. (2014) 'Study on Effect of Different Parameters on Adsorption Efficiency of Low Cost Activated Orange Peels for the Removal of Methylene Blue Dye'*. Int.J.Innov.Sci.Res* 8 (1), 106-111

Tempkin, M. and Pyzhev, V. (1940) 'Heavy Metals Removal and Isotherms Study'*. Acta Physiochim URSS* 12, 217-222

Thomas, H. C. (1944) 'Heterogeneous Ion Exchange in a Flowing System'*. Journal of the American Chemical Society* 66 (10), 1664-1666

Tian, S., Jiang, P., Ning, P., and Su, Y. (2009) 'Enhanced Adsorption Removal of Phosphate from Water by Mixed lanthanum/aluminum Pillared Montmorillonite'*. Chemical Engineering Journal* 151 (1–3), 141-148

Tikariha, A. and Sahu, O.(2013) 'Low Cost Adsorbent for Defluoridation of Water'. *International Journal of Environmental Monitoringand Analysis* 1 (2) 65 - 70

Tschapek, M., Tcheichvili, L., Wasowski, C. (1974) 'The Point of Zero Charge (pzc) of Kaolinite and SiO_2 + Al_2O_3 Mixtures'. *Clay Miner*als 10, 219–229

Tyrrell, T. (1999) 'The Relative Influences of Nitrogen and Phosphorus on Oceanic Primary Production'*. Nature* 400 (6744), 525-531

UNFPA (2011) *State of the World Population 2011: People and Possibilities in a World of 7 Billion* UNFPA, 2011 ISBN 978 0 89714 990 7

Unuabonah, E.I., Olu-Owolabi, B.I., Adebowale, K.O., Yang, L.Z. (2008) 'Removal of Lead and Cadmium from Aqueous Solution by Polyvinyl Alcohol-Modified Kaolinite Clay: A Novel Nanoclay Adsorbent'. Adsorption Science and Technology 26, 383–405

Van Staden, J. and Van der Merwe, J. (1997) 'Evaluation of a Number of Methods for the Determination of Trace Amounts of Phosphates with Flow Injection Analysis(FIA)'*. Water S. A.* 23 (2) 169-174.

Vohla, C., Kõiv, M., Bavor, H. J., Chazarenc, F., and Mander, Ü. (2011) 'Filter Materials for Phosphorus Removal from Wastewater in Treatment wetlands—A Review'*. Ecological Engineering* 37 (1), 70-89

Vohla, C., Alas, R., Nurk, K., Baatz, S., and Mander, Ü. (2007) 'Dynamics of Phosphorus, Nitrogen and Carbon Removal in a Horizontal Subsurface Flow Constructed Wetland'*. Science of the Total Environment* 380 (1–3), 66-74

Vohla, C., Põldvere, E., Noorvee, A., Kuusemets, V., and Mander, Ü. (2005) 'Alternative Filter Media for Phosphorous Removal in a Horizontal Subsurface Flow Constructed Wetland'*. Journal of Environmental Science and Health - Part A Toxic/Hazardous Substances and Environmental Engineering* 40 (6-7), 1251-1264

Vyshak, R. S., Jayalekshmi, S. (2014) 'Soil – An Adsorbent for Purification of Phosphate Contaminated Water' *International Journal of Structural and Civil Engineering Research* 3 (2) 65-77

Walfish S. (2006) 'Analytical Methods: 'A Statistical Perspective on the ICH Q2A and Q2B Guidelines for Validation of Analytical Methods'. *BioPharm International* 19 (12) 28-36

Wang, D., Hu, W., Chen, N., Yu, Y., Tian, C., and Feng, C. (2016) 'Removal of Phosphorus from Aqueous Solutions by Granular Mesoporous Ceramic Adsorbent Based on Hangjin Clay'*. Desalination and Water Treatment* 57 (47), 22400-22412

Wang, S., Jin, X., Pang, Y., Zhao, H., and Zhou, X. (2005) 'The Study of the Effect of pH on Phosphate Sorption by Different Trophic Lake Sediments'. *Journal of Colloid and Interface Science* 285 (2), 448-457

Wang, X. J., Xia, S. Q., Chen, L., Zhao, J. F., Renault, N. J., and Chovelon, J. M. (2006) 'Nutrients Removal from Municipal Wastewater by Chemical Precipitation in a Moving Bed Biofilm Reactor'*. Process Biochemistry* 41 (4), 824-828

Wang, Y.H., Huang, C.B., Hu, Y.H., Hu, Y.M., Lan, Y. (2008) 'Beneficiation of Diasporic-Bauxite Ore by Selective Flocculation with a Polyacrylate Flocculant'. *Minerals Engineering* 21, 664–672

Weber, W. and Morris, J. (1963) 'Intraparticle Diffusion during the Sorption of Surfactants onto Activated Carbon'*. Journal of Sanitary Engineering Division American Society of Civil Engineering* 89 (1), 53-61

Wei, S., Tan, W., Liu, F., Zhao, W., and Weng, L. (2014) 'Surface Properties and Phosphate Adsorption of Binary Systems Containing Goethite and Kaolinite'*. Geoderma* 213, 478-484

Weng, C., Tsai, C., Chu, S., Sharma, Y. (2007) 'Adsorption Characteristics of Copper(II) onto Spent Activated Clay'. *Separation and Purification Technology* 54, 187-197.

Wetzel, R.G. (2001) *Limnology: Lake and River Ecosystems*. 3rd ed., San Diego; Academic Press

Wijesundara, T. (ed.) (2004). 'Low-Cost Defluoridation of Water using Broken Bricks' *30thWEDC International Conference Vientiane, Lao PDR*

Worch, E. (2012) *Adsorption Technology in Water Treatment: Fundamentals, Processes, and Modeling*. Berlin: De Gruyter

Woumfo, E. D., Siéwé, J. M., and Njopwouo, D. (2015) 'A Fixed-Bed Column for Phosphate Removal from Aqueous Solutions using an Andosol-Bagasse Mixture'*. Journal of Environmental Management* 151, 450-460

Xie, J., Lin, Y., Li, C., Wu, D., and Kong, H. (2015) 'Removal and Recovery of Phosphate from Water by Activated Aluminum Oxide and Lanthanum Oxide'*. Powder Technology* 269, 351-357

Xu, Y., Hou, H., Liu, Q., Liu, J., Dou, L., Qian, G. (2016) 'Removal Behaviour Research of Orthophosphates by CaFe-Layered Double Hydroxides' *Desalination and Water Treatment* 57 (17) 7918-7925

Xu,X., Gao, B., Wang, W., and Ni, S.Q. (2009) 'Adsorption of Phosphate from Aqueous Solution onto Modified Wheat Residue: Characteristics, Kinetic and Column Studies'. *Colloids and Surfaces B: Biointerfaces* 7(1) 46-52

Xue, Y., Hou, H., and Zhu, S. (2009) 'Characteristics and Mechanisms of Phosphate Adsorption Onto Basic Oxygen Furnace Slag'*. Journal of Hazardous Materials* 162 (2–3), 973-980

Yadav, A. K., Kaushik, C. P., Haritash, A. K., Kansal, A., and Rani, N. (2006) 'Defluoridation of Groundwater using Brick Powder as an Adsorbent'*. Journal of Hazardous Materials* 128 (2–3), 289-293

Yaghi, N. and Hartikainen, H. (2013) 'Enhancement of Phosphorus Sorption Onto Light Expanded Clay Aggregates by Means of Aluminum and Iron Oxide Coatings'. *Chemosphere* 93 (9), 1879-1886

Yakout, S. and Elsherif, E. (2010) 'Batch Kinetics, Isotherm and Thermodynamic Studies of Adsorption of Strontium from Aqueous Solutions onto Low Cost Rice-Straw Based Carbons'. *Carbon Sci.Technol* 1, 144-153

Yao, Y., Gao, B., Chen, J., and Yang, L. (2013) 'Engineered Biochar Reclaiming Phosphate from Aqueous Solutions: Mechanisms and Potential Application as a Slow-Release Fertilizer'. *Environmental Science & Technology* 47 (15), 8700-8708

Yan, L., Xu, Y., Yu, H., Xin, X., Wei, Q., and Du, B. (2010) 'Adsorption of Phosphate from Aqueous Solution by Hydroxy-Aluminum, Hydroxy-Iron and Hydroxy-iron–aluminum Pillared Bentonites'. *Journal of Hazardous Materials* 179 (1–3), 244-250

Yan, Y., Sun, X., Ma, F., Li, J., Shen, J., Han, W., Liu, X., and Wang, L. (2014) 'Removal of Phosphate from Etching Wastewater by Calcined Alkaline Residue: Batch and Column Studies'. *Journal of the Taiwan Institute of Chemical Engineers* 45 (4), 1709-1716

Yaneva, Z., Koumanova, B., and Allen, S. (2013) 'Applicability Comparison of Different kinetic/diffusion Models for 4-Nitrophenol Sorption on Rhizopus Oryzae Dead Biomass'. *Bulg.Chem.Commun* 45 (2), 161-168

Yang, K., Yan, L., Yang, Y., Yu, S., Shan, R., Yu, H., Zhu, B., and Du, B. (2014) 'Adsorptive Removal of Phosphate by Mg–Al and Zn–Al Layered Double Hydroxides: Kinetics, Isotherms and Mechanisms'. *Separation and Purification Technology* 124 (0), 36-42

Yang, S., Wang, X., Jin, P., and Zhang, Q. (2015) 'Adsorptive Removal of Phosphate by Calcined Kanuma Clay from Aqueous Solution'. *Journal of Water Sustainability* 5 (4), 109-119

Yang, S., Zhao, Y., Chen, R., Feng, C., Zhang, Z., Lei, Z., and Yang, Y. (2013) 'A Novel Tablet Porous Material Developed as Adsorbent for Phosphate Removal and Recycling'. *Journal of Colloid and Interface Science* 396 (0), 197-204

Yang, S., Zhao, Y., Ding, D., Wang, Y., Feng, C., Lei, Z., Yang, Y., and Zhang, Z. (2013) 'An Electrochemically Modified Novel Tablet Porous Material Developed as Adsorbent for Phosphate Removal from Aqueous Solution'. *Chemical Engineering Journal* 220, 367-374

Yang, Y., Zhao, Y. Q., Babatunde, A. O., Wang, L., Ren, Y. X., and Han, Y. (2006) 'Characteristics and Mechanisms of Phosphate Adsorption on Dewatered Alum Sludge'. *Separation and Purification Technology* 51 (2), 193-200

Ye, H., Chen, F., Sheng, Y., Sheng, G., and Fu, J. (2006) 'Adsorption of Phosphate from Aqueous Solution Onto Modified Palygorskites'. *Separation and Purification Technology* 50 (3), 283-290

Yeoman, S., Stephenson, T., Lester, J. N., and Perry, R. (1988) 'The Removal of Phosphorus during Wastewater Treatment: A Review'. *Environmental Pollution* 49 (3), 183-233

Yoon, S., Lee, C., Park, J., Kim, J., Kim, S., Lee, S., and Choi, J. (2014) 'Kinetic, Equilibrium and Thermodynamic Studies for Phosphate Adsorption to Magnetic Iron Oxide Nanoparticles'. *Chemical Engineering Journal* 236 (0), 341-347

Yu, Y., Wu, R., and Clark, M. (2010) 'Phosphate Removal by Hydrothermally Modified Fumed Silica and Pulverized Oyster Shell'. *Journal of Colloid and Interface Science* 350 (2), 538-543

Yuan, X., Xia, W., An, J., Yin, J., Zhou, X., and Yang, W. (2015) 'Kinetic and Thermodynamic Studies on the Phosphate Adsorption Removal by Dolomite Mineral'. *Journal of Chemistry* 2015

Zamparas, M. G. (2015) *Development of Physiochemical Methods for Restoring Eutrophic Water Bodies.* Unpublished PhD Thesis. Patras: University of Patras

Zamparas, M., Drosos, M., Georgiou, Y., Deligiannakis, Y., and Zacharias, I. (2013) 'A Novel Bentonite-Humic Acid Composite Material Bephos™ for Removal of Phosphate and Ammonium from Eutrophic Waters'. *Chemical Engineering Journal* 225, 43-51

Zamparas, M., Gianni, A., Stathi, P., Deligiannakis, Y., and Zacharias, I. (2012) 'Removal of Phosphate from Natural Waters using Innovative Modified Bentonites'. *Applied Clay Science* 62–63, 101-106

Zeng, L., Li, X., and Liu, J. (2004) 'Adsorptive Removal of Phosphate from Aqueous Solutions using Iron Oxide Tailings'. *Water Research* 38 (5), 1318-1326

Zhang, Z., Li, H., Zhu, J., Weiping, L., and Xin, X. (2011) 'Improvement Strategy on Enhanced Biological Phosphorus Removal for Municipal Wastewater Treatment Plants: Full-Scale Operating Parameters, Sludge Activities, and Microbial Features'. *Bioresource Technology* 102 (7), 4646-4653

Zhao, D. and Sengupta, A. K. (1998) 'Ultimate Removal of Phosphate from Wastewater using a New Class of Polymeric Ion Exchangers'. *Water Research* 32 (5), 1613-1625

Zhao, Y., Chen, Y., Zhang, Y., and Liu, S. (2017) *Recent Advance in Black Phosphorus: Properties and Applications* [online] . available from <http://www.sciencedirect.com/science/article/pii/S0254058416309166>

Zhou, H., Jiang, Z., and Wei, S. (2013) 'A Novel Absorbent of Nano-Fe Loaded Biomass Char and its Enhanced Adsorption Capacity for Phosphate in Water'. *Journal of Chemistry* 2013

Zhou, Y., Xing, X., Liu, Z., Cui, L., Yu, A., Feng, Q., and Yang, H. (2008) 'Enhanced Coagulation of Ferric Chloride Aided by Tannic Acid for Phosphorus Removal from Wastewater'. *Chemosphere* 72 (2), 290-298

Zhou, J., Yang, S., Yu, J., and Shu, Z. (2011) 'Novel Hollow Microspheres of Hierarchical zinc–aluminum Layered Double Hydroxides and their Enhanced Adsorption Capacity for Phosphate in Water'. *Journal of Hazardous Materials* 192 (3), 1114-1121

Zhu, M., Ding, K., Xu, S., and Jiang, X. (2009) 'Adsorption of Phosphate on Hydroxyaluminum-and Hydroxyiron-Montmorillonite Complexes'. *Journal of Hazardous Materials* 165 (1), 645-651

Zhu, L. and Zhu, R. (2007) 'Simultaneous Sorption of Organic Compounds and Phosphate to inorganic–organic Bentonites from Water'. *Separation and Purification Technology* 54 (1), 71-76

Zhu, T., Mæhlum, T., Jenssen, P. D., and Krogstad, T. (2003) Phosphorus Sorption Characteristics of a Light-Weight Aggregate''. *Water Science and Technology* 35 (5) 1533-1538

Zhu, T., Jenssen, P., Maehlum, T., and Krogstad, T. (1997) 'Phosphorus Sorption and Chemical Characteristics of Lightweight Aggregates (LWA)-Potential Filter Media in Treatment Wetlands'. *Water Science and Technology* 35 (5), 103-108

Zhu, Z., Zeng, H., Zhu, Y., Yang, F., Zhu, H., Qin, H., and Wei, W. (2013) 'Kinetics and Thermodynamic Study of Phosphate Adsorption on the Porous Biomorph-Genetic Composite of α-Fe2O3/Fe3O4/C with Eucalyptus Wood Microstructure'. *Separation and Purification Technology* 117 (0), 124-130

Zong, E., Wei, D., Wan, H., Zheng, S., Xu, Z., and Zhu, D. (2013) 'Adsorptive Removal of Phosphate Ions from Aqueous Solution using Zirconia-Functionalized Graphite Oxide'*. Chemical Engineering Journal* 221 (0), 193-203